Iron mobilization and reduction by coumarin-type siderophores in roots of *Arabidopsis thaliana*

Dissertation

zur Erlangung des
Doktorgrades der Naturwissenschaften (Dr. rer. nat.)

der

Naturwissenschaftlichen Fakultät I
-Biowissenschaften-

der Martin-Luther-Universität
Halle-Wittenberg

vorgelegt

von Frau Vanessa Paffrath

geb. am 27.05.1991 in Berlin

Gutachter

1. Prof. Dr. Nicolaus von Wirén
2. Prof. Dr. Edgar Peiter
3. Prof. Dr. Stephan Clemens

Halle (Saale), den 05.05.2022

For my parents and my sister.

And Sara, because I promised.

Table of contents

1 Summary 1

2 Introduction 3

2.1 The importance of root exudates for Fe acquisition in plants 3

2.2 Solubility and dissolution mechanisms of Fe in soils 4

2.3 Iron acquisition strategies in plants 7

2.3.1 Iron acquisition in graminaceous plants 7

2.3.2 Iron acquisition in non-graminaceous plants 8

2.3.2.1 Release of coumarin-type phenolics as additional component for Fe acquisition in Strategy I plants 10

2.3.2.2 Biosynthesis and function of coumarins in Fe acquisition 11

2.4 Aim of the study 15

3 Materials and methods 17

3.1 Plant material 17

3.2 Cloning and plant transformation 17

3.3 Generation and selection of double mutant plants 19

3.4 Coumarin standards 20

3.5 Plant growth conditions 20

3.6 Reduction of sideretin 21

3.7 Scanning and fluorescence imaging of plants grown on agar plates 22

3.8 Microscopy analysis 22

3.9 Analysis of root system architecture (RSA) 22

3.10 Shoot chlorophyll analysis 23

3.11 Element analysis 23

3.12 Collection of root exudates and sampling of roots 23

3.13 Determination and quantification of coumarins by UPLC-ESI-MS analysis 24

3.14 Determination of Fe-coumarin complex formation *in vitro* 26

3.15 Fe mobilization assays 27

3.16 Ferric chelate reductase activity assay 28

3.17 Gene expression analysis by qPCR 28

3.18 Statistical analysis 30

4 Results 31

4.1 Coumarin-mediated Fe mobilization and reduction is dependent on pH and buffer strength *in vitro* 31

4.2 Role of fraxetin and sideretin in reduction-mediated Fe acquisition 36

4.3 Supplementation of fraxetin cannot restore Fe deficiency in *irt1-1* plants 40

4.4 Coumarin composition in root exudates and extracts of the *fro2* mutant under Fe-deficient conditions 41

4.5 FRO2 and F6'H1-dependent coumarin synthesis play additive functions in Fe acquisition 43

4.6 Supplementation of fraxetin and sideretin can alleviate Fe deficiency in a *fro2 f6'h1-1* double mutant only at acidic pH 47

4.7 Generation of *fro2 s8h-1* and *fro2 cyp82C4-1* to study the relevance of scopoletin and fraxetin for coumarin-mediated Fe(III) reduction *in planta* 49

4.8 Co-cultivation of *fro2* and *cyp82C4-1* plants can alleviate Fe deficiency-induced chlorosis in *fro2* at acidic pH 52

4.9 Effect of *CYP82C4* over-expression in Col-0 54

4.10 Determination of Fe-coumarin complexes via UPLC-MS/MS 56

4.11 Expression analysis of genes involved in coumarin biosynthesis and secretion in dependence of pH and buffer conditions 63

4.12 pH-dependent changes in abundance and tissue-specific localization of coumarin biosynthesis enzymes 70

4.13 External pH affects coumarin composition in roots and root exudates 72

4.14 pH-dependent release of scopoletin is additionally facilitated in a PDR9-independent manner 76

4.15 MYB72-dependent up-regulation of genes involved in coumarin biosynthesis and secretion and inhibition of *CYP82C4* expression at high pH 81

5 Discussion 85

5.1 pH and buffer conditions distinctively affect Fe(III) mobilization and reduction capacities of individual coumarins 86

5.2 Relevance of non-enzymatic Fe(III) reduction for Fe uptake by Strategy I plants 90

5.3 A multi-layer control of root exudate coumarin composition by environmental pH 96

6 References 101

7 Appendix 115

8 Abbreviations 132

9 Acknowledgement 134

10 Curriculum Vitae 135

11 Eidesstattliche Erklärung/Declaration on oath 138

12 Erklärung über bestehende Vorstrafen und anhängige Ermittlungsverfahren/Declaration concerning Criminal Record and Pending Investigations..... 139

1 Summary

Iron (Fe) is an essential micronutrient for nearly all living organisms including plants. Although Fe is highly abundant in soils, its availability is strongly decreased in well-aerated soils at slightly acidic to alkaline soil pH, limiting plant growth and development in such conditions. Non-graminaceous plants employ a reduction-based strategy (so called Strategy I) for Fe acquisition, which includes rhizosphere acidification, reduction of ferric Fe (Fe(III)), and uptake of ferrous Fe (Fe(II)) by the roots. In some strategy I species, such as *Arabidopsis thaliana* and *Brassica napus*, the release of coumarin-type siderophores was recently shown to assist the reduction-based mechanism by solubilizing ferric Fe from sparingly soluble sources. Although there is mounting evidence that coumarins are essential for plant growth on alkaline soils, several aspects concerning the biochemical mechanisms underlying coumarin-mediated Fe acquisition in dependence of the external pH conditions, including their ability to mediate non-enzymatic Fe(III) reduction, still remain unclear.

The present thesis starts with the characterization of the major coumarins identified so far in Arabidopsis root exudates and known to mobilize Fe by chelation and/or reduction under different pH and buffer conditions *in vitro*. These comprehensive analyses revealed that Fe mobilization in general and/or specifically by reduction depends on the chemical properties of each coumarin as well as the external pH and buffer conditions. Fe(III) mobilization was confined to catechol-harboring coumarins while among them only fraxetin and sideretin were identified to possess also strong Fe(III)-reducing properties. Fraxetin and sideretin exhibited different Fe(III) reduction properties *in vitro* over time and Fe(III) mobilization by sideretin was strongly abolished at alkaline pH (pH 7.5), probably because of the poor stability of sideretin at high external pH conditions. Coumarin resupply assays using the Fe(III)-chelate reductase-deficient mutant *fro2* grown under different conditions of low Fe availability showed that fraxetin and sideretin have the ability to bypass enzymatic Fe(III) reduction via FERRIC REDUCTASE-OXIDASE 2 (FRO2) at the root surface at acidic pH (pH 5.6). Fraxetin but not sideretin was further identified to allow Fe(III) reduction in a FRO2-independent manner at higher pH conditions (i.e., pH 6.5). Resupply experiments using a newly generated *fro2 f6'h1-1* double mutant showed that fraxetin facilitates Fe(III) reduction at pH 6.5 and can largely bypass FRO2 function through synergistic effects with other FERULOYL-CoA 6'-HYDROXYLASE (F6'H1)-dependent coumarins. Furthermore, co-cultivation of *fro2* with the *cyp82C4* mutant, a natural fraxetin over-accumulator, indicated that fraxetin-mediated Fe(III) reduction at acidic pH is indeed relevant *in planta*. The ability of fraxetin to facilitate Fe(III) mobilization by chelation and/or reduction was further supported by the determination of Fe-coumarin complexes by UPLC-MS/MS. This approach allowed the identification of several different Fe(II)/Fe(III)-fraxetin complexes and suggests that coumarins can also dimerize in a Fe-dependent manner.

Since increases in external pH inhibited more sensitively coumarin-mediated Fe(III) reduction rather than their overall Fe(III) mobilization capacities, coumarins assist Fe acquisition in Strategy I plants primarily by increasing Fe(III) solubility by chelation. Nonetheless, by generating double mutants defective in FRO2 activity and coumarin biosynthesis it was possible to estimate *in planta* the contribution of coumarins for Fe(III) reduction.

Furthermore, root exudate and extract analysis of wild-type plants grown under different Fe-limiting conditions and external pH conditions revealed that sideretin was the major catecholic coumarin synthesized and released at acidic to only slightly acidic pH, while fraxetin release was favored at alkaline pH. The apparent difference in the coumarin composition of root extracts and root exudates in dependence of the external pH were largely associated with profound changes in expression of the corresponding genes involved with coumarin biosynthesis and secretion. Among the most contrasting responses were increased transcript levels of *F6'H1* and *S8H* (SCOPOLETIN 8-HYDROXYLASE) as the pH was increased, while *CYP82C4* (CYTOCHROME P450 82C4) expression was strongly inhibited at high pH. The use of *proF6'H1::F6'H1:GFP*, *proS8H::S8H:GFP*, and *proCYP82C4::CYP82C4:GFP* lines allowed to verify these observations at the protein level and additionally revealed that the external pH affects the tissue-specific localization of the enzymes involved with the synthesis of different coumarins in roots. Furthermore, gene expression analysis of different Fe acquisition mutants under different conditions of low Fe availability suggested the transcription factor MYB DOMAIN PROTEIN 72 (MYB72) to be of special importance for the adaptive changes in the gene expression in response to different external pHs. In *myb72-1* plants, the transcriptional up-regulation of several coumarin biosynthesis and transporter genes as well as the repression of *CYP82C4* at alkaline pH were largely absent. Moreover, the secretion of especially catecholic coumarins in *myb72-1* plants was strongly abolished.

Taken together, the present study provides a comprehensive picture on how coumarins assist the reduction-based Fe-acquisition mechanisms by combining both information about the biochemical function of the individual coumarins released by Arabidopsis and the underlying mechanisms that determine the coumarin composition in root exudates in dependence of the external pH. Thereby, chemical properties of individual coumarins determine their efficacy in Fe(III) mobilization both by chelation or reduction, while regulatory features of the corresponding genes responsible for their biosynthesis determine their biological function.

2 Introduction

2.1 The importance of root exudates for Fe acquisition in plants

The ability of plants to efficiently acquire sparingly available nutrients from soil is critical for undisturbed development, growth, and reproduction and thereby affects the productivity and quality of crop plants (Marschner, 2012). As sessile organisms, plants have to deal with temporal and spatial changes in the amount of bioavailable nutrients in the soil solution which is determined by different edaphic and environmental factors (Rengel, 2001; Comerford, 2005; Fageria and Stone, 2006; Hinsinger *et al.*, 2009). Plant adaptive strategies to counteract limited nutrient availability include both morphological and physiological changes. Modulation of root hair development and the elongation and branching of roots of different orders in response to changes in the plant nutritional status and in external nutrient supply are well established (Lynch, 1995; López-Bucio, Cruz-Ramírez and Herrera-Estrella, 2003; Hermans *et al.*, 2006; Gruber *et al.*, 2013; Giehl and von Wirén, 2014). Furthermore, nutrient-deficient plants can induce physiological adaptations including the enhanced expression of membrane transporters for nutrients (Gojon, Nacry and Davidian, 2009) or the remobilization and retranslocation of nutrients from source tissues, intracellular storage proteins and compartments, or from the root apoplast (Loneragan, Snowball and Robson, 1976; Jin *et al.*, 2007; Maillard *et al.*, 2015). Additionally, plants can directly or indirectly influence nutrient availability in the rhizosphere through the secretion of protons, gaseous molecules (e.g. CO_2, O_2), and especially carbon-containing primary and secondary metabolites from roots (Dakora and Phillips, 2002; Bais *et al.*, 2006; Badri and Vivanco, 2009; Sasse, Martinoia and Northen, 2018; Pascale *et al.*, 2020). Such metabolites can directly facilitate nutrient mobilization and uptake (Römheld, 1991; Ström *et al.*, 2002; Johnson and Loeppert, 2006; Suzuki *et al.*, 2006; Schmid *et al.*, 2014; Rajniak *et al.*, 2018) or shape the root microbiome towards beneficial microbes which support nutrient supply, acquisition, and plant growth (Bais *et al.*, 2006; Sasse, Martinoia and Northen, 2018; Pascale *et al.*, 2020). Mobilization comprises thereby all processes that solubilize nutrients including pH decrease, chelation, and reduction.

Root-derived exudates are well-documented to be essential for iron (Fe) acquisition in plants under Fe-limiting conditions (Marschner, Römheld and Kissel, 1986; Rodríguez-Celma *et al.*, 2013; Schmid *et al.*, 2014). Due to its redox-active properties, Fe is an essential element for virtually all living organisms. However, although highly abundant in soils, Fe availability to plants is strongly decreased on well-aerated soils at slightly acidic to alkaline conditions, as it forms only slightly soluble or insoluble minerals (primarily ferric oxides and hydroxides) or organic complexes (Lindsay and Schwab, 1982; Cornell and Schwertmann, 2003; Colombo *et al.*, 2014).

Iron deficiency is a worldwide problem in crop production as it is prevalent on calcareous soils which are often characterized by alkaline pH conditions and represent around one-third of the world's soils (Chen and Barak, 1982; Vose, 1982; Läuchli and Grattan, 2012). A characteristic symptom of Fe deficiency is interveinal chlorosis due to impaired chlorophyll synthesis (Terry and Abadía, 1986). In Fe-deficient plants, chlorosis appears initially on younger leaves, as Fe cannot be readily mobilized from other plant tissues (Taiz *et al.*, 2015). Besides the impairment of chlorophyll synthesis, Fe deficiency also affects the structure and function of the photosynthetic apparatus (Pushnik, Miller and Manwaring, 1984; Eberhard, Finazzi and Wollman, 2008). Iron is therefore a limiting factor for efficient photosynthesis and consequently for plant growth and yield as well as plant product quality (Alvarez-Fernández *et al.*, 2014; Briat, Dubos and Gaymard, 2015).

In plants, Fe deficiency stimulates the enhanced release of different Fe-mobilizing components including phytosiderophores and phenolics like coumarins into the rhizosphere (Brown and Ambler, 1973; Römheld and Marschner, 1983; Hether, Olsen and Jackson, 1984; Takagi, Nomoto and Takemoto, 1984; Schmid *et al.*, 2014; Sisó-Terraza *et al.*, 2016; Rajniak *et al.*, 2018). Besides genotypic differences, the impaired biosynthesis or release of such components diminishes the ability of plants to grow under Fe-limiting conditions (Römheld and Marschner, 1990; Nozoye *et al.*, 2011; Fourcroy *et al.*, 2014; Schmid *et al.*, 2014; Rajniak *et al.*, 2018). A profound knowledge of the basic molecular mechanisms governing Fe acquisition in plants mediated by root-derived exudates can therefore stimulate the development of new breeding, cultivation, and fertilization strategies as well as of new chelators used as agricultural fertilizers to compensate for Fe deficiency-related yield losses. The following sections aim to give an overview of the different mechanisms how Fe is solubilized and dissolved in soils as well as of the basic molecular mechanisms underlying Fe acquisition in plants with special emphasis on coumarin-mediated Fe-acquisition in non-graminaceous plant species such as *Arabidopsis thaliana*.

2.2 Solubility and dissolution mechanisms of Fe in soils

Iron is the fourth most abundant element in the Earth's crust and invariably present in all soils (Mengel *et al.*, 2001; Frey and Reed, 2012). In primary soil minerals, Fe is mainly present as Fe(II) (Mengel *et al.*, 2001). Such minerals are fairly unstable and slowly weathering in the presence of oxygen, which finally leads to the release and oxidation of Fe(II) to Fe(III) and formation of very poorly soluble secondary Fe(III)-oxides and hydroxides (Schwertmann, 1991; Lindsay, 1995). Fe(III) initially precipitates as amorphous Fe and is transformed into more ordered Fe(III)-(hydro)oxides including ferrihydrite, maghemite, lepidocrocite, hematite, and goethite with decreasing solubility as weathering progresses (Lindsay, 1995; Mengel *et al.*,

2001). The latter two represent the most abundant minerals in well-drained soils (Colombo *et al.*, 2014). Given the low solubilities of Fe-(hydro)oxides in soils, the total amount of soluble Fe in the soil solution is typically very low (Uren, 1984; Schwertmann, 1991). In general, the activity of Fe(III) ions is determined by the pH and redox potential of the soil (Schwertmann, 1991; Colombo *et al.*, 2014). Solubilization of Fe(III) from Fe-(hydro)oxides is promoted by acidic and reducing conditions, while precipitation is favored at increasing pH values and redox potentials (Lindsay, 1995; Cornell and Schwertmann, 2003). The minimum solubility of Fe is attained at pH 7.5 to pH 8.5 with an estimated concentration of around 10^{-10} M (Lindsay, 1995). In well-aerated soils with only slightly acidic to alkaline pH conditions, the amount of soluble Fe in the soil solution is therefore insufficient to meet the plant demand, which requires 10^{-6} M to 10^{-5} M soluble Fe for optimal growth (Lindsay and Schwab, 1982; Marschner, 2012).

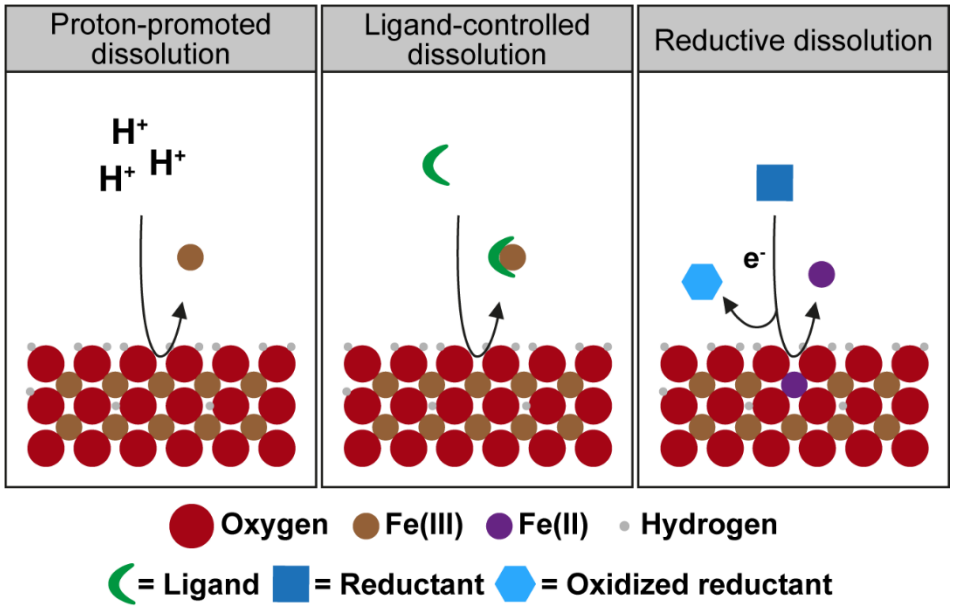

Fig. 1. Schematic representation of the three major Fe dissolution mechanisms of a Fe(III)-(hydro)oxide in natural environments (modified from Schwertmann (1991) and Biswakarma *et al.* (2019)).

As Fe(III)-(hydro)oxides are the main source of Fe for plants and microorganisms in most soils, Fe mobilization, i.e. dissolution, must take place to ensure sufficient Fe supply for organisms and for re-starting the terrestrial Fe cycle (Schwertmann, 1991). However, such minerals possess also very low dissolution kinetics which are influenced by different factors such as the specific surface area of the mineral, the pH, the redox potential, as well as the concentration of acids, reductants, and complexing agents present in the solution phase (Cornell and Schwertmann, 2003; Kraemer, 2004). As shown in Fig. 1, three main mechanisms are thought to accelerate Fe dissolution in natural environments: (i) proton-promoted, (ii) ligand-controlled, and (iii) reductive dissolution (Zinder, Furrer and Stumm, 1986; Schwertmann, 1991; Suter, Banwart and Stumm, 1991). In general, the processes underlying the different surface-controlled dissolution mechanisms are characterized by the adsorption of either protons,

ligands, or reductants on the surface of a Fe mineral which leads to a polarization and subsequent weakening of the Fe-O bonds followed by the detachment of the Fe atom and restoration of the mineral surface by the adsorption of protons (Schwertmann, 1991; Kraemer, 2004). Thereby, the detachment of the Fe atom is usually the rate-limiting step (Cornell and Schwertmann, 2003).

During the proton-promoted dissolution, three protons are adsorbed to the mineral surface facilitating the release of Fe(III) (Cornell and Schwertmann, 2003). Because Fe dissolution by protonation is slow, this process is of only minor importance in comparison to ligand-promoted and especially reductive dissolution in soils and in the rhizosphere (Cornell and Schwertmann, 2003).

The ligand-promoted dissolution relies on the presence of small, Fe-complexing molecules in the soil solution which can be released by microorganisms and plant species under Fe-deficient conditions (Römheld and Marschner, 1986; Sandy and Butler, 2009; Saha *et al.*, 2013). The most common of such molecules are the so-called siderophores, or phytosiderophores if plant-derived, which have a high affinity for Fe(III) and can form soluble Fe(III)-complexes (Schwertmann, 1991; Hider and Kong, 2010; Ahmed and Holmström, 2014). Adsorption of Fe ligands to the mineral surface leads to the formation of surface complexes, which destabilize the coordinative bonds of Fe at the mineral surface by inductive effects and thereby facilitate the detachment of Fe complexed by its ligand (Kraemer, 2004).

Reductive dissolution, in turn, requires the presence of reductants, i.e. electron donors. After adsorption of a reductant, electron transfer takes place and Fe(III) reduction destabilizes the Fe-O bonds and Fe(II) is released (Cornell and Schwertmann, 2003). In natural systems, reductants comprise e.g. phenolics and organic acids originating from exudates of plants and soil microbes as well as humic substances deriving from microbial degradation of organic matter (Marschner, Römheld and Kissel, 1986; Stumm and Sulzberger, 1992; Peiffer and Wan, 2016).

Iron dissolution in soils can be enhanced by the simultaneous presence of multiple ligands or of a reductant and ligand through synergistic effects (Banwart, Davies and Stumm, 1989; Dos Santos Afonso *et al.*, 1990; Reichard, Kretzschmar and Kraemer, 2007; Wang *et al.*, 2015; Schenkeveld *et al.*, 2016; Schenkeveld and Kraemer, 2018). For instance, synergistic Fe mobilization have been reported for organic acids such as oxalate, an inorganic ligand, and siderophores as well as phytosiderophores (Reichard *et al.*, 2005; Reichard, Kretzschmar and Kraemer, 2007). Additionally, synergistic effects have been found for ascorbate, a Fe(III) reductant, and different microbial or plant-derived Fe-complexing molecules (Wang *et al.*, 2015; Schenkeveld *et al.*, 2016). Moreover, trace amounts of Fe(II) have been demonstrated to have catalytic effects on Fe dissolution (Suter *et al.*, 1988; Biswakarma *et al.*, 2019; Kang *et al.*, 2019). Thereby, it is thought that Fe(II), generated e.g. through reductive dissolution,

can accelerate the rate of ligand-controlled Fe dissolution by promoting the detachment of Fe(III)-ligand complexes via electron transfer to Fe(III) at the mineral surface (Biswakarma *et al.*, 2019).

2.3 Iron acquisition strategies in plants

To overcome the limited bioavailability of Fe, plants have evolved two major strategies to acquire Fe from soil (Marschner, Römheld and Kissel, 1986; Römheld and Marschner, 1986). These strategies largely rely on the classical mineral dissolution mechanisms described in the previous section. The main difference between both strategies is the form of Fe which is taken up. While graminaceous plants taken up Fe as an intact Fe(III)-phytosiderophore complex, non-graminaceous plants rely on the reduction of Fe(III) to Fe(II) prior to its uptake.

2.3.1 Iron acquisition in graminaceous plants

Graminaceous plant species such as barley and maize employ a chelation-based strategy, also known as Strategy II (Römheld, 1987). When challenged by Fe deficiency, roots of Strategy II plants release elevated amounts of mugineic acid-type phytosiderophores (PS) into the rhizosphere, which can solubilize and chelate Fe(III) from otherwise insoluble sources (Takagi, Nomoto and Takemoto, 1984; Marschner, Römheld and Kissel, 1986; Ma and Nomoto, 1996). PS are low-molecular-weight metal ligands with high selectivity towards Fe(III) (Ma and Nomoto, 1996; Hider and Kong, 2010). Different PS have been identified in graminaceous plants including e.g. 2'-deoxymugineic acid (DMA), mugineic acid, and epi-hydroxymugineic acid (Kawai, Takagi and Sato, 1988; Ma and Nomoto, 1996). They are synthesized in roots from L-methionine via nicotianamine and DMA (Ma and Nomoto, 1993, 1994). As L-methionine is the precursor, PS biosynthesis is also associated with the methionine recycling pathway (Ma *et al.*, 1995).

The efflux of PS is mediated by TRANSPORTER OF MUGINEIC ACID 1 (TOM1) which resides in the plasma-membrane of the root epidermis, cortex, and endodermis as well as in the central cylinder (Nozoye *et al.*, 2011). Under Fe-sufficient conditions, TOM1 has also been detected in the exodermis of rice roots (Nozoye *et al.*, 2011). Although PS are synthesized continuously throughout the day (Ma and Nomoto, 1996), their release follows a strict diurnal rhythm with a maximum release rate occurring a few hours after onset of the light period (Takagi, Nomoto and Takemoto, 1984; Marschner, Römheld and Kissel, 1986; Mori *et al.*, 1987). Once released into the rhizosphere, PS promote Fe dissolution and bind Fe(III) in a hexadentate fashion via their carboxyl, amine, and hydroxyl groups, thus forming a 1:1 complex (Sugiura *et al.*, 1981; Mino *et al.*, 1983; Kraemer, 2004). Intact Fe(III)-PS complexes are then taken up by specific

transporters, such as YELLOW STRIPE 1 (YS1), which is resides in the plasma-membrane of rhizodermal cells (von Wirén *et al.*, 1994; Curie *et al.*, 2001; Murata *et al.*, 2006).

The ability of PS to mobilize Fe from insoluble Fe-(hydr)oxides is largely pH-independent. PS can efficiently mobilize Fe at neutral to slightly alkaline pH as well as in the presence of high bicarbonate (HCO_3^-) concentrations (Takagi, Nomoto and Takemoto, 1984; Römheld and Marschner, 1986; Takagi, Kamei and Yu, 1988). Interestingly, differences in susceptibility of graminaceous species to Fe deficiency at high pH has been attributed to the quantity and type of PS released rather than the uptake of Fe(III)-PS complexes (Marschner, Römheld and Kissel, 1986; von Wirén, Khodr and Hider, 2000). Since PS are susceptible to microbial degradation which limits their Fe-dissolution capacity (Shi *et al.*, 1988; Takagi, Kamei and Yu, 1988; von Wirén *et al.*, 1993), it is thought that the strict release of high amounts of PS is a strategy to ensure sufficient Fe mobilization (Römheld, 1991; von Wirén *et al.*, 1995). Besides quantity, also the type of PS can affect differentially the Fe mobilization capacity under different soil pHs. For instance, it has been demonstrated that Fe(III)-complexes of hydroxylated PS (e.g. mugineic acid) were less susceptible to protonation under acidic conditions which is thought to decrease complex stability in comparison to non-hydroxylated PS like DMA (von Wirén, Khodr and Hider, 2000).

2.3.2 Iron acquisition in non-graminaceous plants

In contrast to grasses, non-graminaceous plant species such as *Arabidopsis thaliana* and *Brassica napus* rely on a reduction-based strategy, also known as Strategy I. Iron acquisition in such plants typically involves three steps, including (i) acidification of the rhizosphere by the release of protons, (ii) reduction of Fe(III) to Fe(II), and (iii) import of Fe(II) into the roots (Chaney, Brown and Tiffin, 1972; Römheld, 1987). Rhizosphere acidification is achieved by proton extrusion via Fe deficiency-induced H^+-ATPases (Römheld and Kramer, 1983; Guerinot and Yi, 1994). In *Arabidopsis thaliana* (Arabidopsis hereafter), this process mainly relies on the activity of the H^+-ATPase AHA2 (Santi and Schmidt, 2009). The local acidification of the rhizosphere facilitates the solubilization of Fe(III) precipitates (Schwertmann, 1991) and is also assumed to stimulate the enzymatic Fe(III) reduction at the root (Bienfait *et al.*, 1983). Once solubilized, Fe(III) may enter the root apoplast where it can be reduced by members of the FERRIC REDUCTASE-OXIDASE (FRO) gene family, such as FRO2 in Arabidopsis, which is located in root hairs and epidermal cells of Fe-deficient roots (Robinson *et al.*, 1999; Connolly *et al.*, 2003). Readily reduced Fe can be subsequently taken up into root cells by members of the ZIP transporter family located in the plasma-membrane (Guerinot, 2000). In Arabidopsis, this step is mediated by the Fe(II) transporter IRON-REGULATED TRANSPORTER 1 (IRT1) (Eide *et al.*, 1996; Varotto *et al.*, 2002; Vert *et al.*, 2002). The expression of *FRO2* and *IRT1* is

strictly coregulated and highly induced in response to Fe deficiency (Vert, Briat and Curie, 2003).

A key regulator of the Fe acquisition response is the basic helix-loop-helix (bHLH) transcription factor FER-LIKE IRON-DEFICIENCY-INDUCED TRANSCRIPTION FACTOR (FIT) (Colangelo and Guerinot, 2004; Jakoby *et al.*, 2004; Yuan *et al.*, 2005). FIT is necessary to up-regulate *AHA2* and essential for the induction of *FRO2* and *IRT1* expression in response to Fe deficiency (Colangelo and Guerinot, 2004; Jakoby *et al.*, 2004; Ivanov, Brumbarova and Bauer, 2012). A combined co-expression network and FIT-dependent transcriptome analysis indicated FIT as a central regulatory hub that integrates different hormone and stress signals and modulates the response to Fe deficiency (Schwarz and Bauer, 2020). Under Fe-deficient conditions, FIT is activated by a bHLH transcription factor cascade in the root (Gao *et al.*, 2020; Schwarz and Bauer, 2020). In the absence of sufficient Fe, the bHLH transcription factor bHLH121/URI (bHLH subgroup IVb) accumulates in its phosphorylated form (Kim *et al.*, 2019) and interacts with bHLH subgroup IVc proteins including bHLH034, bHLH104, bHLH105 (ILR3), and bHLH115 by forming heterodimers (Gao *et al.*, 2020). These transcription factor complexes can bind to the promoters of their target genes and thereby stimulate the expression of different Fe deficiency-responsive genes, including bHLH subgroup Ib genes (Zhang *et al.*, 2015; Li *et al.*, 2016; Liang *et al.*, 2017). Among them, bHLH038, bHLH039, bHLH100, and bHLH101 are known to activate FIT by the formation of heterodimers (Yuan *et al.*, 2008; Wang *et al.*, 2013). Several genes involved both in Fe uptake and homeostasis have been identified to be regulated in a FIT-dependent manner (Colangelo and Guerinot, 2004; Mai, Pateyron and Bauer, 2016; Schwarz and Bauer, 2020). In order to maintain proper Fe homeostasis, FIT is tightly regulated at both transcriptional and post-translational levels by a sophisticated network integrating different signaling pathways (Kobayashi, 2019; Schwarz and Bauer, 2020). For instance, FIT also transcriptionally induces the expression of *BRUTUS-LIKE1* (*BTSL1*) and *BRUTUS-LIKE2* (*BTSL2*), which encode two E3 ubiquitin ligases, and promote the degradation of FIT (Colangelo and Guerinot, 2004; Rodríguez-Celma *et al.*, 2019). BTSL1 and BTSL2 are further proposed to bind Fe, which is likely to affect their stability providing thereby another layer of regulation (Rodríguez-Celma *et al.*, 2019).

In general, plants employing Strategy I are more susceptible to Fe deficiency than Strategy II plants particularly under alkaline soil conditions (Marschner, Römheld and Kissel, 1986). One reason for this apparent difference is that proton extrusion may be inefficient whenever soil pH is strongly buffered causing insufficient acidification of the local rhizosphere and, hence, resulting in only limited Fe(III) solubilization (Marschner, Römheld and Kissel, 1986; Kraemer, 2004; Colombo *et al.*, 2014). Calcareous soils are characterized by elevated amounts of $CaCO_3$ (calcium carbonate) which can react in the presence of CO_2 to bicarbonate (HCO_3^-), a

strong base which buffers soil pH to 7.5-8.5 and prevents acidification by root-released protons (Lindsay and Schwab, 1982; Lucena, 2000). Within this pH range, the lowest Fe solubility is attained (Lindsay and Schwab, 1982). In addition, the activity of root-bound ferric reductases is strongly reduced as their activity is highly pH-dependent with an optimum at acidic conditions (Bienfait *et al.*, 1983; Romera, Alcántara and de la Guardia, 1992a). Besides this pH-dependent effect, bicarbonate itself has been also shown to inhibit FRO2 activity well as the expression of several Fe acquisition genes (Romera, Alcántara and de la Guardia, 1992a; Lucena *et al.*, 2007).

2.3.2.1 Release of coumarin-type phenolics as additional component for Fe acquisition in Strategy I plants

Despite the strong inhibitory effects of high soil pH and buffering capacity on different components of the Strategy I mechanism, non-graminaceous plants are still able to grow in alkaline and calcareous soils (Terés *et al.*, 2019). The accumulation and enhanced extrusion of phenolics and other low-molecular organic compounds from roots of Strategy I plants has been observed and suggested to support Fe acquisition under Fe-limiting conditions (Brown and Ambler, 1973; Olsen *et al.*, 1981; Marschner and Römheld, 1994). In these early studies, mainly phenolics such as caffeic acid have been assumed to support Fe mobilization and utilization by chelating and/or reducing Fe from insoluble Fe(III) precipitates in the soil (Olsen *et al.*, 1981; Julian, Cameron and Olsen, 1983; Römheld and Marschner, 1983; Hether, Olsen and Jackson, 1984; Mladěnka *et al.*, 2010). The importance of phenolics in Fe acquisition has been described for several different Strategy I plants such as peanut (Römheld and Marschner, 1983), red clover (Jin *et al.*, 2007), and Arabidopsis (Rodríguez-Celma *et al.*, 2013; Schmid *et al.*, 2014; Schmidt *et al.*, 2014). However, the transporters and enzymes involved in Fe deficiency-induced phenolics extrusion and biosynthesis, were only recently identified.

In Arabidopsis, the release of coumarin-type phenolic compounds has been identified to be essential for plant growth under Fe-limiting conditions (Schmid *et al.*, 2014; Schmidt *et al.*, 2014). Coumarins are a large group of 1,2-benzopyrone derivatives which comprise of metabolites with different chemical structures (Harborne, 1999; Bourgaud *et al.*, 2006). Although coumarins are ubiquitously found in higher plants, their concentration, as well as qualitative and quantitative content varies from species to species (Lozhkin and Sakanyan, 2006; Rajniak *et al.*, 2018). In Arabidopsis, Fe deficiency strongly stimulates the biosynthesis and the release of at least four deglycosylated coumarins (Fourcroy *et al.*, 2014; Schmid *et al.*, 2014; Schmidt *et al.*, 2014) which are considered to assist Fe acquisition by chelating and/or reducing Fe (Mladěnka *et al.*, 2010).

2.3.2.2 Biosynthesis and function of coumarins in Fe acquisition

The analysis of root extracts and exudates from Arabidopsis plants grown under Fe-deficient conditions by LC-MS/MS has identified several different coumarins including scopoletin, esculetin, fraxetin, their β-D-glucopyranosides scopolin, esculin, and fraxin, respectively, as well as isofraxidin, 5-methoxyscopoletin, and sideretin (Fourcroy *et al.*, 2014; Schmid *et al.*, 2014; Schmidt *et al.*, 2014; Sisó-Terraza *et al.*, 2016; Ziegler *et al.*, 2017; Rajniak *et al.*, 2018). Coumarin biosynthesis is part of the phenylpropanoid metabolism involving the *ortho*-hydroxylation of cinnamates, trans/cis isomerization of the side chains, and lactonization (Bourgaud *et al.*, 2006; Kai *et al.*, 2008). *Ortho*-hydroxylation is thereby a key process that serves as a branch point away from lignin biosynthesis (Kai *et al.*, 2008).

An essential enzyme involved in the biosynthesis of scopolin and scopoletin derivatives is the 2-oxoglutarate-dependent dioxygenase FERULOYL-CoA 6'-HYDROXYLASE (F6'H1) (Kai *et al.*, 2008; Rodríguez-Celma *et al.*, 2013; Schmid *et al.*, 2014; Schmidt *et al.*, 2014). F6'H1 mediates the *ortho*-hydroxylation of feruloyl-CoA, a key precursor of scopoletin biosynthesis (Fig. 2; Kai *et al.*, 2008), and its expression is strongly induced in roots of Fe-starved plants in a FIT-dependent manner (Schmid *et al.*, 2014). The subsequent trans-cis isomerization and lactonization of 6-hydroxyferuloyl-CoA into scopoletin was recently uncovered to be catalyzed by the BAHD acyltransferase-COUMARIN SYNTHASE (COSY) (Vanholme *et al.*, 2019). Scopoletin is not only one of the most prominent coumarins released by plants under Fe-deficient conditions (Schmid *et al.*, 2014; Clemens and Weber, 2016), but also the precursor for the biosynthesis of the catecholic coumarins fraxetin and sideretin (Rajniak *et al.*, 2018; Siwinska *et al.*, 2018; Tsai *et al.*, 2018). Fraxetin is synthesized from scopoletin via a hydroxylation step catalyzed by the SCOPOLETIN 8-HYDROXYLASE (S8H) (Rajniak *et al.*, 2018; Siwinska *et al.*, 2018; Tsai *et al.*, 2018). In a second hydroxylation step, catalyzed by the cytochrome P450 enzyme CYP82C4, fraxetin is converted into sideretin (Rajniak *et al.*, 2018). Similar to *F6'H1*, *S8H* and *CYP82C4* are also strongly up-regulated by Fe deficiency in a FIT-dependent manner (Murgia *et al.*, 2011; Rajniak *et al.*, 2018; Tsai *et al.*, 2018). However, whereas F6'H1 protein has been detected in rhizodermal and cortical cells of Fe-starved roots, it remains unknown in which cell-types the enzymes S8H and CYP82C4 are present.

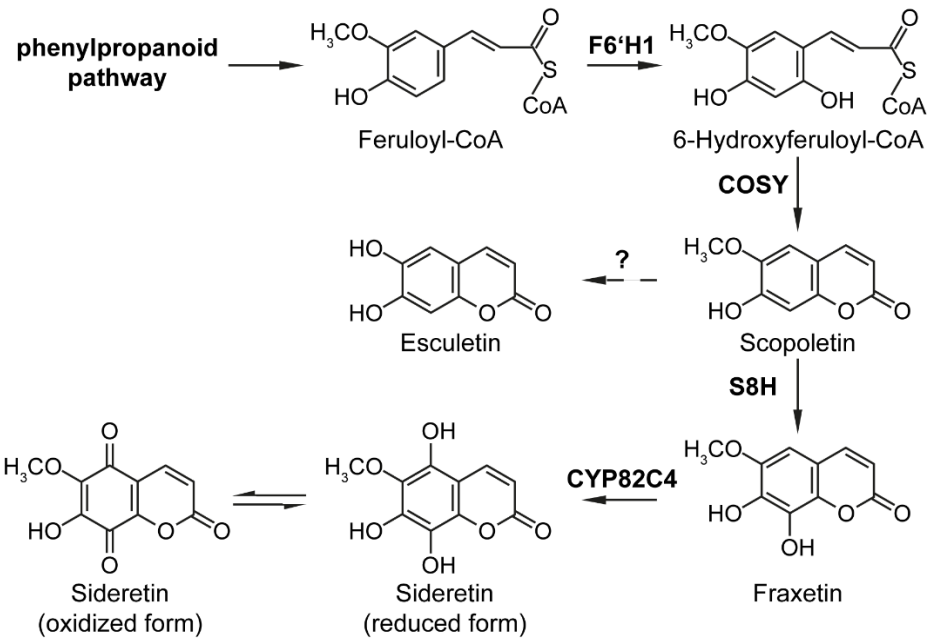

Fig. 2. Coumarin biosynthesis pathway in Arabidopsis. The pathway was drawn according to results from Kai *et. al* (2008), Schmid *et. al* (2014), Schmidt *et. al* (2014), Rajniak *et. al* (2018), Vanholme *et. al* (2019). The question mark indicates that the step leading to esculetin synthesis remains unknown.

Most coumarins identified in Arabidopsis have been detected in their glycosylated and deglycosylated forms. In general, glycosylation and degylcosylation is considered as a mechanism to regulate the localization, availability, and biological activity of phenylpropanoids (Le Roy *et al.*, 2016). In root extracts, coumarins are mainly present in their glycosylated form, while their aglycons prevail in root exudates (Fourcroy *et al.*, 2014; Schmid *et al.*, 2014; Schmidt *et al.*, 2014; Rajniak *et al.*, 2018), suggesting the existence of a degylcosylation step. However, this process is not yet well understood, and it still remains unclear if coumarin degylcosylation takes place before or after coumarin release. So far, only several β-glycosidases facilitating scopolin degylcosylation have been described. The Arabidopsis β-glycosidases BGLU21, BGLU22, and BGLU23 have been shown to specifically deglycosylate scopolin *in vitro* (Ahn *et al.*, 2010). Another β-glycosidase, BGLU42, was recently identified to be essential for the release of scopoletin in response to Fe deficiency and rhizobacteria-mediated induced systemic resistance through the specific degylcosylation of scopolin into scopoletin (Zamioudis, Hanson and Pieterse, 2014; Stringlis *et al.*, 2018).

Coumarin secretion by roots is mainly mediated by the ATP-binding cassette transporter *PLEIOTROPIC DRUG RESISTANCE 9* (PDR9/ABCG37) although further transporters are also likely involved as knocking-out *PDR9* does not completely abolish coumarin secretion in Arabidopsis (Rodríguez-Celma *et al.*, 2013; Fourcroy *et al.*, 2014; Ziegler *et al.*, 2017). The expression of *PDR9* is strongly induced under Fe-limiting conditions especially at alkaline pH (Rodríguez-Celma *et al.*, 2013; Fourcroy *et al.*, 2014; Robe *et al.*, 2021). Under such conditions, PDR9 is localized at the outward facing sides of both epidermal and cortical cells,

while under Fe-sufficient conditions it is mainly present in the epidermis at low abundance (Robe *et al.*, 2021). Coumarin release occurs from the differentiated and mature zones of the root and involves both epidermal cells as well as root hairs (Robe *et al.*, 2021).

Secreted coumarins can directly and indirectly contribute to Fe acquisition by plants. Arabidopsis plants have been shown to indirectly profit from the interaction of coumarins with soil microorganisms (Zamioudis, Hanson and Pieterse, 2014; Stringlis *et al.*, 2018; Harbort *et al.*, 2020). Initially, the root specific R2R3-MYB transcription factor MYB DOMAIN PROTEIN 72 (MYB72), which is required for the onset of induced systemic resistance, was found to be also an integral part of the plant's response to Fe deficiency (Palmer *et al.*, 2013; Zamioudis, Hanson and Pieterse, 2014; Stringlis *et al.*, 2018). MYB72 is required for the induction of several genes involved in Fe homeostasis such as *NICOTIANAMINE SYNTASE 4* (*NAS4*) (Palmer *et al.*, 2013) as well as *BGLU42* and *F6'H1* (Zamioudis, Hanson and Pieterse, 2014). Further studies revealed that F6'H1-dependent coumarins are essential for the assembly of the root-associated microbiome, and disruption of coumarin biosynthesis or secretion lead to an altered microbial community and impaired plant growth under Fe-limiting conditions (Stringlis *et al.*, 2018; Voges *et al.*, 2019; Harbort *et al.*, 2020). Thereby, the secretion of scopoletin and fraxetin seemed to be of major importance for the microbiome composition while sideretin was less important (Stringlis *et al.*, 2018; Harbort *et al.*, 2020). However, antimicrobial activity has been reported for all these coumarins (Stringlis *et al.*, 2018; Voges *et al.*, 2019; Harbort *et al.*, 2020).

Besides indirectly affecting Fe solubilization by interacting with soil microorganisms, coumarins are also suggested to have the capacity to chelate and reduce Fe (Moran *et al.*, 1997; Schmid *et al.*, 2014; Rajniak *et al.*, 2018) and, therefore, to directly facilitate Fe mobilization and potentially assisting in reductive Fe acquisition by plants. Indeed, *in vitro* assays have indicated that the underlying mechanism of coumarins in Fe acquisition by plants involves Fe chelation and reduction (Mladěnka *et al.*, 2010; Schmidt *et al.*, 2014; Rajniak *et al.*, 2018). In general, Fe chelation is considered to be conducted by catechol-harboring coumarins like esculetin, fraxetin, and sideretin, which contain two hydroxyl groups in *ortho* positions (Hider, Liu and Khodr, 2001; Andjelković *et al.*, 2006; Perron and Brumaghim, 2009; Mladěnka *et al.*, 2010). However, a remaining gap in determining Fe-chelating functions of coumarin-type siderophores is that, so far, Fe-coumarin complexes have not been detected in the rhizosphere or root exudate samples. This could be mainly due to analytical challenges involved in the identification of metal-ligand complexes potentially present in relatively low amounts as well as the poor stability during sample preparation and analysis (Alvarez-Fernández *et al.*, 2014). To date, the determination of Fe-coumarin complexes received only little attention. Although Schmidt *et al.* (2014) reported the detection of putative Fe(II)-scopoletin species *in vitro*, they

could not detect any Fe-esculetin or Fe-fraxetin complexes which was unexpected and still remains elusive.

The Fe mobilization capacity of different coumarins has been investigated under different pH and buffer conditions *in vitro* (Mladěnka *et al.*, 2010; Schmid *et al.*, 2014; Sisó-Terraza *et al.*, 2016; Rajniak *et al.*, 2018; Tsai *et al.*, 2018), but similar studies have only partially been done *in vivo*. Coumarin resupply experiments with the coumarin biosynthesis mutants *f6'h1* and *s8h* grown under Fe-limiting conditions at slightly acid pH further supported the involvement of catechol-harboring coumarins in Fe mobilization (Schmid *et al.*, 2014; Rajniak *et al.*, 2018). Interestingly, although the non-catecholic coumarin scopoletin can only poorly mobilize Fe(III) *in vitro*, exogenous supply of scopoletin was able to largely rescue *f6'h1* mutant plants from low Fe availability-induced chlorosis (Schmid *et al.*, 2014; Rajniak *et al.*, 2018). Since scopoletin cannot rescue *s8h* mutants (Rajniak *et al.*, 2018), it is likely that scopoletin can be converted to catecholic coumarins when supplied to *f6'h1* plants. In another study with scopoletin and fraxetin, it was found that supplementation of fraxetin could restore Fe acquisition in both *f6'h1* and *s8h* while scopoletin had no effect (Tsai *et al.*, 2018). However, the ability of esculetin and sideretin to facilitate Fe mobilization and thereby support Fe acquisition in plants under elevated pH conditions remain unclear. Furthermore, *in vivo* studies at alkaline pH and high concentrations of bicarbonate representing more natural conditions as found in calcareous soils are still lacking.

Some phenolics released by roots under Fe-limiting conditions possess Fe reduction capacity but their contribution to efficient Fe(III) reduction is assumed to be only of negligible importance to the overall increased Fe reduction capacity of roots under such conditions (Barrett-Lennard, Marschner and Römheld, 1983; Fourcroy *et al.*, 2016). It has been proposed that coumarins mainly function in Fe mobilization by chelation and that Fe(III) reduction is primarily mediated by FRO2 (Fourcroy *et al.*, 2016). However, the contribution of coumarins to Fe reduction is not yet completely resolved as *fro2* mutant plants grown under sufficient Fe are almost indistinguishable from wild-type plants, suggesting the involvement of FRO2-independent Fe(III) reduction mechanisms. Additionally, it is still uncertain which coumarins have Fe-chelating and -reducing capacity and if they can perform both or only one of these functions *in planta*.

Another largely unknown aspect is why plants produce and release different types of coumarins. For instance, *cyp82C4* mutant plants, which are unable to convert fraxetin into sideretin, are phenotypically similar to wild-type plants even when grown under low Fe availability (Rajniak *et al.*, 2018). Besides the necessity to determine the molecular function of each coumarin and the biological processes they are involved in, it is also important to localize the function of coumarins within and outside roots. Secreted coumarins are suggested to

primarily function in Fe solubilization and to supply membrane-bound FROs with Fe(III) for reduction and/or IRT1 with Fe(II) for uptake (Rodríguez-Celma and Schmidt, 2013; Tsai and Schmidt, 2017b). On the other hand, it is possible that coumarins are also involved in reutilization of root apoplastic Fe, as previously shown for secreted phenolics in red clover grown under Fe deficiency (Jin *et al.*, 2007).

Several studies have indicated that the ability of individual coumarins to assist Fe acquisition by Fe(III) chelation and/or reduction as well as the root exudate composition is influenced by different pH conditions (Sisó-Terraza *et al.*, 2016; Rajniak *et al.*, 2018; Tsai *et al.*, 2018). However, the regulatory mechanisms underlying pH-dependent coumarin biosynthesis and/or secretion are still poorly understood. Furthermore, possible direct effects of high HCO_3^- concentrations, as found in calcareous soils, have not been considered so far. Although a very recent transcriptome analysis of Arabidopsis grown under Fe-deficient conditions at slightly acidic and neutral pH revealed several genes to be differentially regulated in response to the external pH (Tsai and Schmidt, 2020), a comprehensive picture combining both information about the molecular function of individual coumarins as well as coumarin biosynthesis and secretion in dependence of different pH and buffer conditions is still missing.

2.4 Aim of the study

In the past decade, the importance of coumarins for Fe acquisition in non-graminaceous plant species became evident. Although coumarins are suggested to facilitate Fe acquisition in these species by mobilizing Fe through chelation and/or reduction, only little is known about the contribution of the different coumarins to these processes and why it is advantageous for plants to produce a wide variety of different coumarins. In the present study, it was hypothesized that coumarins differ in their ability to chelate and/or reduce Fe(III) and hence to mobilize Fe from insoluble sources in dependence of the external pH. Furthermore, the question was raised whether coumarins can by-pass the enzymatic Fe(III) reduction mediated by FRO2 under certain conditions. Therefore, the main aim of this study was to characterize the coumarins scopoletin, esculetin, fraxetin, and sideretin regarding their molecular function in Fe(III) mobilization in dependence of the external pH and to assign different biological functions to them. To address this aim, the ability of the different coumarins to mobilize and reduce Fe(III) from freshly precipitated Fe-(hydro)oxides under different pH and buffer conditions was assessed both *in vitro* and *in vivo*. Several coumarin resupply experiments were conducted to determine the ability of the individual coumarins to restore Fe-deficiency in the Arabidopsis *fro2* mutant under different conditions of low Fe availability. In addition to that, the coumarin composition of root exudates and extracts of *fro2* and wild-type plants as well as the expression of coumarin biosynthesis and transporter genes was assessed. Furthermore, different

coumarin over-expressing and double mutant lines were generated and phenotypically characterized under different Fe-limiting conditions.

Another aim of the present thesis was to determine and verify the formation of Fe(II)/(III)-coumarin complexes *in vitro* using high resolution liquid chromatography tandem mass spectrometry (LC-MS/MS).

Furthermore, it was aimed to get insights into the regulatory mechanisms that determine the coumarin composition of roots and root exudates. To distinguish between pH- and Fe-deficiency induced responses, gene expression analysis of several genes involved in coumarin biosynthesis and secretion were conducted for wild-type plants grown under different pH conditions in the absence or presence of Fe with different availability to plants. Additionally, the localization of three major coumarin biosynthesis enzymes and the coumarin composition of root exudates and extracts was assessed under these conditions. Finally, gene expression as well as root extract and exudate analysis were also performed for different coumarin biosynthesis and transporter mutants grown under different Fe-limiting conditions.

3 Materials and methods

3.1 Plant material

In this study, the *Arabidopsis thaliana* EMS mutant *fro2* (*frd1-1*) (Yi & Guerinot, 1996) and the corresponding wild-type Columbia *gl1* (Col-*gl1*) were used. Furthermore, the following homozygous T-DNA-insertion lines from the SALK, SM, or GABI collection (all Col-0 background) were used: *f6'h1-1* (At3g13610, SALK_132418C), *s8h-1* (At3g12900, SM_3_27151), *s8h-2* (At3g12900, SM_3_23443), *cyp82C4-1* (At4g31940, SALK_001585), *irt1-1* (At4g19690) (Varotto *et al.*, 2002), *pdr9-2* (At3g53480, SALK_050885) (Fourcroy *et al.*, 2014), *bglu42* (At5g36890, SALK_034026C), *myb72-1* (At1g56160, SAIL_713G10), *myb-10* (At5g65770, SALK_120297C), and *fit* (fit-3, At2g28160, GABI_108C10) (Jakoby *et al.*, 2004).

3.2 Cloning and plant transformation

The GreenGate cloning system (Lampropoulos *et al.*, 2013) was used to generate different constructs for plant expression. Gene-specific promoter and open reading frame fragments were amplified from genomic DNA (gDNA) of the Arabidopsis accession Col-0 (CS 60000). Amplification was performed using the Phusion High-Fidelity DNA Polymerase (New England Biolabs) and the primers shown in Tab. 1. The resulting amplicons were purified on a gel and isolated using the NucleoSpin Gel and PCR Clean-up Kit (Machery-Nagel) according to the manufacturer's instructions. Promoter and open reading frame amplicons were cloned into the GreenGate entry modules pGGA000 and pGGC000, respectively. The correct integration of the amplicon was verified by restriction and the cloned sequences verified by SANGER sequencing. Finally, the individual entry modules were assembled in the GreenGate pGGZ001 binary vector. A phosphinotricin or hygromycin resistance cassette (GreenGate modules pGGF001 or pGGF005, respectively) was included as selection marker.

To achieve a constitutive overexpression of *CYP82C4* (At4g31940), a 1976-bp fragment of the *CYP82C4* open reading frame was expressed under the control of the *35S* promoter from the Cauliflower mosaic virus (CaMV) (GreenGate module pGGA004) and a 1924-bp fragment was expressed under the control of the *UBQ10* promoter (At4g05320; GreenGate module pGGA006).

To investigate the localization of F6'H1, S8H, and CYP82C4, transgenic lines expressing a translational fusion of the proteins with C-terminal GFP under the control of the native promoters were generated. More specifically, to generate *proF6'H1::F6'H1:GFP* a 1166-bp fragment of the *F6'H1* open reading frame was fused to GFP in the C-terminus (GreenGate module pGGD001) and expressed under the control of a 2077-bp fragment of the *F6'H1* promoter. For generating a *proS8H::S8H:GFP* line, a 1534-bp fragment of the *S8H* open

reading frame and a 2023-bp fragment of the promoter were used. In case of the *proCYP82C4::CYP82C4:GFP* reporter line, a 1976-bp fragment of the *CYP82C4* open reading frame and a 1151-bp fragment of the promoter were used.

The *Agrobacterium tumefaciens* strain GV3101 containing the pSOUP helper plasmid was transformed with the final binary vectors. *A. thaliana* wild-type (Col-0) plants were transformed using the flower dip method (Clough and Bent, 1998). T1 transformants were selected on agar plates containing 10 µg mL^{-1} phosphinotricin or 45 µg mL^{-1} hygromycin and 125 µg mL^{-1} ticarcillin while T2 lines were selected only on phosphinotricin or hygromycin. Protein localization studies were conducted using gene:GFP T1 lines. In all other cases, independent homozygous lines were used for experiments.

Table 1. Primer used for cloning.

Transgenic line	**Primer name**	**Primer sequence (5'→3')**
35S::CYP82C4 and *proCYP82C4::CYP82C4:GFP*	ggCYP82C4cds_For1	AACAGGTCTCAGGCTATTCAAACAAGAAATCACCAAAC
35S::CYP82C4 and *proCYP82C4::CYP82C4:GFP*	ggCYP82C4cds_Rev1	AACAGGTCTCACTGACACAAAAAGTTCTTCCTTAAT
proUBQ10::CYP82C4	ggCYP82C4cds_For2	AACAGGTCTCAGGCTAAATGGATACTTCCCTCTTTTCTTTG
proUBQ10::CYP82C4	ggCYP82C4cds_Rev2	AACAGGTCTCACTGACACAAAAAGTTCTTCCTTAATACGTG
proF6'H1::F6'H1:GFP	ggF6'H1pro_For	AACAGGTCTCAACCTCACGAATTCATAACAGATTCACA
proF6'H1::F6'H1:GFP	ggF6'H1pro_Rev	AACAGGTCTCATGTTTGGAATAAAAAAGATAGGAG
proF6'H1::F6'H1:GFP	ggF6'H1cds_For	AACAGGTCTCAGGCTAAATGGCTCCAACACTCTTGAC
proF6'H1::F6'H1:GFP	ggF6'H1cds_Rev	AACAGGTCTCACTGAGATCTTGGCGTAATCGAC
proS8H::S8H:GFP	ggS8Hpro_For	AACAGGTCTCAACCTGCAGAACCGAAATTAGTACCG
proS8H::S8H:GFP	ggS8Hpro_Rev	AACAGGTCTCATGTTTCTCCACACTTCTGCTTGAAAA
proS8H::S8H:GFP	ggS8Hcds_For	AACAGGTCTCAGGCTATGGGTATCAATTTCGAGGACCA
proS8H::S8H:GFP	ggS8Hcds_Rev	AACAGGTCTCACTGACTCGGCACGTGCGAAGTC
proCYP82C4::CYP82C4:GFP	ggCYP82C4pro_For	AACAGGTCTCAACCTGCTCTTTGTGGGCTTTTTGGAT
proCYP82C4::CYP82C4:GFP	ggCYP82C4pro_Rev	AACAGGTCTCATGTTGAGAGTGCAGAAGAGATGTGTGT

3.3 Generation and selection of double mutant plants

The double mutants were generated by crossing of *fro2* plants with *f6'h1-1*, *s8h-1*, and *cyp82C4-1* plants, respectively. Wild-type (Col-0 x Col-*gl1*) and single mutant plants were selected from the same F2 populations to exclude any background effects. Plants were pre-screened for the lack of a functional FRO2 using a ferric-chelate reductase activity assay (FCR assay, see below). Then, the homozygous T-DNA insertion in the *F6'H1*, *S8H*, and *CYP82C4* gene, respectively, was evaluated by PCR. Genomic DNA (gDNA) extraction and PCR was performed either with Phire Plant Direct PCR Kit (Thermo Fisher Scientific) or with MagAttract 96 DNA Plant Core Kit (Qiagen) and 2x Taq Master Mix (Dye Plus, Vazyme Biotech) or DreamTag DNA polymerase (Thermo Fisher Scientific) following the manufacturer's instructions. In order to differentiate between the wild-type alleles and T-DNA insertions, two PCR reactions per sample were conducted using (i) gene-specific primers (GSP_F and GSP_R) or (ii) the reverse gene-specific primer and a T-DNA-specific primer (LBb1.3 for SALK T-DNA lines and Spm32 for SM lines). The primers used for these reactions are listed in Table 2.

Finally, homogenous *fro2* mutation was verified by SANGER sequencing. Therefore, gDNA was extracted from root or shoot material as follows: 100-400 mg fresh harvested plant material was frozen in liquid nitrogen and homogenized via vigorous vortexing using three stainless steel balls (3.0-3.3 mm). 800 µL extraction buffer (1% N-laurylsarcosine, 100 mM Tris-HCl pH 8.0, 10 mM EDTA pH 8.0, and 100 mM NaCl) were added and the samples shortly vortexed followed by the addition of 800 µL phenol/chloroform/3-methyl-1-butanol (25:24:1) and vigorous vortexing. Samples were centrifuged for 3 min (2348 *g* at room temperature). The supernatant was transferred into a new 1.5-mL tube to which 80 µL 3 M sodium acetate pH 5.2 and 800 µL isopropanol were added. After 10 min centrifugation (17949 *g* at 4°C), the supernatant was discarded and 800 µL 70% ethanol (EtOH) were added. Samples were centrifuged for 1 min (17949 *g* at 4°C) and the supernatant discarded. The DNA pellet was shortly dried and resuspended in 80-120 µL 1:10 TRIS-EDTA (TE) pH 8.0 buffer and RNase (RNase A, Qiagen).

The Phusion High-Fidelity DNA Polymerase (New England Biolabs) was used for amplification. Thereby, the following primers were used: ggFRO2cds-F (5'-AACAGGTCTCAGGCTAAGGAGCATGCAACTAGCTTA-3') and ggFRO2cds-R (5'-AACAGGTCTCACTGACCAGCTGAAACTGATAGATTCAAAA-3'). Samples were purified on a 1% agarose gel and the *FRO2* amplicons were isolated from the gel using the NucleoSpin Gel and PCR Clean-up Kit (Machery-Nagel) according to the manufacturer's instructions. Purified amplicons were sequenced using the ggFRO2cds-F primer.

Table 2. Primers used for plant screening regarding T-DNA insertion in the *F6'H1*, *S8H*, or *CYP82C4* gene.

AGI ID	Primer name	Primer Sequence (5'→3')
At3g13610	F6'H1_GSP_F	CCTGTTGCTGTGGAAGAGAAG
At3g13610	F6'H1_GSP_R	GCAGATATCAGGCCAGAACTG
At3g12900	S8H_GSP_F	CGGTAGCCAAGCGTTAAGTAC
At3g12900	S8H_GSP_R	CCACCTGTCATTTTCATTTCG
At4g31940	CYP82C4_GSP_F	TTGTTCCAATCCTTGTTTTCG
At4g31940	CYP82C4_GSP_R	TATGACCCAAGTGCGTCTCTC
	LBb1.3_SALKTDNA	ATTTTGCCGATTTCGGAAC
	Spm32-R	TACGAATAAGAGCGTCCATTTTAGAGTGA

3.4 Coumarin standards

4-methyldaphentin (purity 97%), esculetin (purity 98%, 246573), fraxin (purity ≥ 95%), fraxetin (purity 98%), and scopoletin (purity ≥ 99%) were purchased from Sigma Aldrich. Scopolin (purity ≥ 95%) was purchased from PhytoLab GmbH & Co. KG. Sideretin (purity 95%) was synthesized on demand by Orgentis Chemicals GmbH (Gatersleben, Germany).

3.5 Plant growth conditions

In agar plate experiments, Arabidopsis seeds were surface sterilized in a solution containing 70% (v/v) EtOH and 0.05% (v/v) Triton-X-100 (Roth). Sterilized seeds were precultured on sterile agar plates containing one-half strength Murashige and Skoog (MS) medium (Murashige and Skoog, 1962) (MS medium without Fe was purchased from Ducefa Biochemie) with 40 µM NaFeEDTA (Sigma Aldrich), supplemented with 0.5% sucrose (Ducefa Biochemie) and 2.5 mM MES pH 5.6 (Roth), and solidified with 0.8-1% (w/v) Difco agar (Becton Dickinson). The pH of the medium was adjusted to pH 5.6 with 2 M KOH (Roth) before adding the agar. The plates were incubated at 4°C for 2 d to synchronize seed germination. The plates were then placed vertically inside a growth cabinet under a 22°C/18°C and 10/14 h light/dark regime with the light intensity adjusted to 120 µmol photons m^{-2} sec^{-1}. After 10 d, seedlings were transferred to fresh solid media containing different conditions of low Fe availability. These media contained one-half strength MS supplemented with either freshly prepared 20 µM $FeCl_3$ (Roth) or 15 µM ferrozine (Serva), and buffered with either 2.5 mM MES pH 5.6, 500 µM or 1 mM $NaHCO_3$ (Roth), or 1.25 mM MOPS (AppliChem GmbH). The pH of the different media was adjusted with 2M KOH and 37% HCl (Roth) to pH 5.6 (MES), pH 6.5 (MES and 1mM $NaHCO_3$), and pH 7.5 (MOPS and 500 µM $NaHCO_3$). If not indicated otherwise, 12 seedlings

were cultivated on each square petri dish (120 x 120 mm containing 50 mL solid medium). Plants were assessed after 4 or 6 d of cultivation on treatments depending on the experiment. In the co-cultivation experiment, in total three *fro2* plants were placed on one square plate alternating with three plants of the co-cultivating genotype. The plates were kept vertically in the growth cabined and *fro2* plants were harvested after 11 d.

In coumarin-resupply experiments, esculetin, fraxetin, or scopoletin were dissolved either in methanol (MeOH) or in mQ-H_2O. For the latter, the pH was increased until coumarins were completely dissolved and then adjusted to pH 7.0. Freshly reduced sideretin was dissolved in MeOH. Coumarins were added to autoclaved medium after cooling down. Equal amounts of mQ-H_2O or MeOH (125 µL) were used as mock controls. To avoid the exchange of root exudate components when two different genotypes were grown in the same petri dish, the agar was separated vertically into two segments and horizontally 1 cm above the bottom. The plates were prepared one day before transferring the plants and sideretin-containing plates were kept in darkness. Four seedlings were placed on each agar segment. The plants were grown for 6 d under these conditions. In sideretin re-supply experiments, agar plates were wrapped with aluminum foil up to the shoots or placed into a box to minimize the direct exposure of the roots and root-containing agar to light.

Phenotyping of different Arabidopsis lines to investigate their ability to acquire Fe from soil at high pH was conducted as described in Schmid *et al.* (2014). In brief, plants were cultivated on peat-based substrate (Klaasmann Substrate 1) with soil pH maintained at pH 5.6 (control) or at approximately pH 7.0, achieved by the supplementation of 20 g kg^{-1} $CaCO_3$ (Roth) and 12 g kg^{-1} $NaHCO_3$ (limed). The substrate was prepared two days before sowing the seeds to allow the reaction to reach the equilibrium. Plants were cultivated in 54-pot trays for 19 d. After 6 d, the plant number per pot was reduced to 10. In order to alleviate Fe deficiency symptoms in certain mutant lines, the substrate was supplemented with 2 mL of 0.5 g L^{-1} FeEDDHA (Ducefa Biochemie) three times a week from day 5 onwards.

3.6 Reduction of sideretin

Sideretin stock solutions used for agar plate experiments and *in vitro* Fe-mobilization assays were always freshly prepared in MeOH and reduced by bubbling with hydrogen in the presence of palladium (granular, purity 99.99%, Sigma Aldrich) for ~10 min. During the reduction step, the solution changed its color from orange-brown to light yellow (Fig. 3). The reduction was assumed to be completed when the color remained constant.

Fig. 3. Sideretin stock solutions before (left) and immediately after (right) reduction with hydrogen in the presence of palladium.

3.7 Scanning and fluorescence imaging of plants grown on agar plates

Scanning and fluorescence imaging of plants grown on agar plates was conducted as described in (Schmid *et al.*, 2014). The scanner resolution was set to 600 dots per inch.

3.8 Microscopy analysis

For protein localization studies, roots of *proF6'H1::F6'H1:GFP*, *proS8H::S8H:GFP*, and *proCYP82C4::CYP82C4:GFP* lines cultivated under different Fe and pH conditions, as described above, were first stained with propidium iodide (10 µg mL^{-1}) for 10 minutes (min). Roots were then mounted in water and GFP- and propidium iodide-dependent fluorescence immediately acquired with a confocal laser-scanning microscope (LSM 780, Zeiss, Germany) equipped with 20x/0.8 M27 objective. GFP was excited with a 488 nm Argon laser and the emitted light was detected between 493 nm and 552 nm. Propidium iodide (PI) staining was visualized with a 561 nm laser and detected at 550-650 nm emission range. Z-stacks were acquired using ZEN Black (Zen 2.3 SP1 FP1) while orthogonal views of Z-stacks were prepared with ZEN 2.6 (blue edition) software.

3.9 Analysis of root system architecture (RSA)

The root system architecture (RSA) was analyzed as described by (Gruber *et al.*, 2013). In brief, roots were separated so that they were clearly distinguishable from each another on the agar plate. The plates were scanned in greyscale at 300 dots per inch resolution using an Epson Expression 10000XL scanner (Seiko Epson). To allow for a better quantification of the roots, the contrast of the image was adjusted, and marks were removed using GIMP (version 2.10.22). Roots were analyzed using WinRHIZO Pro 2009 (Regent Instruments, Canada) and the following eight RSA traits were determined: primary root (PR) length, number of lateral

roots (LR), LR length, length of second order LR (TRL), number of second order LRs, average LR length, LR density, and total root length.

3.10 Shoot chlorophyll analysis

Whole shoot samples were weighted and incubated for 1-2 d at 4°C in N,N'-dimethylformamide (Roth). The absorbance of the extracts was measured at 647 nm and 664 nm (UV5Bio, Mettler Toledo, Germany) and the chlorophyll concentration was determined following the protocol of (Porra, Thompson and Kriedemann, 1989).

3.11 Element analysis

For Fe determination, whole shoot samples were dried at 65°C and weighted into polytetrafluoroethylene tubes. Plant material was digested with concentrated HNO_3 (67-69%; Bernd Kraft) and pressurized in a high-performance microwave reactor (UltraCLAVE IV, MLS GmbH). Digested samples were diluted with de-ionized water (Milli-Q Reference A+, Merck Millipore). Element analysis was carried out by high resolution inductively coupled plasma mass spectrometry ((HR)-ICP-MS) (ELEMENT 2, Thermo Fisher Scientific, Germany).

3.12 Collection of root exudates and sampling of roots

Root exudates were collected as described in (Schmid *et al.*, 2014) with some modifications. Sampled plants were grown for 4 d on medium with 20 µM $FeCl_3$ or 15 µM ferrozine and buffered with either 2.5 mM MES to pH 5.6 and pH 6.5, or 1.25 mM MOPS to pH 7.5. One hour after the beginning of the light phase, root exudate sampling was performed on ultrapure water buffered with the buffer used in the agar medium to the corresponding pH for 6 h. Controls containing no plant were also included. Root exudate sample were frozen at -80°C and freeze dried. The freeze-dried samples were resolved in a total volume of 10 mL 100% MeOH and vigorously vortexed. 4-methyldaphnetin (4-MD) dissolved in MeOH (2 µL of 100 µg mL^{-1}) was added as an internal standard. The samples were centrifuged at 4°C for 1 min at 1252 x g, filtered through Chromafil CA-45/25 (0.45 µm pore) filters, and finally concentrated to 0.5 mL using a centrifugal evaporator (Christ ALPHA RVC 2-33 IR). Prepared root exudate samples were stored at -80°C until measurement.

After root exudate collection, plant roots were harvested and snap frozen in liquid nitrogen. Phenolic components were extracted from the frozen roots by adding 100% MeOH with 0.4 µg mL^{-1} 4-MD (400 µL per 100 mg root fresh weight) and homogenizing the tissue with stainless steel balls (3.0-3.3 mm) by vigorously vortexing. The samples were incubated

overnight at 4°C in darkness. After centrifugation at 4°C and 16100 *g* for 10 min, the supernatant was taken, transferred into a new tube and stored at -20°C. A second extraction was performed for 1.5-2 h under the same conditions. The samples were centrifuged and the supernatant was pooled with the first one. Prepared root extracts were stored at -20°C until measurement.

3.13 Determination and quantification of coumarins by UPLC-ESI-MS analysis

Root exudate and extract samples were subjected to ultra-performance liquid chromatography mass spectrometry (UPLC-MS) analysis using a 1290 Infinity II LC system (Agilent Technologies, United States) coupled to a 6490 Triple Quad LC/MS with iFunnel technology (Agilent Technologies, United States).

The Agilent UPLC system was equipped with a reversed phase Acquity UPLC® HSS T3 Column (100 Å, 2.1 mm x 150 mm, 1.8 µm, Waters) and an Acquity UPLC® HSS T3 VanGuard Pre-column (100 Å, 2.1 mm x 5 mm, 1.8 µm, Waters). The column temperature was set to 30°C. For the analysis of esculetin, fraxetin, scopoletin, and their glycosides, the gradient was linear from 0min, 90% solvent A (0.1% (v/v) formic acid in 18mΩ water (Milli-Q)) and 10% solvent B (0.1% (v/v) formic acid in acetonitrile), to 8 min, 20% solvent A and 80% solvent B. For the analysis of sideretin, the gradient was changed linear within 7 min to 70% solvent A and 30% solvent B. In both methods, the solvent composition was then switched back to the initial conditions within 1 min, and then kept constant for another minute to equilibrate the column for the next run. In all cases, the flow rate was 0.4 mL min^{-1} and the injection volume was set to 1 µL.

The eluted coumarins were sprayed into the MS using an ESI source with Agilent Jet Stream technology (Agilent Technologies, United States). The sheath gas temperature was set to 300°C. Mass spectra were acquired in positive and/or negative mode, with capillary voltages of 2 kV and 3 kV, respectively (see Table 3). For tandem mass spectrometry (MS/MS), a collision energy of 18 eV was found to be optimal for all compounds. For data acquisition, a multiple reaction monitoring (MRM) MS experiment was set up. Supplemental Table 2 summarizes the MRM transitions and retention times for the different coumarins. The specific MRM transition for the compound 4-methyldaphnetin (193>147 m/z in pos. mode, 191>145 in neg. mode) was also measured.

A mixture of all coumarins with a final concentration of 0.4 µg mL^{-1} was injected at least every 10 samples to ensure the stability of the measurement and validity of the calibration curve. MS data were analyzed using MassHunter software (B.07.01, Agilent Technologies, United States). Data quantification was performed based on an external calibration curve. A stock solution with a final concentration of 0.8 µg/mL of all coumarins analyzed in this study was

prepared. The calibration standards were prepared by serial dilution of this stock solution (0.8 µg mL^{-1}, 0.7 µg mL^{-1}, 0.6 µg mL^{-1}, 0.5 µg mL^{-1}, 0.4 µg mL^{-1}, 0.3 µg mL^{-1}, 0.2 µg mL^{-1}, 0.1 µg mL^{-1}, 0.05 µg mL^{-1}, and 0.025 µg mL^{-1}). Each standard was measured three times and a linear regression curve was calculated.

Table 3. Multiple reaction monitoring transitions and retention times for LC-MS-based analysis of coumarins.

Compound	Retention time (min)	Precursor ion (m/z)	Product ion (m/z)	Ion mode
4-Methyldaphnetin	4.72	193.0	147.0	Positive
4-Methyldaphnetin	5.26	191.0	145.0	Negative
Esculin	3.02	341.0	179.0	Positive
Esculetin	3.86	179.0	123.0	Positive
Fraxin	3.53	369.0	207.0	Negative
Fraxetin	4.16	209.0	149.0	Positive
Scopolin	3.38	353.0	191.0	Negative
Scopoletin	4.85	193.0	133.0	Positive
Sideretin (oxidized)	4.40	221.0	177.9	Negative

During this study, the UPLC-MS method for coumarin analysis in root exudates and extracts was also transferred to an Orbitrap mass spectrometer. On this device, chromatographic separation was performed on a Vanquish™ UHPLC system (Thermo Fisher Scientific, Germany). Coumarin baseline separation was achieved using the same column and solvents as described above. The applied gradient was as follows: 0 min to 1 min 10% solvent B; linear increase of solvent B to 20% at 5 min, to 30% at 8 min, to 65% at 9 min, to 80% at 9.5 min; 9.5 min to 10 min 80% solvent B. Additional gradient steps to a total run time of 13 min were included to guaranty both column wash and equilibration. The column temperature was set to 30°C and the flow rate to 0.4 mL min^{-1}. The injection volume was 1 µL.

The UHPLC system was coupled to a Q Exactive Plus Mass Spectrometer (Thermo Fisher Scientific, Germany) equipped with a HESI source operating in both positive and negative ion mode. The source values were set in positive mode as follows: spray voltage 3.5 kV; capillary temperature 255°C; S-lens RF level 40; aux gas heater temperature 400°C; sheath gas flow rate 40; aux gas flow rate 10. In negative mode, the spray voltage was set to 2.5 kV, the sheath gas flow rate to 47 and the aux gas flow rate to 11. The retention times and analysis mode for each coumarin are shown in Table 4. A full MS ddMS2 experiment was performed for spectra acquisition. The resolution in the full scan was set to 70,000. For MS/MS experiments a

resolution of 17,500 and an NCE of 30 V was used. MS data were acquired and processed by the Trace Finder Software (v. 4.1., Thermo Fisher Scientific, Germany).

The calibration solutions were prepared as described above. To generate a calibration curve, the peak area on the extracted ion chromatogram (XIC) of the protonated or deprotonated molecule ion, respectively, was used. A least-square regression was applied to best fit the linearity curve. LOQ was found to be 0.0125 µg mL^{-1}. The identification of the compounds in the samples was based on comparison of their retention time and high-resolution m/z spectrum with standards.

As sideretin standards were observed to become oxidized over time and sideretin oxidation during root exudate and extract preparation could not be controlled, the peak areas of both the reduced and oxidized form were added up to allow absolute quantification of sideretin. The error of the calibration standards measured over a time of 7 d was found to be <17%.

Table 4. Coumarin retention times analyzed on the Orbitrap-MS.

Compound	Retention time (min)	Precursor ion (m/z)	Ion mode
4-Methyldaphnetin	5.99	193.04954	Positive
Esculin	3.42	341.0867	Positive
Esculetin	4.58	179.0339	Positive
Fraxin	4.32	369.0827	Negative
Fraxetin	5.14	209.0444	Positive
Scopolin	4.02	355.10236	Positive
Scopoletin	6.12	193.0495	Positive
Sideretin (oxidized)	4.88	221.0916	Negative
Sideretin (reduced)	4.40	223.02481	Negative

3.14 Determination of Fe-coumarin complex formation *in vitro*

To investigate the formation of Fe-coumarin complexes, coumarins were incubated with $FeCl_3$ at different pH's *in vitro*. Therefore, coumarin stock solutions including esculetin, esculin, fraxetin, fraxin, and scopoletin were prepared in 100% MeOH. $FeCl_3$ was dissolved in mQ-H_2O and the pH of the solution was kept either unchanged (pH ~2.2-2.5) or was adjusted with 5 M NaOH to pH ~5.5 or pH ~9.0. The individual coumarins were mixed with $FeCl_3$ in different molar ratios and incubated for 30 min in a thermo-mixer adjusted to 1000 rpm at room temperature in darkness. For esculetin and fraxetin, the following coumarin:Fe molar ratios were investigated: 0.3:1, 0:5:1, 0.7:1, 1:1, 1.5:1, 2:1, 3:1, and 1:2. In case of scopoletin, the coumarin:Fe molar ratio was 1:2 or 2:1. As negative controls, coumarins were incubated with

pure mQ-H_2O or MeOH (1:1 (v/v)). Additionally, esculin and fraxin were incubated with $FeCl_3$ in a molar ratio of 1:1. In order to verify the presence of Fe-coumarin complexes *in vitro*, esculetin and fraxetin were also incubated with $^{58}FeCl_3$ (Trace Sciences International) using a coumarin:Fe molar ratio of 2:1 or 1:2. The pH of $^{58}FeCl_3$ stock solution was not adjusted.
After incubation, all samples were subsequently filtered through Chromafil CA-45/25 (0.45 µm pore) filters and analyzed by UPLC-ESI-MS (Triple Quad and Orbitrap). The gradient of the LC-MS method on the Triple Quad was extended by 1 min 20% solvent A and 80% solvent B for the analysis of the samples shown in Fig. 21, 22, and Annex Figs. 5, 8, and 9 and the mass acquisition window was set to 50-500 m/z. For all further analysis on the Triple Quad, the same LC-MS method described for the analysis of root exudates and extracts was used except that the mass acquisition window was opened to 50-750 m/z. No modifications in the LC-MS method on the Orbitrap were done with the exception of opening the mass acquisition window to 40-1000 m/z.

3.15 Fe mobilization assays

Iron mobilization capacity of pure esculetin, fraxetin, scopoletin, and freshly reduced sideretin standards was determined as a function of pH, buffer strength and time. Therefore, 0.4 mM coumarin dissolved in MeOH was incubated with 0.1 mM $FeCl_3$ buffered with either 2.5 mM MES to pH 5.6 and 6.5, 1 mM, 2 mM, or 2.5 mM $NaHCO_3$ to pH 6.5 and 7.5, or 1.25 mM MOPS pH 7.5. Samples were incubated at room temperature in darkness on a gyratory shaker at 70 rpm (Stuart™ Gyratory rocker SSL3). Aliquots were taken after 10 min, 30 min, 1 h, 3 h, 6 h, and 24 h and directly filtered through Chromafil CA-45/25 (0.45 µm pore) filters. 0.3 mM NaEDTA (Merck), 0.3 mM ascorbic acid (Sigma Aldrich) and MeOH were used as references. The Fe concentration in the filtrates was determined by (HR)-ICP-MS. Additionally, the concentration of reduced Fe was determined using a spectrophotometric approach. Therefore, the absorbance of an aliquot of each filtrate was determined at 562 nm (UV5Bio, Mettler Toledo, Germany) before and after incubation with ferrozine (final concentration 0.4 mM) for 10 min in darkness at room temperature in a thermo-mixer adjusted to 1400 rpm. The difference between both absorbance values was used for Fe(II) quantification based on a calibration curve acquired for the individual buffers. A serial dilution of a 100 µM $FeCl_3$ stock solution in the corresponding buffer was prepared. To fully reduce Fe(III), each calibration standard was incubated with dithiothreitol (DTT, final conc. 20 µM) for 5 h in darkness at room temperature in a thermo-mixer adjusted to 1400 rpm followed by 10 min incubation with ferrozine (final conc. 0.4 mM). The absorbance was determined at 562 nm and a linear regression curve calculated. Three replicates per dilution were included.

3.16 Ferric chelate reductase activity assay

Root ferric chelate reductase activity was determined based on a protocol adapted from (Waters *et al.*, 2006). Ten-d old plants were transferred to one-half strength MS medium supplemented with either freshly prepared 75 µM NaFeEDTA or 50 µM ferrozine buffered with 2.5 mM MES to pH 5.6. After 6 d, part of the root (~3 cm from the root tip) was cut and placed in 0.5 mL buffer solution containing 0.2 mM $CaSO_4$ (AppliChem), 5 mM MES pH 5.5, 0.2 mM ferrozine, and 0.1 mM NaFeEDTA. The reaction was allowed to continue for several hours or overnight in darkness. The color change caused by the formation of a purple Fe(II)-ferrozine complex was visually examined and used as indication for a functional FRO2. No plant controls were included as blanks and roots of *fro2* plants were used as negative control.

3.17 Gene expression analysis by qPCR

Roots were harvested from 14-d old plants grown vertically for 4 d on medium with 20 µM $FeCl_3$ buffered with either 2.5 mM MES to pH 5.6 and pH 6.5, 1 mM $NaHCO_3$ to pH 6.5, or 1.25 mM MOPS to pH 7.5. Roots of 12 individual plants were pooled and directly frozen in liquid nitrogen. The root tissue was homogenized with stainless steel balls (3.0-3.3 mm) on a vortexer while keeping the sample in a frozen state. Total RNA was extracted from the homogenized samples using the NucleoSpin RNA Mini Kit (Machery-Nagel) according to the manufacturer's instruction. The extracted RNA was finally eluted in 20 µL RNase free water supplied by the kit and quantified using a NanoDrop 2000c spectrophotometer (Thermo Fisher Scientific, Germany). cDNA was synthesized from 0.5-1 µg RNA by reverse transcription using the RevertAid First Strand cDNA synthesis Kit (Thermo Fisher Scientific) and oligo(dT) primer or the M-MuLV Reverse Transcriptase (New England Biolabs). A ten- or twenty-times diluted cDNA sample was then used for quantitative real-time (RT) PCR analysis with the CFX384 Touch Real-Time PCR Detection System (Bio-Rad Laboratories) and the iQ SYBR Green Supermix (Bio-Rad Laboratories) or GoTaq qPCR Master Mix (Promega) using the primers listed in Table 5. The samples were analyzed in two technical replicates using the following protocol: one activation cycle for 3 min at 95°C; 40 amplification cycles with 15 sec at 95°C followed by 30 sec 58/60°C (depending on the primer used); one melting curve cycle from 65°C to 95°C in 5 sec (0.5°C increment). Recorded C_t values were exported from the Bio-Rad CFX Manager Software (Version 3.1, Bio-Rad Laboratories) and used for the calculation of PCR amplification efficiency and normalization factors using *ACTIN2* (At3g18780) and *UBQ10* (At4g05320) as reference genes. The PCR amplification efficiency was calculated according to previous instructions (Bustin *et al.*, 2009). Only experiments with an efficiency between 90% to 110% were included. Normalization factors were calculated using geNORM (Vandesompele

et al., 2002). Gene expression levels were expressed as fold changes from either the wild-type or plants grown at pH 5.6 buffered with 2.5 mM MES using the following equation:

$$Fold\ change = \frac{\left(\frac{2^{-C_t GOI}}{NF}\right)_{target\ sample}}{\left(\frac{2^{-C_t GOI}}{NF}\right)_{reference\ sample}}$$

where NF is the calculated normalization factor, C_t is the cycle threshold, and GOI is the investigated gene of interest.

When *UBQ2* (At2g361070) was used as reference gene, recorded C_t values were used to calculate relative changes in gene expression based on the 2^(-Delta Delta C_t) method (Livak and Schmittgen, 2001).

Table 5. List of qPCR primers used in this study.

AGI ID	Primer name	Primer Sequence (5'→3')
At3g18780	ACTIN2_qPCR_F	GACCAGCTCTTCCATCGAGAA
At3g18780	ACTIN2_qPCR_R	CAAACGAGGGCTGGAACAAG
At5g36890	BGLU42_qPCR_F†	ATGGCCTGGGAACTGAAGTC
At5g36890	BGLU42_qPCR_R†	ATTTGTCCAACCTCCGATTG
At4g31940	CYP82C4_qPCR_F	TGTGGTTCAAGAATGGCGGT
At4g31940	CYP82C4_qPCR_R	TCCGACGATACTGAGCCTCC
At3g13610	F6H1_qPCR_F ‡	TGATATCTGCAGGAATGAAACG
At3g13610	F6H1_qPCR_R‡	GGGTAGTAGTTAAGGTTGACTC
At2g28160	FIT_qPCR_F‡	GCGGTATCAATCCTCCTGCT
At2g28160	FIT_qPCR_R‡	GATGGAGCACCTTCTCCT
At1g56160	MYB72_qPCR_F	AGTGGTCAAAGATCGCGTCC
At1g56160	MYB72_qPCR_R	TGTGCTTTGGTCATGAGTGC
At3g53480	PDR9_qPCR_F	ATCTACTCGGCTTGGCTTCG
At3g53480	PDR9_qPCR_R	CGGTGACTCCCACCAATGAA
At3g12900	S8H_qPCR _F	GGCACCAAATCCCTCCCAGA
At3g12900	S8H_qPCR_R	TTTTGCCGTCGTGTGGTTGG
At2g361070	UBQ2_qPCR_F	CCAAGATCCAGGACAAAGAAGGA
At2g361070	UBQ2_qPCR_F	TGGAGACGAGCATAACACTTGC
At4g05320	UBQ10_qPCR_F	CTTCGTCAAGACTTTGACCG
At4g05320	UBQ10_qPCR_R	CTTCTTAAGCATAACAGAGACGAG

†From (Zamioudis, Hanson and Pieterse, 2014)

‡From (Lešková *et al.*, 2017)

In order to approximate normal distribution and to correct for heteroscedasticity in the data sets, fold change values were $\log_2$ transformed prior to principal component analysis (PCA) and hierarchical cluster analysis. All analyses were performed in R (version 4.0.3). Cluster analysis of genes was conducted for the different Fe treatments and genotypes separately, respectively, using Ward's method (Ward.D2) and Euclidean distance.

3.18 Statistical analysis

Statistical analysis was performed using SigmaPlot 11.0 (Systat Software Inc.) and R (version 4.0.3). In R, normality and variance homogeneity were tested using the Shapiro-Wilk test and Levene's test, respectively. For multiple comparison analysis, one-way ANOVA with post hoc Tukey's test ($p \leq 0.05$) was performed. When any of the test assumptions could not be met, data were transformed. If data were still not normally distributed, the non-parametric Kruskal-Wallis (ANOVA on Ranks) test with post hoc Tukey's or Dunn's test ($p \leq 0.05$) was performed. For heteroscedastic data, Welch's *t*-test or Welch's ANOVA with post hoc Games-Howell test ($p \leq 0.05$) was applied. In R, the Benjamini-Hochberg method was used to adjust p-values for multiple comparisons. Data were tested for any outliers using the two-sided Grubbs' test with $p \leq 0.05$, when necessary. Correlation analysis was performed according to Pearson for normally distributed and homoscedastic data or Spearman if any of these assumptions were violated.

4 Results

4.1 Coumarin-mediated Fe mobilization and reduction is dependent on pH and buffer strength *in vitro*

In previous studies, coumarins were described to be important for Fe acquisition in Arabidopsis (Schmid *et al.*, 2014; Rajniak *et al.*, 2018; Tsai *et al.*, 2018). To get a comprehensive picture on how different root-borne coumarins assist plant growth under low Fe availability, their ability to mobilize and reduce Fe(III) at different pH and buffer conditions was first investigated *in vitro*. Therefore, single coumarins including scopoletin, esculetin, fraxetin, and freshly reduced sideretin (final concentration of 400 µM) were incubated with 100 µM Fe (supplied as $FeCl_3$) in solutions buffered with either 2.5 mM MES to pH 5.6 and pH 6.5, 1 mM $NaHCO_3$ to pH 6.5, or 1.25 mM MOPS to pH 7.5. Under these conditions, the supplied Fe was largely precipitated as Fe hydroxides. EDTA and ascorbic acid were included as positive controls for Fe(III) mobilization by chelation and reduction, respectively. The amount of total mobilized Fe and the proportion of reduced Fe (i.e., Fe(II)) was determined after 10 min, 30 min, 1 h, 3 h, 6 h, and 24 h. Fe(II) was assessed spectrophotometrically on the basis of the formation of complexes with the Fe(II) chelator ferrozine.

As expected, EDTA was able to mobilize but not to efficiently reduce Fe(III) under all tested conditions (Figs. 3-6). Independent of the pH and buffer conditions, the total amount of Fe mobilized by EDTA increased over time, but its maximum amount decreased with increasing pH (~94% at pH 5.6 and ~68% at pH 7.5). Ascorbic acid was less efficient than EDTA to mobilize Fe(III), especially at pH 7.5 or in the presence of $NaHCO_3$ (Figs. 3-6). However, ascorbic acid showed the expected strong Fe(III) reduction capacity, reducing 65% to 100% of the total mobilized Fe within 1 h at pH 5.6 and pH 6.5 (Figs. 3-5). However, with increasing time, the proportion of reduced Fe decreased below 35%. At high pH (pH 7.5), not only Fe(III) chelation but also Fe(III) reduction by ascorbic acid was strongly inhibited (Fig. 6).

Among the investigated coumarins, the catecholic coumarins esculetin, fraxetin, and sideretin were the most efficient in mobilizing Fe(III), while scopoletin mobilized only minor amounts of Fe and only at pH 5.6 (Figs. 3-6). Interestingly, Fe(III) mobilization and reduction by the catecholic coumarins was highly dependent on the pH and buffering conditions. Esculetin was able to quickly mobilize Fe(III) reaching maximum values already within 10 to 30 min under all conditions (Figs. 3-6). With increasing pH, the total amount of Fe mobilized by esculetin decreased, reaching ~70% at pH 7.5 compared to 91% at pH 5.6. However, Fe(III) reduction by esculetin was lower in comparison to fraxetin or sideretin, especially at pH 5.6 (Figs. 3-6). At pH 5.6, only 8-12% of the total Fe mobilized by esculetin was reduced (Fig. 3) while the proportion decreased below 8% at pH 6.5 buffered with MES (Fig. 4) and was negligible at pH 7.5 (Fig. 6).

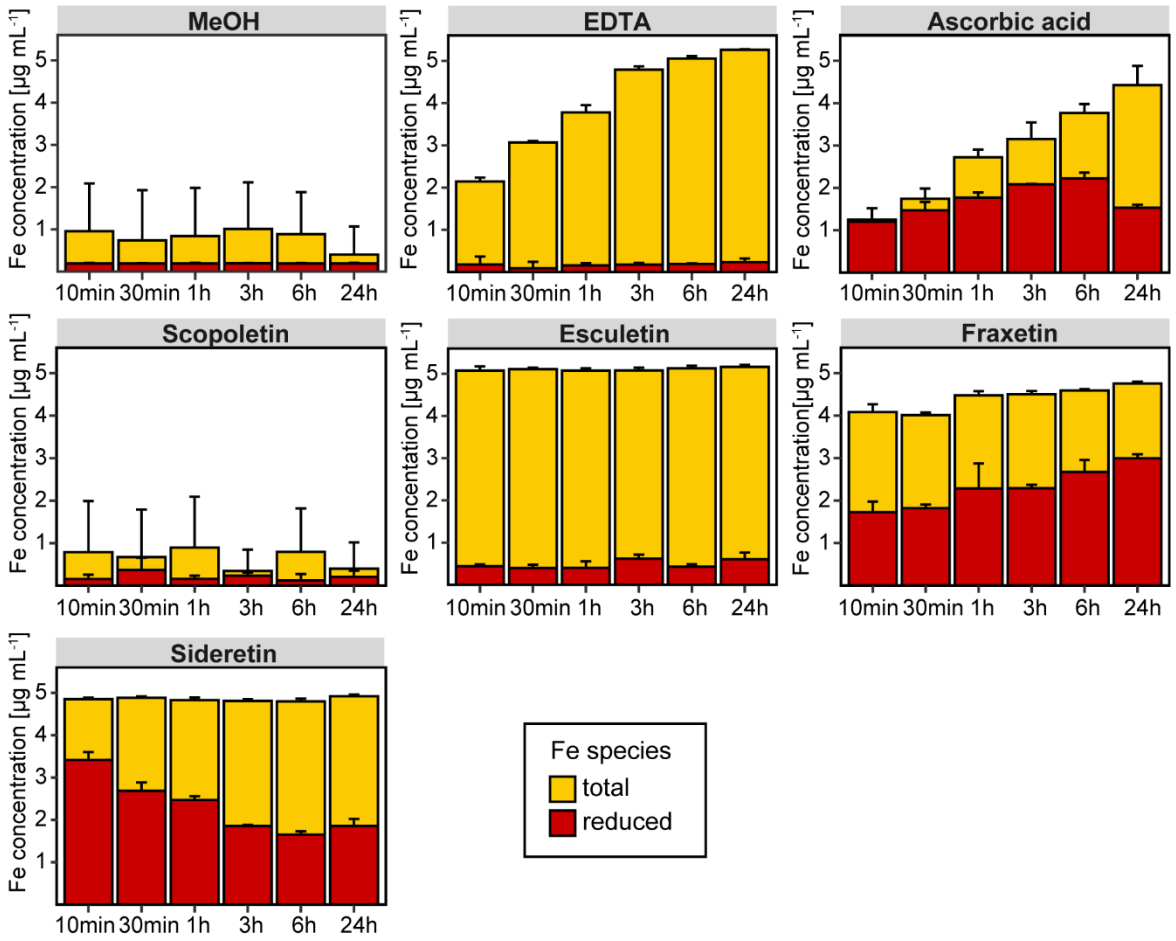

Fig. 3. Ability of different coumarins to mobilize and reduce Fe from freshly precipitated Fe hydroxide at pH 5.6. Time-dependent *in vitro* Fe(III) mobilization (yellow) and reduction (red) from Fe hydroxide precipitates by methanol (MeOH, mock), EDTA, ascorbic acid, scopoletin, esculetin, fraxetin, and sideretin at acidic pH. Compounds were incubated in darkness with 100 µM freshly precipitated Fe (supplied as $FeCl_3$) in 2.5 mM MES buffered to pH 5.6. Aliquots were taken 10 min, 30 min, 1 h, 3 h, 6 h, and 24 h after starting the reaction. The amount of total mobilized Fe was determined by ICP-MS and the amount of reduced Fe was assessed spectrophotometrically on the basis of the formation of Fe(II)-ferrozine complexes. The upper end of the y-axis represents the total amount of Fe used in the experiments. Bars represent means ± s.d. (n = 3 replicates).

Fraxetin was also able to mobilize Fe(III) under all tested conditions and the amount of mobilized Fe after 24 h of incubation decreased with increasing pH (Figs. 3-6). Compared to esculetin, Fe(III) mobilization by fraxetin was slightly slower irrespective of the pH and buffer conditions. Within 10 min, fraxetin mobilized from 44 to 73% of all precipitated Fe which increased by 10-22% within 24 h (Figs. 3-6). In contrast to esculetin, fraxetin exhibited stronger Fe(III) reduction capacity, especially at pH 5.6 and pH 6.5 buffered with $NaHCO_3$. Under these conditions, the proportion of mobilized Fe that was also reduced by fraxetin reached up to around 65% (Figs. 3 and 5). However, only 8% and 5% of the mobilized Fe was reduced by fraxetin after 24 h at pH 6.5 buffered with MES and at pH 7.5, respectively (Figs. 4 and 6).

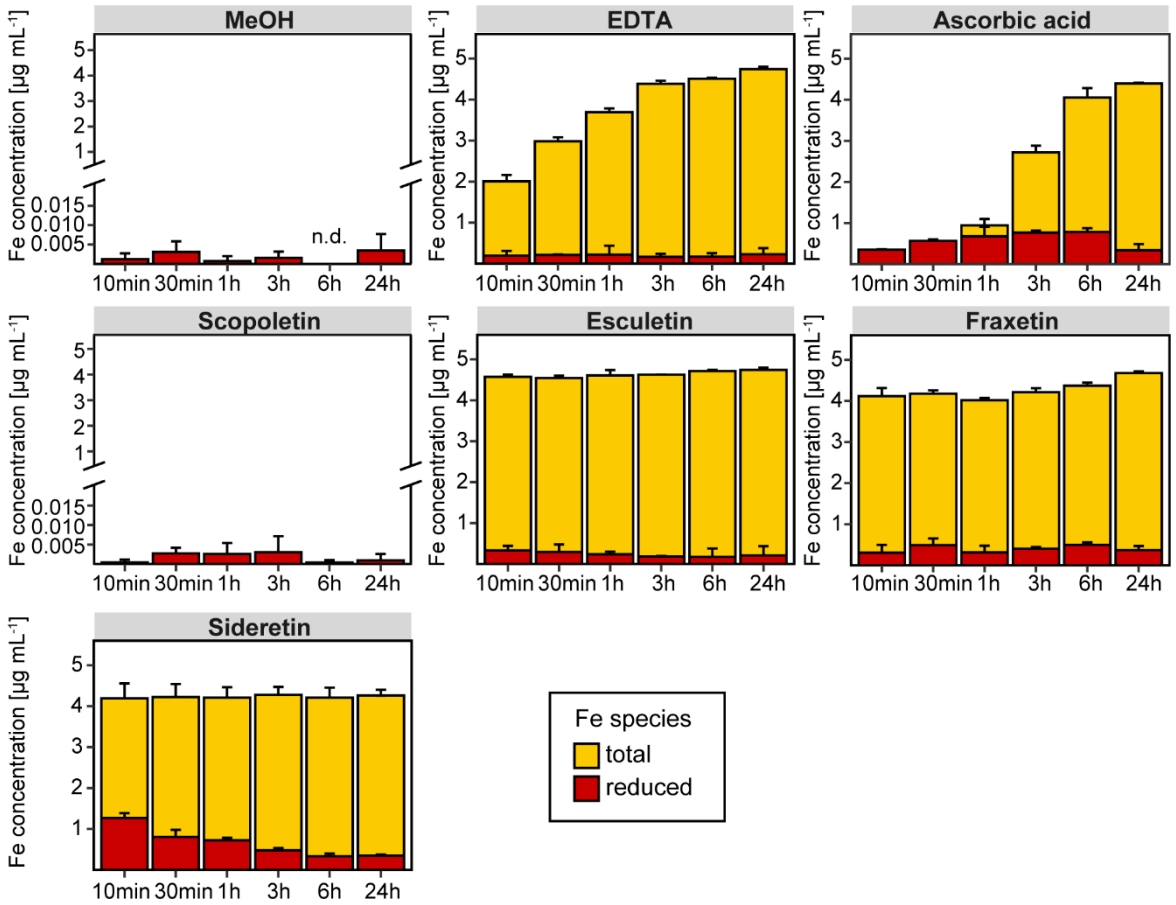

Fig. 4. Ability of different coumarins to mobilize and reduce Fe from freshly precipitated Fe hydroxide at pH 6.5. Time-dependent *in vitro* Fe(III) mobilization (yellow) and reduction (red) from Fe hydroxide precipitates by methanol (MeOH, mock), EDTA, ascorbic acid, scopoletin, esculetin, fraxetin, and sideretin at pH 6.5. Compounds were incubated in darkness with 100 µM freshly precipitated Fe (supplied as $FeCl_3$) in 2.5 mM MES buffered to pH 6.5. Aliquots were taken 10 min, 30 min, 1 h, 3 h, 6 h, and 24 h after starting the reaction. The amount of total mobilized Fe was determined by ICP-MS and the amount of reduced Fe was assessed spectrophotometrically on the basis of the formation of Fe(II)-ferrozine complexes. The upper end of the y-axis represents the total amount of Fe used in the experiments. Bars represent means ± s.d. (n = 3 replicates).

In MES-buffered solutions at pH 5.6 and pH 6.5, sideretin showed fast Fe(III) mobilization, similar to esculetin, mobilizing up to 88% and 76% of the available Fe, respectively (Figs. 3 and 4). Under these conditions, sideretin also showed a strong ability to reduce Fe(III) especially at pH 5.6 and pH 6.5 in presence of $NaHCO_3$ (Figs. 3 and 5). When $NaHCO_3$ was used as buffer, the amount of Fe(III) mobilized by sideretin increased over time from 38% to around 75% of the total amount of present Fe, while the amount of reduced Fe remained nearly constant. At pH 6.5 buffered with MES, sideretin was able to reduce more Fe than the other coumarins, but the amount decreased over time (Fig. 4). In contrast to esculetin and fraxetin, Fe(III) mobilization by sideretin was strongly inhibited at pH 7.5, as only around 9% of the total amount of the present Fe in the solution was mobilized after 24 h (Figs. 3-6). Over time, the amount of reduced Fe in sideretin-containing solutions decreased also at pH 5.6 (Fig. 3), suggesting that putatively formed Fe(II) sideretin complexes possess only low stability. Consequently, after 24 h, the amount of reduced Fe present at pH 5.6 was 38% lower in solution containing sideretin compared to those with fraxetin.

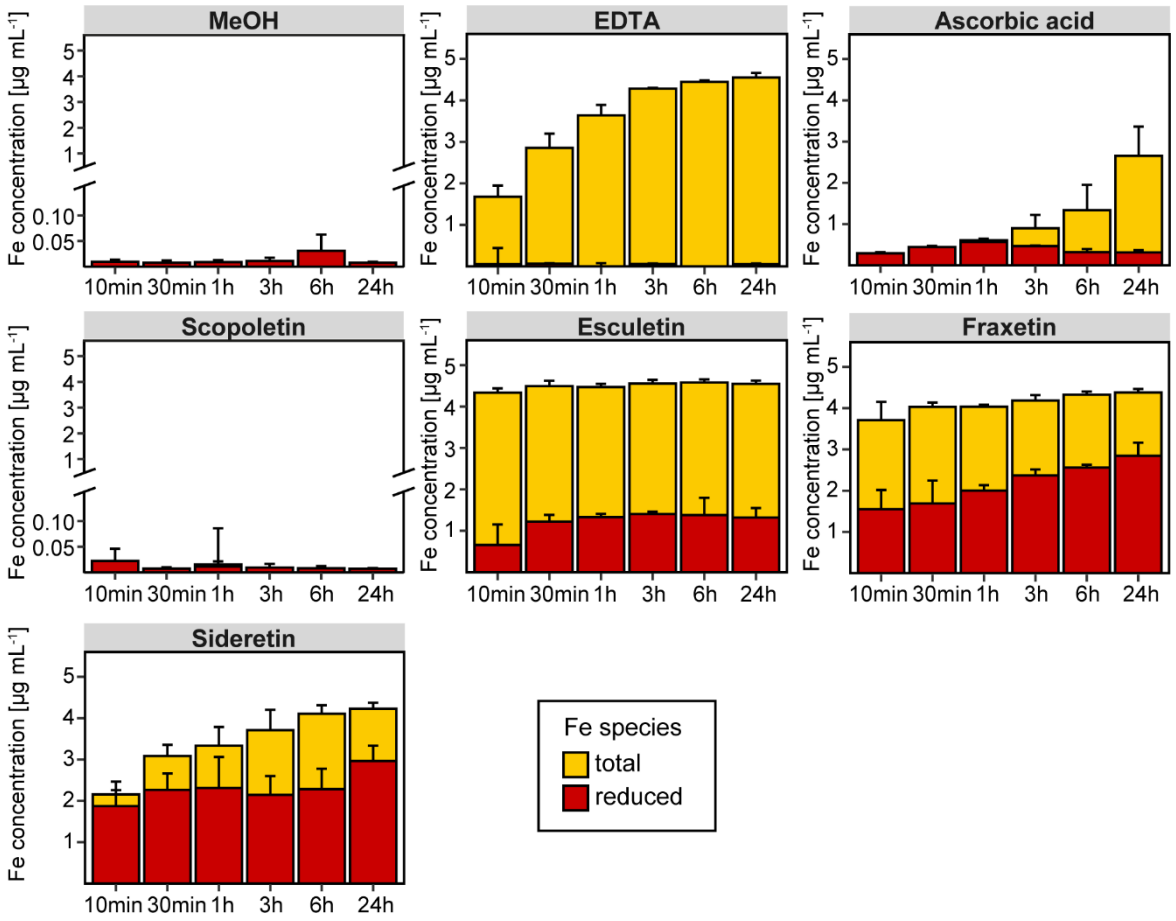

Fig. 5. Ability of different coumarins to mobilize and reduce Fe from freshly precipitated Fe hydroxide at pH 6.5 in the presence of $NaHCO_3$. Time-dependent *in vitro* Fe(III) mobilization (yellow) and reduction (red) from Fe hydroxide precipitates by methanol (MeOH, mock), EDTA, ascorbic acid, scopoletin, esculetin, fraxetin, and sideretin at pH 6.5. Compounds were incubated in darkness with 100 µM freshly precipitated Fe (supplied as $FeCl_3$) in 1 mM $NaHCO_3$. Aliquots were taken 10 min, 30 min, 1 h, 3 h, 6 h, and 24 h after starting the reaction. The amount of total mobilized Fe was determined by ICP-MS and the amount of reduced Fe was assessed spectrophotometrically on the basis of the formation of Fe(II)-ferrozine complexes. The upper end of the y-axis represents the total amount of Fe used in the experiments. Bars represent means ± s.d. (n = 3 replicates).

Besides pH, the observed differences in Fe(III) mobilization and reduction at pH 6.5 buffered with MES or $NaHCO_3$ also indicated an additional effect of the buffer itself. To test this possibility, the ability of fraxetin to mobilize and reduce Fe(III) was determined at pH 6.5 and pH 7.5 in the presence of 0.5 mM, 1 mM, and 2 mM $NaHCO_3$ as described above.

Fe(III) mobilization and reduction by fraxetin at pH 6.5 and 1 mM $NaHCO_3$ were comparable to the results from the first experiment (Figs. 5 and 7), reinforcing the overall reproducibility of the assay. In general, the amounts of Fe(III) mobilized by fraxetin were lower at pH 7.5 in comparison to pH 6.5 (Fig. 7). However, the amount of mobilized Fe(III) over time was comparable between the different $NaHCO_3$ concentrations within pH 6.5 and pH 7.5, respectively. In contrast, the $NaHCO_3$ concentration had a strong effect on the ability of fraxetin to reduce Fe(III). In the presence of 0.5 mM $NaHCO_3$, fraxetin could reduce >86% of the mobilized Fe after 24 h both at pH 6.5 and pH 7.5 whereas at 2 mM $NaHCO_3$ not more than 8% of the mobilized Fe was reduced (Fig. 7). At an intermediate concentration of 1 mM

$NaHCO_3$, around 58% of the total mobilized Fe was reduced to Fe(II) at pH 6.5, while the corresponding value was < 9% at pH 7.5.

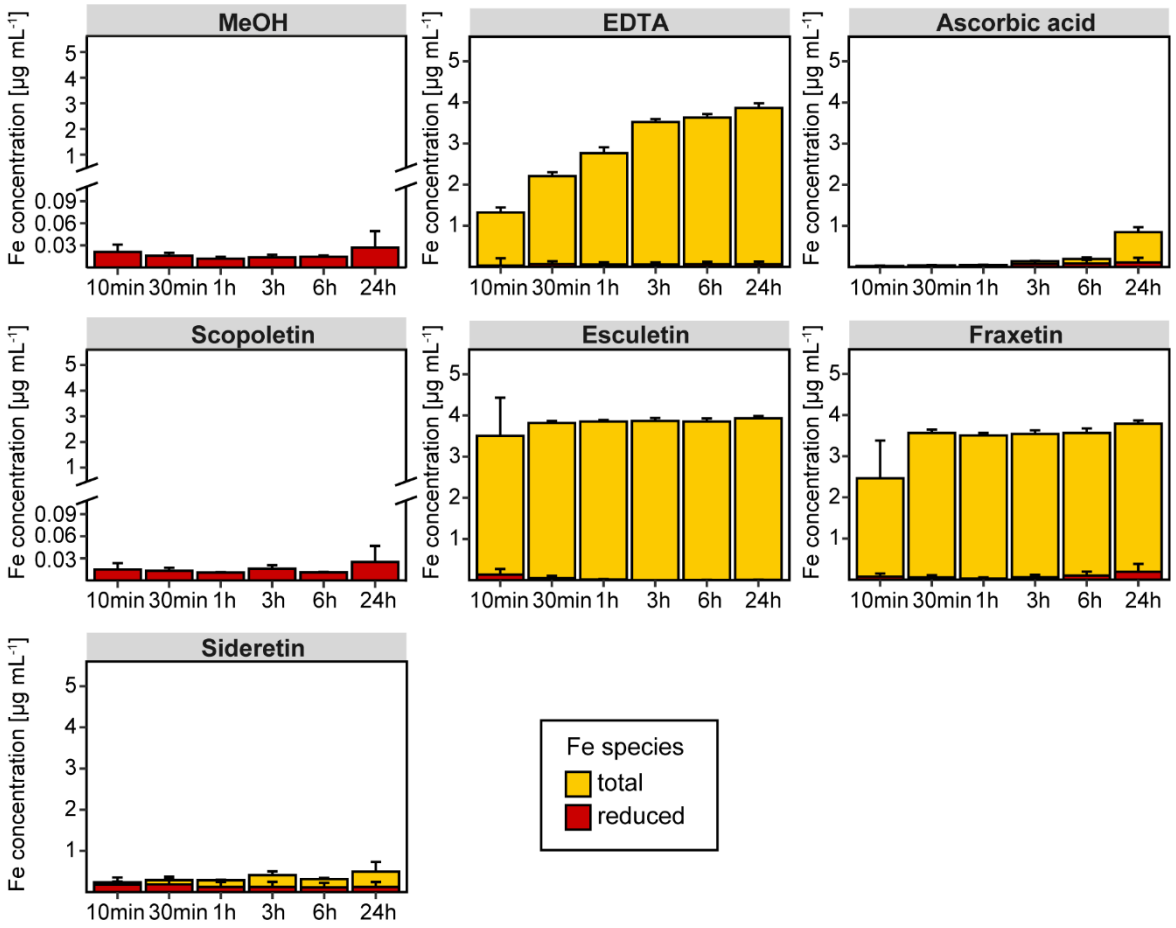

Fig. 6. Ability of different coumarins to mobilize and reduce Fe from freshly precipitated Fe hydroxide at pH 7.5. Time-dependent *in vitro* Fe(III) mobilization (yellow) and reduction (red) from Fe hydroxide precipitates by methanol (MeOH, mock), EDTA, ascorbic acid, scopoletin, esculetin, fraxetin, and sideretin at pH 7.5. Compounds were incubated in darkness with 100 µM freshly precipitated Fe (supplied as $FeCl_3$) in 1.25 mM MOPS buffered to pH 7.5. Aliquots were taken 10 min, 30 min, 1 h, 3 h, 6 h, and 24 h after starting the reaction. The amount of total mobilized Fe was determined by ICP-MS and the amount of reduced Fe was assessed spectrophotometrically on the basis of the formation of Fe(II)-ferrozine complexes. The upper end of the y-axis represents the total amount of Fe used in the experiments. Bars represent means ± s.d. (n = 3 replicates).

Altogether, these results indicate that both Fe(III) mobilization and reduction by coumarins strongly depend on their chemical properties as well as the pH value and buffering strength of the solution. Among the main coumarins described for Arabidopsis, only the catecholate coumarins esculetin, fraxetin, and sideretin can mobilize Fe(III) and only fraxetin and sideretin are also able to reduce considerable amounts of Fe(III) especially at acidic pH (pH 5.6).

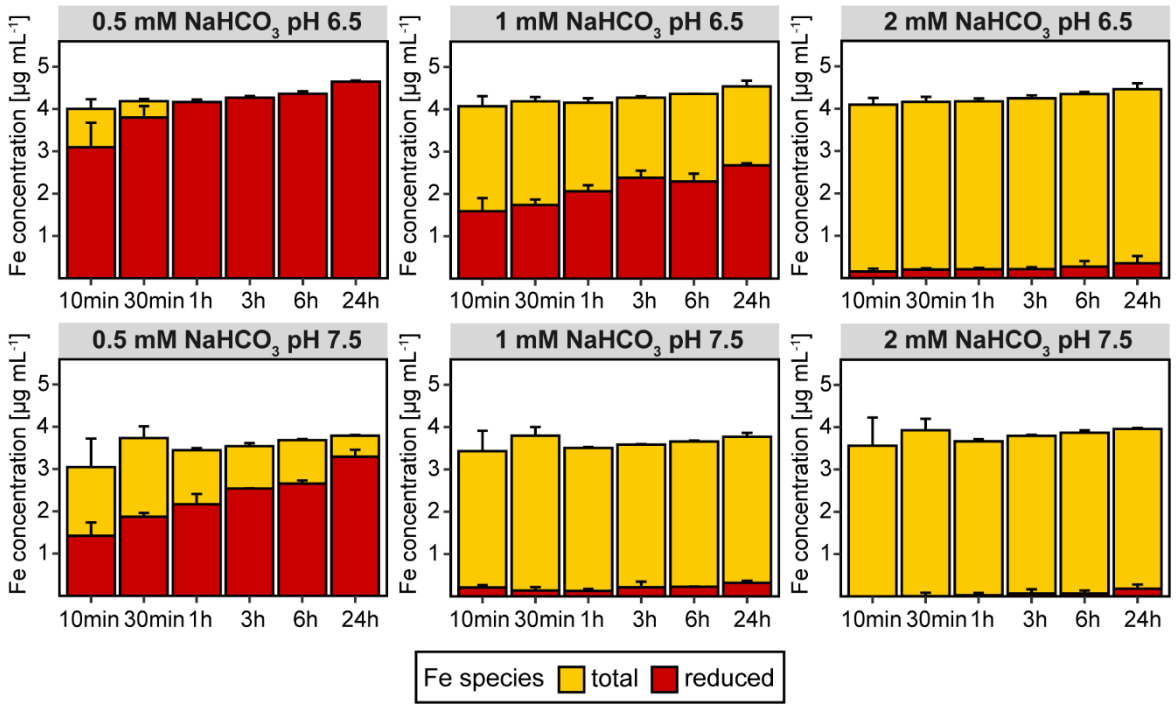

Fig. 7. The effect of buffer strength on fraxetin-mediated Fe mobilization and reduction. Time-dependent *in vitro* Fe(III) mobilization (yellow) and reduction (red) from Fe hydroxide precipitates by fraxetin at different pH and $NaHCO_3$ concentrations. Fraxetin was incubated with 100 µM $FeCl_3$ in 0.5 mM, 1 mM, or 2 mM $NaHCO_3$ buffered to pH 6.5 or pH 7.5. Aliquots were taken after 10 min, 30 min, 1 h, 3 h, 6 h, and 24 h. The amount of total mobilized Fe was determined by ICP-MS and the amount of reduced Fe was assessed spectrophotometrically on the basis of the formation of Fe(II)-ferrozine complexes. The upper end of the y-axis represents the total amount of Fe used in the experiments. Bars represent means ± s.d. (n = 3 replicates).

4.2 Role of fraxetin and sideretin in reduction-mediated Fe acquisition

Given the results gained from the *in vitro* Fe(III)-mobilization and reduction assays, the question was raised whether coumarin-mediated Fe(III) reduction can circumvent the enzymatic Fe(III) reduction via FRO2, at least under certain external pH conditions. To address this question, an agar plate system simulating different conditions of low Fe availability was first set up. Therefore, 10-day-old seedlings of *fro2* and its corresponding wild-type Columbia-*glabra 1* (Col-*gl1*) were pre-cultured on 40 µM FeEDTA and then transferred to one-half strength MS medium with 20 µM $FeCl_3$ buffered with either 2.5 mM MES to pH 5.6 and pH 6.5, 1 mM $NaHCO_3$ to pH 6.5, or 1.25 mM MOPS to pH 7.5. When grown under such conditions, *fro2* plants showed symptoms of Fe-deficiency already at acidic pH (pH 5.6) as indicated by significantly lower chlorophyll and shoot Fe concentrations, and decreased shoot biomass in comparison to the wild type (Fig. 8). This indicates that under this external pH, FRO2-dependent Fe(III) reduction is critical for sufficient acquisition of Fe from sparingly available sources. When the pH was increased, wild-type plants were also affected by Fe-deficiency and significant differences to *fro2* were not observed anymore (Fig. 8).

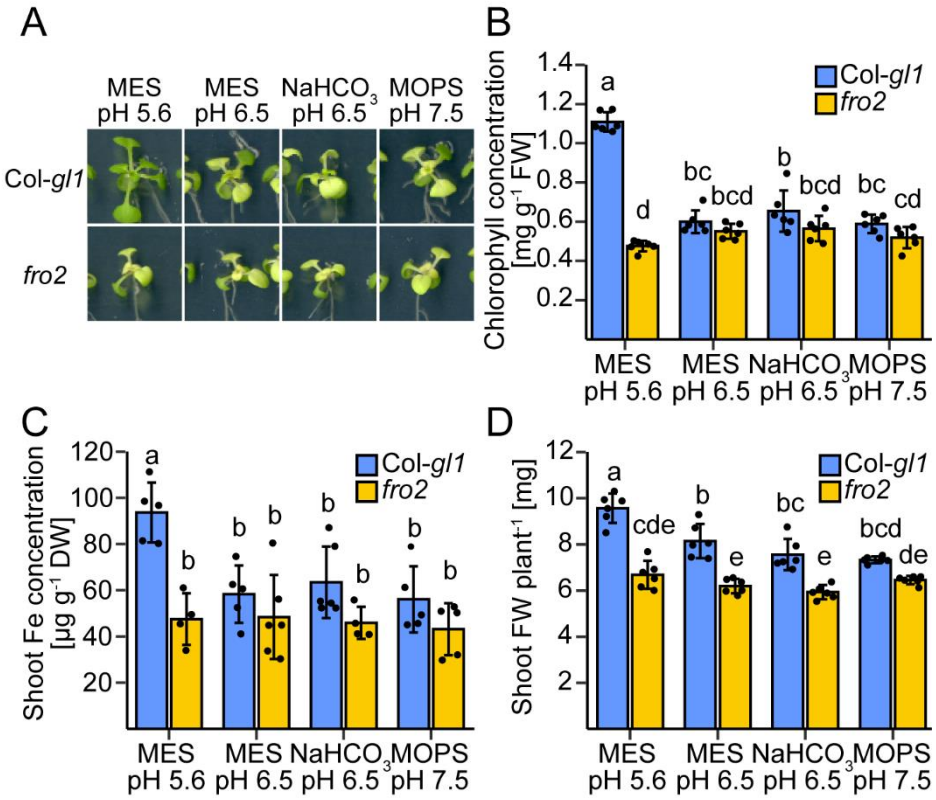

Fig. 8. FRO2 is essential for Fe acquisition at acidic pH. (A-D) Appearance (A), leaf chlorophyll concentration (B), shoot Fe concentration (C), and shoot fresh weight (FW) (D) of wild-type (Col-*gl1*) and *fro2* plants grown for 6 d on different Fe-limiting conditions on agar. Plants were pre-cultured on one-half strength MS medium with 40 µM NaFeEDTA (pH 5.6) for 10 d and then transferred to one-half strength MS medium with 20 µM $FeCl_3$ buffered with either MES to pH 5.6 or pH 6.5, $NaHCO_3$ to pH 6.5, or MOPS to pH 7.5. Bars represent means ± s.d. (n = 4-6 biological replicates). Different letters indicate significant differences according to one-way ANOVA with post-hoc Tukey's test at $p \leq 0.05$.

In the next step, the same growth conditions were used to conduct coumarin re-supply experiments to investigate the ability of different coumarins to recover Fe-deficiency in wild-type and *fro2* plants. Initially, different concentrations of scopoletin, esculetin, and fraxetin were tested to determine the amounts that could be used without causing significant inhibitory effects on plant growth. Due to the limited availability of sideretin, which needs to be synthesized on-demand, this coumarin was not included here. Seedlings pre-cultured with sufficient Fe were transferred to fresh media simulating different conditions of Fe availability as described above and supplemented with either 50 µM, 100 µM, 250 µM, or 500 µM esculetin, fraxetin, or scopoletin, respectively.

Inhibitory effects on the plant growth were observed for scopoletin concentrations ≥100 µM as well as for esculetin and fraxetin concentrations ≥250 µM under certain conditions, while no inhibitory effect was observed for any of the investigated coumarins when supplied at a final concentration of 50 µM (Annex Figs. 1-3). Hence, a coumarin concentration of 50 µM was chosen for further experiments.

In these new experiments, freshly reduced sideretin was also included. Since sideretin was found to be apparently instable at high pH (Rajniak *et al.*, 2018) and solubility in water is

attained only when the pH is increased, in these experiments all coumarins were dissolved in methanol. In a previous study with the coumarin biosynthesis mutants *f6'h1-1* and *s8h*, the external supply of 150 µM sideretin was shown to alleviate Fe deficiency in such plants (Rajniak *et al.*, 2018). In an initial test experiment using the *f6'h1-1* mutant grown under Fe-limiting conditions it was found that the external supply of 100 or 150 µM sideretin could alleviate Fe deficiency to a similar extent, while such effects were less pronounced when only 50 µM sideretin were supplied (data not shown). Hence, given these results and due to its limited availability, sideretin was supplied at a final concentration of 100 µM in all further experiments. Since sideretin was shown to be highly light sensitive (Rajniak *et al.*, 2018), plant roots were shielded from light in these experiments.

As expected from its very low Fe mobilization capacity, scopoletin was not able to prevent Fe deficiency in both wild-type and *fro2* plants independent of the pH conditions (Fig. 9A-F). Although scopoletin was able to significantly increase the chlorophyll levels in wild-type plants at high pH (Fig. 9F), the chlorophyll concentration was still below that of wild-type plants grown under Fe-sufficient conditions at pH 5.6 (Fig. 9B) and young leaves were chlorotic (Fig. 9E). Esculetin, in turn, could alleviate Fe deficiency only in wild-type plants but not in *fro2* plants under the different Fe-limiting conditions (Fig. 9A-F), which was in accordance with its strong ability to mobilize Fe(III) from freshly precipitated Fe-hydroxides *in vitro* (Figs. 3-6). However, esculetin was able to regreen wild-type plants only at pH 6.5 (Fig. 9C).

In contrast to scopoletin and esculetin, supplementation of fraxetin could rescue *fro2* plants from Fe deficiency at pH 5.6 and pH 6.5 and wild-type plants at pH 6.5 (Fig. 9A-D). Under such conditions, the chlorophyll levels in wild-type and *fro2* plants were indistinguishable (Fig. 9B and D). However, although supplementation of fraxetin was still able to significantly increase the chlorophyll concentration of wild-type plants, at alkaline conditions it failed to prevent Fe deficiency in wild-type and *fro2* plants (Fig. 9E and F).

Similar to fraxetin, sideretin was able to significantly alleviate Fe deficiency in *fro2* plants at pH 5.6 although the chlorophyll concentrations still remained below that of wild-type plants (Fig. 9G and H). At pH 6.5, supplementation of sideretin restored Fe deficiency in wild-type plants and increased the chlorophyll concentration in *fro2* plants (Fig. 9I and J). However, *fro2* plants still suffered from Fe deficiency as their young leaves appeared chlorotic (Fig. 9I).

In general, similar results were obtained for scopoletin, esculetin, and fraxetin when dissolved in mQ-water instead of methanol (Annex Fig. 3 and 4). Importantly, prevention of Fe deficiency in *fro2* and wild-type plants by fraxetin supplementation at pH 5.6 and pH 6.5 was also accompanied by significant increases in shoot Fe levels (Annex Fig. 4), demonstrating that the increased chlorophyll levels were indeed associated with enhanced Fe accumulation in shoots.

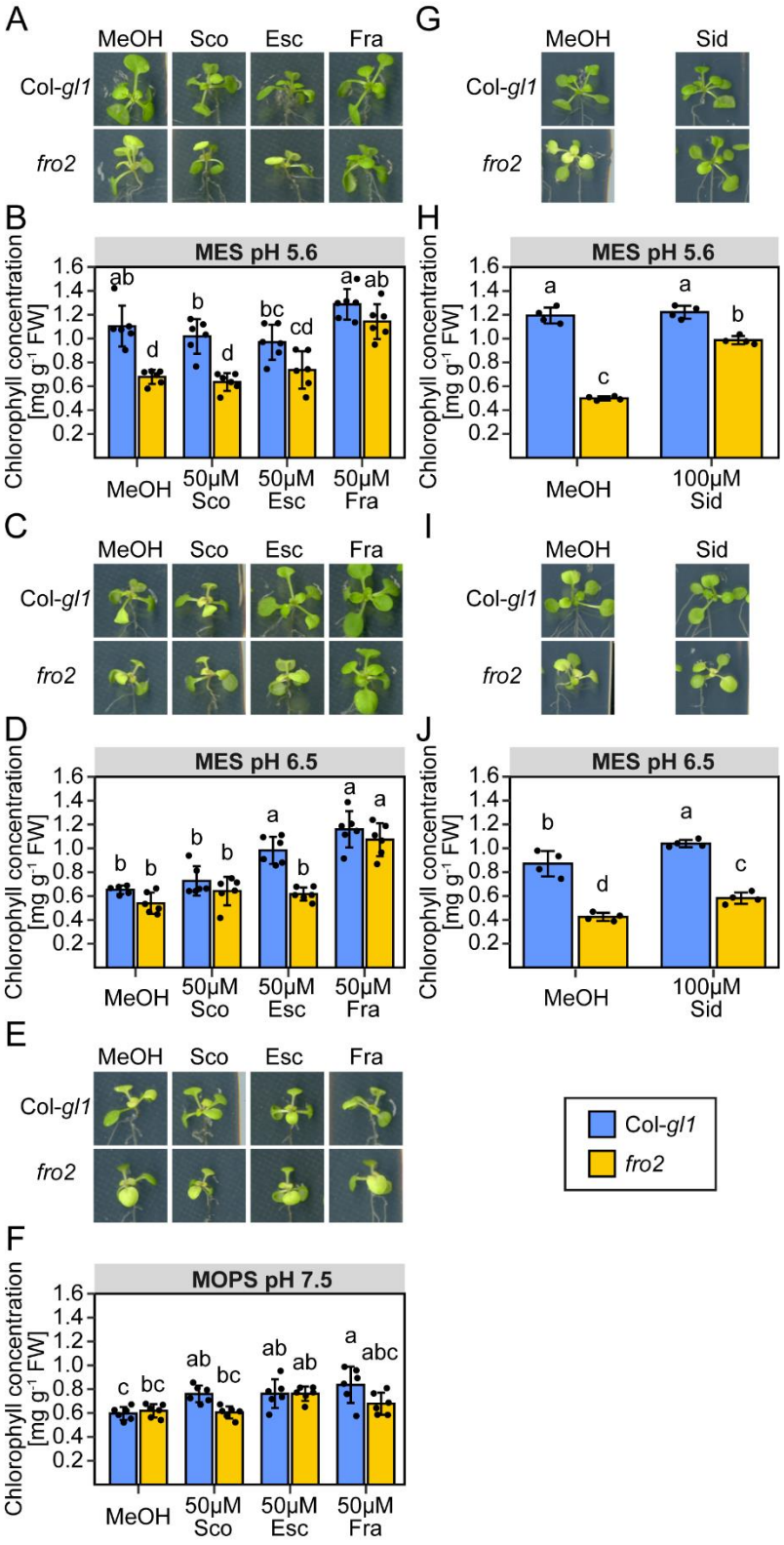

Fig. 9. Effect of coumarin-type siderophores on growth of wild-type and *fro2* plants at different pH. (A-J) Plant appearance (A, C, E, G, I) and leaf chlorophyll concentration (B, D, F, H, J) of wild-type (Col-*gl1*) and *fro2* plants grown for 6 d under different conditions of low Fe availability with or without esculetin, fraxetin, scopoletin, or sideretin. Ten-d-old seedlings pre-cultured one-half strength MS medium with 40 µM Fe-EDTA (pH 5.6) were transferred to one-half strength MS medium with 20µM $FeCl_3$ buffered with either MES to pH 5.6 or pH 6.5, or with MOPS to pH 7.5. The medium was supplemented with either methanol (MeOH, mock), 50 µM esculetin, 50 µM fraxetin, 50 µM scopoletin, or 100 µM sideretin. Bars represent means ± s.d. (n = 4-6 biological replicates). Different letters indicate significant differences according to one-way ANOVA with post-hoc Tukey's test at $p \leq 0.05$.

Taken together, among the deglycosylated coumarins released by Arabidopsis roots, only fraxetin and sideretin were able to restore Fe deficiency in wild-type and/or *fro2* plants. This, however, was strongly dependent on the external pH. Consistent with the *in vitro* Fe-mobilization assays, these results indicate that fraxetin and sideretin can mobilize and reduce Fe(III) at acidic pH and thereby provide sufficient Fe for plants, also if enzymatic Fe(III) reduction via FRO2 is inhibited. This also holds true for fraxetin at pH 6.5, while at this pH sideretin can mobilize but not reduce sufficient Fe(III) to efficiently by-pass FRO2 activity. At slightly alkaline pH, Fe(III) mobilization and reduction by fraxetin and sideretin is limited or absent as their supplementation could not alleviate Fe deficiency symptoms even in wild-type plants.

4.3 Supplementation of fraxetin cannot restore Fe deficiency in *irt1-1* plants

During Fe(III) mobilization by chelation and/or reduction, coumarins are thought to form Fe(II) or Fe(III)-coumarin complexes (Marschner, Römheld and Kissel, 1986; Mladěnka *et al.*, 2010; Schmidt *et al.*, 2014). Hence, a direct uptake of Fe(II)- or Fe(III)-coumarin complexes via a so far unknown transporter into the plant root can be reasoned to explain the supportive effect of fraxetin and sideretin on the growth of wild-type and *fro2* plants under conditions of low Fe availability at pH 5.6 and pH 6.5. In order to test this hypothesis, the ability of fraxetin to mitigate Fe-deficiency in *irt1-1* plants was tested. Under both pH 5.6 and pH 6.5, *irt1-1* plants exhibited severe Fe-deficiency symptoms and no significant differences in the visual appearance and chlorophyll concentrations were observed when this mutant was supplied with fraxetin (Fig. 10). This result indicates that fraxetin is unable to compensate for lacking Fe^{2+} transport activity.

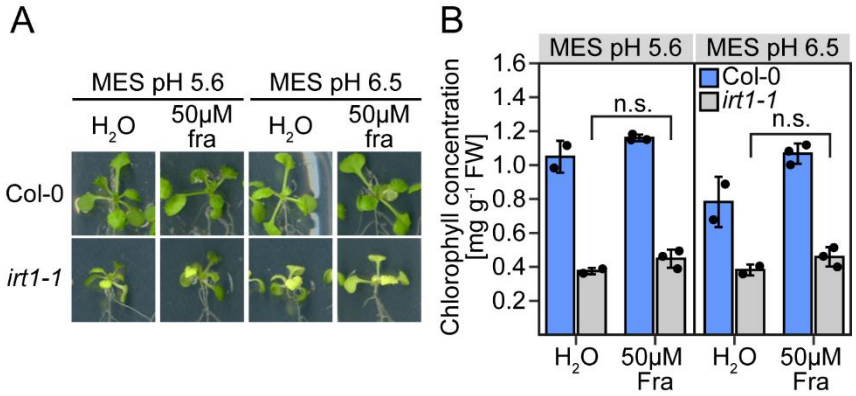

Fig. 10. Supplementation of fraxetin cannot restore Fe deficiency in *irt1-1* plants. (A and B) Plant appearance (A) and leaf chlorophyll concentration (B) of wild-type (Col-0) and *irt1-1* grown for 6 d under conditions of low Fe availability at pH 5.6 and pH 6.5 with and without fraxetin. Wild-type and *irt1-1* plants were pre-cultured one-half strength MS medium with 40 µM Fe-EDTA (pH 5.6) for 10 d and then transferred to one-half strength MS with 20 µM $FeCl_3$ buffered with MES to pH 5.6 or 6.5. The medium was supplemented with mQ-H_2O (mock) or 50 µM fraxetin. Bars represent means ± s.d. (n = 2-3 biological replicates). Student's t-test with $p \leq 0.05$ was used to test for significant differences.

4.4 Coumarin composition in root exudates and extracts of the *fro2* mutant under Fe-deficient conditions

Ferric-chelate reductase activity is essential for Fe acquisition in non-graminaceous plants (Robinson *et al.*, 1999; Connolly *et al.*, 2003). However, *fro2* plants grow better and show less severe symptoms of Fe deficiency than *irt1-1* plants (Vert *et al.*, 2002; Rajniak *et al.*, 2018). Given this fact and the strong ability of fraxetin and sideretin to facilitate Fe(III) reduction as indicated in the previous two sections, it was assessed whether the coumarin composition of root exudates and root extracts is changed in the absence of a functional FRO2. To obtain comparable levels of Fe deficiency at pH 5.6 or pH 6.5, plants were cultivated without added Fe. Under these conditions, *fro2* plants had significantly less chlorophyll at pH 5.6 and pH 6.5 (Fig. 11A and B), while significant differences in the shoot Fe concentration were only detected at pH 5.6 (Fig. 11C).

As expected, the individual coumarins were found mainly in their glycosylated form in root extracts of both genotypes (Fig. 11D, E, and F). Although both wild type and *fro2* were cultivated in the absence of Fe, the concentration of all investigated coumarins was higher in root extracts of *fro2* plants compared to the wild type at pH 5.6 (Fig. 11D and F), whereas at pH 6.5 only the concentration of fraxin, scopoletin, and fraxetin was significantly higher in *fro2* roots (Fig. 11E). In addition, a shift from scopolin/scopoletin toward fraxin/fraxetin synthesis was observed when the external pH was increased from pH 5.6 to pH 6.5, which is in agreement with previous reports (Sisó-Terraza *et al.*, 2016; Rajniak *et al.*, 2018). At pH 6.5, fraxetin exudation rate was 5.1-fold higher in *fro2* and 10.2-fold higher in wild-type plants compared to pH 5.6 (Fig. 11G and H). Sideretin levels increased by ~2.7-fold at pH 6.5 but only in wild-type plants (Fig. 11E). In root exudates, only scopolin and small traces of fraxin were detected indicating that roots remained intact during the sampling period (Fig. 11G, H and I). The exudation rate of deglycosylated coumarins was higher in *fro2* plants than in wild-type plants (Fig. 11I). However, whereas the exudation of scopoletin and fraxetin was significantly higher in *fro2* plants under both pH conditions, *fro2* plants released less sideretin at pH 6.5 than the wild type (Fig. 11H), suggesting that fraxetin is favored over sideretin in the absence of a functional FRO2.

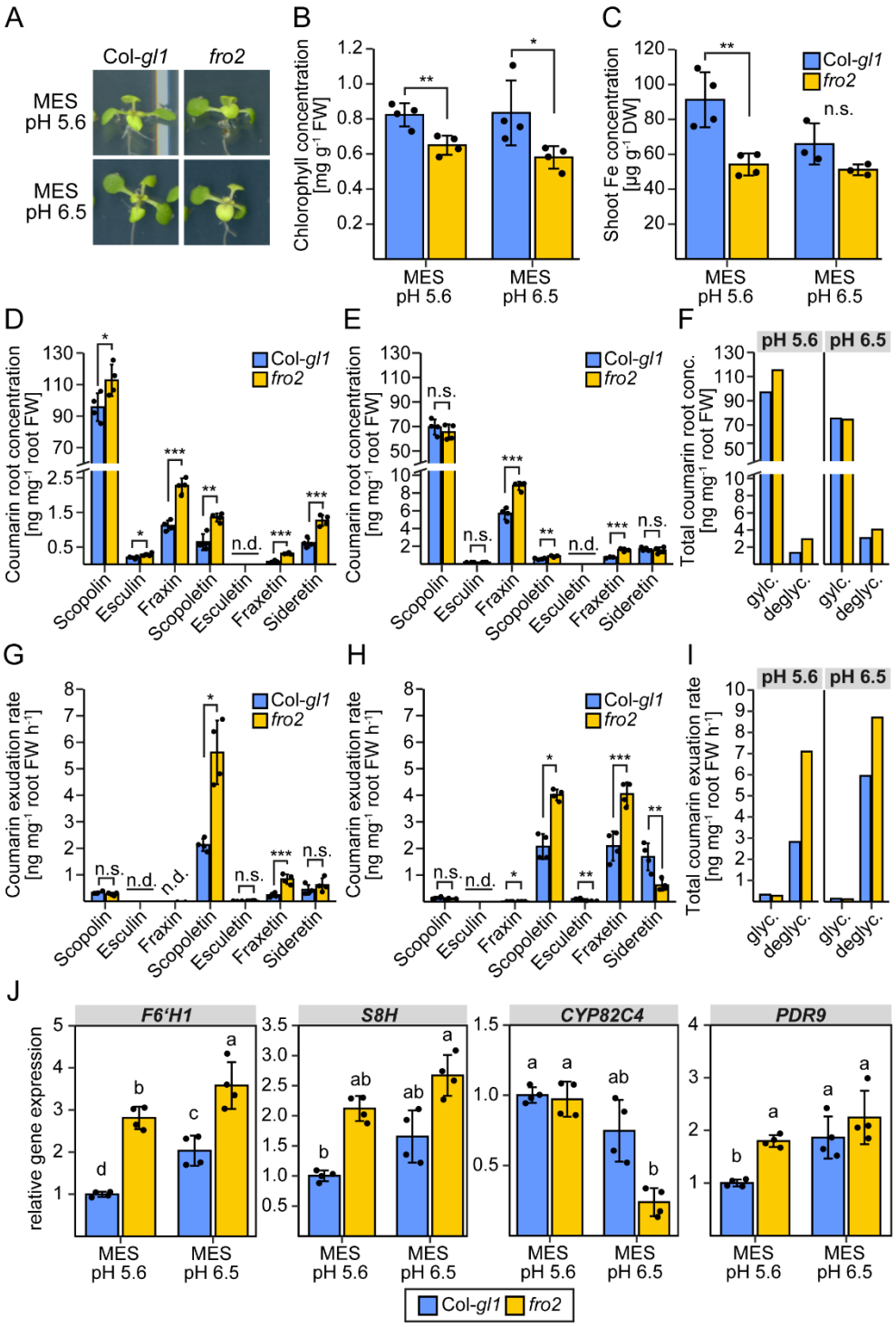

Fig. 11. Root coumarin levels and coumarin exudation rates in wild-type (Col-*gl1*) and *fro2* plants in dependence of the pH. (A-C) Visual appearance (A), leaf chlorophyll concentrations (B), and shoot Fe concentrations (C) of wild-type and *fro2* plants pre-cultured on one-half MS medium with 40 µM Fe-EDTA (pH 5.6) for 10 d and then transferred to one-half MS medium without added Fe (+15 µM ferrozine) buffered with MES to pH 5.6 or pH 6.5 for 4 d. (D-I) Levels of coumarins in root extracts (D and E) and coumarin exudation rate (G and H) at pH 5.6 (D and G) and pH 6.5 (E and H) as determined by UPLC-MS (Orbitrap). Total coumarin concentration in roots (F) and total coumarin exudation rate (I) as sum of glycosylated (glyc; scopolin, esculin, fraxin) and deglycosylated (deglyc.; scopoletin, esculetin, fraxetin, sideretin) coumarins. Root exudates were collected for 6 h in water adjusted to the respective pH and buffered with 2.5 mM MES. (J) Relative gene expression in WT and *fro2* plants grown for 4 d under Fe-limiting conditions at pH 5.6 and pH 6.5. Bars represent means ± s.d. (n = 4 biological replicates). Significant differences are indicated as asterisks according to Student's *t*-test with α=0.05; * $p \leq 0.05$, ** $p \leq 0.01$, *** $p \leq 0.001$. Different letter indicates significant differences according to one-way ANOVA or ANOVA on ranks with post-hoc Tukey's test at $p \leq 0.05$.

Gene expression analysis of the main coumarin biosynthesis genes including *F6'H1*, *S8H*, and *CYP82C4* as well as the root coumarin exporter *PDR9* supported those findings (Fig. 11J). At pH 5.6 and pH 6.5, the expression of *F6'H1* was higher in roots of the *fro2* mutant compared to wild type, while the expression of *S8H* was slightly but not significantly increased. In contrast, the expression of *CYP82C4* was significantly repressed in *fro2* specifically at pH 6.5. The expression of *PDR9*, in turn, was only significantly increased in *fro2* compared to wild type at pH 5.6.

Altogether, these findings suggest that the presence of a functional FRO2 influences not only the amounts but also the composition of coumarins in roots and root exudates of Fe-deficient plants. Furthermore, these results indicate that loss of FRO2 inhibits the release of sideretin at elevated pH conditions while stimulating fraxetin exudation.

4.5 FRO2 and F6'H1-dependent coumarin synthesis play additive functions in Fe acquisition

To further investigate the interplay between FRO2 and coumarins in Fe(III) reduction, a double mutant lacking both a functional FRO2 and F6'H1-dependent coumarin biosynthesis was generated.

Segregating Fe plants were first screened using a ferric-chelate reductase (FCR) assay as indication for the absence of a functional *FRO2* and then tested for T-DNA insertion in the *F6'H1* gene (Fig. 12A-C). Furthermore, the lack of coumarin-derived root fluorescence was used as evidence for an absent coumarin biosynthesis (Fig. 12D). The presence of the *FRO2* mutation (single nucleotide polymorphism G→A) was finally verified by sequencing (Fig. 12E). Homozygous wild type, *fro2*, *f6'h1-1*, and *fro2 f6'h1-1* identified from the F2 population were then transferred to soil for seed propagation.

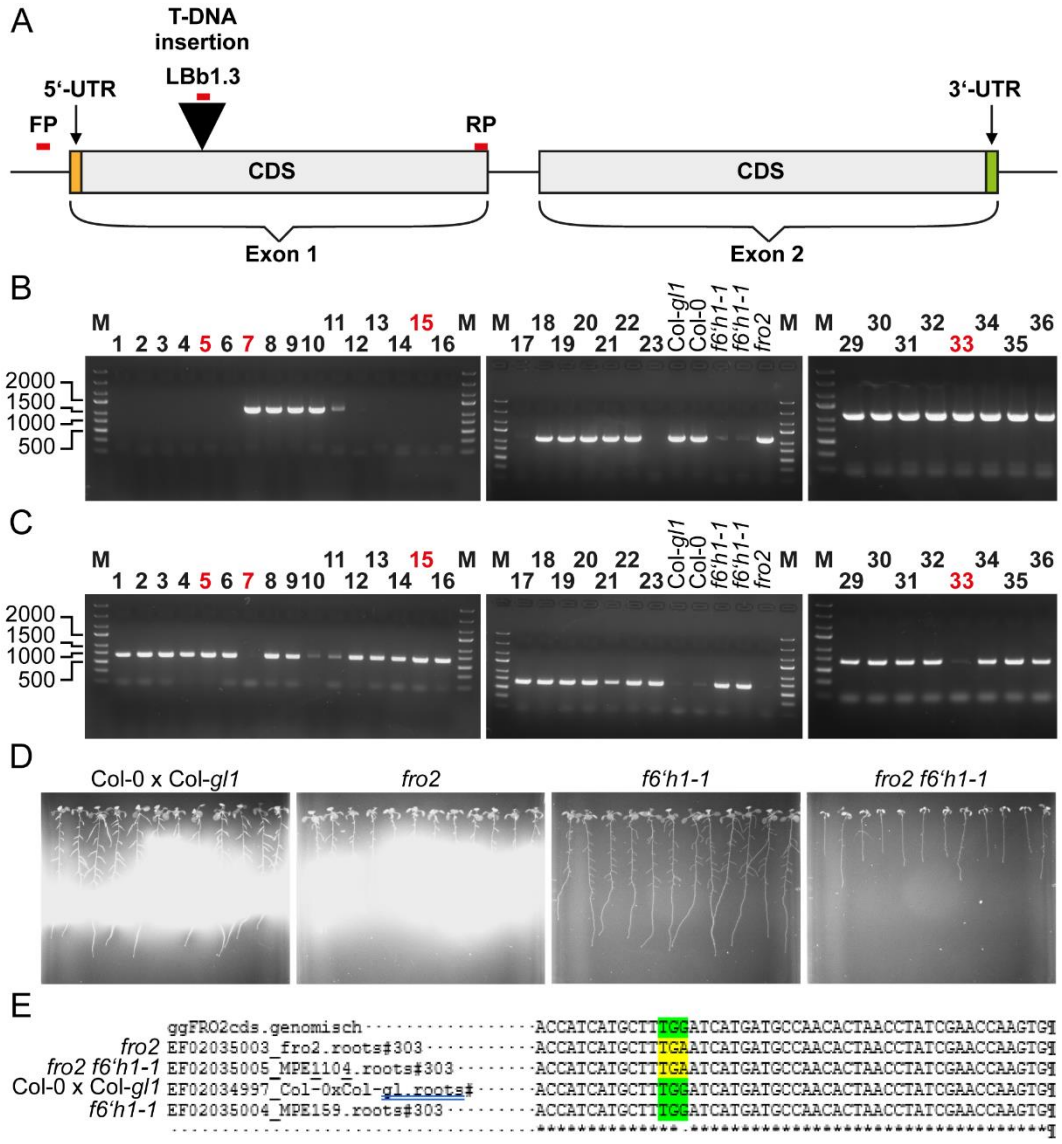

Fig. 12. Isolation of a *fro2 f6h'1-1* double mutant. Isolation of wild-type (Col-0 x Col-*gl1*), single mutant *fro2* and *f6'h1-1* mutants, and double mutant plants (*fro2 f6'h1-1*) from a F2 population obtained after crossing *fro2* and *f6'h1-1* single mutants. (A) Schematic representation of the *F6'H1* gene structure according to SIGnAL (http://signal.salk.edu/) comprising two exons (exon 1: 701 bp; exon 2: 769 bp) separated by an intron of 83 bp. In *f6'h1-1*, the T-DNA insertion is located in the first exon 33 bp downstream of ATG of the coding sequence (CDS). Primer used for PCR are indicated as red lines. UTR: untranslated region; FP: forward primer; LBb1.3: T-DNA specific primer for SALK collection, RP: reverse primer. For primer sequences, see Table 2 (section 3.3). (B and C) PCR results for wild-type *F6'H1* locus (B) and for the presence of the expected T-DNA insertion (C). Red numbers indicate homozygous plants that were selected for further experiments (wild-type (33), *fro2* (7), *f6'h1-1* (15), *fro2 f6'h1-1* (5)). (D) Coumarin-dependent UV fluorescence (365 nm) in roots of wild-type, single mutants, and double mutant plants grown under Fe-limiting conditions as evidence for the absence of coumarins in *f6'h1-1* and *fro2 f6'h1-1* plants. (E) The G→A mutation at position 126 in the first exon of FRO2 was verified by sequencing.

Next, the *fro2 f6'h1-1* double mutant was phenotypically analyzed on substrate and agar plates. On non-limed substrate (control, pH ~5.5), no differences between wild-type and *f6'h1-1* plants were observed while *fro2* appeared more chlorotic and had a significantly reduced chlorophyll concentration and shoot biomass (Fig. 13). However, the *fro2 f6'h1-1* double mutant showed severe symptoms of Fe deficiency and strong growth inhibition, comparable to those observed in *irt1-1* plants (Fig. 13A). In comparison to the wild type, the chlorophyll

concentration and shoot biomass of the double mutant were reduced by ~63% and ~98%, respectively (Fig. 13B and C). Fertilization with Fe-EDDHA could significantly improve the shoot biomass and chlorophyll concentration of the *fro2 f6'h1-1* double mutant under these conditions but was less efficient than for *irt1-1* plants. On limed substrate (pH ~7.0), all mutant lines were highly affected by Fe deficiency and their growth was strongly inhibited in comparison to the wild type (Fig. 13). Under these conditions, no differences between the double and single mutants as well as *irt1-1* were observed anymore and Fe fertilization failed to significantly improve the growth of *fro2 f6'h1-1* or *irt1-1*.

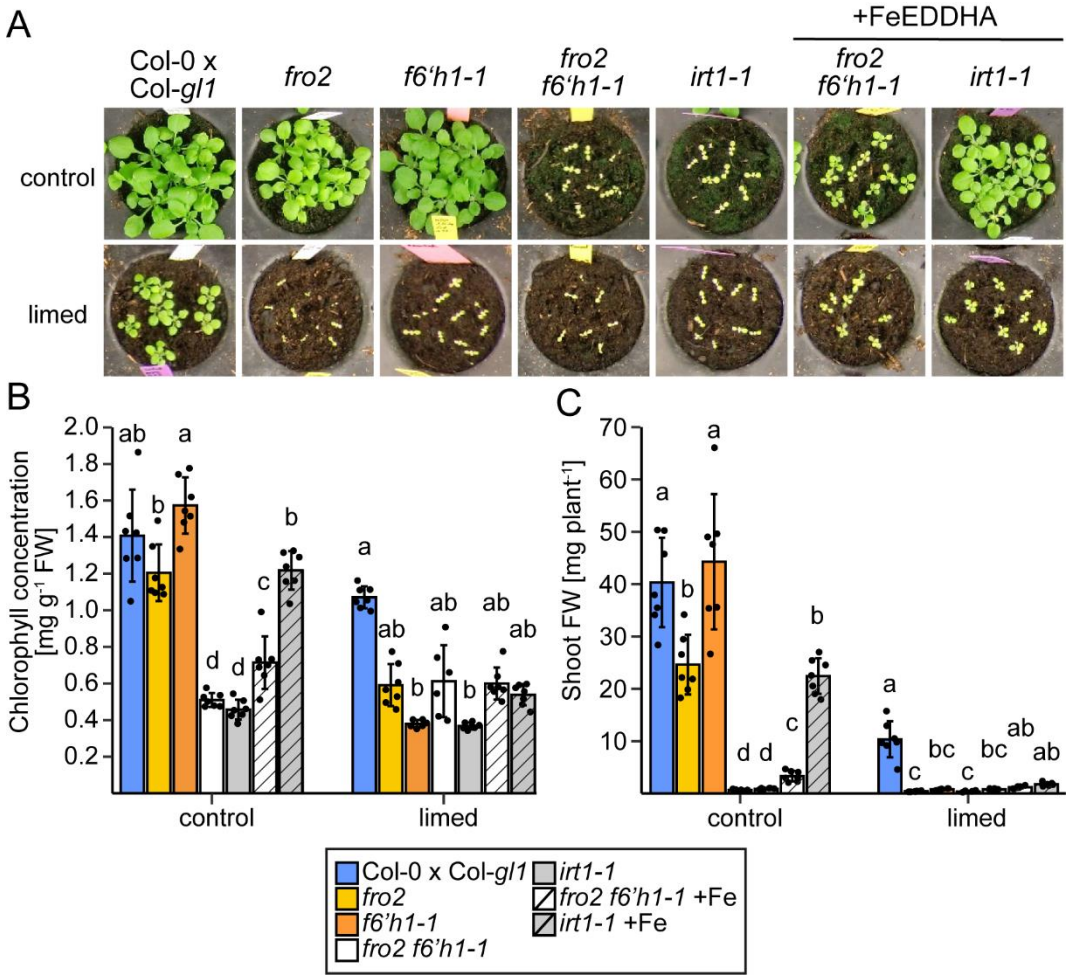

Fig. 13. Chlorosis susceptibility of the *fro2 f6'h1-1* double mutant on solid growth substrate. (A-C) Visual appearance (A), leaf chlorophyll concentration (B), and shoot fresh weight (FW) (C) of wild-type (Col-0 x Col-*gl1*), *fro2*, *f6'h1-1*, *fro2 f6'h1-1* double mutant, and *irt1-1* plants grown for 19 d on non-limed substrate (control) at pH ~5.5 or limed substrate at pH ~7.0. To alleviate leaf chlorosis in *fro2 f6'h1-1* and *irt1-1* plants on limed substrate, plants were supplemented with Fe(III)-EDDHA three times per week. Bars represent means ± s.d. (n = 6-7 biological replicates). Different letters indicate significant differences according to one-way ANOVA with post-hoc Tukey's test at $p \leq 0.05$ or ANOVA on ranks with post-hoc Dunn's test at $p \leq 0.05$ within the individual treatments.

The high susceptibility of *fro2 f6'h1-1* plants to Fe deficiency was also confirmed when plants were grown under axenic conditions of low Fe availability on agar plates (Fig. 14). Compared to the *fro2* and *f6'h1-1* single mutants, the simultaneous disruption of *FRO2* and *F6'H1* resulted in additive phenotypes regarding plant appearance and chlorophyll concentration irrespective

of the pH and buffer conditions (Fig. 14A and B). Similar to what was observed on substrate, the phenotype of the *fro2 f6'h1-1* double mutant was comparable to that of *irt1-1* under all tested conditions. However, shoot Fe concentration did not differ significantly between the single mutants and the *fro2 f6'h1-1* double mutant (Fig. 14C).

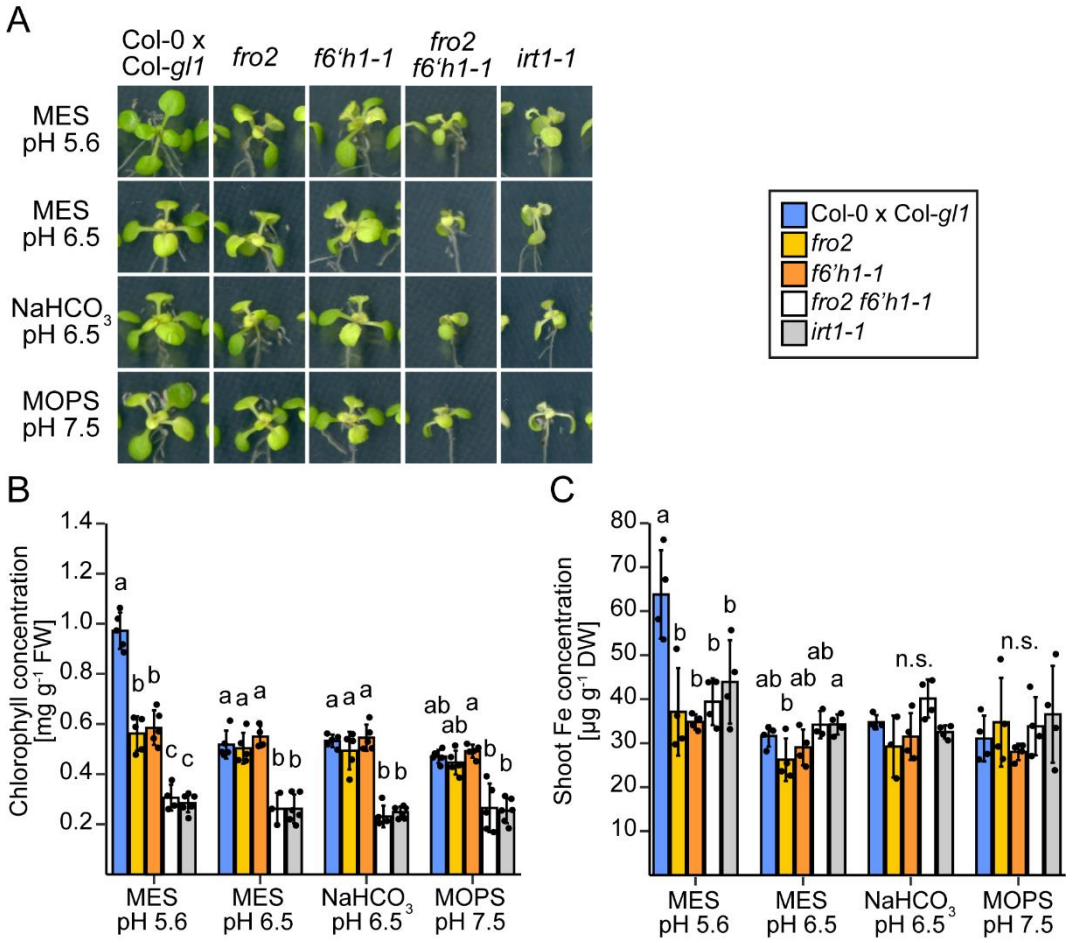

Fig. 14. Chlorosis susceptibility of the *fro2 f6'h1-1* double mutant on agar. (A-C) Visual appearance (A) and concentrations of chlorophyll (B) and Fe (C) in shoots of wild-type (Col-0 x Col-*gl1*), *fro2*, *f6'h1-1*, *fro2 f6'h1-1* double mutant, and *irt1-1* plants after 6 d of cultivation under different conditions of low Fe availability. Ten-d-old seedlings pre-cultured on one-half strength MS medium with 40 µM Fe-EDTA (pH 5.6) were transferred to one-half strength MS with 20 µM $FeCl_3$ buffered with either MES to pH 5.6 or pH 6.5, $NaHCO_3$ to pH 6.5, or MOPS to pH 7.5. Bars represent means ± s.d. (n = 3-6 biological replicates). Different letters indicate significant differences according to one-way ANOVA with post-hoc Tukey's test at $p \leq 0.5$ within the individual treatments.

Taken together, the severe Fe-deficient phenotype of a *fro2 f6'h1-1* double mutant indicates that coumarins and the membrane-bound FRO2 reductase are the only efficient mechanisms for Fe(III) acquisition prior to Fe^{2+} uptake in roots of *A. thaliana*. Furthermore, the less efficient complementation of the *fro2 f6'h1*-1 double mutant with FeEDDHA compared to *irt1-1* suggests that even IRT1-independent Fe import into roots relies on Fe(III) reduction.

4.6 Supplementation of fraxetin and sideretin can alleviate Fe deficiency in a *fro2 f6'h1-1* double mutant only at acidic pH

Although indications for a Fe(III) mobilizing and reductive function of fraxetin and sideretin relevant for plant growth under Fe-limiting conditions at pH 5.6 and pH 6.5 were already found (Fig. 9, Annex Figs. 1-4), in these experiments it was not possible to rule out synergistic effects or negative interactions between the supplied coumarins with those still produced by the *fro2* mutant. Therefore, the absence of both FRO2-dependent Fe(III) reduction and significant coumarin synthesis in the *fro2 f6'h1-1* double mutant offered the chance to investigate *in planta* Fe(III) mobilization and/or reduction of each individual coumarin without the interference of root-borne coumarins.

In line with previous results, the single mutants and double mutant showed Fe deficiency-induced chlorosis under control conditions (MeOH) already at acidic pH (pH 5.6), while wild-type plants showed symptoms of Fe deficiency only at pH 6.5 (Fig. 15). At pH 5.6, the exogenous supply of fraxetin and sideretin alleviated chlorosis and significantly increased the chlorophyll concentration in all lines (Fig. 15A-D). However, this effect resulted in significant increases in shoot fresh biomass only for *fro2* and *f6'h1-1* single mutants supplied with fraxetin (Fig. 16A and C). Furthermore, compared to fraxetin, sideretin was only able to fully rescue *f6'h1-1* plants but not the other mutants from Fe deficiency. At pH 6.5, fraxetin supplementation alleviated Fe deficiency and increased chlorophyll levels in wild-type and single mutant plants but not in the double mutant (Fig. 15A and E, Fig. 16C). This result suggests that synergistic effects between the supplied fraxetin and plant-borne coumarins might favor non-enzymatic Fe(III)-reduction at this pH. The supply of sideretin at pH 6.5 was only efficient for wild-type and *f6'h1-1* plants, as it failed to prevent chlorosis and restore chlorophyll levels and shoot fresh mass of *fro2* and *fro2 f6'h1-1* mutants (Fig. 15B and F, Fig 16D).

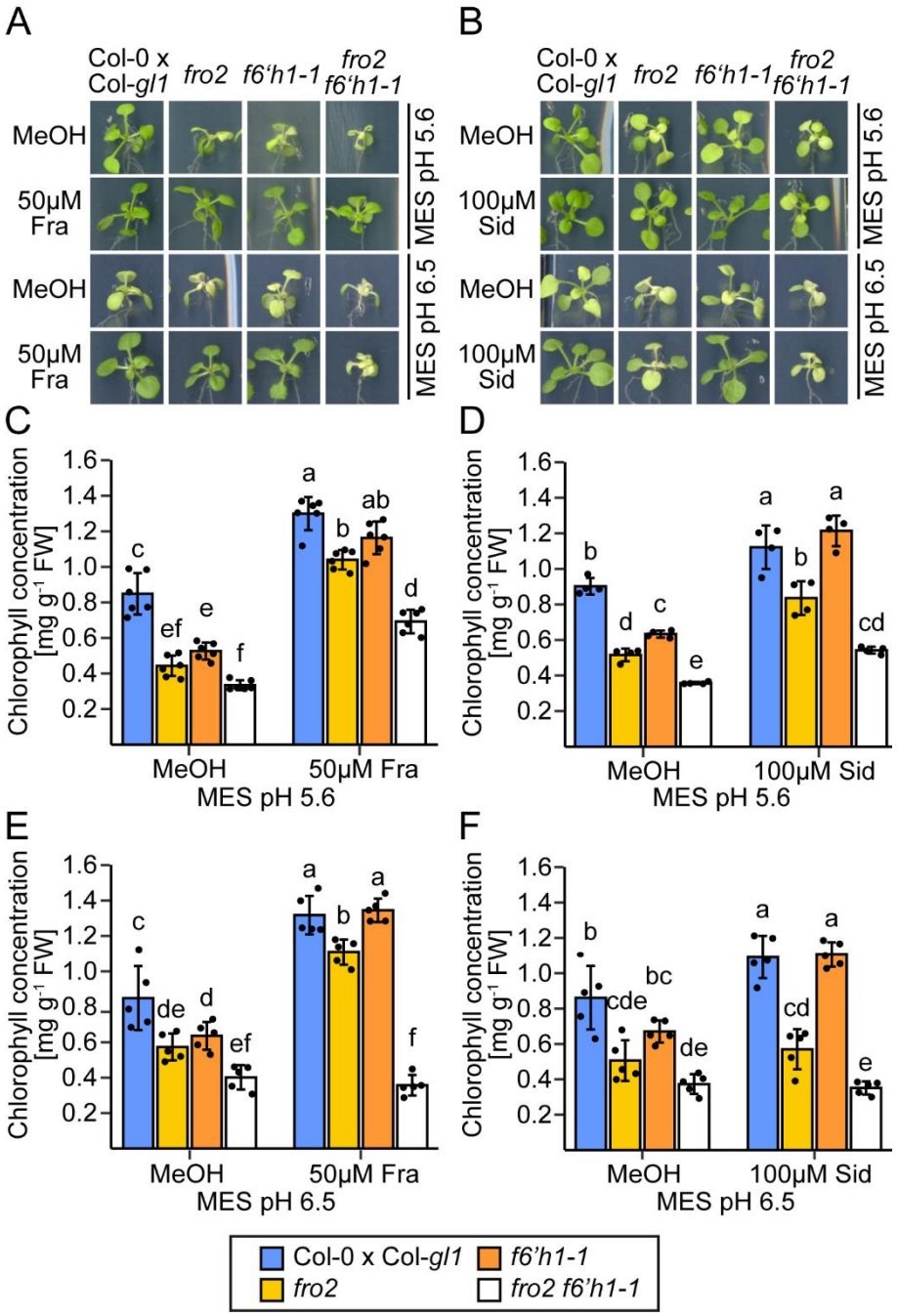

Fig. 15. Effect of fraxetin and sideretin supplementation on Fe deficiency-induced chlorosis of *fro2* and *f6'h1-1* single and double mutant plants. (A-F) Visual appearance (A and B) and leaf chlorophyll concentrations (C-F) of wild-type (Col-0 x Col-*gl1*), *fro2* and *f6'h1-1* single and *fro2 f6'h1-1* double mutant plants grown for 6 d under different conditions of low Fe availability with or without fraxetin (A, C, and E) or sideretin (B, D, and F). Plants were pre-cultured on one-half strength MS medium with 40 µM Fe-EDTA (pH 5.6) for 10 d and then transferred to one-half strength MS with 20 µM $FeCl_3$ buffered with MES to pH 5.6 or pH 6.5 and supplemented with methanol (MeOH, mock), 50 µM fraxetin, or 100 µM sideretin. Bars represent means ± s.d. (n = 4-6 biological replicates composed of two shoots). Different letter indicates significant differences according to one-way ANOVA with post-hoc Tukey's test at $p \leq 0.05$.

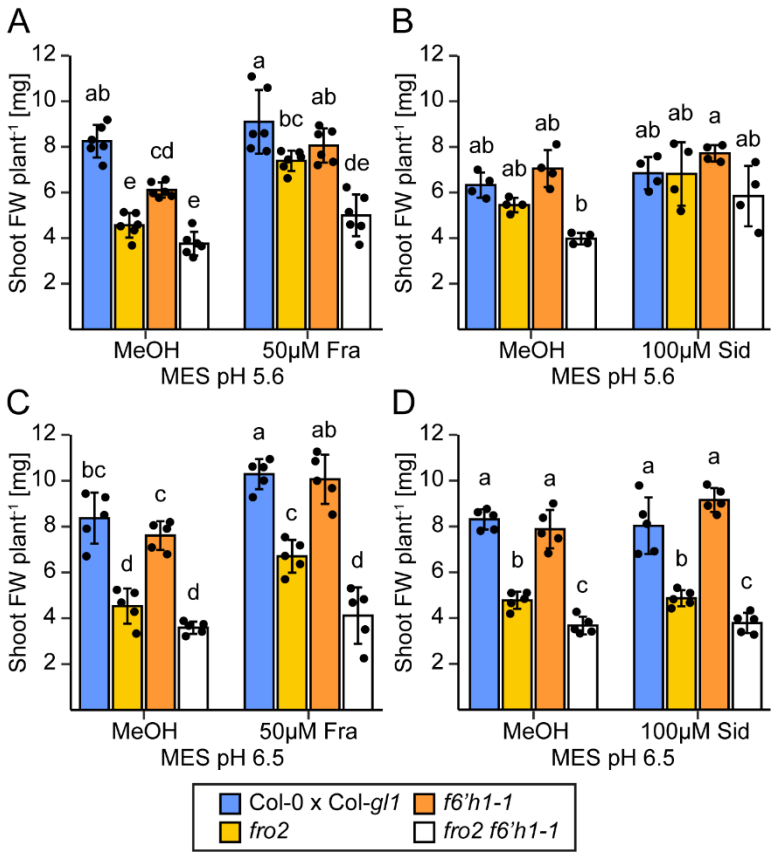

Fig. 16. Effect of fraxetin and sideretin supplementation on shoot biomass of fro2 and f6'h1-1 single and double mutant plants. (A-D) Shoot fresh weight of wild-type (Col-0 x Col-*gl1*), *fro2* and *f6'h1-1* single and *fro2 f6'h1-1* double mutant plants grown for 6 d under different conditions of low Fe availability with or without fraxetin (A and C) or sideretin (B and D). Plants were pre-cultured on one-half strength MS medium with 40 µM Fe-EDTA (pH 5.6) for 10 d and then transferred to one-half strength MS with 20 µM $FeCl_3$ buffered with MES to pH 5.6 or pH 6.5 and supplemented with methanol (MeOH, mock), 50 µM fraxetin, or 100 µM sideretin. Bars represent means ± s.d. (n = 4-6 biological replicates composed of two shoots). Different letter indicates significant differences according to one-way ANOVA with post-hoc Tukey's test at $p \leq 0.05$.

Taken together, these results show that fraxetin and sideretin can mobilize and reduce Fe(III) at acidic pH and thereby by-pass the requirement for enzymatic Fe(III) reduction via FRO2. Furthermore, the results allow to hypothesize synergistic effects between the supplied fraxetin and plant-borne coumarins, which mediate a non-enzymatic Fe(III) reduction at pH 6.5, while at this pH the reduction of Fe(III) mobilized by sideretin requires a functional FRO2.

4.7 Generation of *fro2 s8h-1* and *fro2 cyp82C4-1* to study the relevance of scopoletin and fraxetin for coumarin-mediated Fe(III) reduction *in planta*

The function of certain coumarins in Fe(III) mobilization and reduction might be under- or overestimated if based solely on results from resupply experiments, as relatively large amounts of coumarins are homogeneously supplied at a single time-point, which do not allow to mimic possible spatial-temporal differences in concentration gradients established in a natural soil rhizosphere. Furthermore, this approach has only limited applicability to study coumarin-mediated Fe(III) mobilization and reduction in soil as coumarins possess only very low solubility

in water. Therefore, additional approaches were employed to investigate the role of selected coumarins in root exudates and extracts *in planta*.

Since *s8h* and *cyp82C4* release high levels of scopoletin and fraxetin, respectively, even at acidic pH (Rajniak *et al*., 2018; Fig. 38), *fro2 s8h-1* and *fro2 cyp82C4-1* double mutants were generated to investigate the relevance of scopoletin and especially fraxetin in non-enzymatic Fe(III) reduction *in planta*.

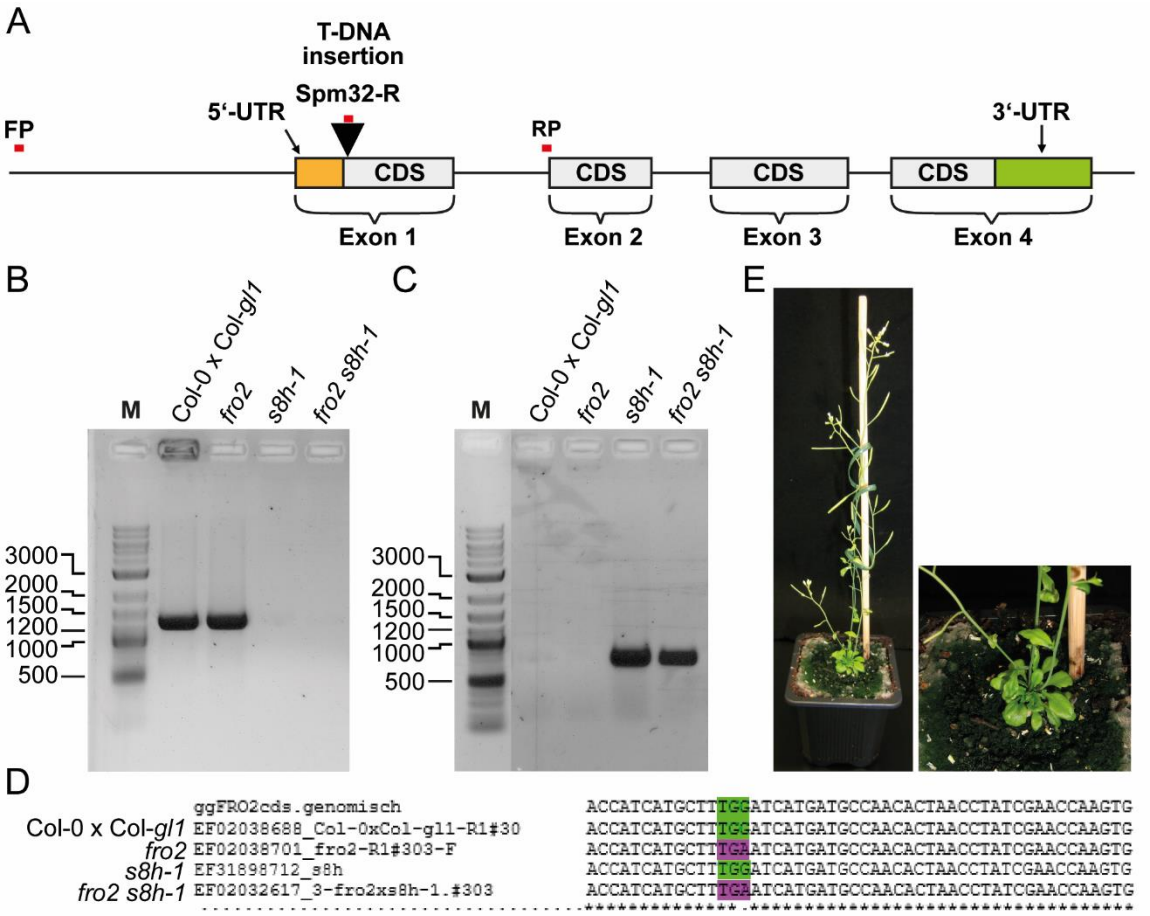

Fig. 17. Isolation of a *fro2 s8h-1* double mutant. Wild-type (Col-0 x Col-*gl1*), single *fro2* and *s8h-1* mutants, and double mutant plants (*fro2 s8h-1*) were selected from the F2 population after crossing *fro2* and *s8h-1* plants. Plants were pre-screened for a functional *FRO2* gene using a ferric-chelate reductase assay. (A) Schematic representation of the *S8H* gene structure. According to SIGnAL (http://signal.salk.edu/), *S8H* has four exons (exon 1: 374 bp; exon 2: 242 bp, exon 3: 325 bp, exon 4: 475 bp; intron 1: 225 bp, intron 2 : 138 bp, intron 3: 100 bp). In *s8h-1*, the T-DNA insertion is located in the first exon 9 bp downstream of ATG of the coding sequence (CDS). Primer used for PCR are indicated as red lines. UTR: untranslated region; FP: forward primer; Spm32-R: T-DNA specific primer for SM collection, RP: reverse primer. For primer sequences, see Table 2 (section 3.3). (B and C) The pre-selected plants were screened for the presence or absence of the T-DNA insertion in the *S8H* gene. PCR results for wild-type *S8H* locus (B) and for the presence of the expected T-DNA insertion (C). (D) The G→A mutation at position 126 in the first exon of FRO2 was verified by sequencing. (E) Appearance of double mutant plants grown on soil for seed propagation. Plants were fertilized with Fe-EDDHA regularly in order to ensure plant growth and seed formation.

For the *fro2* x *s8h-1* cross, the genotypic analysis of plants from the F2 population is shown in Figure 17. T-DNA insertion in the *S8H* gene was verified by PCR using a combination of gene specific and T-DNA insertion-specific primers (Fig. 17A-C) and the expected point-mutation in *FRO2* was confirmed by sequencing (Fig. 17D). Similar to *fro2 f6'h1-1* plants, the *fro2 s8h-1*

double mutant showed clear symptoms of Fe deficiency (Fig. 17E) and had to be fertilized regularly with a highly soluble Fe source to ensure plant growth and seed formation.

Then, homozygous *fro2 s8h-1* double mutant plants and the corresponding wild type and single mutants from the F2 population were phenotypically characterized under conditions of low Fe availability at pH 5.6 and pH 6.5 on agar plates. As shown in Fig. 18, the *fro2 s8h-1* double mutant exhibited substantially reduced shoot growth and significantly lower chlorophyll concentration compared to the wild-type and single mutant plants at both pH 5.6 and pH 6.5 (Fig. 18). At pH 5.6, *s8h-1* plants were less affected by Fe-deficiency and showed significantly higher chlorophyll levels than *fro2* plants. If *fro2 s8h-1* indeed over-accumulate scopoletin, which was not yet verified, then these results suggest that scopoletin has no or only minor effects in Fe(III) reduction.

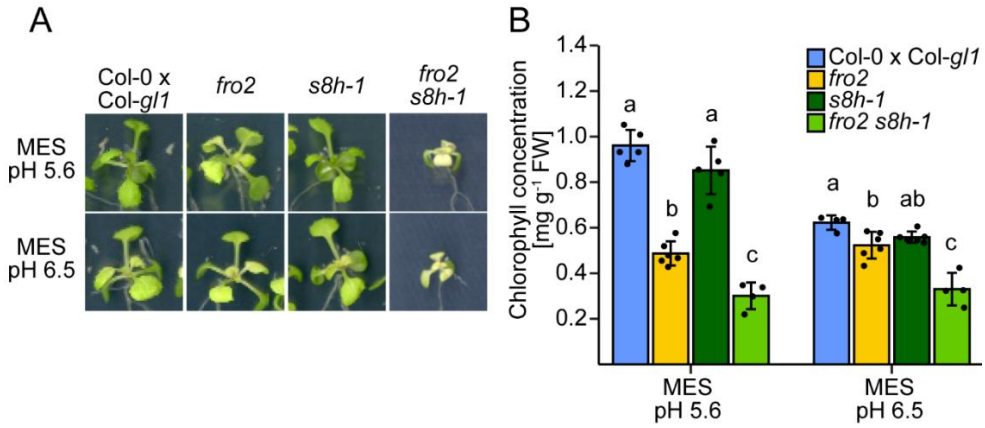

Fig. 18. Initial characterization of a *fro2 s8h-1* double mutant on Fe limiting conditions. (A and B) Visual appearance (A) and leaf chlorophyll concentrations (B) of wild-type (Col-0 x Col-*gl1*), *fro2*, *s8h-1*, and *fro2 s8h-1* plants grown for 6 d under different conditions of low Fe availability on agar plates. Plants were pre-cultured on one-half strength MS medium with 40 µM Fe-EDTA (pH 5.6) for 10 d and then transferred to one-half strength MS with 20 µM $FeCl_3$ buffered with MES to pH 5.6 or pH 6.5. Bars represent means ± s.d. (n = 4-6 biological replicates). Different letters indicate significant differences according to one-way ANOVA with post-hoc Tukey's test at $p \leq 0.05$ within the different treatments.

For the selection of a *fro2 cyp82C4-1* double mutant, a slightly different strategy was followed. Since the initial attempts using ferric-chelate reductase activity failed to identify plants homozygous for the mutation in *FRO2*, the F3 population of the *fro2* x *cyp82C4-1* cross was eventually grown on soil and first screened for homozygous T-DNA insertion in the *CYP82C4* gene followed by sequencing to verify homozygous *FRO2* mutation (Fig. 19A-D). Nine plants were finally identified as homozygous both for *fro2* and *cyp82C4* (Fig. 19E). As these plants grew, they developed severe symptoms of Fe deficiency. This result is somehow unexpected, as disruption of *CYP82C4* results in the release of high levels of fraxetin (Rajniak *et al.*, 2018). If this response is maintained in the double mutant, which still awaits confirmation, these preliminary results could suggest that sideretin synthesis and release plays the most critical role in Fe acquisition in the absence of a functional FRO2 at acidic pH.

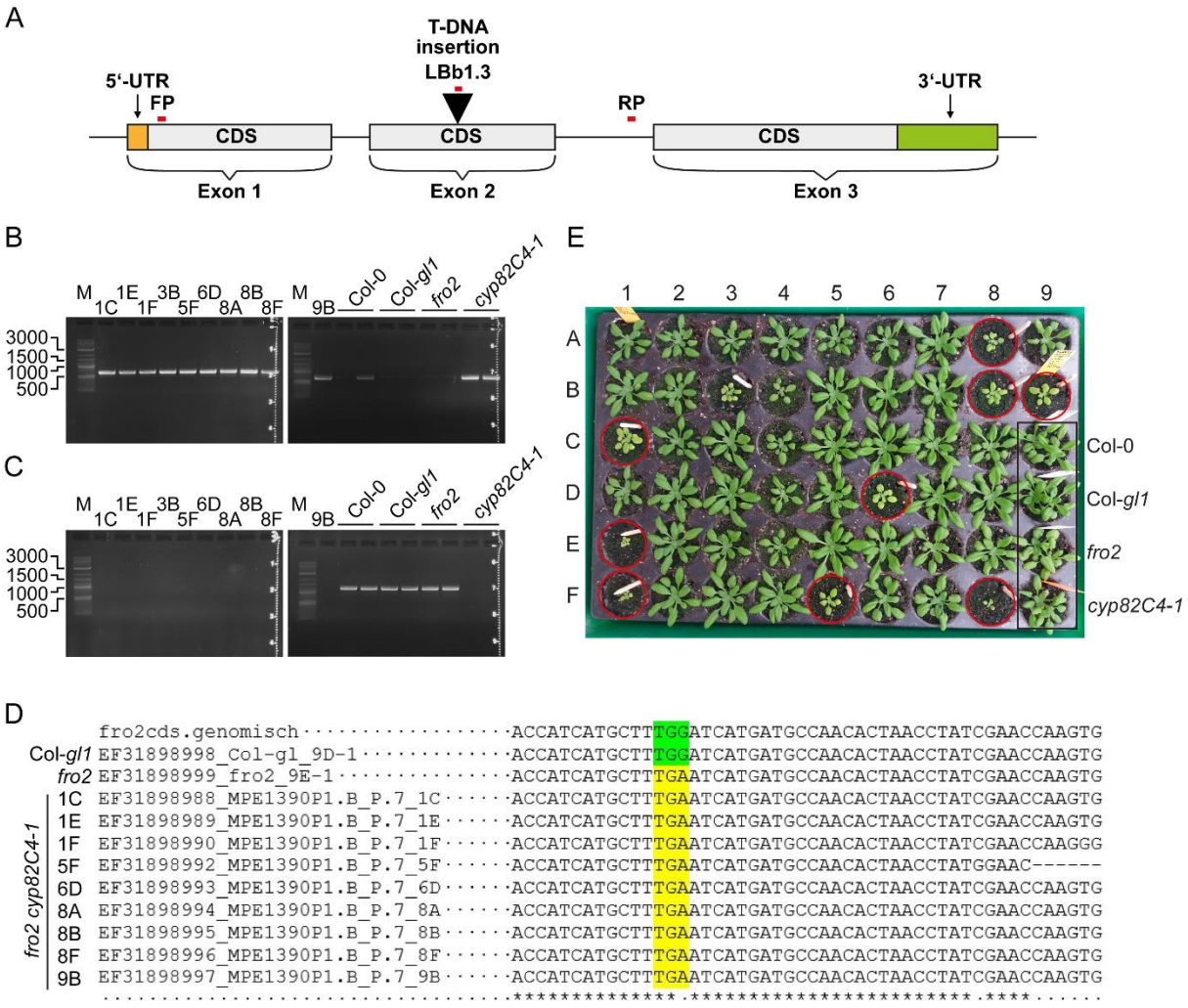

Fig. 19. Isolation of a *fro2 cyp82C4-1* double mutant. Double mutant plants (*fro2 cyp82C4-1*) were selected from the F3 population after crossing *fro2* and *cyp82C4-1* plants. Soil-grown plants were pre-screened for a T-DNA insertion in the *CYP82C4* gene by PCR. (A) Schematic representation of the *CYP82C4* gene structure. According to SIGnAL (http://signal.salk.edu/), *CYP82C4* has three exons (exon 1: 524 bp; exon 2: 476 bp, exon 3: 885 bp; intron 1: 99 bp, intron 2: 253 bp). In cyp82C4-*1*, the T-DNA insertion is located in the second exon 216 bp upstream of the second exon start. Primer used for PCR are indicated as red lines. UTR: untranslated region; FP: forward primer; LBb1.3: T-DNA specific primer for SALK collection, RP: reverse primer. For primer sequences, see Table 2 (section 3.3). B and C) The pre-selected plants were screened for the presence or absence of the T-DNA insertion in the *CYP82C4* gene. PCR results for the presence of the expected T-DNA insertion (B) and for wild-type *CYP82C4* locus (C). (D) The G→A mutation at position 126 in the first exon of FRO2 was verified by sequencing. (E) Appearance of different plants from the F3 population grown for 25 d on soil during double mutant selection. Plants finally verified as homozygous for *fro2* and *cyp82C4* are indicated by red circles. Plants were fertilized with Fe-EDDHA regularly in order to ensure plant growth and seed formation.

4.8 Co-cultivation of *fro2* and *cyp82C4-1* plants can alleviate Fe deficiency-induced chlorosis in *fro2* at acidic pH

Since it was not possible to analyze the root exudates of *fro2 cyp82C4-1* before the end of this thesis, the proposed function of fraxetin in non-enzymatic Fe(III) reduction was investigated by co-cultivating *fro2* and *cyp82C4-1* under conditions of low Fe availability at pH 5.6 and pH 6.5 (Fig. 20A). As *cyp82C4-1* synthesize and exude very high levels of fraxetin (Rajniak *et al.*, 2018), this mutant was used as a natural fraxetin "supplier" to *fro2* plants.

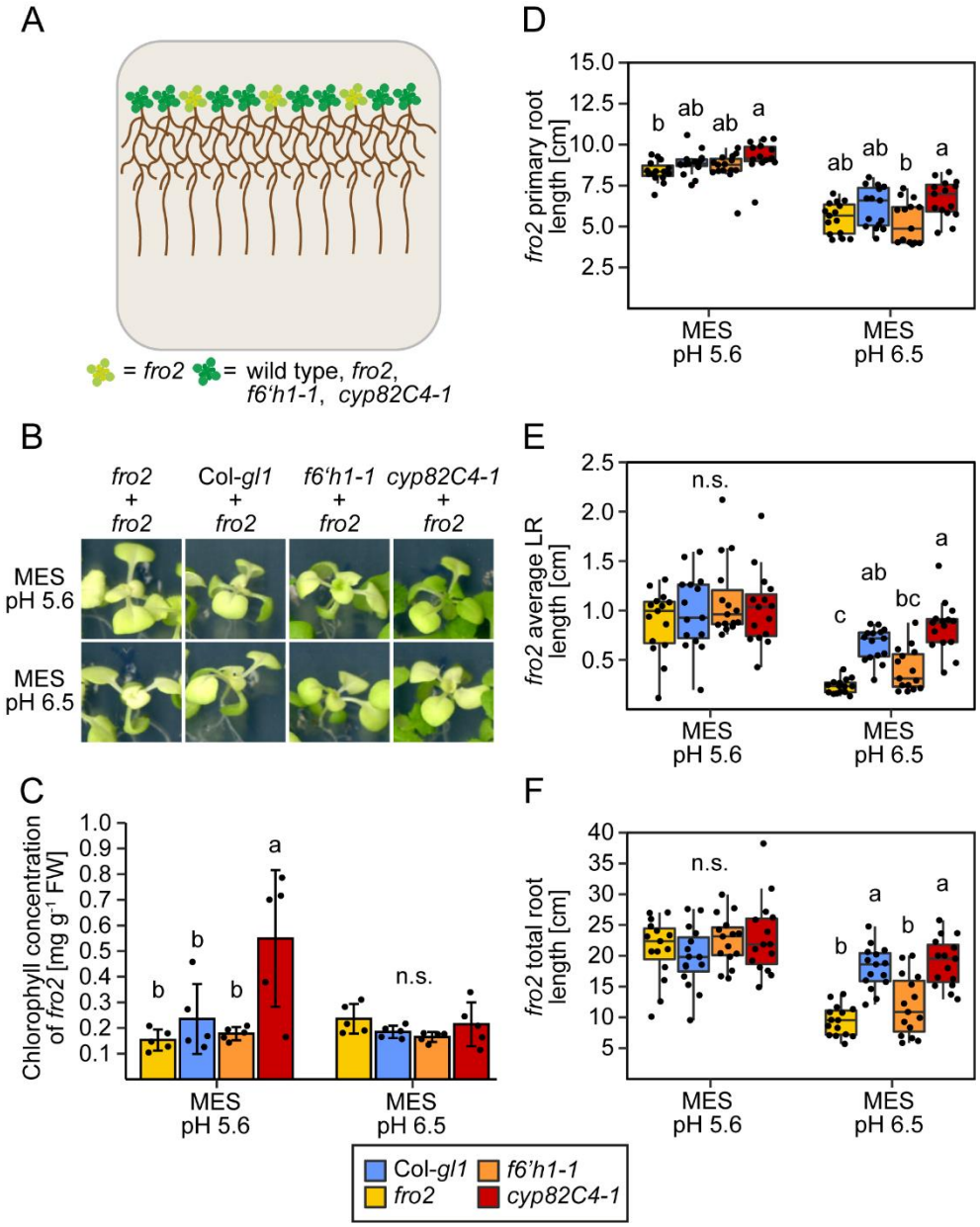

Fig. 20. Co-cultivation of *fro2* with *cyp82C4* alleviates leaf chlorosis at acidic pH. Schematic representation of the experiment (A), shoot appearance (B), leaf chlorophyll concentrations (C), primary root length (D), average lateral root length (E), and total root length (F) of *fro2* plants co-cultivated either with itself or with Col-*gl1* (wild-type), *f6'h1-1*, or *cyp82C4-1*. Plants were pre-cultured on one-half strength MS medium with 40 µM Fe-EDTA (pH 5.6) for 10 d and then transferred to one-half strength MS with 20 µM $FeCl_3$ buffered with MES to pH 5.6 or pH 6.5 for another 11 d. Bars represent means ± s.d. (n = 5 biological replicates composed of three shoots). Box plots horizontal lines show medians (n = 15 biological replicates), box limits indicate the 25th and 75th percentiles and whiskers extend to 5th and 95th percentiles. Different letters indicate significant differences according to one-way ANOVA or ANOVA on ranks with post-hoc Tukey's test at $p \leq 0.05$.

At acidic pH (pH 5.6), *fro2* plants co-cultivated with *cyp82C4-1* appeared greener and had a significantly increased chlorophyll concentration in comparison to *fro2* co-cultivated with itself (Fig. 20B and C). When co-cultivated at pH 6.5, none of the investigated genotypes could alleviate Fe deficiency in *fro2*. However, co-cultivation with wild type and *cyp82C4-1* significantly increased the total root length of *fro2* plants by increasing the average lateral root

length but not the primary root length under these conditions (Fig. 20E and F). Such changes in the root system architecture of *fro2* plants were not observed at pH 5.6.

Taken together, these results provide further support *in planta* that fraxetin facilitates non-enzymatic Fe(III) reduction at acidic pH.

4.9 Effect of *CYP82C4* over-expression in Col-0

Considering that sideretin has faster Fe(III) reduction kinetics than fraxetin at pH 5.6 and pH 6.5 (Fig. 3 and 4; Rajniak *et al.*, 2018) it was then attempted to increase sideretin synthesis and release in wild-type (Col-0) plants by overexpressing *CYP82C4*. To this end, two promoters were used: the *35S* promoter of CaMV and the *UBQ10* promoter of *A. thaliana*. The expression of *CYP82C4* in several independent, homozygous transgenic lines was verified by quantitative real-time (RT) PCR. Finally, three and four independent lines with different levels of overexpression were selected for *35S::CYP82C4* and *proUBQ10::CYP82C4* (Fig. 21A and B), respectively.

Irrespective of the growth conditions and the promoter used for the overexpression of *CYP82C4*, no differences were observed in plant appearance and chlorophyll concentration between the wild type (Col-0) and overexpression lines (Fig. 21C and D). Furthermore, in comparison to the *cyp82C4-1* mutant, which releases more fraxetin and virtually no sideretin, no differences were observed when over-expressors were grown on non-limed or limed substrate (Fig. 21E).

These results suggest that simply overexpressing *CYP82C4* is insufficient to improve plant growth under limiting Fe conditions. As the root exudate composition of *CYP82C4* overexpression lines was not yet assessed, it remains unclear if high transcript levels of *CYP82C4* ultimately resulted in higher sideretin production and release.

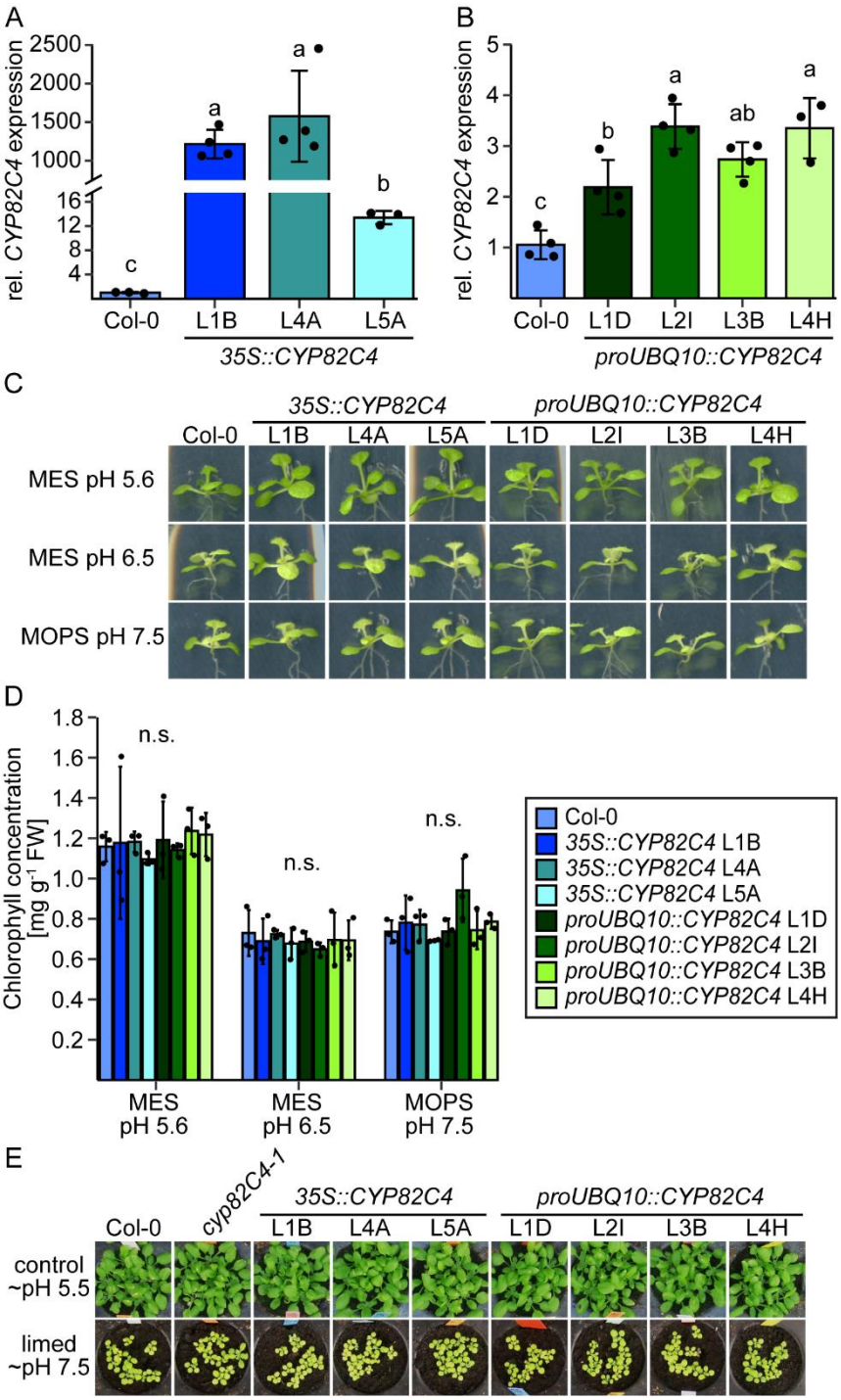

Fig. 21. Over-expression of *CYP82C4* in wild-type plants does not affect plant growth under different Fe-limiting conditions. (A-B) Relative expression of *CYP82C4* in roots of *35S::CYP82C4* (A) and *proUBQ10::CYP82C4* (B) plants in comparison to wild-type plants (Col-0). Plants were either cultivated on sufficient Fe (100 µM Fe-EDTA) for 16 d (A) or pre-cultured on one-half strength MS medium with 40µM FeEDTA (pH 5.6) for 10 d and transferred to one-half strength MS medium with 20µM $FeCl_3$ buffered with MES to pH 5.6 for 6 d (B). (C and D) Appearance (C) and leaf chlorophyll concentrations (D) of different *CYP82C4* over-expression lines after 6 d cultivation under different low Fe availability conditions. Plants were pre-cultured for 10 d on one-half strength MS medium with 40µM Fe-EDTA (pH 5.6) and transferred to one-half strength MS with 20µM $FeCl_3$ buffered with either MES to pH 5.6 or pH 6.5, or MOPS to pH 7.5. Plant roots were shaded from light. Bars represent means ± s.d. (n = 3-4 biological replicates). (E) Plant appearance of wild-type, *cyp82C4-1*, *35S::CYP82C4*, and *proUBQ10::CYP82C4* plants frown for 17 d on non-limed substrate (control) at pH ~5.5 or limed substrate (limed) at pH ~7.0. Significant differences are indicated as asterisks according to Student's *t*-test with α=0.05; * $p \leq 0.05$, ** $p \leq 0.01$, *** $p \leq 0.001$ (B). Different letters indicate significant differences according to one-way ANOVA or ANOVA on ranks with post-hoc Tukey's test at $p \leq 0.05$.

4.10 Determination of Fe-coumarin complexes via UPLC-MS/MS

Since coumarins, especially those harboring a catechol group have the capacity to mobilize Fe(III) by chelation and/or reduction it was assumed that they can form Fe(II)/Fe(III)-coumarin complexes to keep Fe in solution. In order to verify this hypothesis, the formation of Fe-coumarin complexes *in vitro* was evaluated by LC-MS/MS (Triple Quad). Therefore, scopoletin, esculetin, and fraxetin were incubated in aqueous solution with $FeCl_3$ at different pHs. Chromatographic separation was performed using a reverse-phase column and all samples were analyzed in both positive and negative ionization mode. However, different Fe-species for esculetin and fraxetin were found only in negative mode (Figs. 22 and 23; Annex Fig. 5), whereas Fe-scopoletin complexes were detected only in positive mode (Annex Figs. 6 and 11).

In order to determine optimal reaction conditions to study Fe(II)/(III)-coumarin complex formation, in a first step, esculetin, which can chelate but not reduce Fe(III) and fraxetin, which can chelate and reduce Fe(III), were incubated at different molar ratios with $FeCl_3$ at pH 5.5. Coumarin:Fe ratios of 0.3:1, 0.5:1, 0.7:1, 1:1, 1.5:1, and 3:1 were investigated and the acquired mass-to-charge (m/z) range was set to 50-500. Representative chromatograms for esculetin and fraxetin incubated with Fe (coumarin:Fe ratio 3:1) are shown in Fig. 22A and 23A, respectively. In all samples, the $[FeCl_4]^-$ molecular ion at m/z 197.8 eluted at the solvent front as shown exemplarily in Fig. 22B. The isotopic profile was not exactly as expected (see Annex Fig. 7) potentially due to some overlap of the different isotopic peaks. In all cases, the respective free ligand was detected as the largest peak in the chromatograms. Consistence with the retention times (RT) found for the pure coumarin standards, esculetin mainly eluted at 3.4 min (Fig. 22C) and fraxetin at 3.8 min (Fig. 23B). Beside the highly abundant molecular peak $[M-H]^-$ corresponding to the free ligand, several additional peaks were found to co-elute. In the case of esculetin, the molecular peak of the free ligand was detected at m/z 177.0 and additional peaks at m/z 355.0 and m/z 407.9 were assigned as esculetin deprotonated dimer adduct $[2M-H]^-$ and a Fe(III)-$(esculetin)_2$ complex $[Fe+2M-4H]^-$, respectively (Fig. 22C). Furthermore, a peak at m/z 353.0 was also observed suggesting the presence of an esculetin dimer $[2M-3H]^-$ which eluted after the esculetin peak (Fig. 22D). For fraxetin samples, three different peaks were found to co-elute with the free ligand peak $[M-H]^-$ (m/z 207.0) (Fig. 23B). The peak at m/z 191.8 was not conclusively identified but could correspond to a hydroxyesculetin semi-quinone $[M-CH_3-H]^-$ with an expected m/z of 192.0. The peak at m/z 467.9 indicated the presence of a Fe(III)-$(fraxetin)_2$ complex $[2M+Fe-4H]^-$, while a less intense peak at m/z 438.9 suggested the presence of a Fe(II)-$(hydroxyesculetin\ semi\text{-}quinone)_2$ complex $[Fe+2M-2CH_3-3H]^-$. Additional detected peaks corresponded to hydroxyesculetin quinone $[M-CH_3-2H]^-$ (m/z 190.9) and fraxetin dimer $[2M-3H]^-$ (m/z 413.0) which were found to elute after the fraxetin peak (Fig. 23C and D).

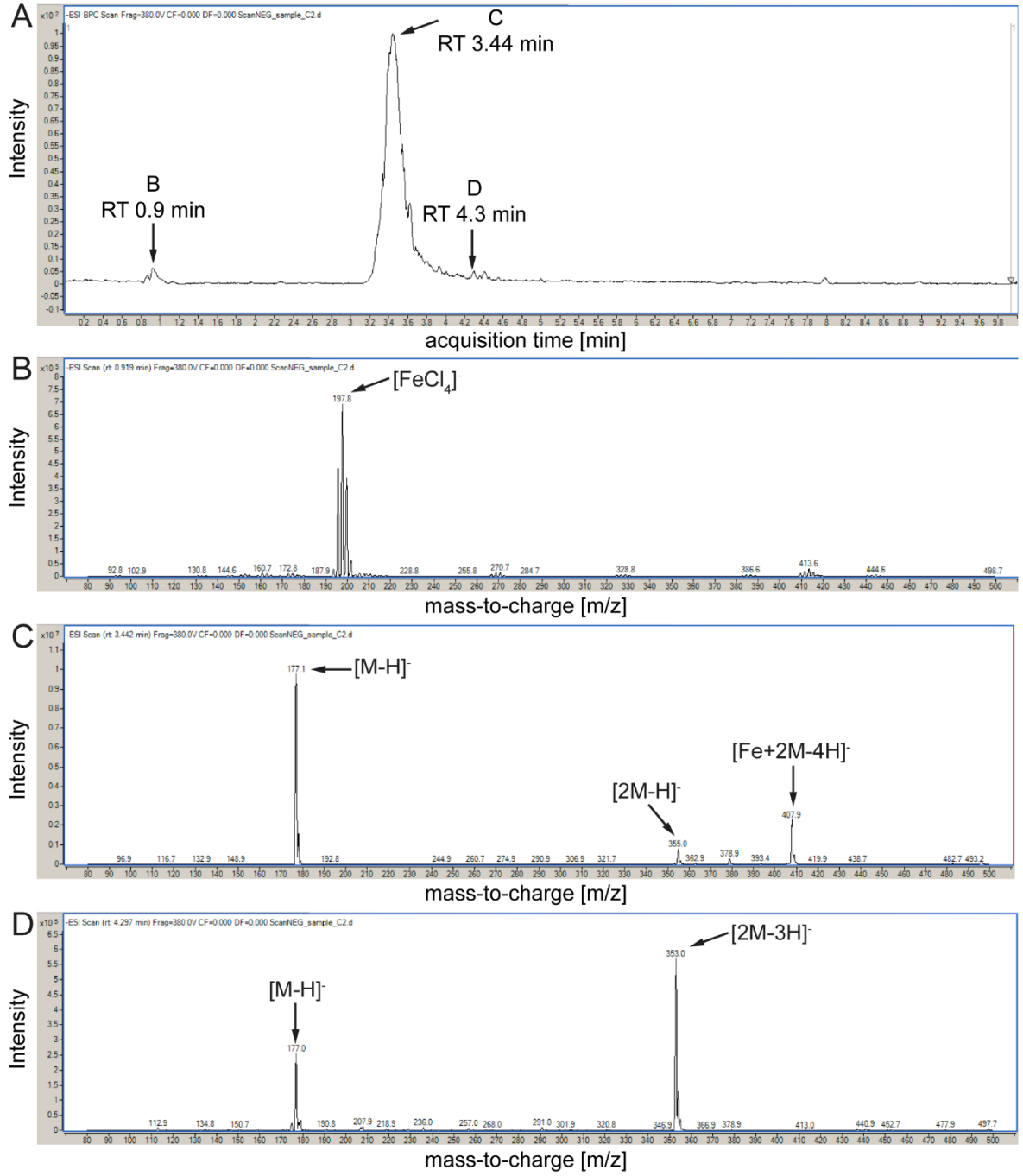

E

Esculetin:Fe ratio	Signal Intensity (Peak area) *10^6		
	m/z 177.1	**m/z 355.0**	**m/z 407.9**
1.5:1	110.0	66.0	2.9
1.0:1	100.0	55.0	1.9
0.7:1	82.5	40.0	1.1
0.5:1	85.0	41.0	1.0
0.3:1	47.9	20.0	0.8

Fig. 22. Analytical detection of Fe-esculetin complexes *in vitro*. (A) Representative chromatogram for esculetin incubated with $FeCl_3$ at pH 5.5. (B-D) Representative mass spectra (negative mode) after 0.919 min (B), 3.442 min (C), and 4.297 min (D) as indicated in A. Esculetin was dissolved in MeOH and incubated with freshly prepared $FeCl_3$ solution adjusted to pH 5.5. The coumarin:Fe ratio was set to 3:1. Samples were incubated for 30 min at room temperature and 1000 rpm in darkness. After subsequent filtration, samples were analyzed by UPLC-MS/MS (Triple Quad). (E) Signal intensity (peak area) for selected mass-to-charge (m/z) ratios in dependence of the indicated esculetin:Fe ratios. M = free ligand.

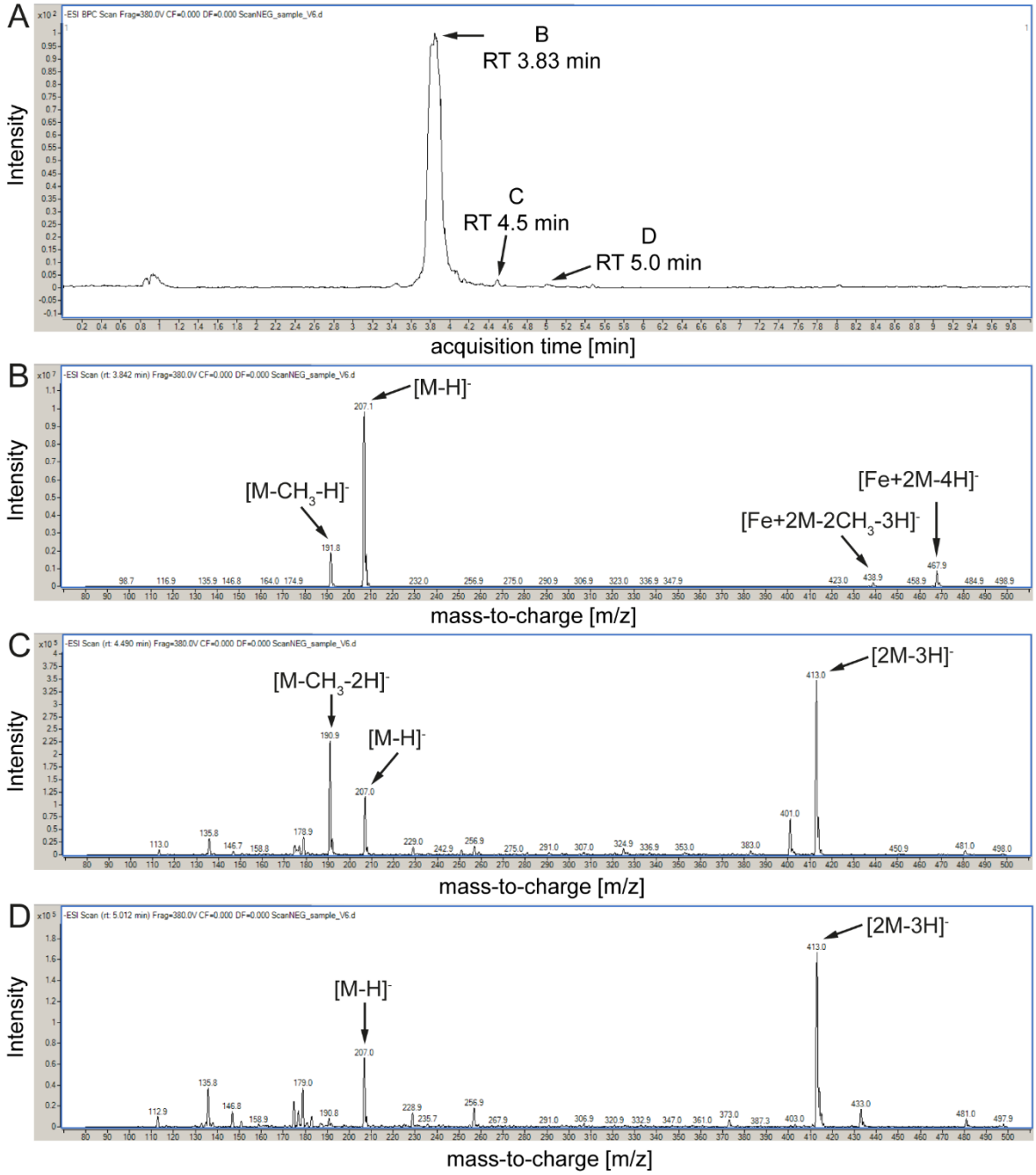

E

Fraxetin:Fe ratio	Signal Intensity (Peak area) $*10^6$	
	m/z 207.0	**m/z 467.9**
3:1	96.5	7.2
1.5:1	78.4	3.2
1.0:1	68.6	2.7
0.7:1	66.0	1.5
0.5:1	44.5	0.9
0.3:1	25.6	0.4

Fig. 23. Analytical detection of Fe-fraxetin complexes *in vitro*. (A) Representative chromatogram for fraxetin incubated with $FeCl_3$ at pH 5.5. (B-D) Representative mass spectra (negative mode) after 3.842 min (B), 4.490 min (C), and 5. 012 min (D) as indicated in A. Fraxetin was dissolved in MeOH and incubated with freshly prepared $FeCl_3$ solution adjusted to pH 5.5. The coumarin:Fe ratio was set to 3:1. Samples were incubated for 30 min at room temperature and 1000 rpm in darkness. After subsequent filtration, samples were analyzed by UPLC-MS/MS (Triple Quad). (E) Signal intensity (peak area) for selected mass-to-charge (m/z) ratios in dependence of the indicated fraxetin:Fe ratios. M = free ligand.

To investigate whether esculetin and fraxetin can also form Fe-coumarin complexes of higher stoichiometry, the investigated m/z-range was extended to m/z 1000 (Annex Fig. 8). However, no evidence was found for the formation of Fe-(coumarin)$_3$ or higher complexes.
The peak areas of the molecule peak of the free ligand and the Fe(III)-(coumarin)$_2$ complexes were compared for the different investigated coumarin:Fe ratios (Fig. 22E and 23E). For both esculetin and fraxetin, the peak area of the corresponding Fe(III)-coumarin complexes decreased in a non-linear fashion with decreasing coumarin concentration. A similar trend was also observed for the esculetin adduct (m/z 355.0) found in esculetin samples (Fig. 22E).

Next, the formation of Fe-coumarin complexes was investigated under acidic (pH ~2.5) and alkaline (pH ~9.0) pH conditions for scopoletin, esculetin, and fraxetin. For further experiments, a coumarin:Fe ratio of 2:1 was chosen as only Fe-(coumarin)$_2$ complexes were detected and the investigated m/z-range was set to m/z 750. Independent of the pH conditions, similar results were obtained for esculetin and fraxetin as those recorded at pH 5.5 (Annex Figs. 9 and 10). In general, the peak intensity of the Fe(III)-(fraxetin)$_2$ complex (m/z 467.9) slightly increased at alkaline pH, while the peak intensity of the Fe(III)-(esculetin)$_2$ complex (m/z 407.9) was unchanged. The peak intensites of the esculetin and fraxetin dimers (m/z 353.0 and m/z 413, respectively) decreased under alkaline conditions. Additionally, no Fe-coumarin complexes with a stoichiometry higher than 1:2 (Fe:coumarin) were detected under any of the pH conditions.
For scopoletin, a peak at m/z 316.0 was observed under all pH conditions (Annex Fig. 11). This peak corresponded to the previously reported double-charged Fe(II)-(scopoletin)$_3$ complex (Schmidt *et al.*, 2014). However, further Fe-scopoletin species as put to evidence by Schmidt *et al.* (2014) could not be found. Instead, the presence of scopoletin dimers (m/z 381.0 negative mode and m/z 383.0 positive mode) and trimers (m/z 571.0 negative mode and 573.0 positive mode) were detected (see Annex Fig. 11D and E). Under alkaline conditions, however, neither scopoletin dimers nor trimers were detected. Additionally, when coumarins were incubated without Fe, the formation of coumarin dimers and trimers was not observed or such peaks showed only low intensities (Annex Fig. 12). These results suggests that Fe acts as a possible catalyzer in coumarin dimerization.

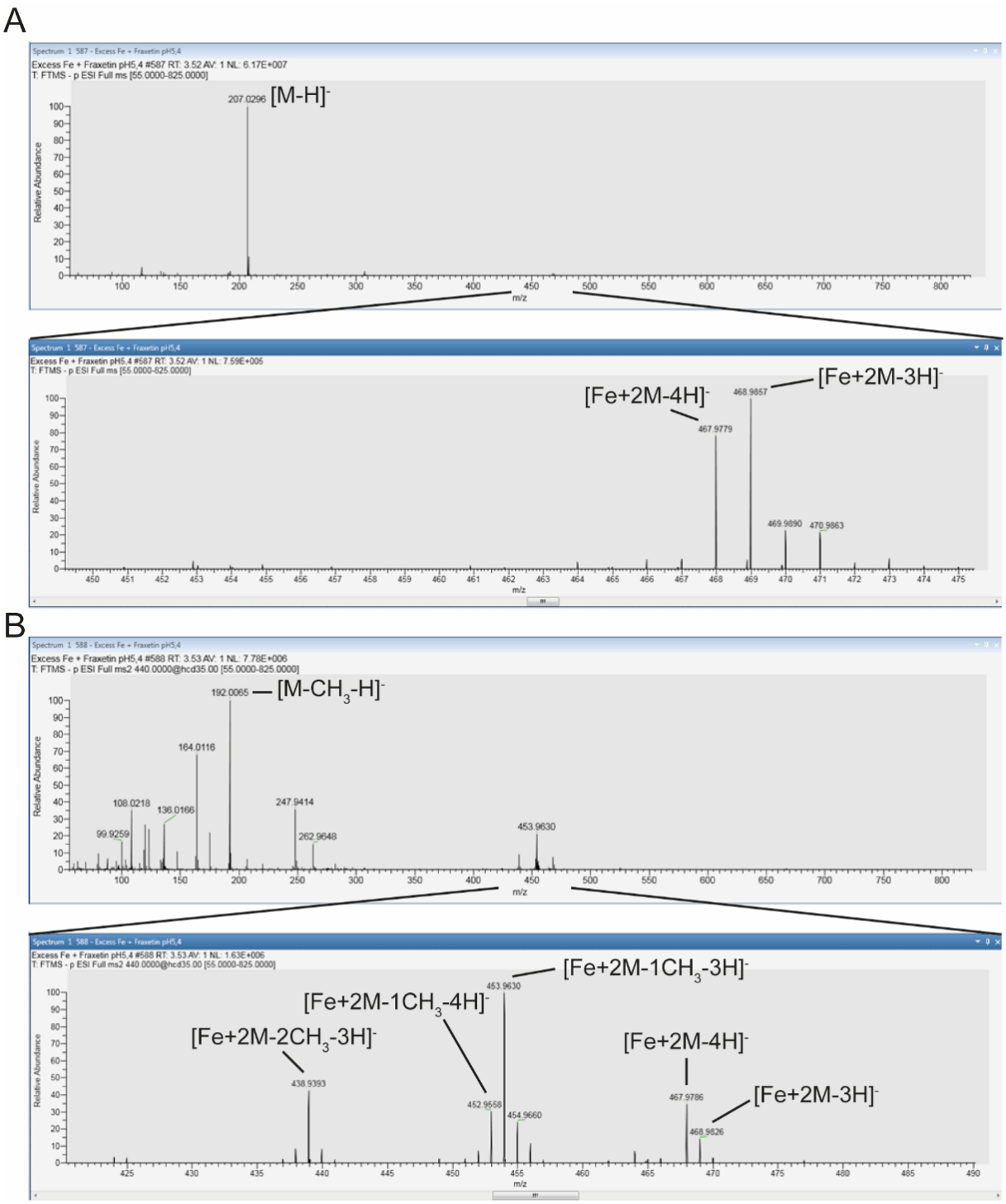

Fig. 24. Detection of Fe(II)/Fe(III)-fraxetin complexes by UPLC-HRMS. (A and B) Full MS (A) and MS2 (B) scans of fraxetin incubated with $FeCl_3$ at pH 5.4. Fraxetin was dissolved in MeOH and incubated with freshly prepared $FeCl_3$ solution adjusted to pH 5.4. The fraxetin:Fe ratio was set to 1:2. Samples were incubated for 30 min at room temperature and 1000 rpm in darkness. After subsequent filtration, samples were analyzed by UPLC-HRMS (Orbitrap) in negative mode. M = free ligand.

To further verify the formation of Fe:coumarin complexes *in vitro*, an isotopically labeled $^{58}FeCl_3$ standard was used. The enrichment of ^{58}Fe in the standard was verified by ICP-MS and was found to be >95% (Annex Fig. 13). If Fe-coumarin chelates are formed during the incubation period, the corresponding peaks were expected to be shifted in the mass spectrum by two units. For such experiments, only fraxetin was used (Fe:coumarin ratio 2:1) and sample

analysis was conducted using an Orbitrap mass spectrometer which offers higher mass resolution than Triple Quad MS. To assess the repeatibility of the results obtained with Triple Quad MS, first samples originating from the incubation of fraxetin with $FeCl_3$ not enriched with ^{58}Fe were analyzed with Oritrap MS.

Similar to the results shown in Fig. 23, the most prominent peak detected was the molecule peak of fraxetin (m/z 207.0296; Fig. 24A) while additional peaks corresponding to hydroxyesculetin semi-quinone (m/z 192.0065) and different Fe-fraxetin species were of much lower relative abundance. Among the observed Fe-fraxetin species, both Fe(II)- and Fe(III)-$(fraxetin)_2$ complexes at m/z 468.9857 and m/z 467.9779, respectively, were found. Futhermore, the presence of Fe(II)/(III)-(fraxetin)(hydroxyesculetin quinone) complexes (m/z 453.9630 and 452.9558, respectively) and a Fe(II)-$(hydroxyesculetin\ semi\text{-}quinone)_2$ complex (m/z 438.9393) were observed. In accordance with the previous measurements, the different Fe-fraxetin species were only detected at the same retention time of the respective free coumarin. However, when fraxetin was incubated with $^{58}FeCl_3$, no mass shifts were observed for any of the detected Fe-fraxetin species (Fig. 25). This result suggested that the detected Fe-coumarin complexes were formed in the UPLC-MS/MS system probably by ^{56}Fe exchange from Fe residues on the column rather than in solution. Notably, Fe-coumarin complexes of similar intensities were also observed in samples when pure coumarins were not incubated with $FeCl_3$ (Fig. 26 and Annex Fig. 12) and even when the samples were directly injected into the mass spectrometer (without LC separation).

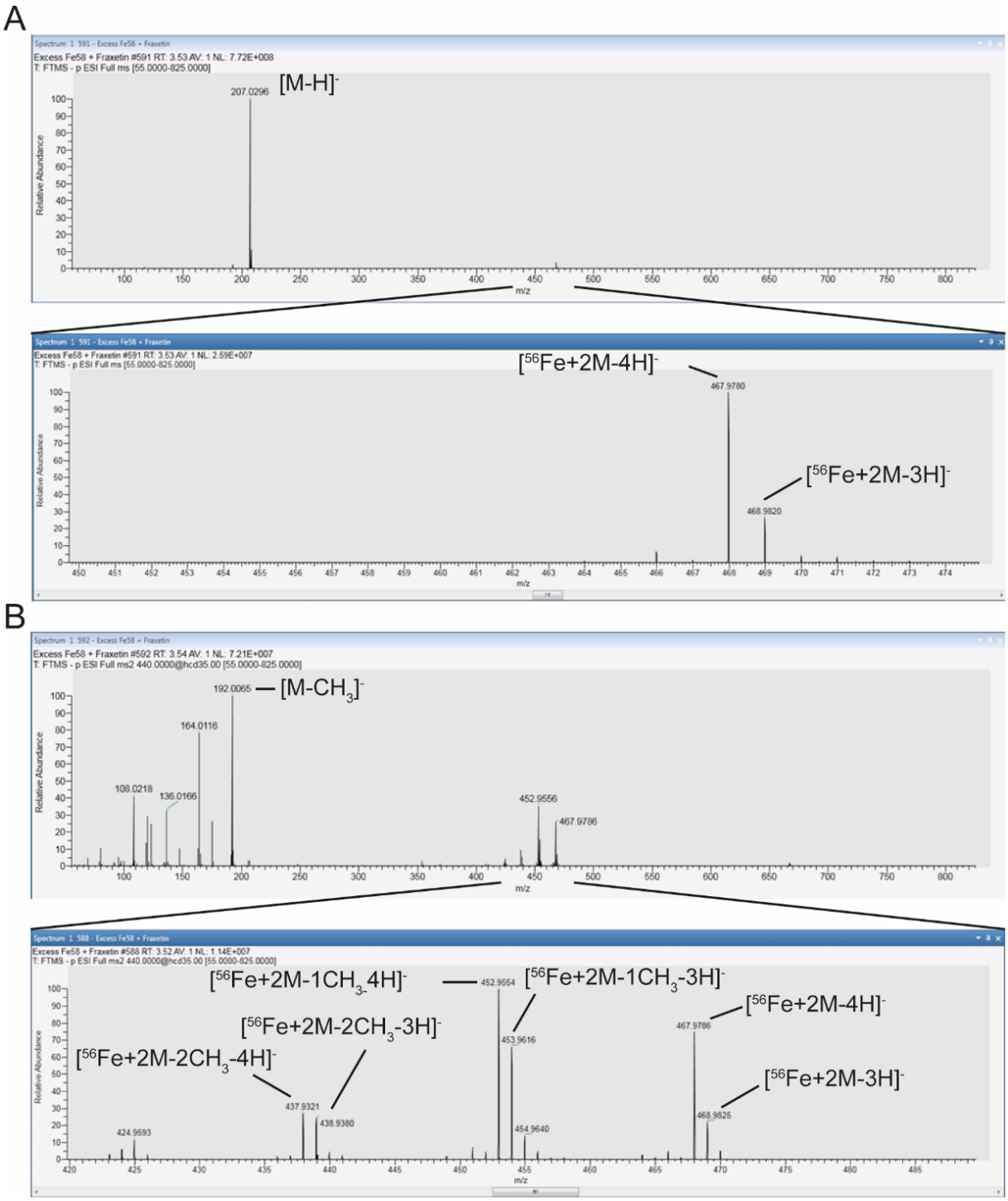

Fig. 25. Detection of Fe-fraxetin species when using $^{58}FeCl_3$. (A and B) Representative full MS (A) and MS2 (B) scans (negative mode) of fraxetin incubated with $^{58}FeCl_3$. Fraxetin was dissolved in MeOH and incubated with freshly prepared $^{58}FeCl_3$ solution. The fraxetin:Fe retio was set to 1:2. The sample was incubated for 30 min at room temperature and 1000 rpm in darkness. After subsequent filtration, samples were analyzed by UPLC-HRMS (Orbitrap). M = free ligand.

In summary, the results suggest that scopoletin, esculetin, and fraxetin can dimerize in a Fe-dependent fashion. Furthermore, the results indicate that scopoletin, esculetin, and fraxetin can form complexes with Fe(III) and scopoletin and fraxetin with Fe(II). However, further efforts are required i) to obtain the conditions for the Fe:coumarin complex formation in solution using

the isotopically enriched $^{58}FeCl_3$ standard; and ii) to establish the appropriate methods to regenerate the column to minimize Fe contamination during liquid chromatography.

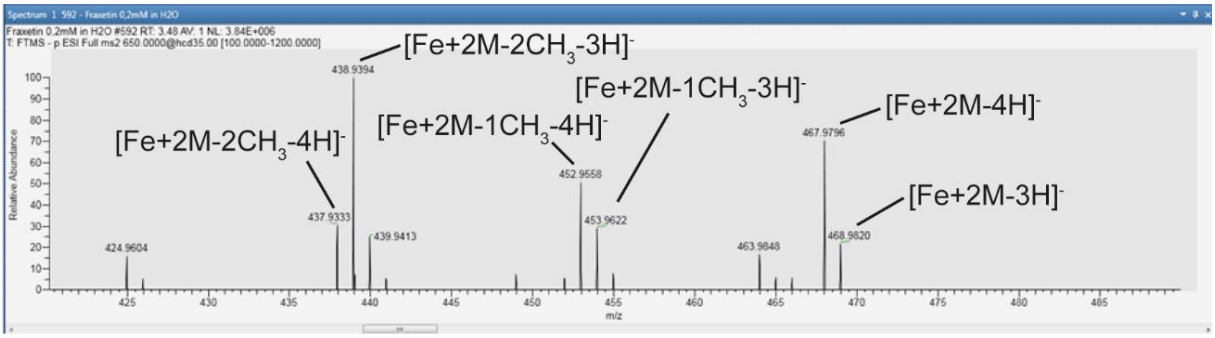

Fig. 26. Detection of Fe-fraxetin complexes without external addition of Fe. Full MS2 scan (negative mode) of 0.2 mM fraxetin incubated in mQ-H_2O without Fe for 30 min at room temperature and 1000 rpm in darkness. After subsequent filtration, the sample was analyzed by UPLC-HRMS (Orbitrap). M = free ligand.

4.11 Expression analysis of genes involved in coumarin biosynthesis and secretion in dependence of pH and buffer conditions

Recent studies have indicated that the coumarin composition of root exudates and extracts is influenced by the external pH (Sisó-Terraza *et al.*, 2016; Rajniak *et al.*, 2018) but the underlying mechanisms are largely unknown. Therefore, it was investigated whether coumarin biosynthesis and/or release are affected by different pH and buffer conditions and whether the external pH can act independently of the plant nutritional status. In an initial step, the effect of Fe, pH and buffers on in the expression of genes involved in coumarin biosynthesis and secretion was assessed. In order to distinguish between responses induced by external pH or the plants' Fe status, plants were exposed to different external pH and buffer conditions in the presence of highly soluble Fe (i.e., FeEDDHA), non-available Fe (i.e., $FeCl_3$) or without added Fe (i.e. 0 Fe). The concentration of FeEDDHA and $FeCl_3$ was adjusted in such a way that plants received the same final amount of Fe. As FeEDDHA possesses a high stability over a wide pH range, this source was considered to allow sufficient Fe supply to the plants under all tested pH and buffer conditions. This was confirmed as plants grown in the presence of FeEDDHA did not develop Fe-deficiency symptoms even when cultivated at alkaline pH (Fig. 27A and B). When $FeCl_3$ was used as the Fe source, chlorophyll concentrations decreased gradually over time in plants cultivated at pH 6.5 and pH 7.5, reaching the lowest levels after 4 days (Fig. 27C and D). At pH 5.6, chlorophyll concentrations also decreased after 2 days but recovered after 4 d (Fig. 27C and D), probably because the coumarins released in response to the initial Fe deficiency helped plants to acquire more Fe. In the absence of Fe, chlorosis worsened and chlorophyll levels decreased gradually under all pH conditions (Fig. 27E and F). Altogether, this initial physiological characterization indicated that the expected conditions

were achieved to investigate Fe-, pH- and buffer-dependent transcriptional responses of Fe-acquisition genes in roots.

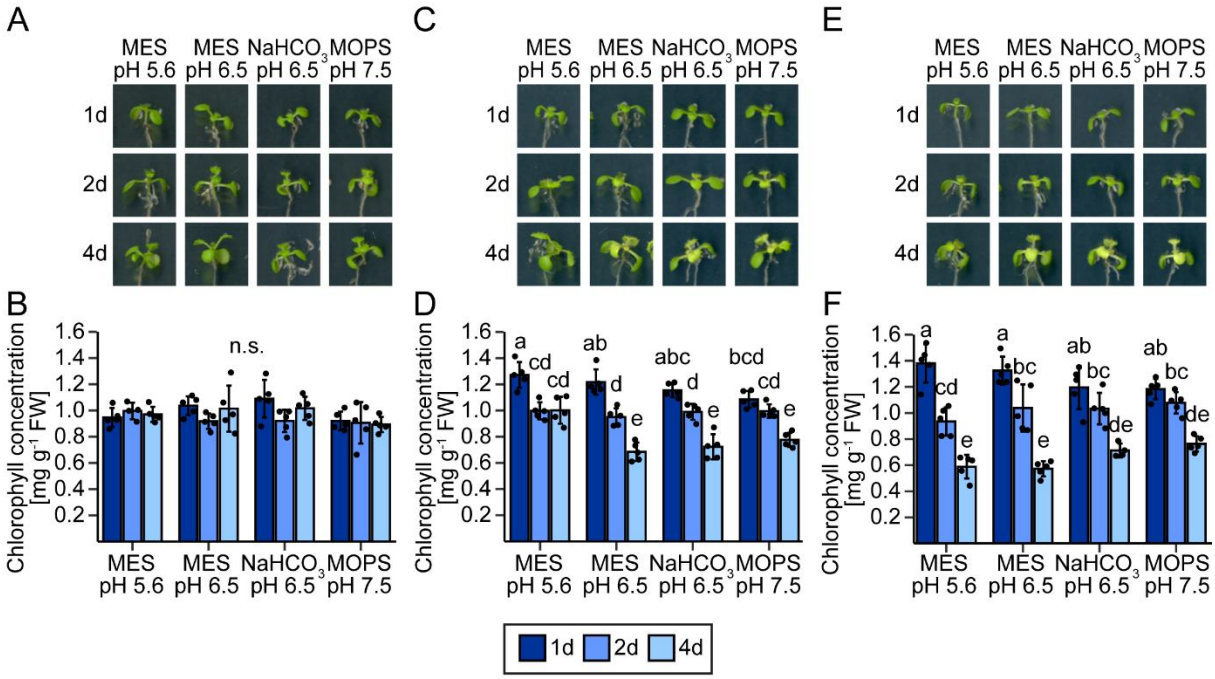

Fig. 27. Physiological characterization of the Fe nutritional status of plants exposed to different Fe sources and external pH and buffer conditions. Appearance (A, C, E) and chlorophyll concentration (B, D, F) of wild-type (Col-0) plants grown for 1 d, 2 d, or 4 d under different pH and buffer conditions in the presence of FeEDDHA (A and B), $FeCl_3$ (C and D), or without added Fe (E and F). Plants were pre-cultured for 10 d on one-half strength MS medium with 40 µM FeEDTA (pH 5.6) and then transferred to one-half strength MS medium with either 80 µM FeEDDHA, 20 µM $FeCl_3$, or without added Fe plus 15 µM ferrozine to inactivate any Fe contaminants. Different pH values were adjusted with different buffers as indicated. The total amount of Fe effectively supplied in the FeEDDHA and $FeCl_3$ treatments was the same. Bars represent means ± s.d. (n = 4-5 biological replicates). Different letters indicate significant differences according to one-way ANOVA with post-hoc Tukey's test at $p \leq 0.05$.

Next, the expression levels of *FIT*, *MYB72*, *F6'H1*, *S8H*, *CYP82C4*, *BGLU42*, and *PDR9* were determined in roots collected from plants grown under the conditions described above. Results were expressed as fold changes relative to plants grown for 1 day on MES pH 5.6 of the respective Fe treatment. In order to capture the main variability in the expression patterns of all investigated genes in dependence of the investigated pH and buffer conditions, a principal component analysis (PCA) for each Fe treatment and time point was conducted (Fig. 28).

PCA revealed clear differences between the investigated pH and buffer conditions both for the different Fe treatments and time points. When Fe was supplied as FeEDDHA, the different pHs and buffers induced distinct expression patterns in roots (Fig. 28A-C), despite plants were showing no signs of Fe deficiency (see Fig. 27A and B). According to PCA, pH 5.6 and pH 7.5 induced the most contrasting transcriptional changes. These distinct expression profiles were induced rapidly as a clear separation along principal component (PC) 1, which explained more than 50% of the variation at all time points, was already observed 1 day after transfer (Fig. 28A-C).

In overall, similar results were also observed when $FeCl_3$ was supplied as the Fe source (Fig. 28D-F). However, a main difference compared to FeEDDHA was that the transcriptional changes induced by pH 5.6 buffered with MES separated more clearly from all other conditions, especially from 2 days after transfer onwards. A clear separation of this pH from all other conditions also persisted when no external Fe was supplied to plants (Fig. 28G-I).

Interestingly, in the presence of FeEDDHA there was no substantial overlap between MES and bicarbonate at pH 6.5, while under $FeCl_3$ and especially under no added Fe these two buffers triggered strongly overlapping responses. These results suggest that bicarbonate itself can trigger specific transcriptional responses, which are probably overruled by Fe deficiency.

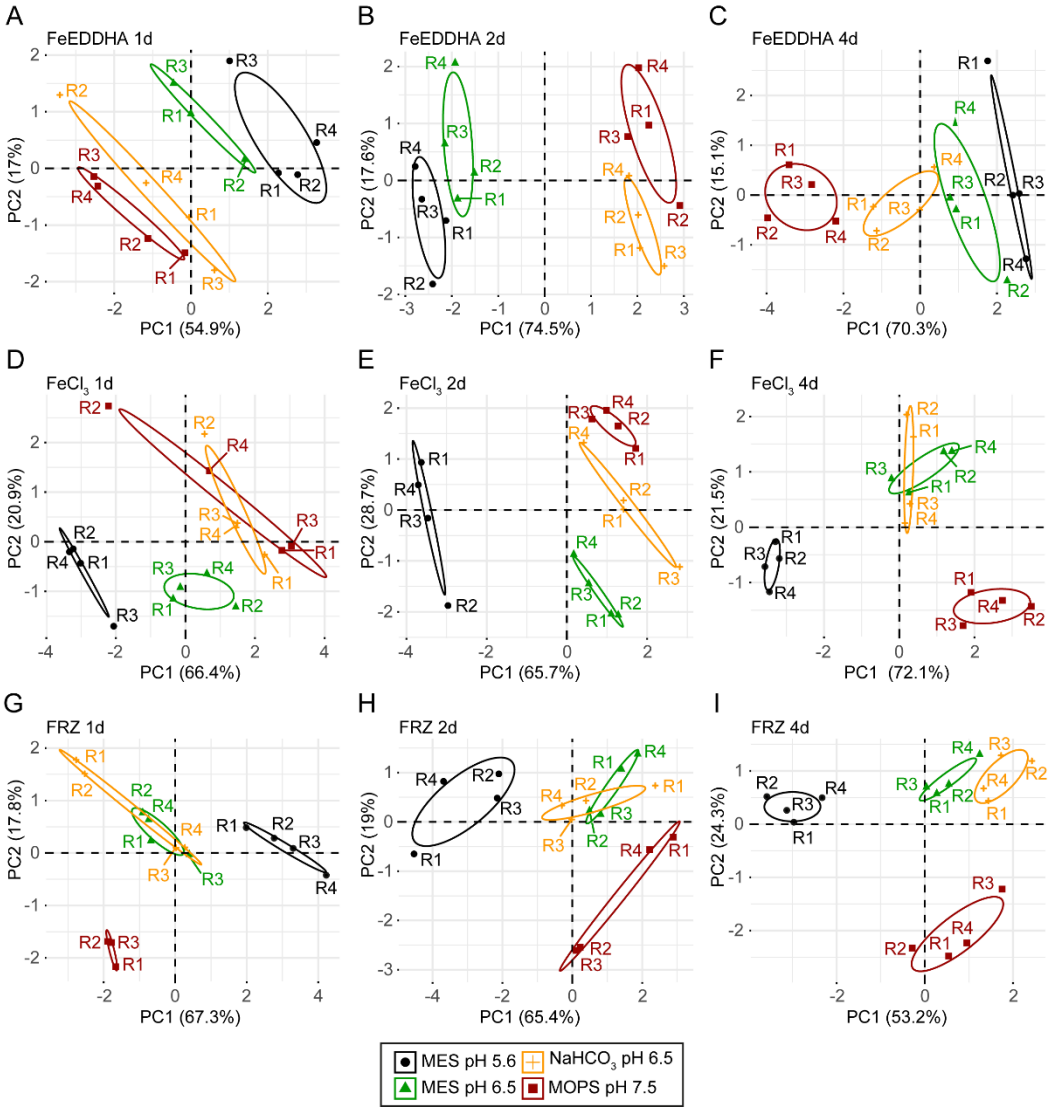

Fig. 28. Principle component analysis (PCA) of the variation in gene expression in response to the plant's Fe status and external pH and buffer conditions. PCAs are based on the relative expression of *FIT*, *MYB72*, *F6'H1*, *S8H*, *CYP82C4*, *BGLU42*, and *PDR9* in roots of wild-type (Col-0) plants grown for 1 d, 2 d, or 4 d under different pH and buffer conditions in the presence of FeEDDHA (A-C), $FeCl_3$ (D-F), or zero Fe (G-I), respectively. Ten day-old plants pre-cultured on one-half strength MS medium with 40 µM FeEDTA (pH 5.6) were transferred to one-half strength MS medium with either 80 µM FeEDDHA, 20 µM $FeCl_3$, or without added Fe plus 15 µM ferrozine to inactivate any Fe contaminants. Different pH values were adjusted with different buffers as indicated. The total amount of Fe effectively supplied in the FeEDDHA and $FeCl_3$ treatments was the same. Plotted are PC1 against PC2. Percent variation explained by each PC is indicated in each plot.

In order to determine whether transcriptional changes under each Fe scenario are associated with the nutritional Fe status of plants, all obtained transcriptional data were correlated with the chlorophyll concentration. As all investigated genes are induced by Fe deficiency (Colangelo and Guerinot, 2004; Jakoby *et al.*, 2004; Palmer *et al.*, 2013; Fourcroy *et al.*, 2014; Schmid *et al.*, 2014; Pan *et al.*, 2015; Rajniak *et al.*, 2018; Stringlis *et al.*, 2018), significant negative correlations with shoot chlorophyll were determined only when Fe was omitted from the medium or supplied as $FeCl_3$ but not when supplied as FeEDDHA (Fig. 29). Under such conditions, *FIT* and *S8H* expression showed the highest negative correlations with shoot chlorophyll concentrations. A moderate correlation was determined also for *BGLU42* but only under $FeCl_3$ (Fig. 29B). For all other genes, correlations with chlorophyll concentrations were low ($r^2 \leq 0.5$) or absent ($r^2 \leq 0.3$) independent of the Fe treatment (Fig. 29B and C). The lower correlation of *MYB72* expression with shoot chlorophyll levels compared to *FIT* suggests that expression of the transcription factor *MYB72* is not only ruled by the plant nutritional Fe status.

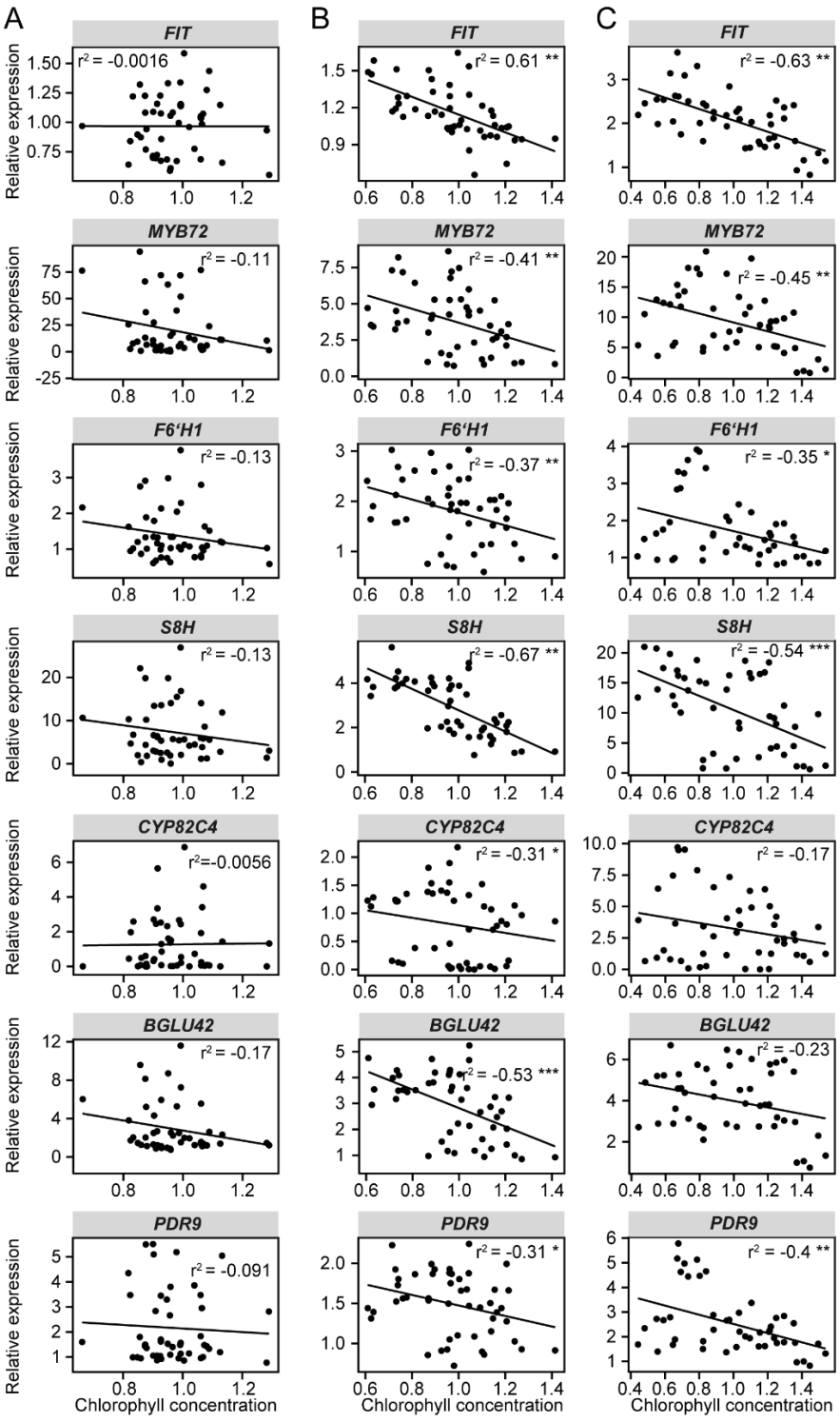

Fig. 29. Correlation analysis of gene expression levels and shoot chlorophyll concentrations in response to different Fe, pH, and buffer conditions. (A-C) Correlation plots of the relative root expression of *FIT*, *MYB72*, *F6'H1*, *S8H*, *CYP82C4*, *BGLU42*, and *PDR9* with the chlorophyll concentration in shoots of wild-type (Col-0) plants grown for 1 d, 2 d, and 4 d under different pH and buffer conditions in the presence of FeEDDHA (A), $FeCl_3$ (B), or zero Fe (C), respectively. Plants were pre-cultured on one-half strength MS medium with 40 µM FeEDTA (pH 5.6) for 10 d and then transferred to one-half strength MS medium with either 80 µM FeEDDHA, 20 µM $FeCl_3$, or without added Fe plus 15 µM ferrozine to inactivate any Fe contaminants. The medium was buffered with either MES to pH 5.6 or pH 6.5, $NaHCO_3$ (1 mM) to pH 6.5, or MOPS to pH 7.5, respectively. The total amount of Fe effectively supplied in the FeEDDHA and $FeCl_3$ treatments was the same. Gene expression levels were calculated as fold changes referring to plants grown for 1 d on MES pH 5.6 of the respective Fe treatment. r^2 values define correlation coefficients according to Pearson or Spearman. Asterisks indicate statistical significance of the correlation with * $p \leq 0.05$, ** $p \leq 0.01$, *** $p \leq 0.001$.

To determine which of the genes related with coumarin biosynthesis or secretion are more strongly co-regulated and how their expression is associated with *FIT* and *MYB72* in dependence of the different Fe conditions, hierarchical cluster analysis was conducted (Fig. 30). Similar clusters were obtained when Fe was present in the medium irrespective of its form and solubility (Fig. 30A and B). Under such conditions, *S8H* clustered together with *MYB72*, and *F6'H1* with *FIT* while *CYP82C4* stood separately. Close co-regulation of *S8H* with *MYB72* was also observed when Fe was omitted from the medium (Fig. 30C). The transcriptional response of *PDR9* was always clustered with *FIT* and *F6'H1*, irrespective of the external Fe supply, while *BGLU42* was more closely co-regulated with *MYB72* and *S8H* but only when Fe was present in the medium (Fig. 30). In the absence of Fe, the expression of *CYP82C4* and *BGLU42* clustered more closely with *FIT*, however, less closely than *F6'H1* and *PDR9* (Fig. 30C).

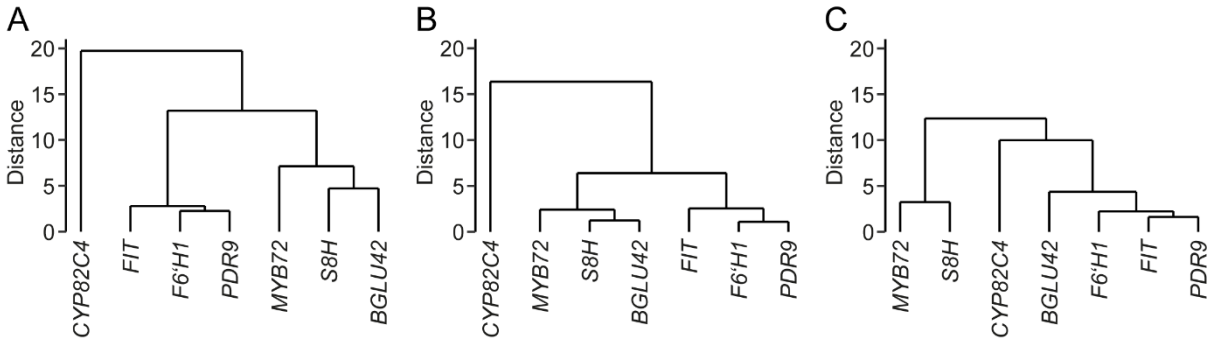

Fig. 30. Hierarchical cluster analysis of gene expression in response to different conditions of Fe availability. (A-C) Dendrogram of the relative expression of *FIT*, *MYB72*, *F6'H1*, *S8H*, *CYP82C4*, *BGLU42*, and *PDR9* in roots of wild-type plants grown for 1 d, 2 d, and 4 d under different pH and buffer conditions in the presence of FeEDDHA (A), $FeCl_3$ (B), or zero Fe (C). Ten-d-old plants pre-cultured on one-half strength MS medium with 40 µM FeEDTA (pH 5.6) were transferred to one-half strength MS medium with either 80 µM FeEDDHA, 20 µM $FeCl_3$, or without added Fe plus 15 µM ferrozine to inactivate any Fe contaminants. The medium was buffered with either MES to pH 5.6 or pH 6.5, $NaHCO_3$ (1 mM) to pH 6.5, or MOPS to pH 7.5, respectively. The total amount of Fe effectively supplied in the FeEDDHA and $FeCl_3$ treatments was the same. Gene expression levels were calculated as fold changes from plants grown for 1 d on MES pH 5.6 of the respective Fe treatment and $\log_2$ transformed. The ordinate axis indicates the distance between different clusters.

Since the most contrasting effect between the different pH and buffer conditions were observed after 4 days on the treatments (Fig. 28), the expression of the individual investigated genes was assessed in more detail at this time point (Fig. 31).

The expression of *FIT* was slightly induced by higher external pH values as long as Fe was not added or only supplied as a sparingly available form. Compared to *FIT*, the expression of *MYB72* responded even more strongly to increases in the external pH (Fig. 31). This response was fast, as it was detected already 1 day after transfer (Annex Figs. 14-16). Interestingly, the pH-dependent regulation of MYB72 was largely independent of the Fe status of shoots, as it was maintained even in plants grown in the presence of FeEDDHA (Fig. 27A and B). These results suggest that the transcription factors FIT and MYB72 respond to partially distinct signaling cascades.

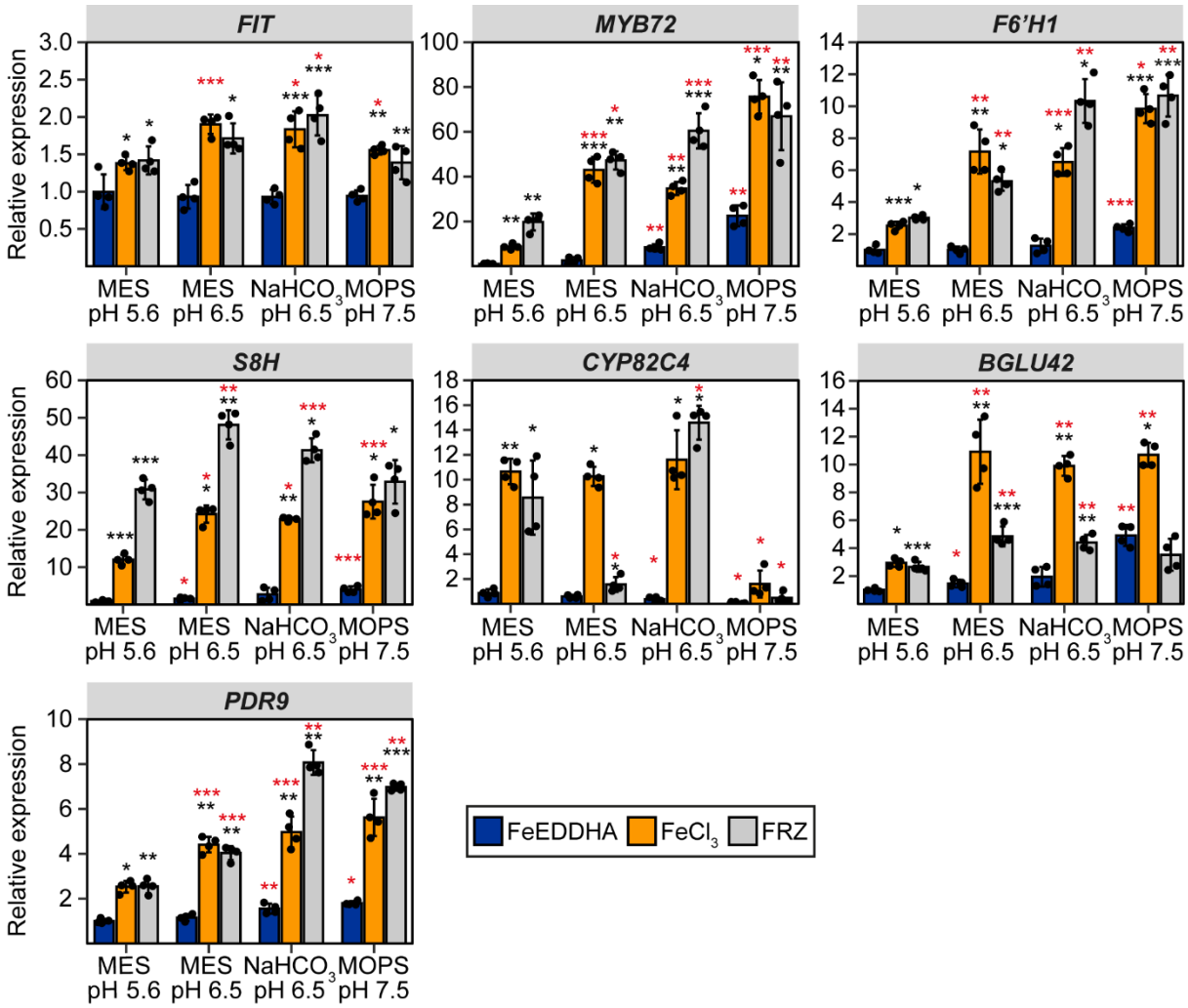

Fig. 31. Analysis of the expression of genes involved in coumarin biosynthesis and secretion in dependence of to the plant's Fe status and external pH and buffer conditions. Relative expression of *FIT*, *MYB72*, *F6'H1*, *S8H*, *CYP82C4*, *BGLU42*, and *PDR9* in roots of wild-type (Col-0) plants grown for 4 d under different Fe, pH and buffer conditions. After 10 d of pre-culture on one-half strength MS medium with 40 µM FeEDTA (pH 5.6), plants were transferred to one-half strength MS medium with either 80 µM FeEDDHA, 20 µM $FeCl_3$ or without added Fe plus 15 µM ferrozine to inactivate any Fe contaminants (FRZ). Different pH values were adjusted with different buffers as indicated. The total amount of Fe effectively supplied in the FeEDDHA and $FeCl_3$ treatments was the same. Gene expression levels were calculated as fold change compared to plants grown in the presence of FeEDDHA at pH 5.6. Bars indicate means ± s.d. (n = 4 biological replicates). Significant differences are indicated as asterisks according to Student's *t*-test, Welch's *t*-test or Mann-Whitney U test with α=0.05; * $p \leq 0.05$, ** $p \leq 0.01$, *** $p \leq 0.001$. Black asterisks indicate comparisons between $FeCl_3$ or zero Fe vs. FeEDDHA grown plants at the different pH and buffer conditions, respectively. Red asterisks indicate comparisons between MES pH 6.5, $NaHCO_3$ pH 6.5, or MOPS pH 7.5 vs MES pH 5.6 grown plants for the individual Fe treatments. Changes in gene expression over time (all time points) are additionally shown in Annex Figures 14-16.

Among the coumarin biosynthesis genes, *S8H* showed the strongest fold-change response to Fe availability and pH conditions. *S8H* expression was consistently induced by high pH, especially under conditions that induced Fe deficiency. Additionally, *S8H* transcription levels determined in plants grown in the absence of Fe were around 1.8 to 2.5-fold higher compared to $FeCl_3$ at pH 5.6 and pH 6.5. *F6'H1* expression increased with increasing pH especially under $FeCl_3$ and no added Fe. However, the most striking transcriptional response was detected for *CYP82C4*, whose expression was strongly repressed when the external pH was raised to 7.5

(Fig. 31). The inhibitory effect of alkaline pH on *CYP82C4* expression was observed as soon as 1 day after transfer when Fe was supplied to the medium, while it was partially attenuated when Fe was absent from the external medium (Annex Figs. 14-16). At all other external pH conditions, *CYP82C4* transcript levels were significantly enhanced when Fe was absent or supplied as $FeCl_3$. Thereby, *CYP82C4* expression was comparable under the different Fe treatments except for pH 6.5 buffered with MES. Under this condition, the lack of Fe from the external medium did not lead to any changes in *CYP82C4* expression. The expression of *BGLU42* and *PDR9* was slightly induced as the external pH was increased when Fe was provided as FeEDDHA. Under conditions of low Fe availability when Fe was not added or supplied as $FeCl_3$, *BGLU42* expression was consistently induced by elevated pH conditions, whereas *PDR9* transcription increased with increasing pH especially under no added Fe (Fig. 31). Thereby, *BGLU42* expression levels were significantly lower in plants when Fe was absent.

To summarize, the qPCR data indicated that the expression of genes involved in coumarin biosynthesis and secretion is distinctively affected by the external pH while pH buffers play a rather minor role. Alkaline pH can trigger transcriptional changes largely independent of the plant nutritional Fe status, but this response can be further amplified by Fe deficiency. Furthermore, the data suggest that high pH conditions have a stronger effect on the transcriptional expression of genes involved in coumarin biosynthesis than coumarin secretion.

4.12 pH-dependent changes in abundance and tissue-specific localization of coumarin biosynthesis enzymes

Given the noticeable differences in the transcriptional regulation of coumarin biosynthesis genes in response to different external pH conditions, the hypothesis was tested whether the pH conditions also affect the abundance and tissue-specific localization of the corresponding proteins. Therefore, transgenic lines expressing F6'H1-GFP, S8H-GFP, or CYP82C4-GFP under the control of the respective native promoters from Col-0 were generated. After the selection of representative lines, one T2 line for each construct was used for protein localization studies. Since the expression levels of *F6'H1*, *S8H*, and *CYP82C4* are low when Fe is supplied as FeEDDHA (Fig. 31), pH-dependent responses were assessed only in the absence of Fe or in the presence of $FeCl_3$.

Confocal imaging of plants expressing *proF6'H1::F6'H1:GFP* or *proS8H::S8H-GFP*, revealed a dramatic increase in the protein levels of F6'H1 and S8H in the root hair zone at elevated pH values (i.e., pH ≥ 6.5) irrespective of the buffer or Fe condition (Fig. 32A-B and 33A-B). In agreement with previous findings reported by Schmid *et al.* (2014), F6'H1 protein was detected in epidermal and cortical cells both in the presence and absence of Fe (Fig. 32A and 33A). In

contrast to F6'H1, the external pH conditions had a strong effect on the cell type-specific localization of S8H. At pH 5.6 and pH 6.5 buffered with MES, S8H protein was strongly confined to epidermal cells, while exposure of plants to pH 7.5 or pH 6.5 buffered with bicarbonate induced a prominent accumulation of S8H in cortical cells (Fig. 32B and 33B).

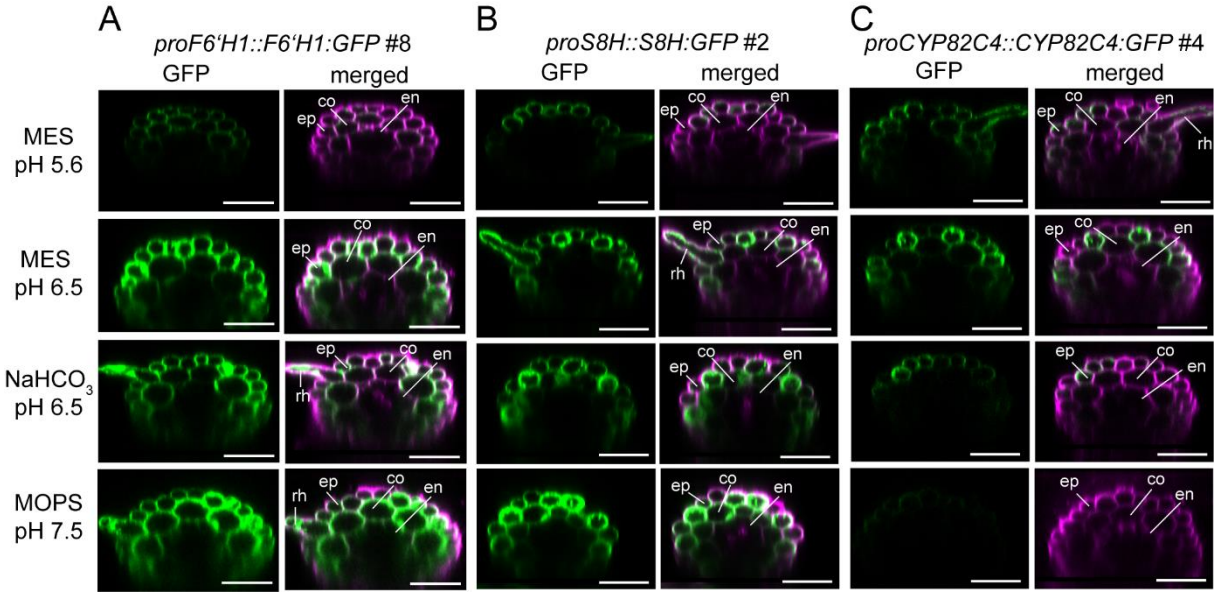

Fig. 32. pH-dependent abundance and tissue-specific localization of F6'H1-, S8H- and CYP82C4-GFP fused proteins in roots exposed to different external pH and buffer conditions in the presence of $FeCl_3$. (A-C) GFP-dependent fluorescence (green) and merged GFP and propidium iodide (magenta) signals of *proF6'H1::F6'H1:GFP* (A), *proS8H::S8H:GFP* (B) and *proCYP82C4::CYP82C4:GFP* (C) translational fusions. Plants were pre-cultured for 10 d on one-half strength MS medium with 40 µM FeEDTA (pH 5.6) and then transferred to one-half strength MS medium with 20 µM $FeCl_3$ buffered with either MES to pH 5.6 or pH 6.5, $NaHCO_3$ to pH 7.5, or MOPS to pH 7.5. Shown are transverse sections reconstituted from Z-stack images taken from representative lines. Root tissue layers are labeled as ep: epidermis, rh: root hairs, co: cortex, en: endodermis. Scale bars = 50 µm.

In line with the qPCR results (Fig. 30), also CYP82C4 protein accumulation was repressed at pH 7.5 (Fig. 32C and 33C). In overall, CYP82C4 was mainly localized in the epidermis but weak fluorescence was also detected in cortical cells. The increase of external pH from 5.6 to pH 6.5 slightly increased the accumulation of CYP82C4 when $FeCl_3$ was provided and buffered by MES.

Together, the data indicate that the external pH and buffer conditions also affect the abundance and tissue-specific localization of the coumarin biosynthesis proteins in roots.

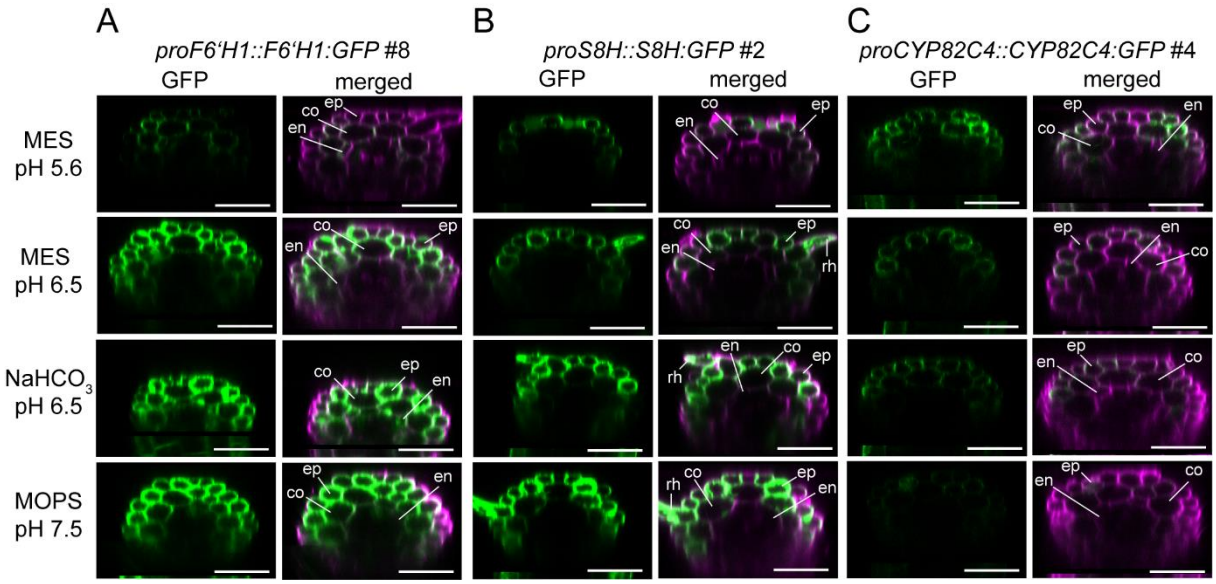

Fig. 33. pH-dependent abundance and tissue-specific localization of F6'H1-, S8H- and CYP82C4-GFP fused proteins in roots exposed to different external pH and buffer conditions in the absence of Fe. (A-C) GFP-dependent fluorescence (green) and merged GFP and propidium iodide (magenta) signals of *proF6'H1::F6'H1:GFP* (A), *proS8H::S8H:GFP* (B) and *proCYP82C4::CYP82C4:GFP* (C) translational fusions. Plants were pre-cultured for 10 d on one-half strength MS medium with 40 µM FeEDTA (pH 5.6) and then transferred to one-half strength MS medium without added Fe and buffered with either MES to pH 5.6 or pH 6.5, $NaHCO_3$ to pH 6.5, or MOPS to pH 7.5. Shown are transverse sections reconstituted from Z-stack images taken from representative lines. Root tissue layers are labeled as ep: epidermis, rh: root hairs, co: cortex, en: endodermis. Scale bars = 50 µm.

4.13 External pH affects coumarin composition in roots and root exudates

The partially distinct effects of external pH and buffering conditions on the accumulation of coumarin biosynthesis enzymes are expected to alter the amounts of the different coumarins that are produced and released by Arabidopsis roots. To investigate this possibility, the coumarin composition in root extracts and exudates of wild-type plants (Col-0) was assessed by UPLC-MS/MS. Plants were cultivated as described in previous sections and root extracts and exudates were collected after 4 days. As bicarbonate strongly repressed the signal of the internal standard 4-methyldaphnetin (Annex Fig. 17), a coumarin species not produced by Arabidopsis and that was spiked prior to sample analysis, root exudates and root extracts collected from plants exposed to bicarbonate were not analyzed.

As expected, in root extracts, the glycosylated coumarins (i.e. scopolin, esculin, and fraxin) were more abundant than the corresponding deglycosylated forms (Fig. 34A). Overall, coumarin levels in roots were significantly higher in plants grown in the absence of Fe as compared to those grown with $FeCl_3$. The most prominent coumarin determined in root extracts was scopolin irrespective of the Fe treatment and external pH (Fig. 34A). When $FeCl_3$ was supplied as the Fe source, scopolin concentration was largely unaffected by the external pH, while its amount significantly decreased as the external pH increased under Fe-deprived conditions. This is most likely due to an enhanced release of its aglycon scopoletin and an increased conversion into fraxetin especially at pH 6.5 under severe Fe limitation (Fig. 34A

and 35A). In contrast, esculin and fraxin concentrations in roots increased consistently as the pH was raised irrespective of Fe (Fig. 34A). However, the relative concentration increments of these two catecholic coumarins was higher under $FeCl_3$-supplied conditions especially as the pH was raised from 6.5 to pH 7.5. The sideretin concentration in roots also significantly increased at pH 6.5, while it strongly decreased at pH 7.5. In contrast, esculetin and fraxetin accumulated in roots as the pH increased, while scopoletin concentrations remained largely unaffected by the different external pH conditions. Despite the clear pH-dependent changes in root concentration of most individual coumarins, when the concentration of all coumarins detected in roots were combined, the external pH had a minor effect on the total levels of non-glycosylated coumarins (Fig. 34B). This was mainly because the slight decrease in scopolin levels was largely compensated by increases in esculin and fraxin (Fig. 34A). In the case of the non-glycosylated coumarins, the lacking responsiveness of scopoletin to pH changes contrasted with significant increases in the levels of esculetin, fraxetin, and sideretin at higher external pH values and resulted in increased total levels of non-glycosylated coumarins as pH was raised (Fig. 34B).

Given the noticeable differences in the concentration of the different coumarin glycosides and their corresponding aglycons in roots according to the external pH conditions (Fig. 34), the percentage of deglycosylated coumarin in relation to its corresponding glycoside in root extracts was additionally calculated. For scopoletin/scopolin, the percentage was always below 1.5%, while the percentage of fraxetin to fraxin increased from around 9% and 21% in the absence and presence of Fe at pH 5.6, respectively, to more than 30% at pH 7.5. This suggests that scopolin deglycosylation mainly occurs during or after its exudation, while significant fraxin deglycosylation can already occur inside roots. Furthermore, these data indicate that scopolin synthesis in roots is largely pH independent but its deglycosylation during or after exudation is responsive to the external pH. In the case of fraxin/fraxetin, both the synthesis and deglycosylation are regulated in a pH-dependent manner.

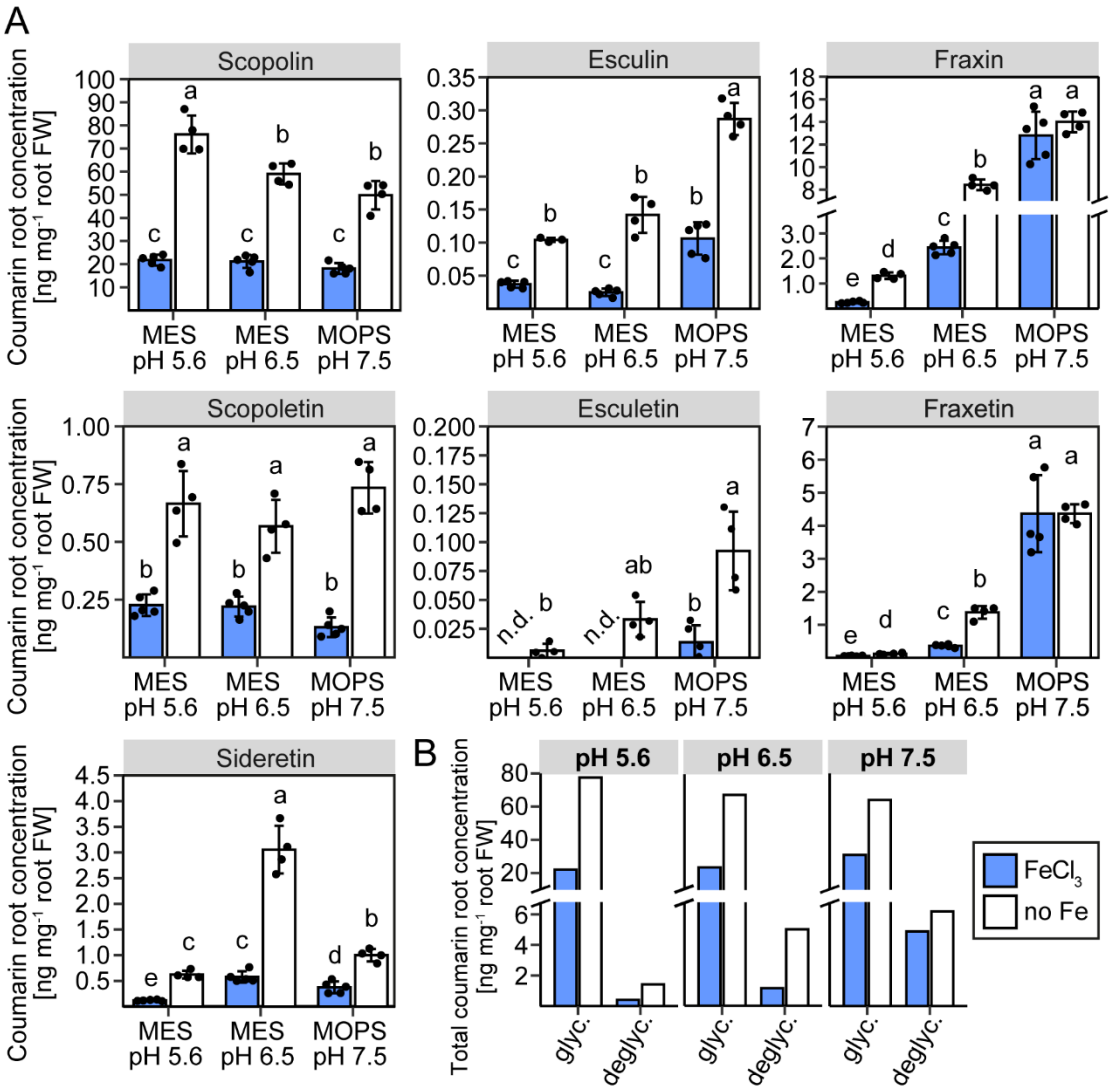

Fig. 34. Coumarin concentrations in roots of plants exposed to different Fe and external pH conditions. (A) Coumarin root concentration of wild-type (Col-0) plants grown for 4 d under different Fe-limiting conditions in the presence (blue bars; $FeCl_3$) or absence (white bars; no Fe) of Fe. Plants were pre-cultured for 10 d on one-half strength MS medium with 40 µM FeEDTA (pH 5.6) and then transferred to one-half strength medium with 20 µM $FeCl_3$ or without added Fe and 15 µM ferrozine buffered with either 2.5 mM MES to pH 5.6 or pH 6.5, or MOPS to pH 7.5. Level of coumarins in root extracts as determined by UPLC-MS (Triple Quad for $FeCl_3$ samples; Orbitrap for ferrozine (no Fe) samples). Bars represent means ± s.d. (n = 4-5 biological replicates). Significant differences are indicated by asterisks according to Student's *t*-test with α=0.05; * $p \leq 0.05$, ** $p \leq 0.01$, *** $p \leq 0.001$. Different letters indicate significant differences according to one-way ANOVA with post-hoc Tukey's test at $p \leq 0.05$ or Welch's ANOVA with post-hoc Games-Howell test at $p < 0.05$. (B) Total coumarin root concentration as sum of glycosylated (glyc; scopolin, esculin, fraxin) and deglycosylated (deglyc.; scopoletin, esculetin, fraxetin, sideretin) coumarins. n.d.: not detected.

Among the glycosylated coumarins, only scopolin and fraxin were found at low amounts in root exudates especially when $FeCl_3$ was present in the media (Fig. 35A). While fraxin was detected only at pH 7.5, scopolin was found at all three pH conditions. The release of deglycosylated forms, in turn, was stimulated more strongly when no Fe was added (Fig. 35A). The most prominent coumarins determined in root exudates were fraxetin and sideretin. While sideretin predominated at pH 5.6 and pH 6.5, fraxetin became the major coumarin in exudates at pH 7.5. In overall, the exudation of scopoletin, esculetin, and fraxetin was stimulated by higher external pH conditions, irrespective of whether Fe was present or not. In contrast, when the

pH increased to pH 7.5 the exudation of sideretin was strongly inhibited. These results are in line with the strong repression of *CYP82C4* expression and protein accumulation when the external pH is alkaline (see Figs. 31-33). In consequence, although the total amount of deglycosylated coumarins exuded by roots was not substantially changed when the external pH increased from 6.5 to 7.5 (Fig. 35B), the composition of the exudates was significantly altered.

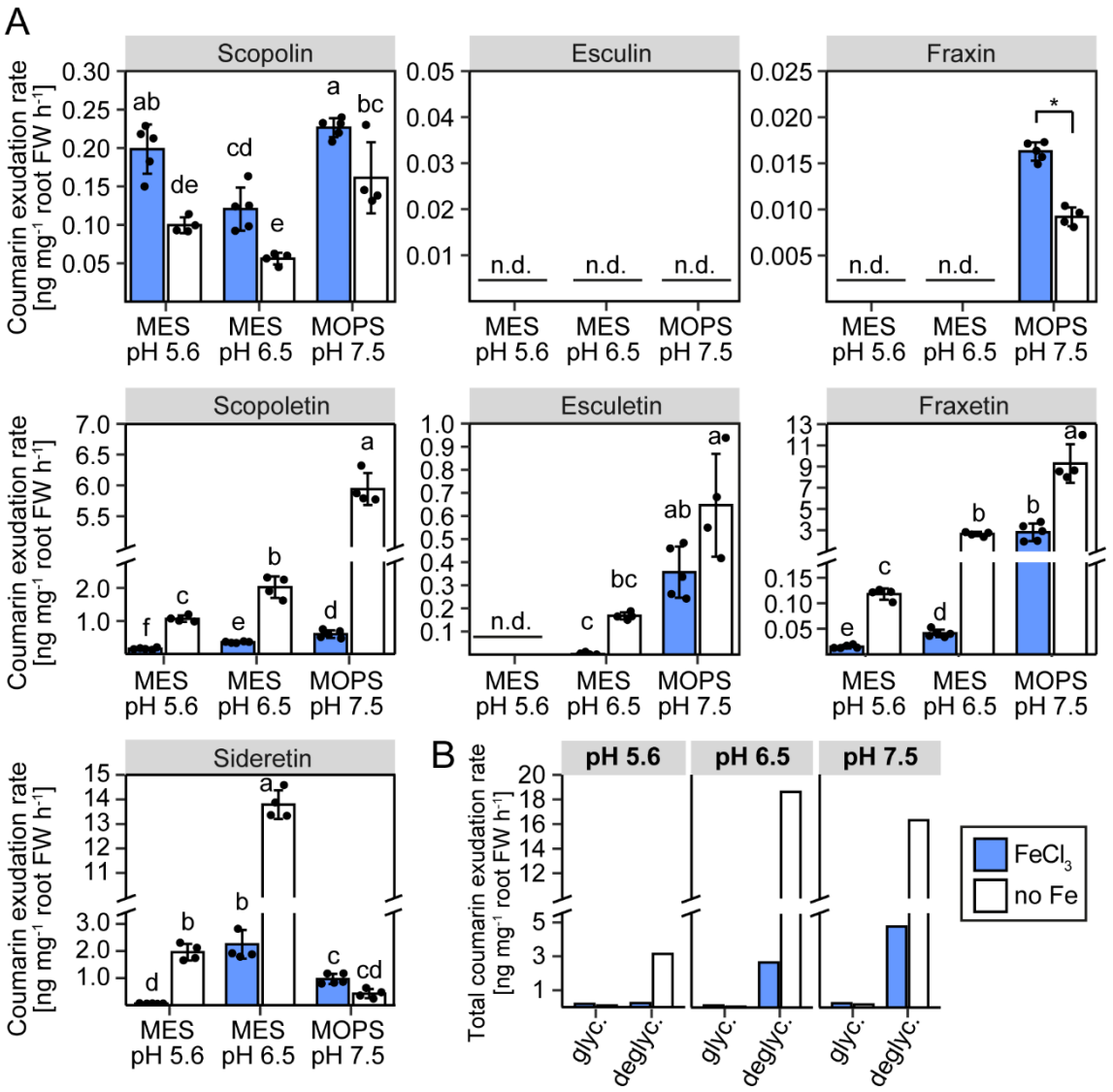

Fig. 35. Coumarin exudation rates of plants exposed to different Fe and external pH conditions. (A) Coumarin exudation rate of wild-type (Col-0) plants grown for 4 d under different Fe-limiting conditions in the presence (blue bars; $FeCl_3$) or absence (white bars; no Fe) of Fe. Plants were pre-cultured for 10 d on one-half strength MS medium with 40 µM FeEDTA (pH 5.6) and then transferred to one-half strength medium with 20 µM $FeCl_3$ or without added Fe and 15 µM ferrozine buffered with either 2.5 mM MES to pH 5.6 or pH 6.5, or MOPS to pH 7.5. After 4 d, root exudates were collected for 6 h on MES or MOPS buffer adjusted to the respective pH. Coumarins were determined by UPLC-MS (Triple Quad for root exudates of plants grown in the presence of $FeCl_3$; Orbitrap for root exudates of plants grown in the presence of ferrozine). Bars represent means ± s.d. (n = 4-5 biological replicates). Significant differences are indicated by asterisks according to Student's *t*-test with α=0.05; * $p \leq 0.05$, ** $p \leq 0.01$, *** $p \leq 0.001$. Different letters indicate significant differences according to one-way ANOVA with post-hoc Tukey's test at $p \leq 0.05$ or ANOVA on ranks with post-hoc Dunn's test at $p < 0.05$. (B) Total coumarin root concentration as sum of glycosylated (glyc; scopolin, esculin, fraxin) and deglycosylated (deglyc.; scopoletin, esculetin, fraxetin, sideretin) coumarins. n.d.: not detected.

Altogether, the data indicate that the external pH determines the amount and composition of coumarins in roots and root exudates by affecting coumarin biosynthesis, deglycosylation and, possibly, secretion. Sideretin is the major catecholic coumarin synthesized and released at pH 5.6 and pH 6.5, while fraxetin becomes the predominant catecholic coumarin at pH 7.5. Furthermore, the data suggest that coumarin deglycosylation is a pH-dependent process that can take place already inside roots, or during or after exudation depending on the type of coumarin.

4.14 pH-dependent release of scopoletin is additionally facilitated in a PDR9-independent manner

Given the observation that deglycosylation of the different coumarins preferentially takes place either inside roots or during/after exudation it was then assessed whether PDR9-mediated coumarin secretion responds to external pH changes and pH-dependent changes in coumarin synthesis or secretion are altered if specific biosynthetic steps are disturbed. A PCA analysis revealed clear differences in the coumarin composition of root extracts and exudates of wild-type, *s8h-2*, *cyp82C4-1*, and *pdr9-2* mutant plants (Fig. 36). Irrespective of the external pH the coumarin composition of *s8h-2* roots was the most distinctive compared to wild-type plants (Fig. 36A-C). With regard to the coumarin composition of root exudates, the most prominent separations were detected when S8H- or CYP82C4-dependent steps were disturbed rather than when secretion via PDR9 was impaired independently of the external pH (Fig. 36D-F).

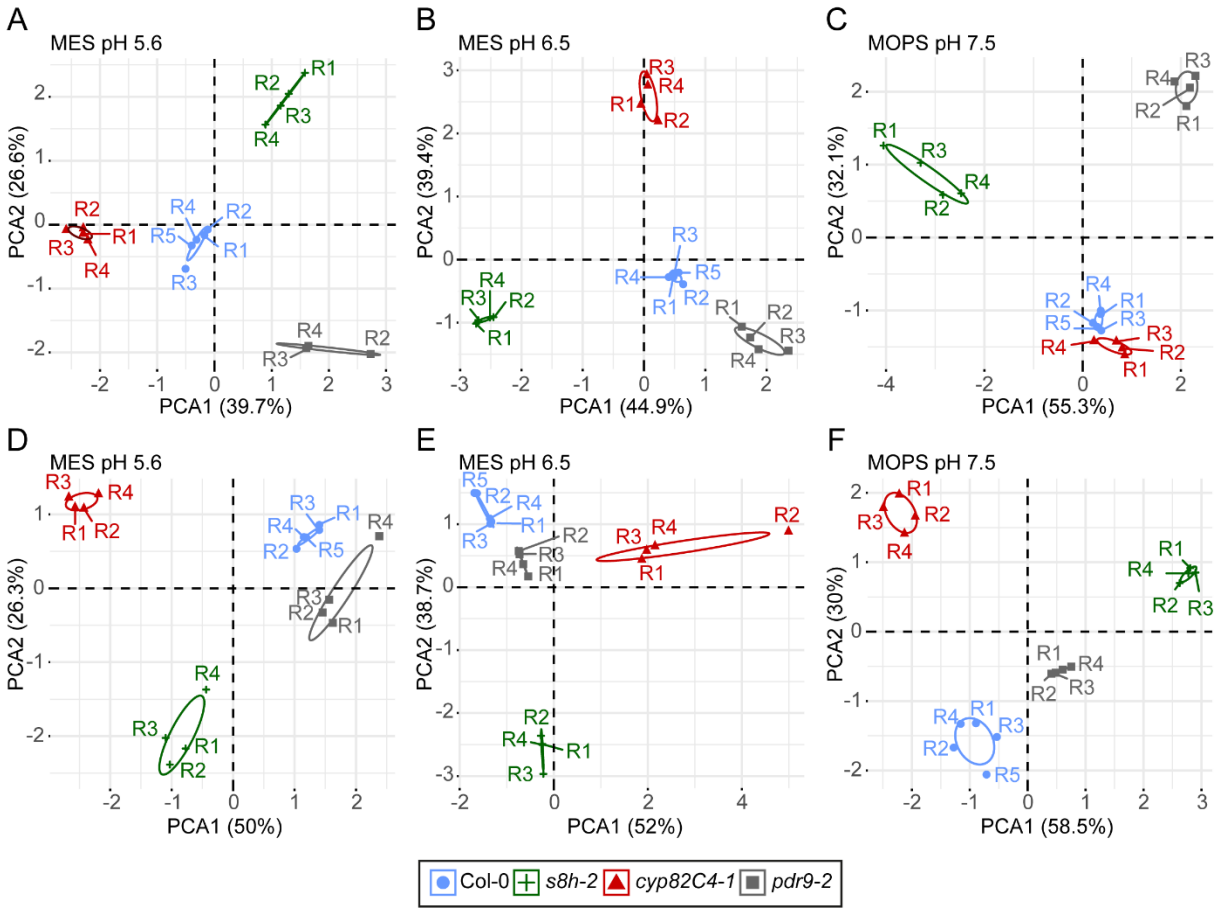

Fig. 36. Principle component analysis (PCA) of coumarin root concentrations and exudation rates of wild type and coumarin biosynthesis and secretion mutants under different external pH conditions. (A-F) PCAs are based on the coumarin root concentration (A-C) and root exudation rate (D-F) of wild-type (Col-0), *s8h-2*, *cycp82C4-1*, and *pdr9-2* plants grown for 4 d under different conditions of low Fe availability. Plants were pre-cultured for 10 d on one-half strength MS medium with 40 µM NaFeEDTA (pH 5.6) and then transferred to one-half strength MS medium with 20 µM $FeCl_3$ buffered with either MES to pH 5.6 or pH 6.5, or MOPS to pH 7.5. Root exudates were collected for 6 h on MES or MOPS buffer adjusted to the respective pH. Coumarins were analyzed with UPLC-MS (Triple Quad for wild-type, *s8h-2*, and *cyp82C4-1*; Orbitrap for *pdr9-2* samples). PCA is based on coumarin root concentrations and exudation rates of wild-type plants as shown in Fig. 34 and 35. Plotted are PC1 against PC2. Percent variation explained by each PC is indicated in each plot.

Considering each coumarin individually, no or only trace amounts of fraxin, fraxetin, and sideretin were detected in root extracts of *s8h-2* plants while scopolin and scopoletin over-accumulated (Fig. 37A). The total coumarin concentration in roots of *s8h-2* plants was increased up to 4.7-fold compared to the wild type and was almost exclusively composed of scopolin (Fig. 37B). Interestingly, by impairing processing of scopolin/scopoletin to catecholic coumarins in roots of *s8h-2* plants, these two coumarins exhibited much more pronounced pH-dependent accumulation than in wild-type plants (Fig. 37A). Although scopoletin levels also increased in *s8h-2* roots, the relative proportion of scopoletin to scopolin was only slightly enhanced with respect to the wild type, suggesting that the scopolin/scopoletin ratio in roots is largely constant and that significant intracellular deglycosylation of scopolin does not take place even when very large amounts of scopolin are synthesized.

In agreement with a previous study (Rajniak *et al.*, 2018), fraxin and fraxetin over-accumulated in roots of *cyp82C4-1* plants (Fig. 37A). In *cyp82C4-1* roots, the concentration of fraxin increased by around 45.8-, 10.8-, and 1.7-fold as compared to the wild type under pH 5.6, 6.5, and 7.5, respectively. A similar pattern, although at smaller fold-changes, was also detected for fraxetin (Fig. 37A). The less pronounced concentration differences with increasing external pH were due to further increases in the concentrations of fraxin and fraxetin as the pH was increased from pH 6.5 to 7.5 in roots of wild-type but not *cyp82C4-1* plants. This result suggests that the absence of functional CYP82C4 allows fraxin accumulation beyond wild type levels but also limits the stimulation of fraxin synthesis by high external pH conditions. Furthermore, the absence of CYP82C4 does not affect fraxin deglycosylation as the percentage of fraxetin to fraxin remained nearly constant at pH 6.5 and pH 7.5. Although scopolin and esculin levels also increased significantly in root extracts of *cyp82C4-1* plants, fraxin and fraxetin were mainly responsible for the overall higher total amount of glycosylated and deglycosylated coumarins in root extracts of this mutant compared to wild type (Fig. 37B). The absence of PDR9 led to significant root accumulation of scopolin, esculin, fraxin, and sideretin irrespectively of the pH (Fig. 37A). Scopoletin levels also increased in *pdr9-2* roots but only at pH 7.5. In overall, the pH-dependent changes in the root concentration of all coumarins followed a similar pattern as in the wild type. This suggests that the absence of PDR9 does not affect the pH-induced changes in coumarin biosynthesis in roots. Interestingly, esculin accumulated at the highest levels in *pdr9-2* root extracts and showed clear increases as the external pH was elevated (Fig. 37A).

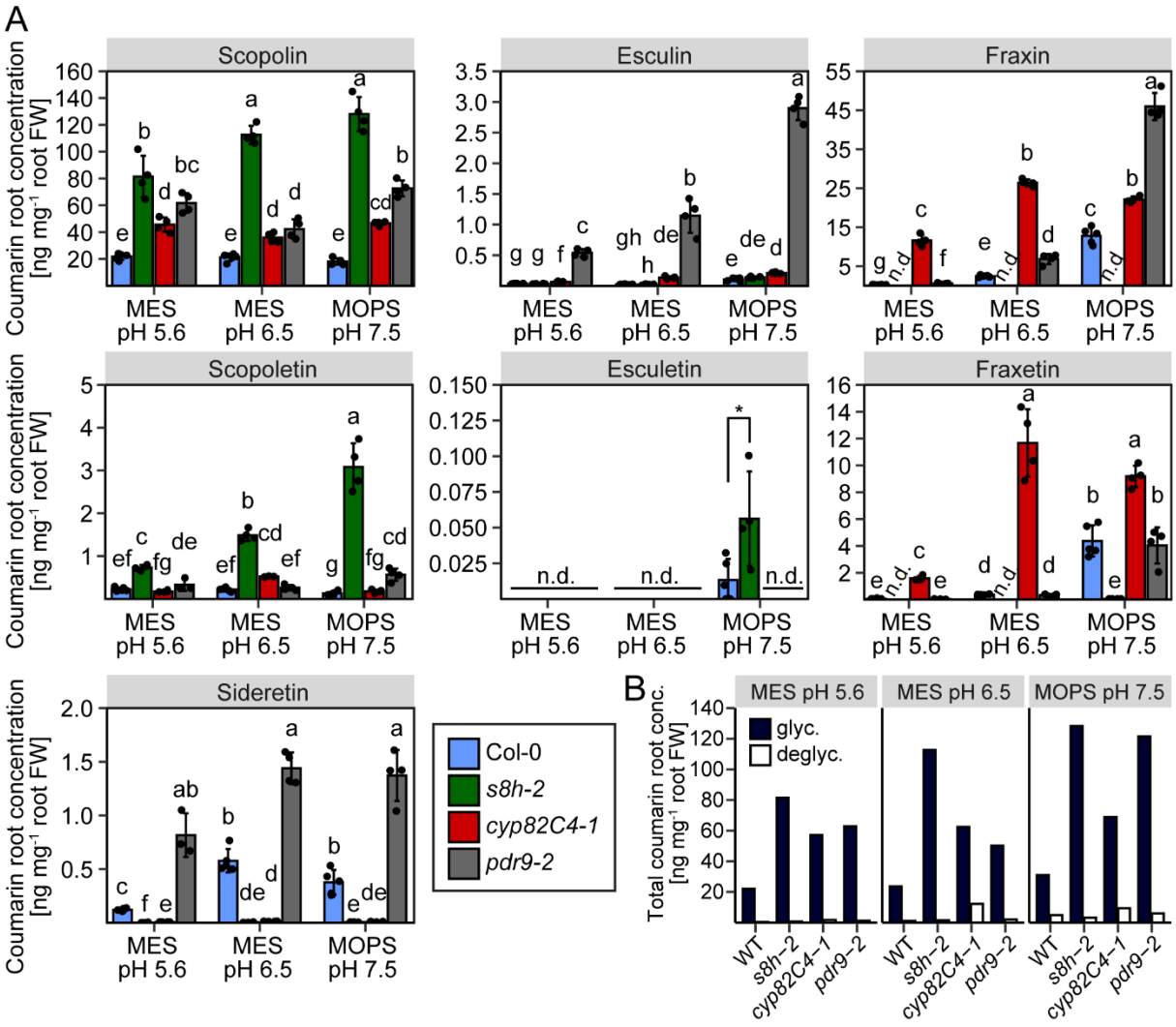

Fig. 37. pH-dependent changes in root accumulation of coumarins in biosynthesis and transport mutants. (A) Concentrations of indicated coumarin in roots of wild-type (Col-0), *s8h-2*, *cyp82C4-1*, and *pdr9-2* plants grown for 4 d under different conditions of low Fe availability. After 10 d pre-culture on one-half strength MS medium with 40 µM NaFeEDTA (pH 5.6), plants were transferred to one-half strength MS medium with 20 µM $FeCl_3$ buffered with either MES to pH 5.6 or 6.5, or MOPS to pH 7.5. Coumarins were analyzed with UPLC-MS (Triple Quad for wild-type, *s8h-2*, and *cyp82C4-1*; Orbitrap for *pdr9-2* samples). Coumarin root concentrations for wild-type plants are as shown in Fig. 35. Bars represent means ± s.d (n = 3-5 biological replicates). Significant differences are indicated as asterisks according to Student's *t*-test with α=0.05; * $p \leq 0.05$, ** $p \leq 0.01$, *** $p \leq 0.001$. Different letters indicate significant differences according to one-way ANOVA with post-hoc Tukey's test at $p \leq 0.05$ or Welch's ANOVA with post-hoc Games-Howell test with $p \leq 0.05$. (B) Total coumarin concentration in roots as sum of glycosylated (glyc.; scopoletin, esculin, fraxin) and deglycosylated (deglyc.; scopoletin, esculetin, fraxetin, sideretin) coumarins. n.d.: not detected.

In agreement with the root extract profiling, *s8h-2* plants also released up to 7.3- and 9.4-fold more scopolin and scopoletin compared to the wild-type plants (Fig. 38A). Thereby, the high pH-dependent stimulation of scopoletin exudation was only slightly enhanced in *s8h-2* compared to wild-type plants as the pH increased from pH 6.5 to 7.5. *cyp82C4-1* plants, in turn, exuded more fraxetin than wild type under all pH conditions (Fig. 38A). However, the relative increments of fraxetin in root exudates as the external pH was elevated from pH 6.5 to 7.5 were less pronounced in the mutant. Since a similar pattern was also observed for fraxin in root extracts (Fig. 37A), these results may suggest that a maximum biosynthetic rate for

fraxin/fraxetin is achieved in *cyp82C4* mutants. Because fraxetin levels were strongly increased in root exudates of *cyp82C4-1* plants, these plants released the largest total amount of deglycosylated coumarins among all assessed genotypes (Fig. 38B).

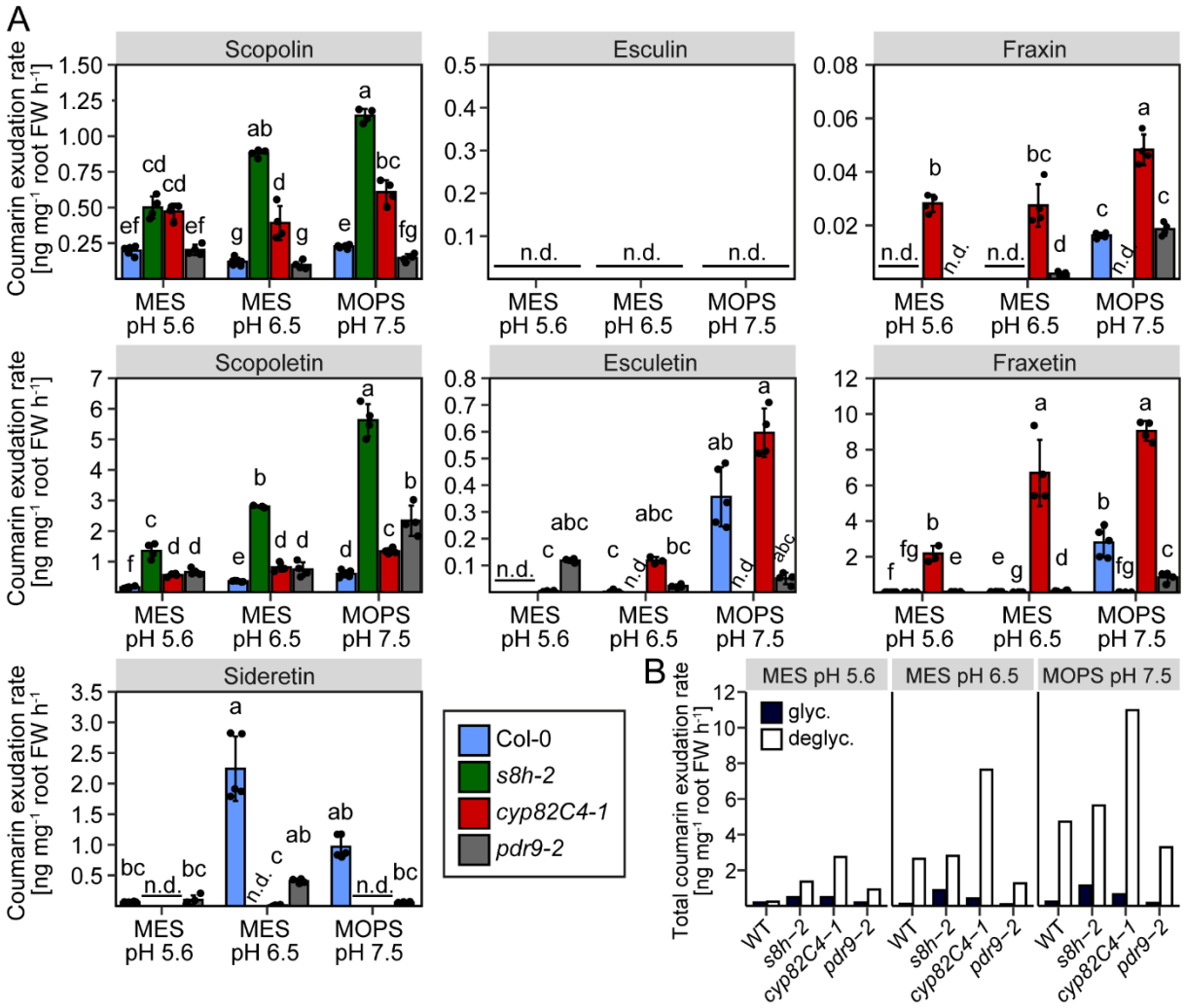

Fig. 38. pH-dependent changes in root exudation rates of coumarins in biosynthesis and transport mutants. (A) Exudation rates of indicated coumarins from roots of wild-type (Col-0), *s8h-2*, *cyp82C4-1*, and *pdr9-2* plants grown for 4 d under different conditions of low Fe availability. After 10 d pre-culture on one-half strength MS medium with 40 µM NaFeEDTA (pH 5.6), plants were transferred to one-half strength MS medium with 20 µM $FeCl_3$ buffered with either MES to pH 5.6 or 6.5, or MOPS to pH 7.5. Root exudates were collected for 6 h on MES and MOPS buffer adjusted to the respective pH. Coumarins were analyzed with UPLC-MS (Triple Quad for wild-type, *s8h-2*, and *cyp82C4-1*; Orbitrap for *pdr9-2* samples). Coumarin exudation rate of wild-type plants are as shown in Fig. 34. Bars represent means ± s.d (n = 3-5 biological replicates). Different letters indicate significant differences according to one-way ANOVA with post-hoc Tukey's test at $p \leq 0.05$, ANOVA on ranks with post-hoc Dunn's test at $p < 0.05$, or Welch's ANOVA with post-hoc Games-Howell test with $p \leq 0.05$. (B) Total coumarin exudation rate as sum of glycosylated (glyc.; scopoletin, esculin, fraxin) and deglycosylated (deglyc.; scopoletin, esculetin, fraxetin, sideretin) coumarins. n.d.: not detected.

Disruption of PDR9-mediated coumarin secretion resulted in low levels of most coumarins in root exudates especially at elevated pH (Fig. 38A). One exception was scopoletin, whose exudation from *prd9-2* roots was significantly enhanced, especially at alkaline conditions. These results are in line with previous findings reported by Ziegler *et al.* (2017) and suggests

that scopoletin exudation involves an additional unknown transporter which allows scopoletin exudation in a pH-dependent manner.

Taken together, these data indicate that disruption of the central coumarin biosynthesis pathway towards highly hydroxylated coumarins leads to an overaccumulation of certain coumarins and additionally enhances the total amount of coumarins in roots and root exudates. Furthermore, the data suggest that exudation of catecholic coumarins is mainly facilitated via PDR9, probably in a pH-dependent manner, while scopoletin may be exuded additionally by a yet unknown transporter.

4.15 MYB72-dependent up-regulation of genes involved in coumarin biosynthesis and secretion and inhibition of *CYP82C4* expression at high pH

Since gene expression analysis of wild-type plants indicated that the external pH affects the transcriptional regulation of different genes involved in coumarin biosynthesis and secretion (Figs. 28 and 31; Annex Figs. 14-16), the question was raised whether such pH-induced changes prevail in different mutants defective in coumarin biosynthesis or secretion as well as in Fe uptake and Fe-deficiency signaling.

In general, distinct changes in transcript levels of individual genes in the different mutants were observed (Fig. 39A). The absence of functional FRO2 or F6'H1 led to overall comparable changes in the transcript profile of the examined genes irrespective of pH and buffer conditions, except for *S8H* which was repressed in *f6'h1-1* root at pH 7.5 (Fig. 39A). Interestingly, in all coumarin-related mutants, the induction of *FIT* expression by high pH conditions was partially prevented. The expression of *MYB72*, in turn, was less affected. Furthermore, the expression of *CYP82C4* was significantly reduced already in *fro2* and *f6'h1-1* at pH 5.6 compared to wild type and all other mutant lines (Fig. 39A).

Although scopolin and scopoletin levels were strongly increased in root extracts and exudates of *s8h-2* plants under all pH and buffer conditions (Figs. 37 and 38), the transcriptional expression of *F6'H1* was only slightly enhanced compared to wild type. In *cyp82C4*-1 plants, which accumulate more fraxin and fraxetin in their roots and root exudates irrespective of the pH and buffer conditions (Figs. 37 and 38), *S8H* expression in roots was even significantly reduced compared to wild type (Fig. 39A; Annex Fig. 18). These results suggest that the increased synthesis of scopolin/scopoletin and fraxin/fraxetin in *s8h* and *cyp82C4* mutants, respectively, involves further regulatory mechanisms that act at the post-transcriptional level.

The absence of induced *FIT* expression by elevated pH conditions was also observed in *bglu42* and *pdr9-2* but not in *myb72-1* and *myb10* (Fig. 39A). Apart from *FIT*, gene expression in *bglu42* plants was largely comparable to that of the wild type. For *pdr9-2*, the most striking

difference was the lack of *S8H* up-regulation by pH 7.5 and bicarbonate buffered conditions at pH 6.5.

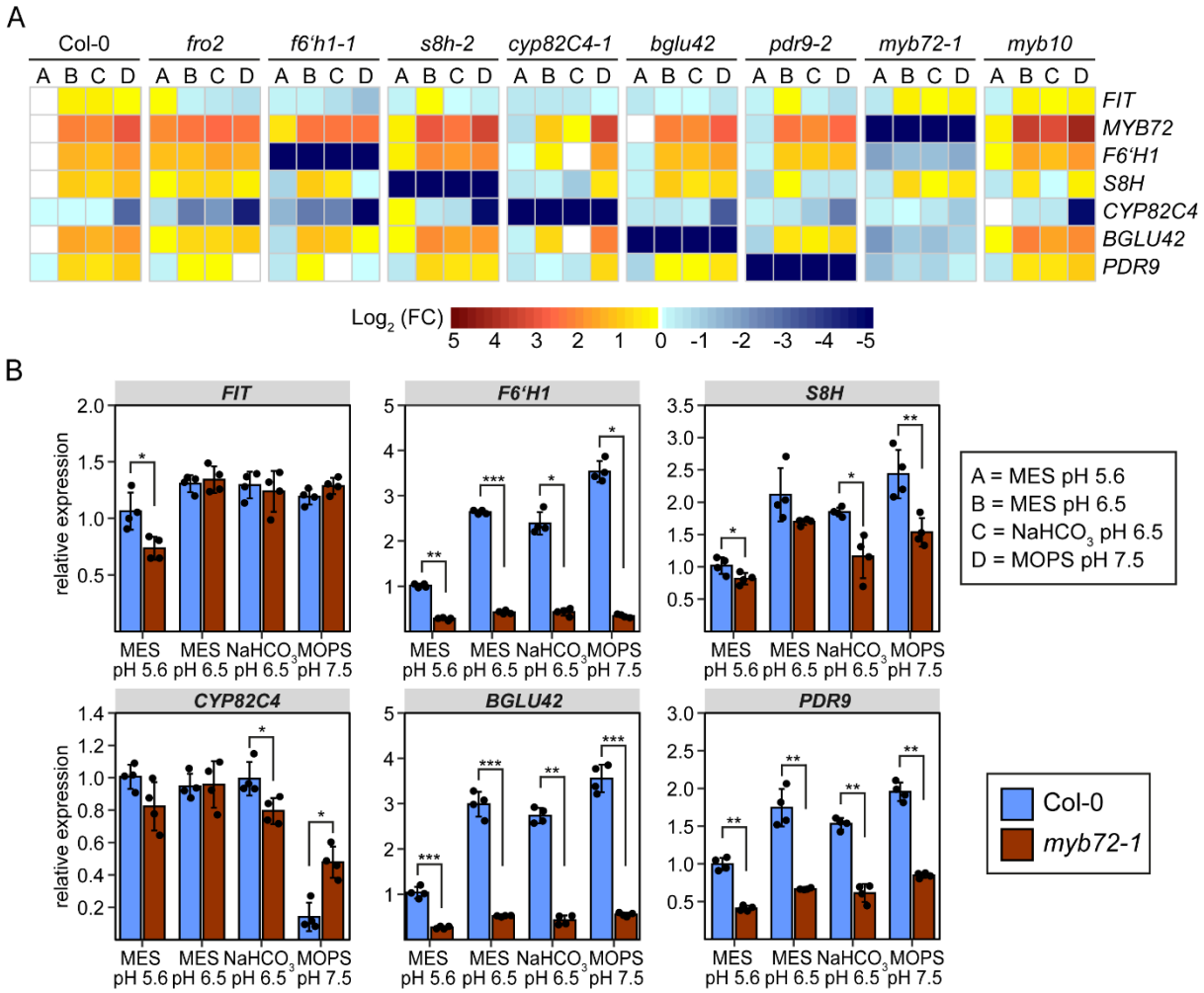

Fig. 39. Expression profiles of genes involved in coumarin biosynthesis and secretion in different mutant lines exposed to conditions of low Fe availability at different external pH and buffers. (A) Heatmap of $\log_2$ fold changes (FC) in transcript levels of *FIT*, *MYB72*, *F6'H1*, *S8H*, *CYP82C4*, *BGLU42*, and *PDR9* in roots of wild-type (Col-0), *fro2*, *f6'h1-1*, *s8h-2*, *cyp82C4-1*, *bglu42*, *pdr9-2*, *myb72-1*, and *myb10* plants grown under different conditions of low Fe availability for 4 d. (B) Relative expression of *FIT*, *F6'H1*, S8H, *CYP82C4*, *BGLU42*, and *PDR9* in Col-0 and *myb72-1* plants. Bars represent means ± s.d (n = 4 biological replicates). Significant differences are indicated by asterisks according to Student's *t*-test with α=0.05; * $p \leq 0.05$, ** $p \leq 0.01$, *** $p \leq 0.001$. Plants were pre-cultured on one-half strength MS medium with 40 µM FeEDTA (pH 5.6) and then were transferred to one-half strength MS medium with 20 µM $FeCl_3$ buffered with either MES to pH 5.6 or pH 6.5, $NaHCO_3$ to pH 6.5 (1 mM), or MOPS to pH 7.5. Relative expression levels were calculated as fold changes from Col-0 plants grown for 4 d on MES pH 5.6 and $\log_2$ transformed.

In overall, the strongest changes in gene expression were observed for *myb72-1* (Fig. 39A). In these plants, the expression of *F6'H1*, BGLU42, *PDR9* and, less dramatically, *S8H* was significantly decreased mostly irrespective of the pH and buffer conditions (Fig. 39A and B). However, one striking difference was observed for *CYP82C4*. The expression of this gene was hardly decreased in *myb72-1* roots at pH 5.6 and pH 6.5 but increased by around 3.4-fold at pH 7.5 compared to the wild type. As a result, the alkaline pH-induced *CYP82C4* inhibition was

less pronounced, providing initial evidence that MYB72 may act as a negative regulator of *CYP82C4* under this condition.

Although MYB10 is described to be functionally redundant to MYB72 (Palmer *et al.*, 2013), gene expression in *myb10* plants was largely comparable to the wild type (Fig. 39A and E). In these plants, only *S8H* transcript levels were reduced, while *MYB72* and *BGLU42* expression were significantly enhanced. This further supports the importance of MYB72 in the transcriptional regulation of different genes involved in coumarin biosynthesis and secretion in response to Fe deficiency and different external pH conditions.

Considering the detected MYB72-dependent transcriptional regulation of coumarin-related genes, the coumarin composition of root extracts and root exudates of the *myb72-1* mutant was assessed. Compared to the wild type (see Fig. 34 or 36), *myb72-1* plants accumulated comparable amounts of scopolin in its roots while all other coumarins were less abundant, especially when the external pH was increased (Fig. 40A). The overall pH-dependent changes for the different coumarins were comparable except for sideretin whose concentration in root extracts was not decreased at pH 7.5. Root exudate profiling revealed that the release of coumarins in *myb72-1* was largely diminished compared to wild-type plants irrespective of the pH (Fig. 40B; for wild type root exudates see Fig. 34 and 38).

Taken together, these data indicate that MYB72 functions as an integral part in the transcriptional regulation of genes involved in coumarin biosynthesis and secretion under Fe-deficient conditions in a pH-dependent manner. Furthermore, these data suggest that MYB72 is also involved in the transcriptional repression of *CYP82C4* at high external pH.

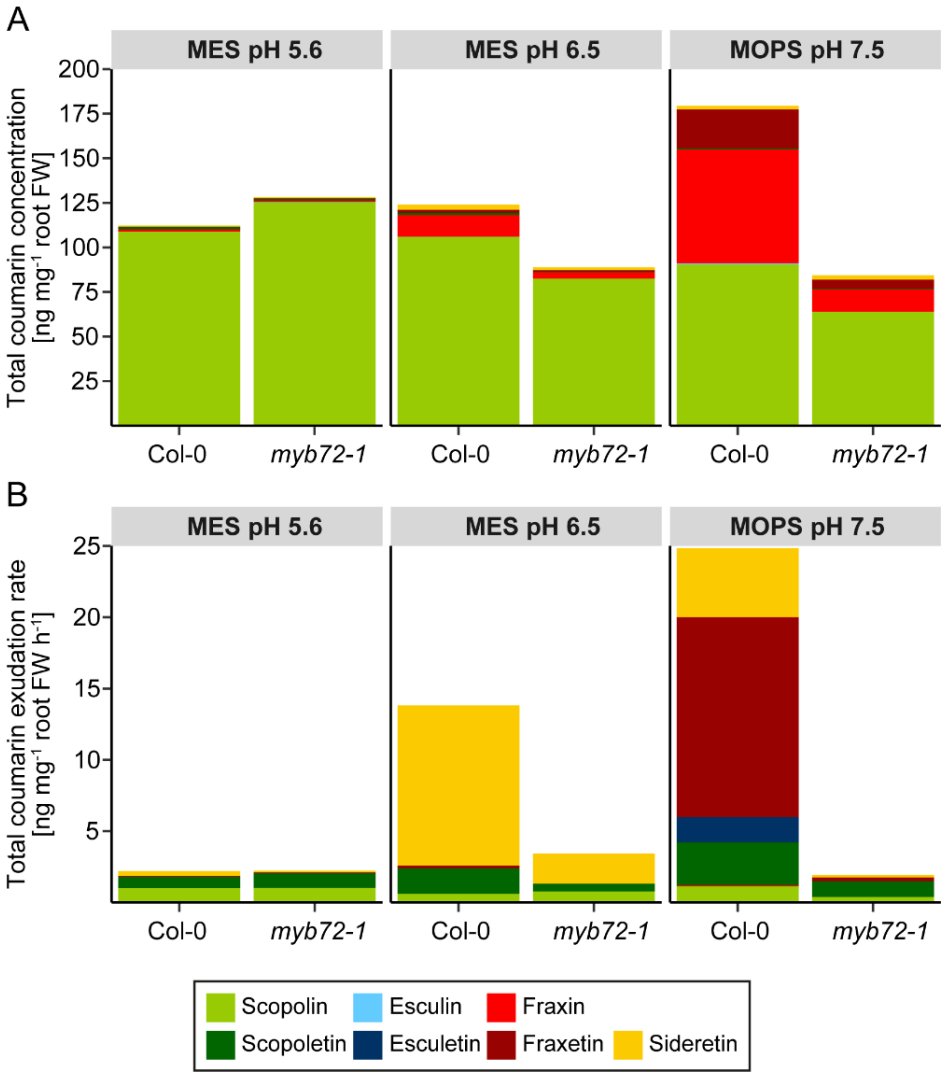

Fig. 40. Coumarin accumulation and secretion in *myb72-1* mutant plants. (A) Coumarin root concentrations and (B) exudation rates of wild-type (Col-0) and *myb72-1* plants grown for 4 d under different conditions of low Fe availability. After 10 d pre-culture on one-half strength MS medium with 40 µM NaFeEDTA (pH 5.6), plants were transferred to one-half strength MS medium with 20 µM $FeCl_3$ buffered with either MES to pH 5.6 or 6.5, or MOPS to pH 7.5. Root exudates were collected for 6 h on MES or MOPS buffer adjusted to the respective pH. Coumarins were analyzed with UPLC-MS (Triple Quad). Coumarin root concentrations and exudation rates of wild-type plants are as shown in Figs. 34 and 35. The experiments were carried out at the same time. Bars represent the sum of the mean values of the different coumarins (n = 4-5 biological replicates).

5 Discussion

The release of different metabolites from the root is an essential mechanism in plants to facilitate nutrient mobilization and acquisition from soil (Römheld, 1991; Dakora and Phillips, 2002; Ström *et al.*, 2002; Johnson and Loeppert, 2006; Suzuki *et al.*, 2006; Schmid *et al.*, 2014; Rajniak *et al.*, 2018). Root-derived exudates are well-documented to be crucial for the acquisition of Fe in both graminaceous and non-graminaceous plant species especially in soils with slightly acidic to alkaline pH where Fe solubility is very low (Marschner, Römheld and Kissel, 1986; Kobayashi and Nishizawa, 2012). While the release of Fe(III)-chelating PS in graminaceous plants is well established, several aspects governing the identity, function, and synthesis of phenolics and other low molecular-weight organic compounds released by non-graminaceous plants are still under investigation. In the past decade, the identification of coumarins as a class of phenolic compounds released by Arabidopsis and rapeseed plants in response to Fe deficiency has revived the importance of such root metabolites for Fe acquisition in Strategy I plants and stimulated the identification of the underlying biosynthetic and transport pathways (Rodríguez-Celma *et al.*, 2013; Fourcroy *et al.*, 2014; Schmid *et al.*, 2014; Schmidt *et al.*, 2014; Ziegler *et al.*, 2017; Rajniak *et al.*, 2018; Tsai *et al.*, 2018; Vanholme *et al.*, 2019). To date, several different coumarins have been described and the main molecular players involved in coumarin biosynthesis and secretion are largely known. However, although coumarins are suggested to facilitate Fe acquisition by directly chelating and/or reducing Fe(III) (Mladěnka *et al.*, 2010; Schmid *et al.*, 2014; Rajniak *et al.*, 2018), much less is known about their individual contribution to these processes especially considering the external pH and buffer conditions prevailing in soils. It also remained unclear how the external pH can alter the coumarin composition of root exudates.

By combining physiological investigations and growth assays with reverse genetic approaches, the present work extends the knowledge about the function of coumarin-type siderophores in Fe acquisition in Strategy I plants in dependence of the external pH and buffer conditions. Among the main coumarins synthesized and released by Arabidopsis, the present study identifies fraxetin and sideretin as being able to facilitate non-enzymatic Fe(III) reduction and to bypass FRO2 at pH 5.6 and pH 6.5. Fraxetin-mediated Fe(III) reduction is shown here to be relevant *in planta*. Furthermore, LC-MS/MS analysis allowed the identification of different Fe(II) and/or Fe(III)-complexes for catecholic coumarins *in vitro*.

The present thesis also explores the molecular mechanisms determining the coumarin composition in root exudates in response to different external pH and buffer conditions. The results from this study reveal that the external pH induces considerable changes in the expression of different genes involved in coumarin biosynthesis and secretion which entails profound changes in the coumarin composition in roots and root exudates. Most strikingly, it

was found that *CYP82C4* expression is strongly inhibited by high pH conditions, largely explaining the shift from sideretin synthesis and release towards fraxetin under such conditions. Finally, evidence was raised that MYB72 plays a critical role in adjusting the expression of genes involved in coumarin biosynthesis and secretion to the external pH.

5.1 pH and buffer conditions distinctively affect Fe(III) mobilization and reduction capacities of individual coumarins

Catechol-harboring phenolic compounds are most potent in chelating and thus solubilizing Fe from otherwise insoluble sources (Andjelković *et al.*, 2006; Perron and Brumaghim, 2009; Mladěnka *et al.*, 2010; Schmid *et al.*, 2014; Sisó-Terraza *et al.*, 2016; Rajniak *et al.*, 2018; Tsai *et al.*, 2018). In line with these findings, *in vitro* assays at different pH and buffer conditions over time using the four main coumarins known in Arabidopsis revelated that Fe(III) mobilization is confined to catecholic coumarins including esculetin, fraxetin, and sideretin (Figs. 3-7). However, even among these, specific features were detected. In general, esculetin was strong in Fe(III) mobilization but a poor Fe(III) reductant, while fraxetin and sideretin could mobilize and reduce Fe(III). Additionally, sideretin-mediated Fe(III) mobilization was more sensitively affected by high pH compared to fraxetin.

Overall, the ability of the different catecholate coumarins to mobilize and/or reduce Fe(III) decreases as the pH increases (Figs. 3-6). Thereby, Fe(III) reduction was observed especially for fraxetin and sideretin and largely confined to pH 5.6 and pH 6.5, while Fe(III) mobilization by esculetin, fraxetin, and sideretin was observed under all pH conditions and largely comparable. This is most likely due to the fact that Fe(II)-complexes are preferentially formed at acidic pH, whereas Fe(III)-complexes occur at pH > 7 (Schweigert, Zehnder and Eggen, 2001). Only at alkaline pH, Fe(III) mobilization by sideretin was strongly diminished (Fig. 6), probably as a result of the low stability of sideretin at high pH as identified in a previous study (Rajniak *et al.*, 2018). These results demonstrate that besides the presence of a catecholate group, further structural differences affect the chemical properties of the different coumarins produced and released by Arabidopsis and determine their pH- and buffer-dependent Fe(III) mobilization capacity both by chelation and reduction. Although only little is known about the chemistry of sideretin in dependence of the pH, different mechanisms can be assumed to decrease its stability at high pH. For instance, sideretin has been described to get readily oxidized when exposed to air and its redox potential was found to be around 300 mV lower compared to fraxetin at pH 6.5 (Rajniak *et al.*, 2018). Since oxidation becomes easier as the pH increases, the higher susceptibility of sideretin to oxidation may be an explanation for its instability and hence inability to facilitate Fe mobilization at high external pH compared to esculetin and fraxetin. The overall susceptibility of coumarins towards opening of their lactone

ring under alkaline conditions may also play a relevant role for their function in Fe acquisition (Bowden, Hanson and Taylor, 1968; Garrett, Lippold and Mielck, 1971). However, whether the additional hydroxyl group of sideretin compared to fraxetin increases its susceptibility to lactone ring cleavage remains to be elucidated.

Besides the pH, also the buffer strength affected the ability of coumarins to reduce Fe(III) (Fig. 7). Considering that Fe(III) reduction strongly decreases as the pH increases and catecholate ligands form Fe(III)-complexes preferentially under high pH conditions, the ability of coumarins to reduce Fe(III) can be assumed to be strongly limited whenever the pH is efficiently buffered to neutral and alkaline conditions. An effect of bicarbonate itself on the stability of coumarins appears unlikely as Fe(III) mobilization by fraxetin was only slightly reduced when the $NaHCO_3^-$ concentration was increased (Fig. 7). The observed repression of the internal standard signal during LC-MS/MS analysis of especially root exudate samples collected from plants exposed to bicarbonate indicate ion-suppressing effects much likely due to the presence of elevated salt concentrations (Annesley, 2003). Given the structural similarity of the internal standard, similar effects on the detection of the other investigated coumarins can be assumed. One way to counteract ion suppression in such samples could be to modify the sample preparation by e.g. by including a solid-phase extraction step to remove bicarbonate from the samples.

The investigated catecholic coumarins further differed in their ability to mobilize and/or reduce Fe(III) over time. In general, esculetin and sideretin showed initially faster kinetics compared to fraxetin (Figs. 3-6). While the amount of mobilized and reduced Fe(III) by fraxetin-containing solutions largely increased over time irrespective of the pH and buffer conditions, the maximum amount of Fe(III) mobilized by esculetin and sideretin was already reached after 10 min of incubation and remained nearly constant until the end of the assay. In contrast, the concentration of reduced Fe(III) in sideretin-containing solutions was maximum after 10 min but strongly decreased as the time proceeds. Such kinetic differences in Fe(III) reduction between fraxetin and sideretin were also previously reported by Rajniak *et al.* (2018) who conducted similar experiments at pH 5 and pH 7 over 2 h. However, since the total amount of reduced Fe by sideretin considerably decreased over time while that of fraxetin increased, it can be assumed that putatively formed Fe(II)-sideretin complexes possess only low stability. This could be related to the ability of ligands with high affinity for Fe(III), e.g. catechols, to facilitate the auto-oxidation of complexed Fe(II) in the presence of oxygen yielding the corresponding Fe(III) complex especially under elevated pH conditions (Hider, Liu and Khodr, 2001; Perron and Brumaghim, 2009). Because the Fe(II) oxidation rate varies between different polyphenols, such as gallolyl- and catechol-harboring compounds, and because catecholate ligands form more stable complexes with trivalent than divalent ions (Hider, Liu and Khodr, 2001; Schweigert, Zehnder and Eggen, 2001; Perron and Brumaghim, 2009; Perron *et al.*, 2010), putative Fe(II)-sideretin and Fe(II)-fraxetin complexes might differ in the

rate by which they become auto-oxidized. This is reasonable as fraxetin and sideretin are already known to differ in their redox capacities (Rajniak *et al.*, 2018).

The ability of sideretin to mobilize and reduce considerable amounts of Fe(III) very quickly might be an explanation why it is advantageous for plants to synthesize this coumarin in addition to fraxetin which is already quite efficient in Fe(III) mobilization and reduction. In plants, it may allow fast Fe(III) mobilization before readily accessible Fe(III), e.g. from freshly precipitated $Fe(OH)_3$, further oxidizes and becomes immobilized. To date, sideretin synthesis and release appear to be dispensable as the disruption of its synthesis in *cyp82C4* mutants does not result in any noticeable phenotype compared to the wild type (Rajniak *et al.*, 2018). Sideretin was also recently reported to be dispensable in root microbiota assembly under Fe-limiting conditions (Harbort *et al.*, 2020). As the appearance of growth phenotypes and significant changes in the composition of root-associated microbial communities requires time, the short-time kinetic differences between sideretin and fraxetin become less relevant over the long run, as long as at least one of them is produced. However, the unique redox capacity of sideretin and the fact that its biosynthesis is widely conserved in eudicots (Rajniak *et al.*, 2018) suggest that there are conditions under which sideretin function becomes more critical. For instance, considering the high susceptibility of sideretin to oxidation and its lower redox potential compared to fraxetin (Rajniak *et al.*, 2018), sideretin might become especially important when oxygen availability is limited, i.e. when the redox potential (E_h) of soils is low. Besides pH, soil E_h is another important parameter that affects redox reactions in soils and thus influences various biological and biogeochemical processes including nutrient solubility and the assembly of microbial communities (Sims and Patrick Jr., 1978; Schwab and Lindsay, 1983; Cornell and Schwertmann, 2003; Rabenhorst, Hively and James, 2009; Husson, 2013). Soil E_h fluctuates usually between -300 and +900 mV and is affected by different abiotic factors, including soil moisture, temperature, and availability of organic matter or of metals. Furthermore, plants and especially microorganism can directly influence the redox potential of their surrounding soil, leading to considerable variation of soil E_h in space and time (Fageria and Stone, 2006; Fiedler, Vepraskas and Richardson, 2007; Husson, 2013). Hence, the release of sideretin might allow plants to mobilize Fe(III) both by chelation and reduction over a broader range of redox conditions. This could be of primary relevance for temporal and spatial fluctuations in soil E_h, since anaerobic conditions increase Fe solubility in general, and plants require a soil E_h of +300 to +700 mV for proper growth (Volk, 1939; Schwab and Lindsay, 1983; Husson, 2013). However, further research is needed including a detailed investigation of the redox potentials of fraxetin and sideretin as a function of pH as well as the assessment whether such conditions are of physiological relevance for Fe acquisition in Strategy I plants.
Although catecholic coumarins are more efficient in Fe(III) mobilization both by chelation and reduction, a possible involvement of the non-catecholic coumarin scopoletin in these

processes remains under debate. Previously, Schmidt *et al.* (2014) reported that scopoletin solutions gave rise to similar UV/vis spectra as observed for esculetin and fraxetin when incubated with an Fe(II) or Fe(III) salt at alkaline pH. Since the observed shifts in the absorption maxima compared to the free ligands were originating from ligand-to-metal charge transfer bands, the authors assigned these optical spectra to the corresponding Fe(II)-coumarin complexes. A possible role of scopoletin in Fe mobilization by chelation and/or reduction was further suggested by the identification of different Fe(II)-scopoletin species by UPLC-MS/MS (Schmidt *et al.*, 2014; Baune *et al.*, 2020), which were also partially detected in the presented study (Annex Fig. 11). Recently, scopoletin has also been reported to possess the highest Fe(III)-mobilization capacity compared to esculetin and fraxetin *in vitro* when the Fe mineral lepidocrocite served as Fe source at pH 8.5 (Baune *et al.*, 2020). The authors attributed this to the involvement of different coumarin oxidation products, which are formed through the reduction of Fe(III). For instance, scopoletin can be demethylated to esculetin which is a catecholic coumarin that can efficiently mobilize Fe(III) (Figs. 3-6; Baune *et al.*, 2020; Schmid *et al.*, 2014). Besides differences in pH and buffer conditions and reaction time compared to the assays presented in this study, such redox reactions between coumarins and Fe are also strongly associated with the mineral surface. Hence, given the apparent differences in the used Fe sources, surface chemistry-related issues might be an explanation for the observed differences in the Fe(III)-mobilization capacity of scopoletin versus fraxetin. Thus, the importance of such mechanisms for Fe acquisition by plants may differ from case-to-case. Since *s8h* mutants, which over-accumulate scopoletin in root exudates irrespective of the external pH (Fig. 38), show severe Fe-deficiency symptoms under conditions of low Fe availability compared to its wild type (Rajniak *et al.*, 2018; Siwinska *et al.*, 2018; Tsai *et al.*, 2018), scopoletin appears not to play a major role in Fe solubilization.

Since coumarin-mediated Fe solubilization involves the formation of Fe(II) and/or Fe(III)-coumarin complexes, the formation of Fe(II)/Fe(III) complexes for scopoletin, esculetin, and fraxetin was determined *in vitro* by UPLC-MS/MS. Although Schmidt *et al.* (2014) previously failed to detect any Fe-esculetin or Fe-fraxetin complex by mass spectrometry, a Fe(III)-esculetin complex and different Fe(II)/(III)-fraxetin complexes were detected in this study, when these ligands were incubated with freshly precipitated Fe-hydroxide. This is in line with reported UV/Vis spectroscopy data which previously suggested the existence of such complexes (Schmidt *et al.*, 2014; Zhang *et al.*, 2021). Furthermore, the dimerization of esculetin, fraxetin, and scopoletin as well as the formation of scopoletin trimers in a Fe-dependent fashion was observed (Fig. 22 and 23; Annex Figs. 11D and E, 12). Similar findings were also recently reported by Baune *et al.* (2020) after incubation of esculetin and fraxetin with different Fe minerals at different pH values. In agreement with the present findings, the authors also observed Fe-coumarin complexes to only co-elute with the respective free ligand,

which has been proposed to be due to chromatographic instability of such Fe-coumarin species, i.e. the complexes start to dissociate as soon as the excess ligand is separated from the complex. Whereas previous studies used the observation of the expected isotopic pattern of Fe for identification of different Fe-coumarin complexes (Schmidt *et al.*, 2014; Baune *et al.*, 2020), this study aimed to verify the formation of Fe-coumarin complexes *in vitro* by using $^{58}FeCl_3$ as Fe source during the incubation step. However, the expected mass shift of the corresponding ^{58}Fe-fraxetin species could not be detected (Fig. 25). Considering that Fe-coumarin complexes were also detected when samples were not brought in contact with Fe prior to analysis (Fig. 26; Annex Fig. 12), it is possible that Fe was already present in the UPLC-MS/MS system, even accumulated there and yielded to memory effects. Such residual Fe probably derived from prior injection of samples enriched with Fe. In previous studies, partial dissociation of metal-ligand species has been described to occur during chromatographic separation resulting in metal contamination of the respective column even for thermodynamically stable metal-ligand chelates such as Fe-PS chelates (Weber *et al.*, 2001; Xuan *et al.*, 2006; Köster *et al.*, 2011). Hence, partial dissociation and new formation of Fe-coumarin complexes may have occurred, and the presence of large amounts of ^{56}Fe in the column led to a strong dilution of the ^{58}Fe initially complexed by fraxetin *in vitro*. Furthermore, as the pH could not be monitored exactly in the small volume used for incubation, the possibility cannot be ruled out that the applied incubation conditions, especially regarding pH, were not suitable for the formation of Fe-coumarin complexes *in vitro*.

5.2 Relevance of non-enzymatic Fe(III) reduction for Fe uptake by Strategy I plants

Several studies have indicated the importance of coumarin-mediated Fe(III) mobilization from otherwise insoluble sources in Strategy I plants (Schmid *et al.*, 2014; Schmidt *et al.*, 2014; Fourcroy *et al.*, 2016; Rajniak *et al.*, 2018; Tsai *et al.*, 2018). Coumarin resupply experiments with the Arabidopsis coumarin biosynthesis mutants *f6'h1-1* and *s8h* demonstrated that supplementation of esculetin, fraxetin, and sideretin can largely prevent Fe deficiency in these mutants, especially at acidic pH conditions (Schmid *et al.*, 2014; Rajniak *et al.*, 2018; Tsai *et al.*, 2018). Nonetheless, the physiological relevance of coumarin-mediated Fe(III) reduction still remained unclear. Although two previous studies have indicated that Fe(III) reduction by coumarins plays only a negligible role under Fe-limiting conditions, their experiments were conducted only at high pH, and thus the involvement of specific coumarins in Fe(III) reduction may have been overlooked (Barrett-Lennard, Marschner and Römheld, 1983; Fourcroy *et al.*, 2016). In the present work, it has been shown that fraxetin and sideretin can efficiently bypass the enzymatic Fe(III) reduction via FRO2 at acidic pH (pH 5.6) (Fig. 9; Annex Figs. 1-4). The fact that lacking coumarins in the *fro2* background leads to severe Fe deficiency (Figs. 13 and

14) reinforces a major role of coumarins in Fe(III) mobilization. Since the *fro2 f6'h1-1* double mutant was largely rescued by external supply of fraxetin and sideretin (Figs. 15 and 16), interferences by other F6'H1-dependent coumarins or root-derived components released by *fro2* under such conditions can be excluded. Compared to the *fro2* single mutant, which grew and was relatively green at slightly acidic pH, the *fro2 f6'h1-1* double mutant grew only poorly and became highly chlorotic under such conditions (Figs. 13 and 14). These results provide strong genetic support for the relevance of coumarin-dependent Fe(III) reduction. Interestingly, the initial phenotypical analysis of a newly generated *fro2 cyp82C4-1* double mutant revealed that its Fe deficiency symptoms are as severe as for *fro2 f6'h1-1* (Fig. 13 and 19). If confirmed in more detailed experiments, this could indicate that sideretin is the most critical coumarin for Fe(III) reduction. Although sideretin has a strong ability to reduce Fe(III) at slightly acidic conditions (Fig. 3), more experimental evidence will be required to demonstrate if that is indeed the case. One possibility to address this question would be to test whether the external supply of sideretin but not of fraxetin can alleviate the growth of *fro2 cyp82C4-1* at acidic pH.

Co-cultivation of *fro2* with *cyp82C4-1*, which releases very high levels of fraxetin (Fig. 38), have revealed that enhanced fraxetin levels in the rhizosphere can in fact alleviate Fe deficiency and promote root growth of *fro2* plants at pH 5.6 (Fig. 20). These results indicated that fraxetin-mediated Fe(III) reduction especially at acidic to slightly acidic pH is indeed relevant *in planta* and further suggested that coumarins might also contribute to root morphological changes in response to Fe deficiency by affecting the root system architecture. A similar stimulating effect on root morphology has been previously described for the coumarin 1,2-benzopyron (Abenavoli *et al.*, 2008). The importance of fraxetin in the absence of a functional FRO2 in plants is further supported by the observation that fraxetin synthesis and release is favored over sideretin in *fro2* plants especially at elevated pH conditions (Fig. 11). However, the more severe Fe-deficiency symptoms of *fro2* plants compared to the wild type indicate that the enhanced fraxetin levels in root exudates are still insufficient to fully bypass enzymatic Fe(III) reduction by FRO2 (Fig. 8). Interestingly, fraxetin supplementation was unable to alleviate Fe deficiency of *irt1-1* plants (Fig. 10), demonstrating that IRT1-mediated Fe(II) uptake is still required and that an efficient uptake of intact Fe(II)/Fe(III)-coumarin complexes is very unlikely. This applies especially as supplementation of higher fraxetin concentrations (≥250 µM) was shown to have inhibitory effects on plant growth (section 4.2; Annex Fig. 1). This result provides further support to previous findings from Fourcroy *et al.* (2016) that the growth media from Fe-deprived wild-type plants can regreen wild-type but not *irt1-1* plants when grown on $FeCl_3$ at high pH.

Under slightly acidic pH conditions at pH 6.5, the external supply of sideretin could restore Fe deficiency only in wild-type and *f6'h1-1* plants, while fraxetin was able to recover Fe deficiency

also in *fro2* (Fig. 9, 15, 16). These results indicated clear differences in reduction capacity between the two major catecholic coumarins released by Arabidopsis when the pH increases: while sideretin can still facilitate Fe(III) mobilization presumably by chelation but loses its capacity to reduce Fe(III), fraxetin can efficiently mobilize Fe(III) both by chelation and reduction. Although the *in vitro* experiments presented in this study indicated that sideretin possesses even higher Fe(III)-reductive properties than fraxetin at pH 6.5 (Fig. 4), the apparent differences could be due to the lower stability of sideretin itself and of putative Fe(II)-sideretin complexes at elevated pH as well as to the higher susceptibility of sideretin to undergo spontaneous oxidation (Rajniak *et al.*, 2018). Of note, external supply of fraxetin was not able to rescue the *fro2 f6'h1-1* double mutant at pH 6.5 (Figs. 15 and 16). This could indicate that at this pH, fraxetin relies on the presence of other F6'H1-dependent coumarins to reduce sufficient Fe(III) in the absence of FRO2. Up to date, synergistic interactions of coumarins have been described only with other components such as ascorbate which was shown to enhance Fe mobilization by esculetin from calcareous soils (Schenkeveld *et al.*, 2016). The possibility of synergistic interactions among coumarins are of great interest as they could extend the functional range of the individual components and further support the understanding of how coumarins mediate Fe acquisition in total and why it is advantageous for Strategy I plants to produce a wide range of different coumarins. Evaluating the effect of supplied mixtures of coumarins to the growth medium to recover Fe deficiency of the double mutants isolated in this study could help to obtain insights into whether and which plant-derived coumarins can act synergistically in Fe(III) mobilization both by chelation and reduction.

Since coumarin-mediated Fe(III) reduction was strongly limited at high pH and strongly buffered conditions *in vitro* (Fig. 3-7), the inability of externally supplied coumarins to alleviate Fe deficiency of *fro2* at pH 7.5 was expected (Fig. 9; Annex Fig. 1-4). However, esculetin and fraxetin were still able to mobilize considerable amounts of Fe *in vitro* under such conditions but none of them alleviated Fe deficiency in wild-type plants irrespective of their applied concentration. As the activity of root-bound reductases such as FRO2 has been described to be strongly impaired under such conditions (Bienfait *et al.*, 1983; Romera, Alcántara and de la Guardia, 1992b), this could be an explanation for the absence of a supportive effect. However, this finding is in contrast to previous studies, which have reported that growth medium from Fe-deprived Arabidopsis plants and supplementation of pure fraxetin were able to largely recover Fe deficiency in wild-type and *f6'h1-1* or *s8h* plants at pH 7.0-7.5, respectively (Fourcroy *et al.*, 2016; Tsai *et al.*, 2018). Furthermore, it has been shown that *S8H* overexpression in the background of Arabidopsis accession Col-0 significantly improves plant growth under Fe-limiting conditions at high external pH (Tsai *et al.*, 2018). This indicates that Fe(III) mobilization by fraxetin from otherwise insoluble source is relevant in plants under such conditions. Besides differences in the plant cultivation systems, buffer conditions, and

concentration of the applied coumarins, it remains elusive why the supplementation of especially catecholic coumarins including esculetin and fraxetin even at concentrations of up to 500 µM was insufficient to alleviate Fe deficiency in wild-type plants at high pH in the present study.

Root exudate analysis of wild-type plants revealed that sideretin is especially released at pH 6.5 while fraxetin exudation is highest at alkaline pH (Fig. 33). Hence, these two coumarins are primarily released outside the pH range in which they exhibited their strongest Fe(III) reducing capacities *in vitro* and in supplementation experiments. This indicates that the main function of coumarins during Fe acquisition in Strategy I plants is the chelation of Fe(III) rather than Fe(III) reduction (Fig. 41). Nevertheless, coumarin-mediated Fe(III) reduction might be still relevant for Fe acquisition in Strategy I plants especially under specific growth conditions which limit FRO2 activity already at slightly acidic to near-neutral pH. This assumption is supported by the observation that, under relatively acidic pH conditions, *fro2* plants exhibited stronger Fe-deficiency symptoms under axenic growth conditions than in soils (Figs. 8, 13, and 14). Hence, soil microbes could potentially help *fro2* plants by providing not only Fe(III)-chelators but also Fe(III)-reductants. For instance, some microbes have been described to produce extracellular Fe(III) reductases, which have been proposed to mediate reduction for direct uptake of Fe^{2+} in such species (Cowart, 2002; Schröder, Johnson and de Vries, 2003). This is reasonable as coumarins are known to influence the composition root microbial communities (Stringlis *et al.*, 2018; Voges *et al.*, 2019; Harbort *et al.*, 2020) and coumarin release was found to be enhanced in the absence of a functional FRO2 already at acidic pH (Fig. 11). Since inoculation of Arabidopsis with a synthetic community of bacterial commensals has been recently reported to alleviate Fe deficiency and improve plant growth under conditions of low Fe availability in a FRO2-dependent manner at alkaline pH (Harbort *et al.*, 2020), and *fro2* plants are severely affected by Fe deficiency also on calcareous soils (Fig. 13), such processes might be of particular importance under acidic pH conditions.

Coumarins may also play a role under other conditions when FRO2 is inhibited. For instance, excess copper has been reported to inhibit FRO2 activity (Barton *et al.*, 2000; Waters and Armbrust, 2013) and is also known to increase the accumulation and release of phenolic compounds in different plant species such as Jerusalem artichokes and sunflower (Cabello-Hurtado *et al.*, 1998; Yaoya *et al.*, 2004; Meier *et al.*, 2012). Furthermore, substantial natural variation for FRO2 expression and root ferric-chelate reductase activity has been identified in natural accessions of *A. thaliana* (Satbhai *et al.*, 2017). Hence, the importance of Fe(III) reduction by coumarins might differ among individual Arabidopsis accession lines. Recent studies have revealed already that the metabolite composition of root exudates including coumarins varies among Arabidopsis accessions (Siwinska *et al.*, 2014; Mönchgesang *et al.*, 2016; Tsai *et al.*, 2018; Perkowska *et al.*, 2021). However, it remains to be elucidated whether

genotypic differences in FRO2-dependent ferric-chelate reductase activity causally affect the synthesis and release of Fe(III)-reducing coumarins.

The results from the present thesis also indicate that plant-derived coumarins possess a high potential for Fe acquisition that might not yet be fully exploited by certain genotypes, like the accession Col-0 of *A. thaliana*. For instance, it may be attempted to increase the release of fraxetin and sideretin at an external pH where their ability to reduce Fe(III) is not strongly limited, and to stimulate the release of esculetin, which has a particularly strong Fe(III) mobilizing capacity that is largely insensitive to external pH conditions to improve plant growth under different conditions of low Fe availability. Together, these results could provide a basis for the development of new strategies to breed Fe deficiency-tolerant crops and to implement approaches to use coumarins as natural Fe-chelators in organic farming.

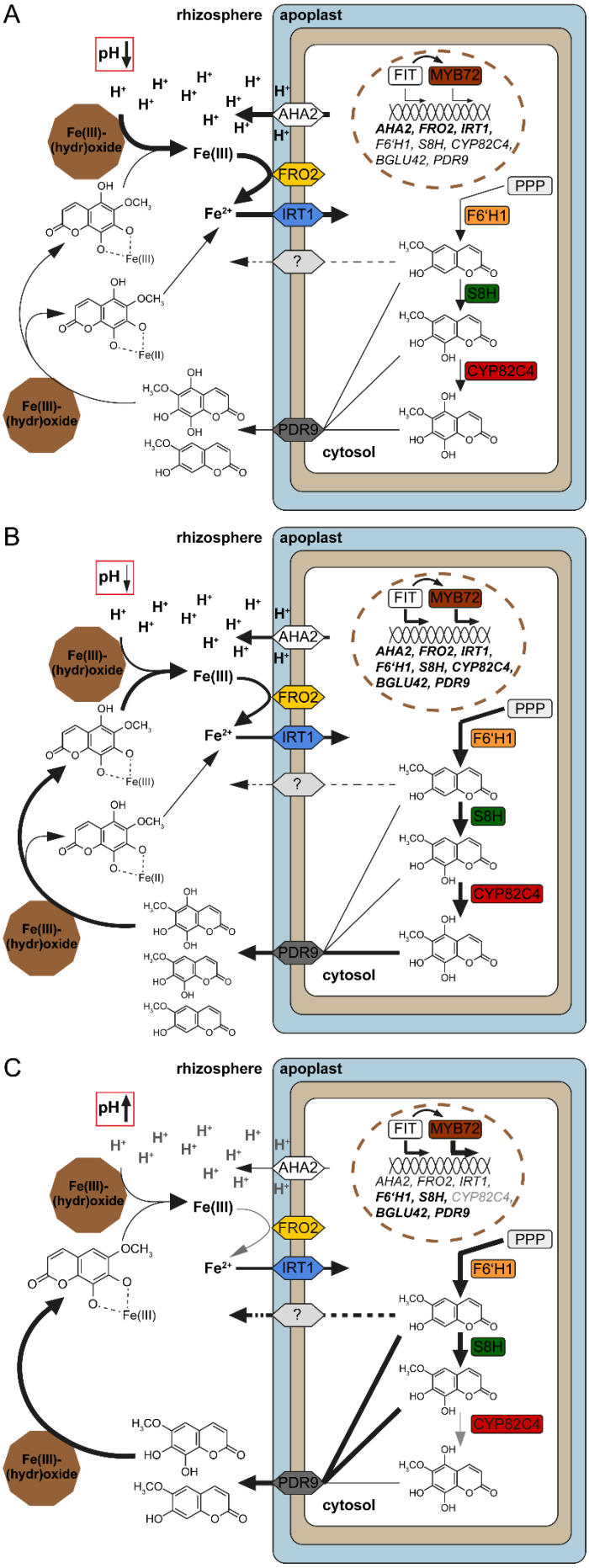

Fig. 41. Proposed model for coumarin-dependent functions in Fe acquisition under different pH and buffer scenarios. Function of coumarins in Fe acquisition at (A) acidic pH (~pH 5.5), (B) slightly acidic pH (~pH 6.5), or (C) alkaline pH (~pH 7.5). Under Fe-limiting conditions at acidic to slightly acidic pH, Fe acquisition is mainly achieved by proton-mediated acidification of the rhizosphere which enhances Fe solubility from otherwise insoluble sources, followed by the enzymatic reduction of Fe(III) at the root surface, and subsequent uptake of Fe^{2+}. As the external pH increases, proton-mediated acidification of the rhizosphere becomes strongly limited. In calcareous soils, high amounts of bicarbonate (HCO_3^-) are present which can efficiently buffer the released protons. Additionally, the enzymatic Fe(III) reduction via FRO2 is strongly inhibited under such conditions. Different Strategy I species, such as *A. thaliana*, can release coumarin-type siderophores to facilitate Fe acquisition. Coumarins assist the reduction-based Fe acquisition via Fe(III) reduction and chelation. The catecholic coumarins sideretin and fraxetin are capable of reducing Fe(III) at acidic to slightly acidic pH, respectively. Under these conditions, coumarin-mediated Fe(III) reduction can even complement lacking FRO2 activity. In general, coumarin levels in root exudates are increased in response to elevations in the external pH. Environmental pH conditions also determine the composition of the coumarins released. At acidic to slightly acidic pH, especially sideretin is released, while at alkaline pH conditions fraxetin becomes the most prominent coumarin. At least in part, this shift requires the action of the transcription factor MYB72, which is required to fully inhibit *CYP82C4* expression at alkaline pH conditions. In contrast to all other coumarins, the accumulation of the non-catecholic coumarin scopoletin in root exudates relies additionally on a yet unidentified transporter (indicated by question mark).
In the model, the boxes represent an epidermal root cell; in general, the thickness of the arrows indicates the importance of respective mechanism at different external pH conditions. Dashed arrows indicate proposed chemical reactions and interactions. Enhanced gene expression is indicated in bold. For simplicity, coumarins in the cells are depicted in their aglycon form. The process of coumarin deglycosylation is discussed in more detail in section 5.3. PPP: phenylpropanoid pathway.

5.3 A multi-layer control of root exudate coumarin composition by environmental pH

Besides an overall enhanced coumarin exudation by different Strategy I plant species under Fe-deficient conditions, the coumarin composition of root exudates has been indicated to be affected by the external pH conditions (Sisó-Terraza *et al.*, 2016; Rajniak *et al.*, 2018; Tsai *et al.*, 2018). In the present study, a combination of gene expression analysis and root extract and exudate analysis of wild-type and different mutant plants grown under different conditions of Fe availability as well as pH and buffer conditions has been employed to investigate the underlying mechanisms. Relative to pH 5.6, these analyses revealed that at pH 6.5 the expression of coumarin biosynthesis- and secretion-related genes increases (Fig. 31). Under alkaline pH conditions (i.e., pH 7.5) Fe deficiency further increases transcript levels of MYB72 relative to those of FIT, which promotes coumarin synthesis up to the level of fraxetin but inhibits sideretin biosynthesis (Fig. 31). Furthermore, this study investigated whether bicarbonate itself impacts the expression of genes involved in coumarin biosynthesis and secretion as it has been shown previously for *AHA2*, *FRO2*, and *IRT1* (Lucena *et al.*, 2007). Interestingly, the expression of the investigated genes remained largely unaffected by the presence of bicarbonate as any bicarbonate-related effects observed under sufficient Fe conditions were largely overruled by Fe deficiency (Fig. 28 and 31; Annex Figs. 14-16). This emphasizes the importance of coumarin exudation as alternative mechanism to the well-known reduction-based mechanism of Fe acquisition in Strategy I plants, as the latter is strongly inhibited by high pH and in presence of bicarbonate in calcareous soils (Bienfait *et al.*, 1983; Marschner, Römheld and Kissel, 1986; Romera, Alcántara and de la Guardia, 1992b; Kraemer, 2004; Lucena *et al.*, 2007; Colombo *et al.*, 2014). In agreement with this notion, a recent study demonstrated that local adaptation of Arabidopsis accessions to soils with elevated carbonate levels is more strongly related to higher exudation rates of protons and coumarins rather than to enhanced ferric-chelate reductase activity (Terés *et al.*, 2019).

The distinctive transcriptional regulation of the coumarin biosynthesis genes especially at alkaline pH represents a fundamental mechanism to modify the coumarin composition in roots and root exudates in response to the external pH. While the transcript levels and protein abundance of F6'H1 and especially S8H are strongly enhanced by elevated external pH conditions, CYP82C4 expression and protein accumulation is strongly inhibited at alkaline pH (Fig. 31-33). A recent genome-wide transcriptome study found that *CYP82C4* was among the genes most strongly repressed by high pH (Tsai and Schmidt, 2020). This indicates that external alkaline conditions determine the ratio of sideretin-to-fraxetin released by plants already at the transcriptional level. The fact that Fe(III) mobilization by sideretin is largely diminished (Fig. 6) probably due to its low stability under such conditions (see section 5.1 and

5.2) further supports this assumption. Since root exudate and root extract analysis showed that sideretin biosynthesis and release predominate at pH 5.6 and pH 6.5 while fraxetin was more abundant at pH 7.5 (Figs. 34 and 35), the importance of fraxetin for Fe acquisition under alkaline conditions was confirmed. Additionally, Tsai *et al.* (2018) have reported that the amount of released fraxetin in 22 Arabidopsis accession lines correlates positively with growth under high pH. This also explains why *cyp82C4* mutants, which over-produce fraxetin (Fig. 38) are indistinguishable from wild-type plants under different pH conditions (Rajniak *et al.*, 2018). Besides its higher capability to facilitate Fe(III) mobilization compared to sideretin at high external pH (Fig. 6 and 9), fraxetin is also known to be important for the assembly of the root microbiome in calcareous soil while sideretin is largely dispensable (Stringlis *et al.*, 2018; Voges *et al.*, 2019; Harbort *et al.*, 2020). Furthermore, synthesis and release of fraxetin but not of scopoletin and sideretin has been shown to be essential for the growth-promoting effect of bacterial commensals on Arabidopsis under conditions of low Fe availability (Harbort *et al.*, 2020).

Besides the distinctive changes in the expression of *S8H* and *CYP82C4*, the external pH also affects the cell type-specific localization of the two enzymes in roots. While CYP82C4 localization was largely confined to the epidermis, S8H expanded from epidermal to cortical cells when plants were grown under $NaHCO_3$-buffered conditions at alkaline pH (Figs. 32 and 33). The expanded cell type-specific localization of S8H in response to alkaline pH is in agreement with results of a spectral imaging approach that indicated that fraxin synthesis takes place in both the epidermis and cortex (Robe *et al.*, 2021).

A phylogenetic analysis of the genes conferring the sideretin pathway in different plant species revealed that *F6'H1* and *S8H* (i.e. scopoletin and fraxetin synthesis) are conserved in all examined Brassicaceae analyzed species, while *CYP82C4* (i.e. sideretin synthesis) was lost independently in several members of this family (Rajniak *et al.*, 2018). Considering the strong evidence that fraxetin is most advantageous for Fe acquisition in Strategy I plants at alkaline pH, this suggests that sideretin synthesis and release underlies a tight regulation in plants in dependence of the external pH. The transcriptional regulation of the investigated coumarin biosynthesis and secretion genes is directly controlled by FIT (Murgia *et al.*, 2011; Rodríguez-Celma *et al.*, 2013; Schmid *et al.*, 2014; Rajniak *et al.*, 2018; Tsai *et al.*, 2018). However, also MYB72 has been indicated to be associated with plant survival under Fe-limiting conditions by e.g. inducing the expression of distinct genes involved in coumarin biosynthesis and secretion (Zamioudis, Hanson and Pieterse, 2014). Although the expression of both *FIT* and *MYB72* has been shown to be induced by Fe deficiency (Palmer *et al.*, 2013; Zamioudis, Hanson and Pieterse, 2014), gene expression analysis revealed that they responded distinctively at the transcriptional level to different external pH conditions (Fig. 31; Annex Figs. 14-16). While *FIT* expression was only slightly induced and only when Fe was absent or Fe availability was low,

MYB72 transcription was considerably enhanced in response to increasing external pH, largely in a Fe status-independent manner. Although *MYB72* has been shown to be a direct target of FIT (Sivitz *et al.*, 2012), this finding indicates that MYB72 is part of an additional signaling cascade which modulates transcriptional regulation of downstream targets according to the external pH. However, up to date, only little is known on how the external pH is sensed and the corresponding signals are transduced in plants (Tsai and Schmidt, 2021). *Trans*-acting factors have been hypothesized to be involved in gene expression changes in response to the external pH by "transporting" information about the environmental pH to the nucleus, where they can interfere or override signaling cascades induced by other external stimuli (Gautam, Tsai and Schmidt, 2021; Tsai and Schmidt, 2021). Hence, MYB72 may function as a node of convergence for the Fe deficiency signal and the external pH signal to regulate the expression of several genes involved in coumarin biosynthesis and secretion. The strong repression of several genes involved in coumarin biosynthesis and secretion in *myb72-1* plants (Fig. 39; Annex Fig. 18) further supports this hypothesis. However, it remains enigmatic why *myb72* mutants do not show any visible phenotype in comparison to the wild type when grown under conditions of low Fe availability, as coumarin levels in root exudates of *myb72-1* plants are strongly decreased (Fig. 40).

Among the genes most strongly repressed in *myb72-1* plants were *F6'H1*, *BGLU42*, and *PDR9* (Fig. 39; Annex Fig. 18). While only *BGLU42* has been previously proposed to be a direct target of MYB72, *PDR9* has been found being induced in response to colonialization with the plant growth-promoting rhizobacterium *Pseudomonas fluorescens* WCS417 in a MYB72-dependent manner (Palmer *et al.*, 2013; Zamioudis, Hanson and Pieterse, 2014). In contrast, the absence of MYB72 largely diminished the repression of *CYP82C4* at high pH raising evidence that MYB72 may act as a transcriptional activator for some or as repressor for other genes. Interestingly, *S8H* expression appeared largely independent of MYB72, as expression levels were only slightly down-regulated in *myb72-1*. Thus, it is possible that *S8H* expression responds to an MYB72-independent signaling cascade. In fact, it has been recently shown that the ectopic expression of the *IRONMAN* peptides *IMA1* and *IMA2* can improve plant growth on calcareous soil by enhancing coumarin biosynthesis and release of especially fraxetin through increased expression of *S8H* at high external pH (Gautam, Tsai and Schmidt, 2021). IRONMAN/FE-UPTAKE-INDUCING PEPTIDES (IMA/FEP) are a novel family of peptides that have been described to be essential for Fe uptake in plants presumably through activation of bHLH proteins subgroup Ib such as *bHLH38* and *bHLH39* (Grillet *et al.*, 2018; Hirayama *et al.*, 2018). Furthermore, Tsai and Schmidt (2020) have recently suggested bHLH proteins of the subgroup Ib to have a direct or indirect role in the pH dependent regulation of Fe uptake as they have been identified to be highly upregulated at optimal pH but strongly downregulated at high pH. Since these bHLH proteins are essential to activate FIT in roots (Yuan *et al.*, 2008;

Wang *et al.*, 2013), their weaker expression at alkaline pH may indicate that MYB72 function becomes more prominent to orchestrate distinctive changes in the transcriptional regulation of coumarin biosynthesis and secretion genes and also for the coumarin composition in root exudates under such conditions (Fig. 41). However, further research is needed to elucidate the underlying mechanisms involved in sensing of the external pH and perception of this environmental stimulus to induce distinctive physiological and morphological adaptations in plants.

Besides affecting coumarin biosynthesis, the present gene expression analysis also suggested that elevated pH conditions can directly affect the *PDR9* expression independent of the Fe status (Fig. 31; Annex Figs. 14-16). However, as this effect was less dramatic than for genes encoding coumarin biosynthesis enzymes, pH-dependent changes in the composition of root exudates are more likely determined at the level of biosynthesis rather than export. However, to investigate a possible influence of external pH and buffers on PDR9-mediated coumarin secretion additional experiments, such as transport assays in oocytes (Pike *et al.*, 2019) are required. Noteworthy, the lack of functional PDR9 does not completely abolish coumarin secretion (Fig. 38; Fourcroy *et al.*, 2014; Ziegler *et al.*, 2017), suggesting the involvement of further transporters in coumarin release. As only the concentration of catecholate coumarins was decreased in root exudates of *pdr9-2* plants (Fig. 38), these yet unidentified transporters appear especially relevant for the export of scopoletin. Interestingly, also NtPDR3 from *Nicotiana tabacum*, which is the closest homolog of AtPDR9, has been shown to preferentially transport catechol-harboring coumarins (Lefèvre *et al.*, 2018).

The external pH might also alter the coumarin composition of root exudates by affecting the deglycosylation of the coumarin glycosides. It is thought that deglycosylation is a pivotal step to turn glycosylated coumarins into biologically active compounds. In the case of esculin and fraxin, deglycosylation sets the catechol group free that is critical for Fe binding. Although it remains elusive where such a deglycosylation step may take place, published models have suggested that coumarin deglycosylation occurs inside the root, which was mainly based on the reported promoter activity of BGLU42 in epidermal cells of *A. thaliana* (Zamioudis, Hanson and Pieterse, 2014; Tsai and Schmidt, 2017a; Robe *et al.*, 2021). The present study indicates that coumarin deglycosylation is a pH-dependent process and that deglycosylation of catecholic and non-catecholic coumarins occurs at different locations. The root extract and root exudate data obtained for different external pH conditions indicated that scopolin synthesis in roots is largely independent of pH, while its degylcosylation and the consequent accumulation of scopoletin in root exudates is affected by the external pH (Figs. 34A and 35A). Indeed, among β-glycosidases, BGLU42 has been identified to specifically deglycosylate scopolin (Ahn *et al.*, 2010; Zamioudis, Hanson and Pieterse, 2014; Stringlis *et al.*, 2018). In

contrast, fraxin and fraxetin accumulated in both roots and root exudates responded to the external pH, suggesting that fraxin deglycosylation is a pH-dependent process. This probably also applies to esculin/esculetin as their accumulation in roots and root exudates followed a similar pattern as fraxin and fraxetin. Although no sideretin glycoside was determined due to the lack of an authentic standard, different studies have reported the detection of a sideretin glycoside in roots (Ziegler *et al.*, 2017; Chutia, Abel and Ziegler, 2019). However, the results from gene expression analysis presented in this study indicated that sideretin synthesis rather than deglycosylation is diminished by high pH (pH 7.5) conditions (Fig. 31-33; Annex Figs. 14-16). The root extract and exudate data of the present study also provided indications that scopolin deglycosylation mainly takes place during or after its exudation, while significant fraxin deglycosylation can already occur inside root cells (see section 4.13). Based on the high sideretin concentrations detected in root extracts (Fig. 35A), it is also hypothesized that significant deglycosylation of its corresponding glycoside can happen already within root cells. However, further research is needed to identify the enzymes carrying out coumarin deglycosylation.

6 References

Abenavoli, M.R. *et al.* (2008) 'Effects of different allelochemicals on root morphology of Arabidopsis thaliana', *Allelopathy Journal*, 22(1), pp. 245–252.

Ahmed, E. and Holmström, S.J.M. (2014) 'Siderophores in environmental research: roles and applications', *Microbial Biotechnology*, 7(3), pp. 196–208. doi:10.1111/1751-7915.12117.

Ahn, Y.O. *et al.* (2010) 'Scopolin-hydrolyzing β-glucosidases in roots of Arabidopsis', *Plant and Cell Physiology*, 51(1), pp. 132–143. doi:10.1093/pcp/pcp174.

Alvarez-Fernández, A. *et al.* (2014) 'Metal species involved in long distance metal transport in plants', *Frontiers in plant science*, 5, pp. 105–105. doi:10.3389/fpls.2014.00105.

Andjelković, M. *et al.* (2006) 'Iron-chelation properties of phenolic acids bearing catechol and galloyl groups', *Food Chemistry*, 98(1), pp. 23–31. doi:10.1016/j.foodchem.2005.05.044.

Annesley, T.M. (2003) 'Ion Suppression in Mass Spectrometry', *Clinical Chemistry*, 49(7), pp. 1041–1044. doi:10.1373/49.7.1041.

Badri, D.V. and Vivanco, J.M. (2009) 'Regulation and function of root exudates', *Plant, Cell & Environment*, 32(6), pp. 666–681. doi:10.1111/j.1365-3040.2009.01926.x.

Bais, H.P. *et al.* (2006) 'The role of root exudates in rhizosphere interactions with plants and other organisms', *Annual Review of Plant Biology*, 57(1), pp. 233–266. doi:10.1146/annurev.arplant.57.032905.105159.

Banwart, S., Davies, S. and Stumm, W. (1989) 'The role of oxalate in accelerating the reductive dissolution of hematite (α-Fe2O3) by ascorbate', *Colloids and Surfaces*, 39(2), pp. 303–309. doi:10.1016/0166-6622(89)80281-1.

Barrett-Lennard, E.G., Marschner, H. and Römheld, V. (1983) 'Mechanism of Short Term FeIII Reduction by Roots 1: Evidence against the Role of Secreted Reductants', *Plant Physiology*, 73(4), pp. 893–898. doi:10.1104/pp.73.4.893.

Barton, L.L. *et al.* (2000) 'Inhibition of ferric chelate reductase in alfalfa roots by cobalt, nickel, chromium, and copper', *Journal of Plant Nutrition*, 23(11–12), pp. 1833–1845. doi:10.1080/01904160009382146.

Baune, M. *et al.* (2020) 'Importance of oxidation products in coumarin-mediated Fe(hydr)oxide mineral dissolution', *BioMetals*, 33(6), pp. 305–321. doi:10.1007/s10534-020-00248-y.

Bienfait, H.F. *et al.* (1983) 'Characterization of ferric reducing activity in roots of Fe-deficient Phaseolus vulgaris', *Physiologia Plantarum*, 59(2), pp. 196–202. doi:10.1111/j.1399-3054.1983.tb00757.x.

Biswakarma, J. *et al.* (2019) 'Fe(II)-Catalyzed Ligand-Controlled Dissolution of Iron(hydr)oxides', *Environmental Science & Technology*, 53(1), pp. 88–97. doi:10.1021/acs.est.8b03910.

Bourgaud, F. *et al.* (2006) 'Biosynthesis of coumarins in plants: a major pathway still to be unravelled for cytochrome P450 enzymes', *Phytochemistry Reviews*, 5(2), pp. 293–308. doi:10.1007/s11101-006-9040-2.

Bowden, K., Hanson, M.J. and Taylor, G.R. (1968) 'Reactions of carbonyl compounds in basic solutions. Part I. The alkaline ring fission of coumarins', *Journal of the Chemical Society B: Physical Organic*, (0), pp. 174–177. doi:10.1039/J29680000174.

Briat, J.-F., Dubos, C. and Gaymard, F. (2015) 'Iron nutrition, biomass production, and plant product quality', *Trends in Plant Science*, 20(1), pp. 33–40. doi:10.1016/j.tplants.2014.07.005.

Brown, J.C. and Ambler, J.E. (1973) '"Reductants" Released by Roots of Fe-Deficient Soybeans1', *Agronomy Journal*, 65(2), pp. 311–314. doi:10.2134/agronj1973.00021962006500020037x.

Bustin, S.A. *et al.* (2009) 'The MIQE Guidelines: Minimum Information for Publication of Quantitative Real-Time PCR Experiments', *Clinical Chemistry*, 55(4), pp. 611–622. doi:10.1373/clinchem.2008.112797.

Cabello-Hurtado, F. *et al.* (1998) 'Coumarins in helianthus tuberosus : characterization, induced accumulation and biosynthesis', *Phytochemistry*, 49(4), pp. 1029–1036. doi:10.1016/S0031-9422(97)01036-4.

Chaney, R.L., Brown, J.C. and Tiffin, L.O. (1972) 'Obligatory Reduction of Ferric Chelates in Iron Uptake by Soybeans', *Plant Physiology*, 50(2), pp. 208–213. doi:10.1104/pp.50.2.208.

Chen, Y. and Barak, P. (1982) 'Iron Nutrition of Plants in Calcareous Soils', in Brady, N.C. (ed.) *Advances in Agronomy*. Academic Press, pp. 217–240. doi:10.1016/S0065-2113(08)60326-0.

Chutia, R., Abel, S. and Ziegler, J. (2019) 'Iron and Phosphate Deficiency Regulators Concertedly Control Coumarin Profiles in Arabidopsis thaliana Roots During Iron, Phosphate, and Combined Deficiencies', *Frontiers in Plant Science*, 10, p. 113. doi:10.3389/fpls.2019.00113.

Clemens, S. and Weber, M. (2016) 'The essential role of coumarin secretion for Fe acquisition from alkaline soil', *Plant Signaling & Behavior*, 11(2), p. e1114197. doi:10.1080/15592324.2015.1114197.

Clough, S.J. and Bent, A.F. (1998) 'Floral dip: a simplified method for Agrobacterium -mediated transformation of Arabidopsis thaliana', *The Plant Journal*, 16(6), pp. 735–743. doi:10.1046/j.1365-313x.1998.00343.x.

Colangelo, E.P. and Guerinot, M.L. (2004) 'The Essential Basic Helix-Loop-Helix Protein FIT1 Is Required for the Iron Deficiency Response', *The Plant Cell*, 16(12), pp. 3400–3412. doi:10.1105/tpc.104.024315.

Colombo, C. *et al.* (2014) 'Review on iron availability in soil: interaction of Fe minerals, plants, and microbes', *Journal of Soils and Sediments*, 14(3), pp. 538–548. doi:10.1007/s11368-013-0814-z.

Comerford, N.B. (2005) 'Soil Factors Affecting Nutrient Bioavailability', in BassiriRad, H. (ed.) *Nutrient Acquisition by Plants: An Ecological Perspective*. Berlin, Heidelberg: Springer Berlin Heidelberg, pp. 1–14. doi:10.1007/3-540-27675-0_1.

Connolly, E.L. *et al.* (2003) 'Overexpression of the FRO2 Ferric Chelate Reductase Confers Tolerance to Growth on Low Iron and Uncovers Posttranscriptional Control', *Plant Physiology*, 133(3), p. 1102. doi:10.1104/pp.103.025122.

Cornell, R.M. and Schwertmann, U. (2003) *The Iron Oxides: Structure, Properties, Reactions, Occurences and Uses*. 2nd edition. Wiley-VCH Verlag GmbH & Co. KGaA.

Cowart, R.E. (2002) ‘Reduction of iron by extracellular iron reductases: implications for microbial iron acquisition’, *Archives of Biochemistry and Biophysics*, 400(2), pp. 273–281. doi:10.1016/S0003-9861(02)00012-7.

Curie, C. *et al.* (2001) ‘Maize yellow stripe1 encodes a membrane protein directly involved in Fe(III) uptake’, *Nature*, 409(6818), pp. 346–349. doi:10.1038/35053080.

Dakora, F.D. and Phillips, D.A. (2002) ‘Root exudates as mediators of mineral acquisition in low-nutrient environments’, *Plant and Soil*, 245(1), pp. 35–47. doi:10.1023/A:1020809400075.

Dos Santos Afonso, M. *et al.* (1990) ‘The reductive dissolution of iron oxides by ascorbate: The role of carboxylate anions in accelerating reductive dissolution’, *Journal of Colloid and Interface Science*, 138(1), pp. 74–82. doi:10.1016/0021-9797(90)90181-M.

Eberhard, S., Finazzi, G. and Wollman, F.-A. (2008) ‘The Dynamics of Photosynthesis’, *Annual Review of Genetics*, 42(1), pp. 463–515. doi:10.1146/annurev.genet.42.110807.091452.

Eide, D. *et al.* (1996) ‘A novel iron-regulated metal transporter from plants identified by functional expression in yeast’, *Proceedings of the National Academy of Sciences*, 93(11), p. 5624. doi:10.1073/pnas.93.11.5624.

Fageria, N.K. and Stone, L.F. (2006) ‘Physical, Chemical, and Biological Changes in the Rhizosphere and Nutrient Availability’, *Journal of Plant Nutrition*, 29(7), pp. 1327–1356. doi:10.1080/01904160600767682.

Fiedler, S., Vepraskas, M.J. and Richardson, J.L. (2007) ‘Soil Redox Potential: Importance, Field Measurements, and Observations’, in Sparks, D.L. (ed.) *Advances in Agronomy*. Academic Press, pp. 1–54. doi:10.1016/S0065-2113(06)94001-2.

Fourcroy, P. *et al.* (2014) ‘Involvement of the ABCG37 transporter in secretion of scopoletin and derivatives by Arabidopsis roots in response to iron deficiency’, *New Phytologist*, 201(1), pp. 155–167. doi:10.1111/nph.12471.

Fourcroy, P. *et al.* (2016) ‘Facilitated Fe Nutrition by Phenolic Compounds Excreted by the Arabidopsis ABCG37/PDR9 Transporter Requires the IRT1/FRO2 High-Affinity Root Fe2+ Transport System’, *Molecular Plant*, 9(3), pp. 485–488. doi:10.1016/j.molp.2015.09.010.

Frey, P.A. and Reed, G.H. (2012) ‘The Ubiquity of Iron’, *ACS Chemical Biology*, 7(9), pp. 1477–1481. doi:10.1021/cb300323q.

Gao, F. *et al.* (2020) ‘The Transcription Factor bHLH121 Interacts with bHLH105 (ILR3) and Its Closest Homologs to Regulate Iron Homeostasis in Arabidopsis’, *The Plant Cell*, 32(2), p. 508. doi:10.1105/tpc.19.00541.

Garrett, E.R., Lippold, B.C. and Mielck, J.B. (1971) ‘Kinetics and Mechanisms of Lactonization of Coumarinic Acids and Hydrolysis of Coumarins I’, *Journal of Pharmaceutical Sciences*, 60(3), pp. 396–405. doi:10.1002/jps.2600600312.

Gautam, C.K., Tsai, H.-H. and Schmidt, W. (2021) ‘IRONMAN Tunes Responses to Iron Deficiency in Concert with Environmental pH’, *bioRxiv*, p. 2021.02.16.431461. doi:10.1101/2021.02.16.431461.

Giehl, R.F.H. and von Wirén, N. (2014) ‘Root Nutrient Foraging’, *Plant Physiology*, 166(2), p. 509. doi:10.1104/pp.114.245225.

Gojon, A., Nacry, P. and Davidian, J.-C. (2009) 'Root uptake regulation: a central process for NPS homeostasis in plants', *Physiology and Metabolism*, 12(3), pp. 328–338. doi:10.1016/j.pbi.2009.04.015.

Grillet, L. *et al.* (2018) 'IRON MAN is a ubiquitous family of peptides that control iron transport in plants', *Nature Plants*, 4(11), pp. 953–963. doi:10.1038/s41477-018-0266-y.

Gruber, B.D. *et al.* (2013) 'Plasticity of the Arabidopsis Root System under Nutrient Deficiencies', *Plant Physiology*, 163(1), p. 161. doi:10.1104/pp.113.218453.

Guerinot, M.L. (2000) 'The ZIP family of metal transporters', *Biochimica et Biophysica Acta (BBA) - Biomembranes*, 1465(1), pp. 190–198. doi:10.1016/S0005-2736(00)00138-3.

Guerinot, M.L. and Yi, Y. (1994) 'Iron: Nutritious, Noxious, and Not Readily Available', *Plant Physiology*, 104(3), pp. 815–820. doi:10.1104/pp.104.3.815.

Harborne, J.B. (1999) 'Classes and Functions of Secondary Products from Plants', in *Chemicals from Plants*. WORLD SCIENTIFIC / IMPERIAL COLLEGE PRESS, pp. 1–25. doi:10.1142/9789812817273_0001.

Harbort, C.J. *et al.* (2020) 'Root-Secreted Coumarins and the Microbiota Interact to Improve Iron Nutrition in Arabidopsis', *Cell Host & Microbe*, 28(6), pp. 825-837.e6. doi:10.1016/j.chom.2020.09.006.

Hermans, C. *et al.* (2006) 'How do plants respond to nutrient shortage by biomass allocation?', *Trends in Plant Science*, 11(12), pp. 610–617. doi:10.1016/j.tplants.2006.10.007.

Hether, N.H., Olsen, R.A. and Jackson, L.L. (1984) 'Chemical identification of iron reductants exuded by plant roots', *Journal of Plant Nutrition*, 7(1–5), pp. 667–676. doi:10.1080/01904168409363231.

Hider, R.C. and Kong, X. (2010) 'Chemistry and biology of siderophores', *Natural Product Reports*, 27(5), pp. 637–657. doi:10.1039/B906679A.

Hider, R.C., Liu, Z.D. and Khodr, H.H. (2001) 'Metal chelation of polyphenols', in *Methods in Enzymology*. Academic Press, pp. 190–203. doi:10.1016/S0076-6879(01)35243-6.

Hinsinger, P. *et al.* (2009) 'Rhizosphere: biophysics, biogeochemistry and ecological relevance', *Plant and Soil*, 321(1), pp. 117–152. doi:10.1007/s11104-008-9885-9.

Hirayama, T. *et al.* (2018) 'The Putative Peptide Gene FEP1 Regulates Iron Deficiency Response in Arabidopsis', *Plant and Cell Physiology*, 59(9), pp. 1739–1752. doi:10.1093/pcp/pcy145.

Husson, O. (2013) 'Redox potential (Eh) and pH as drivers of soil/plant/microorganism systems: a transdisciplinary overview pointing to integrative opportunities for agronomy', *Plant and Soil*, 362(1), pp. 389–417. doi:10.1007/s11104-012-1429-7.

Ivanov, R., Brumbarova, T. and Bauer, P. (2012) 'Fitting into the Harsh Reality: Regulation of Iron-deficiency Responses in Dicotyledonous Plants', *Molecular Plant*, 5(1), pp. 27–42. doi:10.1093/mp/ssr065.

Jakoby, M. *et al.* (2004) 'FRU (BHLH029) is required for induction of iron mobilization genes in Arabidopsis thaliana', *FEBS Letters*, 577(3), pp. 528–534. doi:10.1016/j.febslet.2004.10.062.

Jin, C.W. *et al.* (2007) 'Iron Deficiency-Induced Secretion of Phenolics Facilitates the Reutilization of Root Apoplastic Iron in Red Clover', *Plant Physiology*, 144(1), p. 278. doi:10.1104/pp.107.095794.

Johnson, S.E. and Loeppert, R.H. (2006) 'Role of Organic Acids in Phosphate Mobilization from Iron Oxide', *Soil Science Society of America Journal*, 70(1), pp. 222–234. doi:10.2136/sssaj2005.0012.

Julian, G., Cameron, H.J. and Olsen, R.A. (1983) 'Role of chelation by ortho dihydroxy phenols in iron absorption by plant roots', *Journal of Plant Nutrition*, 6(2), pp. 163–175. doi:10.1080/01904168309363078.

Kai, K. *et al.* (2008) 'Scopoletin is biosynthesized via ortho-hydroxylation of feruloyl CoA by a 2-oxoglutarate-dependent dioxygenase in Arabidopsis thaliana', *The Plant Journal*, 55(6), pp. 989–999. doi:10.1111/j.1365-313X.2008.03568.x.

Kang, K. *et al.* (2019) 'Low Fe(II) Concentrations Catalyze the Dissolution of Various Fe(III) (hydr)oxide Minerals in the Presence of Diverse Ligands and over a Broad pH Range', *Environmental Science & Technology*, 53(1), pp. 98–107. doi:10.1021/acs.est.8b03909.

Kawai, S., Takagi, S. -I. and Sato, Y. (1988) 'Mugineic acid-family phytosiderophores in root-secretions of barley, corn and sorghum varieties', *Journal of Plant Nutrition*, 11(6–11), pp. 633–642. doi:10.1080/01904168809363829.

Kim, S.A. *et al.* (2019) 'The iron deficiency response in Arabidopsis thaliana requires the phosphorylated transcription factor URI', *Proceedings of the National Academy of Sciences*, 116(50), p. 24933. doi:10.1073/pnas.1916892116.

Kobayashi, T. (2019) 'Understanding the Complexity of Iron Sensing and Signaling Cascades in Plants', *Plant and Cell Physiology*, 60(7), pp. 1440–1446. doi:10.1093/pcp/pcz038.

Kobayashi, T. and Nishizawa, N.K. (2012) 'Iron Uptake, Translocation, and Regulation in Higher Plants', *Annual Review of Plant Biology*, 63(1), pp. 131–152. doi:10.1146/annurev-arplant-042811-105522.

Köster, J. *et al.* (2011) 'Evaluation of different column types for the hydrophilic interaction chromatographic separation of iron-citrate and copper-histidine species from plants', *Selected Papers from the 28th International Symposium on Chromatography*, 1218(30), pp. 4934–4943. doi:10.1016/j.chroma.2011.03.036.

Kraemer, S.M. (2004) 'Iron oxide dissolution and solubility in the presence of siderophores', *Aquatic Sciences*, 66(1), pp. 3–18. doi:10.1007/s00027-003-0690-5.

Lampropoulos, A. *et al.* (2013) 'GreenGate - A Novel, Versatile, and Efficient Cloning System for Plant Transgenesis', *PLOS ONE*, 8(12), p. e83043. doi:10.1371/journal.pone.0083043.

Läuchli, A. and Grattan, S.R. (2012) 'Soil pH Extremes', in *Plant Stress Physiology*. Wallingford: CAB International, pp. 194–209.

Le Roy, J. *et al.* (2016) 'Glycosylation Is a Major Regulator of Phenylpropanoid Availability and Biological Activity in Plants', *Frontiers in Plant Science*, 7, p. 735. doi:10.3389/fpls.2016.00735.

Lefèvre, F. *et al.* (2018) 'The Nicotiana tabacum ABC transporter NtPDR3 secretes O-methylated coumarins in response to iron deficiency', *Journal of Experimental Botany*, 69(18), pp. 4419–4431. doi:10.1093/jxb/ery221.

Lešková, A. *et al.* (2017) 'Heavy Metals Induce Iron Deficiency Responses at Different Hierarchic and Regulatory Levels', *Plant Physiology*, 174(3), p. 1648. doi:10.1104/pp.16.01916.

Li, X. *et al.* (2016) 'Two bHLH Transcription Factors, bHLH34 and bHLH104, Regulate Iron Homeostasis in Arabidopsis thaliana', *Plant Physiology*, 170(4), p. 2478. doi:10.1104/pp.15.01827.

Liang, G. *et al.* (2017) 'bHLH transcription factor bHLH115 regulates iron homeostasis in Arabidopsis thaliana', *Journal of Experimental Botany*, 68(7), pp. 1743–1755. doi:10.1093/jxb/erx043.

Lindsay, W.L. (1995) 'Chemical reactions in soils that affect iron availability to plants. A quantative approach', in Abadía, J. (ed.) *Iron Nutrition in Soils and Plants: Proceedings of the Seventh International Symposium on Iron Nutrition and Interactions in Plants, June 27–July 2, 1993, Zaragoza, Spain*. Dordrecht: Springer Netherlands, pp. 7–14. doi:10.1007/978-94-011-0503-3_2.

Lindsay, W.L. and Schwab, A.P. (1982) 'The chemistry of iron in soils and its availability to plants', *Journal of Plant Nutrition*, 5(4–7), pp. 821–840. doi:10.1080/01904168209363012.

Livak, K.J. and Schmittgen, T.D. (2001) 'Analysis of Relative Gene Expression Data Using Real-Time Quantitative PCR and the 2−ΔΔCT Method', *Methods*, 25(4), pp. 402–408. doi:10.1006/meth.2001.1262.

Loneragan, J.F., Snowball, K. and Robson, A. (1976) 'Remobilization of Nutrients and its Significance in Plant Nutrition', in *Transport and Transfer Process in Plants*. Academic Press.

López-Bucio, J., Cruz-Ramírez, A. and Herrera-Estrella, L. (2003) 'The role of nutrient availability in regulating root architecture', *Current Opinion in Plant Biology*, 6(3), pp. 280–287. doi:10.1016/S1369-5266(03)00035-9.

Lozhkin, A.V. and Sakanyan, E.I. (2006) 'Natural coumarins: Methods of isolation and analysis', *Pharmaceutical Chemistry Journal*, 40(6), pp. 337–346. doi:10.1007/s11094-006-0123-6.

Lucena, C. *et al.* (2007) 'Bicarbonate blocks the expression of several genes involved in the physiological responses to Fe deficiency of Strategy I plants', *Functional Plant Biology*, 34(11), pp. 1002–1009. doi:10.1071/FP07136.

Lucena, J.J. (2000) 'Effects of bicarbonate, nitrate and other environmental factors on iron deficiency chlorosis. A review', *Journal of Plant Nutrition*, 23(11–12), pp. 1591–1606. doi:10.1080/01904160009382126.

Lynch, J. (1995) 'Root Architecture and Plant Productivity', *Plant physiology*, 109(1), pp. 7–13. doi:10.1104/pp.109.1.7.

Ma, J.F. *et al.* (1995) 'Biosynthesis of Phytosiderophores, Mugineic Acids, Associated with Methionine Cycling *', *Journal of Biological Chemistry*, 270(28), pp. 16549–16554. doi:10.1074/jbc.270.28.16549.

Ma, J.F. and Nomoto, K. (1993) 'Two Related Biosynthetic Pathways of Mugineic Acids in Gramineous Plants', *Plant Physiology*, 102(2), pp. 373–378. doi:10.1104/pp.102.2.373.

Ma, J.F. and Nomoto, K. (1994) 'Incorporation of Label from 13C-, 2H-, and 15N-Labeled Methionine Molecules during the Biosynthesis of 2[prime]-Deoxymugineic Acid in Roots of Wheat', *Plant Physiology*, 105(2), pp. 607–610. doi:10.1104/pp.105.2.607.

Ma, J.F. and Nomoto, K. (1996) 'Effective regulation of iron acquisition in graminaceous plants. The role of mugineic acids as phytosiderophores', *Physiologia Plantarum*, 97(3), pp. 609–617. doi:10.1111/j.1399-3054.1996.tb00522.x.

Mai, H.-J., Pateyron, S. and Bauer, P. (2016) 'Iron homeostasis in Arabidopsis thaliana: transcriptomic analyses reveal novel FIT-regulated genes, iron deficiency marker genes and functional gene networks', *BMC Plant Biology*, 16(1), p. 211. doi:10.1186/s12870-016-0899-9.

Maillard, A. *et al.* (2015) 'Leaf mineral nutrient remobilization during leaf senescence and modulation by nutrient deficiency', *Frontiers in Plant Science*, 6, p. 317. doi:10.3389/fpls.2015.00317.

Marschner, H. (2012) *Marschner's Mineral Nutrition of Higher Plants*. 3rd edition. Academic Press.

Marschner, H. and Römheld, V. (1994) 'Strategies of plants for acquisition of iron', *Plant and Soil*, 165(2), pp. 261–274. doi:10.1007/BF00008069.

Marschner, H., Römheld, V. and Kissel, M. (1986) 'Different strategies in higher plants in mobilization and uptake of iron', *Journal of Plant Nutrition*, 9(3–7), pp. 695–713. doi:10.1080/01904168609363475.

Meier, S. *et al.* (2012) 'Influence of copper on root exudate patterns in some metallophytes and agricultural plants', *Ecotoxicology and Environmental Safety*, 75, pp. 8–15. doi:10.1016/j.ecoenv.2011.08.029.

Mengel, K. *et al.* (2001) 'Iron', in Inoue, K. et al. (eds) *Principles of Plant Nutrition*. Dordrecht: Springer Netherlands, pp. 553–571. doi:10.1007/978-94-010-1009-2_13.

Mino, Y. *et al.* (1983) 'Mugineic acid-iron(III) complex and its structurally analogous cobalt(III) complex: characterization and implication for absorption and transport of iron in gramineous plants', *Journal of the American Chemical Society*, 105(14), pp. 4671–4676. doi:10.1021/ja00352a024.

Mladěnka, P. *et al.* (2010) 'In vitro interactions of coumarins with iron', *Advances in Biomolecular and Medicinal Chemistry*, 92(9), pp. 1108–1114. doi:10.1016/j.biochi.2010.03.025.

Mönchgesang, S. *et al.* (2016) 'Natural variation of root exudates in Arabidopsis thaliana-linking metabolomic and genomic data', *Scientific Reports*, 6(1), p. 29033. doi:10.1038/srep29033.

Moran, J.F. *et al.* (1997) 'Complexes of Iron with Phenolic Compounds from Soybean Nodules and Other Legume Tissues: Prooxidant and Antioxidant Properties', *Free Radical Biology and Medicine*, 22(5), pp. 861–870. doi:10.1016/S0891-5849(96)00426-1.

Mori, S. *et al.* (1987) 'Dynamic state of mugineic acid and analogous phytosiderophores in Fe-deficient barley', *Journal of Plant Nutrition*, 10(9–16), pp. 1003–1011. doi:10.1080/01904168709363628.

Murashige, T. and Skoog, F. (1962) 'A Revised Medium for Rapid Growth and Bio Assays with Tobacco Tissue Cultures', *Physiologia Plantarum*, 15(3), pp. 473–497. doi:10.1111/j.1399-3054.1962.tb08052.x.

Murata, Y. *et al.* (2006) 'A specific transporter for iron(III)–phytosiderophore in barley roots', *The Plant Journal*, 46(4), pp. 563–572. doi:10.1111/j.1365-313X.2006.02714.x.

Murgia, I. *et al.* (2011) 'Arabidopsis CYP82C4 expression is dependent on Fe availability and circadian rhythm, and correlates with genes involved in the early Fe deficiency response', *Journal of Plant Physiology*, 168(9), pp. 894–902. doi:10.1016/j.jplph.2010.11.020.

Nozoye, T. *et al.* (2011) 'Phytosiderophore efflux transporters are crucial for iron acquisition in graminaceous plants', *The Journal of biological chemistry*. 2010/12/14 edn, 286(7), pp. 5446–5454. doi:10.1074/jbc.M110.180026.

Olsen, R.A. *et al.* (1981) 'Chemical aspects of the Fe stress response mechanism in tomatoes', *Journal of Plant Nutrition*, 3(6), pp. 905–921. doi:10.1080/01904168109362887.

Palmer, C.M. *et al.* (2013) 'MYB10 and MYB72 Are Required for Growth under Iron-Limiting Conditions', *PLOS Genetics*, 9(11), p. e1003953. doi:10.1371/journal.pgen.1003953.

Pan, I.-C. *et al.* (2015) 'Post-Transcriptional Coordination of the Arabidopsis Iron Deficiency Response is Partially Dependent on the E3 Ligases RING DOMAIN LIGASE1 (RGLG1) and RING DOMAIN LIGASE2 (RGLG2)*', *Molecular & Cellular Proteomics*, 14(10), pp. 2733–2752. doi:10.1074/mcp.M115.048520.

Pascale, A. *et al.* (2020) 'Modulation of the Root Microbiome by Plant Molecules: The Basis for Targeted Disease Suppression and Plant Growth Promotion', *Frontiers in Plant Science*, 10, p. 1741. doi:10.3389/fpls.2019.01741.

Peiffer, S. and Wan, M. (2016) 'Reductive Dissolution and Reactivity of Ferric (Hydr)oxides: New Insights and Implications for Environmental Redox Processes', in *Iron Oxides*. John Wiley & Sons, Ltd, pp. 31–52. doi:10.1002/9783527691395.ch3.

Perkowska, I. *et al.* (2021) 'Identification and Quantification of Coumarins by UHPLC-MS in Arabidopsis thaliana Natural Populations', *Molecules*, 26(6), p. 1804. doi:10.3390/molecules26061804.

Perron, N.R. *et al.* (2010) 'Kinetics of iron oxidation upon polyphenol binding', *Dalton Transactions*, 39(41), pp. 9982–9987. doi:10.1039/C0DT00752H.

Perron, N.R. and Brumaghim, J.L. (2009) 'A Review of the Antioxidant Mechanisms of Polyphenol Compounds Related to Iron Binding', *Cell Biochemistry and Biophysics*, 53(2), pp. 75–100. doi:10.1007/s12013-009-9043-x.

Pike, S. *et al.* (2019) 'Using Xenopus laevis Oocytes to Functionally Characterize Plant Transporters', *Current Protocols in Plant Biology*, 4(1), p. e20087. doi:10.1002/cppb.20087.

Porra, R.J., Thompson, W.A. and Kriedemann, P.E. (1989) 'Determination of accurate extinction coefficients and simultaneous equations for assaying chlorophylls a and b extracted with four different solvents: verification of the concentration of chlorophyll standards by atomic absorption spectroscopy', *Biochimica et Biophysica Acta (BBA) - Bioenergetics*, 975(3), pp. 384–394. doi:10.1016/S0005-2728(89)80347-0.

Pushnik, J.C., Miller, G.W. and Manwaring, J.H. (1984) 'The role of iron in higher plant chlorophyll biosynthesis, maintenance and chloroplast biogenesis', *Journal of Plant Nutrition*, 7(1–5), pp. 733–758. doi:10.1080/01904168409363238.

Rabenhorst, M.C., Hively, W.D. and James, B.R. (2009) 'Measurements of Soil Redox Potential', *Soil Science Society of America Journal*, 73(2), pp. 668–674. doi:10.2136/sssaj2007.0443.

Rajniak, J. *et al.* (2018) 'Biosynthesis of redox-active metabolites in response to iron deficiency in plants', *Nature Chemical Biology*, 14(5), pp. 442–450. doi:10.1038/s41589-018-0019-2.

Reichard, P.U. *et al.* (2005) 'Goethite Dissolution in the Presence of Phytosiderophores: Rates, Mechanisms, and the Synergistic Effect of Oxalate', *Plant and Soil*, 276(1), pp. 115–132. doi:10.1007/s11104-005-3504-9.

Reichard, P.U., Kretzschmar, R. and Kraemer, S.M. (2007) 'Dissolution mechanisms of goethite in the presence of siderophores and organic acids', *Physical Chemistry of Soils and Aquifers: A Special Issue in Honor of Garrison Sposito*, 71(23), pp. 5635–5650. doi:10.1016/j.gca.2006.12.022.

Rengel, Z. (2001) 'Genotypic Differences in Micronutreint Use Efficiency in Crops', *Communications in Soil Science and Plant Analysis*, 32(7–8), pp. 1163–1186. doi:10.1081/CSS-100104107.

Robe, K. *et al.* (2021) 'Coumarin accumulation and trafficking in Arabidopsis thaliana: a complex and dynamic process', *New Phytologist*, 229(4), pp. 2062–2079. doi:10.1111/nph.17090.

Robinson, N.J. *et al.* (1999) 'A ferric-chelate reductase for iron uptake from soils', *Nature*, 397(6721), pp. 694–697. doi:10.1038/17800.

Rodríguez-Celma, J. *et al.* (2013) 'Mutually Exclusive Alterations in Secondary Metabolism Are Critical for the Uptake of Insoluble Iron Compounds by Arabidopsis and Medicago truncatula', *Plant Physiology*, 162(3), p. 1473. doi:10.1104/pp.113.220426.

Rodríguez-Celma, J. *et al.* (2019) 'Arabidopsis BRUTUS-LIKE E3 ligases negatively regulate iron uptake by targeting transcription factor FIT for recycling', *Proceedings of the National Academy of Sciences*, 116(35), p. 17584. doi:10.1073/pnas.1907971116.

Rodríguez-Celma, J. and Schmidt, W. (2013) 'Reduction-based iron uptake revisited', *Plant Signaling & Behavior*, 8(11), p. e26116. doi:10.4161/psb.26116.

Romera, F.J., Alcántara, E. and de la Guardia, M.D. (1992a) 'Effects of bicarbonate, phosphate and high pH on the reducing capacity of Fe-deficient sunflower and cucumber plants', *Journal of Plant Nutrition*, 15(10), pp. 1519–1530. doi:10.1080/01904169209364418.

Romera, F.J., Alcántara, E. and de la Guardia, M.D. (1992b) 'Effects of bicarbonate, phosphate and high pH on the reducing capacity of Fe-deficient sunflower and cucumber plants', *Journal of Plant Nutrition*, 15(10), pp. 1519–1530. doi:10.1080/01904169209364418.

Römheld, V. (1987) 'Different strategies for iron acquisition in higher plants', *Physiologia Plantarum*, 70(2), pp. 231–234. doi:10.1111/j.1399-3054.1987.tb06137.x.

Römheld, V. (1991) 'The role of phytosiderophores in acquisition of iron and other micronutrients in graminaceous species: An ecological approach', *Plant and Soil*, 130(1), pp. 127–134. doi:10.1007/BF00011867.

Römheld, V. and Kramer, D. (1983) 'Relationship Between Proton Efflux and Rhizodermal Transfer Cells Induced by Iron Deficiency', *Zeitschrift für Pflanzenphysiologie*, 113(1), pp. 73–83. doi:10.1016/S0044-328X(83)80020-8.

Römheld, V. and Marschner, H. (1983) 'Mechanism of Iron Uptake by Peanut Plants', *Plant Physiology*, 71(4), p. 949. doi:10.1104/pp.71.4.949.

Römheld, V. and Marschner, H. (1986) 'Evidence for a Specific Uptake System for Iron Phytosiderophores in Roots of Grasses 1', *Plant Physiology*, 80(1), pp. 175–180. doi:10.1104/pp.80.1.175.

Römheld, V. and Marschner, H. (1990) 'Genotypical differences among graminaceous species in release of phytosiderophores and uptake of iron phytosiderophores', in El Bassam, N., Dambroth, M., and Loughman, B.C. (eds) *Genetic Aspects of Plant Mineral Nutrition*. Dordrecht: Springer Netherlands, pp. 77–83. doi:10.1007/978-94-009-2053-8_12.

Saha, R. *et al.* (2013) 'Microbial siderophores: a mini review', *Journal of Basic Microbiology*, 53(4), pp. 303–317. doi:10.1002/jobm.201100552.

Sandy, M. and Butler, A. (2009) 'Microbial Iron Acquisition: Marine and Terrestrial Siderophores', *Chemical Reviews*, 109(10), pp. 4580–4595. doi:10.1021/cr9002787.

Santi, S. and Schmidt, W. (2009) 'Dissecting Iron Deficiency-Induced Proton Extrusion in Arabidopsis Roots', *The New Phytologist*, 183(4), pp. 1072–1084.

Sasse, J., Martinoia, E. and Northen, T. (2018) 'Feed Your Friends: Do Plant Exudates Shape the Root Microbiome?', *Trends in Plant Science*, 23(1), pp. 25–41. doi:10.1016/j.tplants.2017.09.003.

Satbhai, S.B. *et al.* (2017) 'Natural allelic variation of FRO2 modulates Arabidopsis root growth under iron deficiency', *Nature Communications*, 8(1), p. 15603. doi:10.1038/ncomms15603.

Schenkeveld, W.D.C. *et al.* (2016) 'Synergistic Effects between Biogenic Ligands and a Reductant in Fe Acquisition from Calcareous Soil', *Environmental Science & Technology*, 50(12), pp. 6381–6388. doi:10.1021/acs.est.6b01623.

Schenkeveld, W.D.C. and Kraemer, S.M. (2018) 'Constraints to Synergistic Fe Mobilization from Calcareous Soil by a Phytosiderophore and a Reductant', *Soil Systems*, 2(4). doi:10.3390/soilsystems2040067.

Schmid, N.B. *et al.* (2014) 'Feruloyl-CoA 6′-Hydroxylase1-Dependent Coumarins Mediate Iron Acquisition from Alkaline Substrates in Arabidopsis', *Plant Physiology*, 164(1), p. 160. doi:10.1104/pp.113.228544.

Schmidt, H. *et al.* (2014) 'Metabolome Analysis of Arabidopsis thaliana Roots Identifies a Key Metabolic Pathway for Iron Acquisition', *PLOS ONE*, 9(7), p. e102444. doi:10.1371/journal.pone.0102444.

Schröder, I., Johnson, E. and de Vries, S. (2003) 'Microbial ferric iron reductases', *FEMS Microbiology Reviews*, 27(2–3), pp. 427–447. doi:10.1016/S0168-6445(03)00043-3.

Schwab, A.P. and Lindsay, W.L. (1983) 'Effect of Redox on the Solubility and Availability of Iron', *Soil Science Society of America Journal*, 47(2), pp. 201–205. doi:10.2136/sssaj1983.03615995004700020005x.

Schwarz, B. and Bauer, P. (2020) 'FIT, a regulatory hub for iron deficiency and stress signaling in roots, and FIT-dependent and -independent gene signatures', *Journal of Experimental Botany*, 71(5), pp. 1694–1705. doi:10.1093/jxb/eraa012.

Schweigert, N., Zehnder, A.J.B. and Eggen, R.I.L. (2001) 'Chemical properties of catechols and their molecular modes of toxic action in cells, from microorganisms to mammals', *Environmental Microbiology*, 3(2), pp. 81–91. doi:10.1046/j.1462-2920.2001.00176.x.

Schwertmann, U. (1991) 'Solubility and dissolution of iron oxides', *Plant and Soil*, 130(1), pp. 1–25. doi:10.1007/BF00011851.

Shi, W.-M. *et al.* (1988) 'The occurrence of mugineic acid in the rhizosphere soil of barley plant', *Soil Science and Plant Nutrition*, 34(4), pp. 585–592. doi:10.1080/00380768.1988.10416473.

Sims, J.L. and Patrick Jr., W.H. (1978) 'The Distribution of Micronutrient Cations in Soil Under Conditions of Varying Redox Potential and pH', *Soil Science Society of America Journal*, 42(2), pp. 258–262. doi:10.2136/sssaj1978.03615995004200020010x.

Sisó-Terraza, P. *et al.* (2016) 'Accumulation and Secretion of Coumarinolignans and other Coumarins in Arabidopsis thaliana Roots in Response to Iron Deficiency at High pH', *Frontiers in Plant Science*, 7, p. 1711. doi:10.3389/fpls.2016.01711.

Sivitz, A.B. *et al.* (2012) 'Arabidopsis bHLH100 and bHLH101 Control Iron Homeostasis via a FIT-Independent Pathway', *PLOS ONE*, 7(9), p. e44843. doi:10.1371/journal.pone.0044843.

Siwinska, J. *et al.* (2014) 'Identification of QTLs affecting scopolin and scopoletin biosynthesis in Arabidopsis thaliana', *BMC Plant Biology*, 14(1), p. 280. doi:10.1186/s12870-014-0280-9.

Siwinska, J. *et al.* (2018) 'Scopoletin 8-hydroxylase: a novel enzyme involved in coumarin biosynthesis and iron-deficiency responses in Arabidopsis', *Journal of Experimental Botany*, 69(7), pp. 1735–1748. doi:10.1093/jxb/ery005.

Stringlis, I.A. *et al.* (2018) 'MYB72-dependent coumarin exudation shapes root microbiome assembly to promote plant health', *Proceedings of the National Academy of Sciences*, 115(22), pp. 5213–5222. doi:10.1073/pnas.1722335115.

Ström, L. *et al.* (2002) 'Organic acid mediated P mobilization in the rhizosphere and uptake by maize roots', *Soil Biology and Biochemistry*, 34(5), pp. 703–710. doi:10.1016/S0038-0717(01)00235-8.

Stumm, W. and Sulzberger, B. (1992) 'The cycling of iron in natural environments: Considerations based on laboratory studies of heterogeneous redox processes', *Geochimica et Cosmochimica Acta*, 56(8), pp. 3233–3257. doi:10.1016/0016-7037(92)90301-X.

Sugiura, Y. *et al.* (1981) 'Structure, properties, and transport mechanism of iron(III) complex of mugineic acid, a possible phytosiderophore', *Journal of the American Chemical Society*, 103(23), pp. 6979–6982. doi:10.1021/ja00413a043.

Suter, D. *et al.* (1988) 'Catalytic dissolution of iron(III)(hydr)oxides by oxalic acid in the presence of Fe(II)', *Naturwissenschaften*, 75(11), pp. 571–573. doi:10.1007/BF00377723.

Suter, D., Banwart, S. and Stumm, W. (1991) 'Dissolution of hydrous iron(III) oxides by reductive mechanisms', *Langmuir*, 7(4), pp. 809–813. doi:10.1021/la00052a033.

Suzuki, M. *et al.* (2006) 'Biosynthesis and secretion of mugineic acid family phytosiderophores in zinc-deficient barley', *The Plant Journal*, 48(1), pp. 85–97. doi:10.1111/j.1365-313X.2006.02853.x.

Taiz, L. *et al.* (2015) *Plant Physiology and Development*. 6th edition. Sunderland: Sinauer Associates Incorporated.

Takagi, S. -I., Kamei, S. and Yu, M. -H. (1988) 'Efficiency of iron extraction from soil by mugineic acid family phytosiderophores', *Journal of Plant Nutrition*, 11(6–11), pp. 643–651. doi:10.1080/01904168809363830.

Takagi, S. -I., Nomoto, K. and Takemoto, T. (1984) 'Physiological aspect of mugineic acid, a possible phytosiderophore of graminaceous plants', *Journal of Plant Nutrition*, 7(1–5), pp. 469–477. doi:10.1080/01904168409363213.

Terés, J. *et al.* (2019) 'Soil carbonate drives local adaptation in Arabidopsis thaliana', *Plant, cell & environment*. 2019/06/18 edn, 42(8), pp. 2384–2398. doi:10.1111/pce.13567.

Terry, N. and Abadía, J. (1986) 'Function of iron in chloroplasts', *Journal of Plant Nutrition*, 9(3–7), pp. 609–646. doi:10.1080/01904168609363470.

Tsai, H.-H. *et al.* (2018) 'Scopoletin 8-Hydroxylase-Mediated Fraxetin Production Is Crucial for Iron Mobilization', *Plant Physiology*, 177(1), p. 194. doi:10.1104/pp.18.00178.

Tsai, H.-H. and Schmidt, W. (2017a) 'Mobilization of Iron by Plant-Borne Coumarins', *Trends in Plant Science*, 22(6), pp. 538–548. doi:10.1016/j.tplants.2017.03.008.

Tsai, H.-H. and Schmidt, W. (2017b) 'One way. Or another? Iron uptake in plants', *New Phytologist*, 214(2), pp. 500–505. doi:10.1111/nph.14477.

Tsai, H.-H. and Schmidt, W. (2020) 'pH-dependent transcriptional profile changes in iron-deficient Arabidopsis roots', *BMC Genomics*, 21(1), p. 694. doi:10.1186/s12864-020-07116-6.

Tsai, H.-H. and Schmidt, W. (2021) 'The enigma of environmental pH sensing in plants', *Nature Plants*, 7(2), pp. 106–115. doi:10.1038/s41477-020-00831-8.

Uren, N.C. (1984) 'Forms, reactions and availability of iron in soils', *Journal of Plant Nutrition*, 7(1–5), pp. 165–176. doi:10.1080/01904168409363183.

Vandesompele, J. *et al.* (2002) 'Accurate normalization of real-time quantitative RT-PCR data by geometric averaging of multiple internal control genes', *Genome Biology*, 3(7), p. research0034.1. doi:10.1186/gb-2002-3-7-research0034.

Vanholme, R. *et al.* (2019) 'COSY catalyses trans–cis isomerization and lactonization in the biosynthesis of coumarins', *Nature Plants*, 5(10), pp. 1066–1075. doi:10.1038/s41477-019-0510-0.

Varotto, C. *et al.* (2002) 'The metal ion transporter IRT1 is necessary for iron homeostasis and efficient photosynthesis in Arabidopsis thaliana', *The Plant Journal*, 31(5), pp. 589–599. doi:10.1046/j.1365-313X.2002.01381.x.

Vert, G.A. *et al.* (2002) 'IRT1, an Arabidopsis Transporter Essential for Iron Uptake from the Soil and for Plant Growth', *The Plant Cell*, 14(6), p. 1223. doi:10.1105/tpc.001388.

Vert, G.A., Briat, J.-F. and Curie, C. (2003) 'Dual regulation of the Arabidopsis high-affinity root iron uptake system by local and long-distance signals', *Plant physiology*. 2003/04/10 edn, 132(2), pp. 796–804. doi:10.1104/pp.102.016089.

Voges, M.J.E.E.E. *et al.* (2019) 'Plant-derived coumarins shape the composition of an Arabidopsis synthetic root microbiome', *Proceedings of the National Academy of Sciences*, 116(25), p. 12558. doi:10.1073/pnas.1820691116.

Volk, N.J. (1939) 'The Effect of Oxidation-Reduction Potential on Plant Growth', *Agronomy Journal*, 31(8), pp. 665–670. doi:10.2134/agronj1939.00021962003100080001x.

Vose, P.B. (1982) 'Iron nutrition in plants: A world overview', *Journal of Plant Nutrition*, 5(4–7), pp. 233–249. doi:10.1080/01904168209362954.

Wang, N. *et al.* (2013) 'Requirement and Functional Redundancy of Ib Subgroup bHLH Proteins for Iron Deficiency Responses and Uptake in Arabidopsis thaliana', *Molecular Plant*, 6(2), pp. 503–513. doi:10.1093/mp/sss089.

Wang, Z. *et al.* (2015) 'Synergistic Effect of Reductive and Ligand-Promoted Dissolution of Goethite', *Environmental Science & Technology*, 49(12), pp. 7236–7244. doi:10.1021/acs.est.5b01191.

Waters, B.M. *et al.* (2006) 'Mutations in Arabidopsis Yellow Stripe-Like1 and Yellow Stripe-Like3 Reveal Their Roles in Metal Ion Homeostasis and Loading of Metal Ions in Seeds', *Plant Physiology*, 141(4), p. 1446. doi:10.1104/pp.106.082586.

Waters, B.M. and Armbrust, L.C. (2013) 'Optimal copper supply is required for normal plant iron deficiency responses', *Plant Signaling & Behavior*, 8(12), p. e26611. doi:10.4161/psb.26611.

Weber, G. *et al.* (2001) 'Determination of phytosiderophores by anion-exchange chromatography with pulsed amperometric detection', *Journal of Chromatography A*, 928(2), pp. 171–175. doi:10.1016/S0021-9673(01)01140-2.

von Wirén, N. *et al.* (1993) 'Influence of microorganisms on iron acquisition in maize', *Soil Biology and Biochemistry*, 25(3), pp. 371–376. doi:10.1016/0038-0717(93)90136-Y.

von Wirén, N. *et al.* (1994) 'Iron Inefficiency in Maize Mutant ys1 (Zea mays L. cv Yellow-Stripe) Is Caused by a Defect in Uptake of Iron Phytosiderophores', *Plant Physiology*, 106(1), p. 71. doi:10.1104/pp.106.1.71.

von Wirén, N. *et al.* (1995) 'Competition between Micro-Organisms and Roots of Barley and Sorghum for Iron Accumulated in the Root Apoplasm', *The New Phytologist*, 130(4), pp. 511–521.

von Wirén, N., Khodr, H. and Hider, R.C. (2000) 'Hydroxylated phytosiderophore species possess an enhanced chelate stability and affinity for iron(III)', *Plant physiology*, 124(3), pp. 1149–1158. doi:10.1104/pp.124.3.1149.

Xuan, Y. *et al.* (2006) 'Separation and identification of phytosiderophores and their metal complexes in plants by zwitterionic hydrophilic interaction liquid chromatography coupled to electrospray ionization mass spectrometry', *Journal of Chromatography A*, 1136(1), pp. 73–81. doi:10.1016/j.chroma.2006.09.060.

Yaoya, S. *et al.* (2004) 'Umbelliferone Released from Hairy Root Cultures of Pharbitis nil Treated with Copper Sulfate and Its Subsequent Glucosylation', *Bioscience, Biotechnology, and Biochemistry*, 68(9), pp. 1837–1841. doi:10.1271/bbb.68.1837.

Yuan, Y.X. *et al.* (2005) 'AtbHLH29 of Arabidopsis thaliana is a functional ortholog of tomato FER involved in controlling iron acquisition in strategy I plants', *Cell Research*, 15(8), pp. 613–621. doi:10.1038/sj.cr.7290331.

Yuan, Y.X. *et al.* (2008) 'FIT interacts with AtbHLH38 and AtbHLH39 in regulating iron uptake gene expression for iron homeostasis in Arabidopsis', *Cell Research*, 18(3), pp. 385–397. doi:10.1038/cr.2008.26.

Zamioudis, C., Hanson, J. and Pieterse, C.M.J. (2014) 'β-Glucosidase BGLU42 is a MYB72-dependent key regulator of rhizobacteria-induced systemic resistance and modulates iron deficiency responses in Arabidopsis roots', *New Phytologist*, 204(2), pp. 368–379. doi:10.1111/nph.12980.

Zarzana, C.A. *et al.* (2015) 'Iron Fluoroanions and Their Clusters by Electrospray Ionization of a Fluorinating Ionic Liquid', *Journal of The American Society for Mass Spectrometry*, 26(9), pp. 1559–1569. doi:10.1007/s13361-015-1160-8.

Zhang, C. *et al.* (2021) 'Interpretation of the differential UV–visible absorbance spectra of metal-NOM complexes based on the quantum chemical simulations for the model compound esculetin', *Chemosphere*, 276, p. 130043. doi:10.1016/j.chemosphere.2021.130043.

Zhang, J. *et al.* (2015) 'The bHLH Transcription Factor bHLH104 Interacts with IAA-LEUCINE RESISTANT3 and Modulates Iron Homeostasis in Arabidopsis', *The Plant Cell*, 27(3), p. 787. doi:10.1105/tpc.114.132704.

Ziegler, J. *et al.* (2017) 'Arabidopsis Transporter ABCG37/PDR9 contributes primarily highly oxygenated Coumarins to Root Exudation', *Scientific Reports*, 7(1), p. 3704. doi:10.1038/s41598-017-03250-6.

Zinder, B., Furrer, G. and Stumm, W. (1986) 'The coordination chemistry of weathering: II. Dissolution of Fe(III) oxides', *Geochimica et Cosmochimica Acta*, 50(9), pp. 1861–1869. doi:10.1016/0016-7037(86)90244-9.

7 Appendix

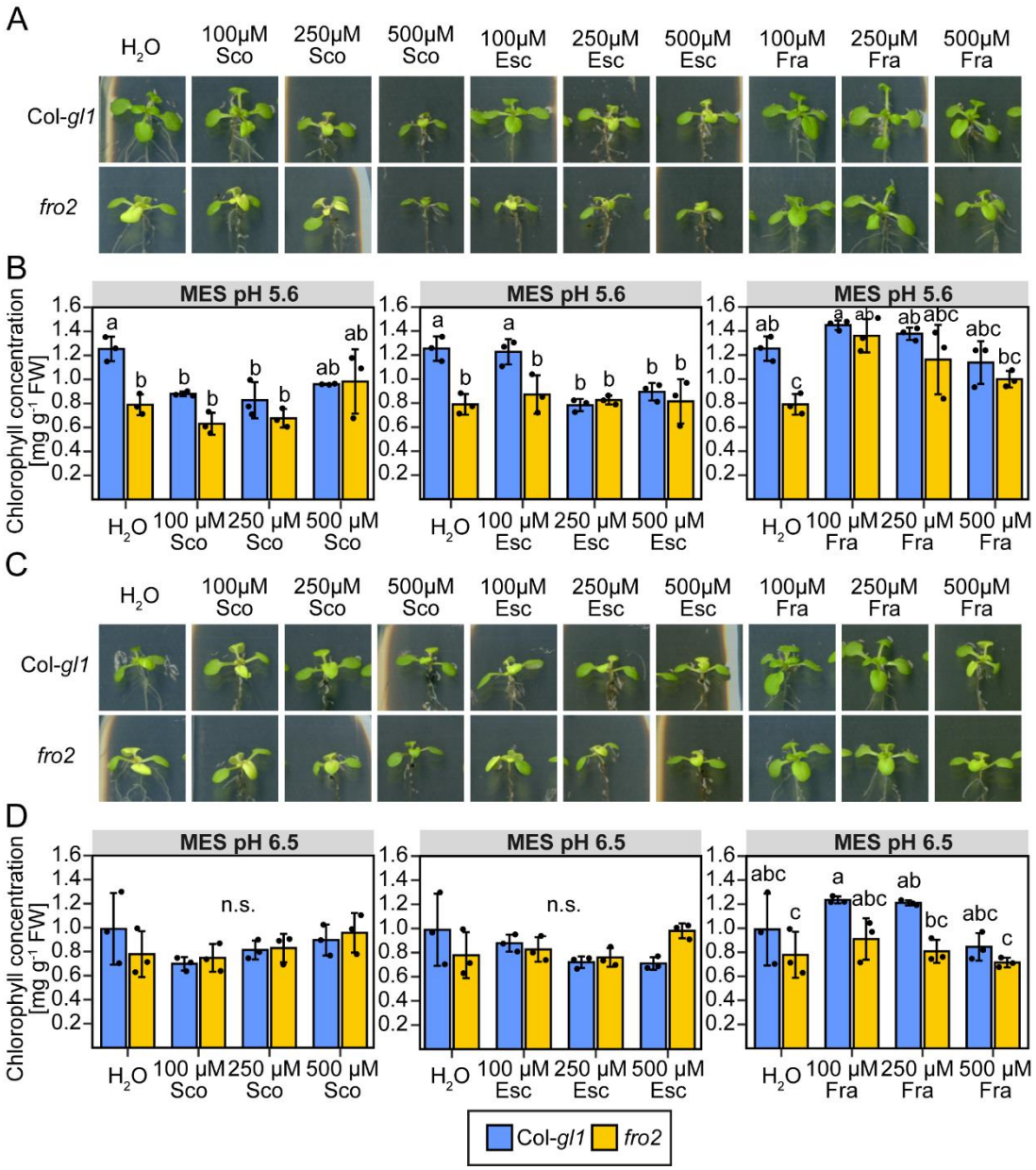

Annex Fig. 1. Influence of different concentrations of esculetin, fraxetin, and scopoletin on the growth of wild-type (Col-*gl1*) and *fro2* plants on Fe-limiting conditions at pH 5.6 and pH 6.5. (A-D) Plant appearance (A and C) and leaf chlorophyll concentration (B and D) of Col-*gl1* and *fro2* plants grown for 6 d under different conditions of low Fe availability at pH 5.6 and 6.5 with or without esculetin, fraxetin, and scopoletin. Plants were pre-cultured for 10 d on one-half strength MS medium with 40 µM NaFeEDTA (pH 5.6) and then transferred to one-half strength MS medium with 20 µM $FeCl_3$ buffered with MES to pH 5.6 or pH 6.5. The medium was supplemented with mQ-H_2O (mock) or 100, 250, or 500 µM esculetin, fraxetin, or scopoletin, respectively. Bars represent means ± s.d. (n = 3 biological replicates). Different letters indicate significant differences according to one-way ANOVA or ANOVA on ranks with post-hoc Tukey's test at $p \leq 0.05$. n.s.: not significant.

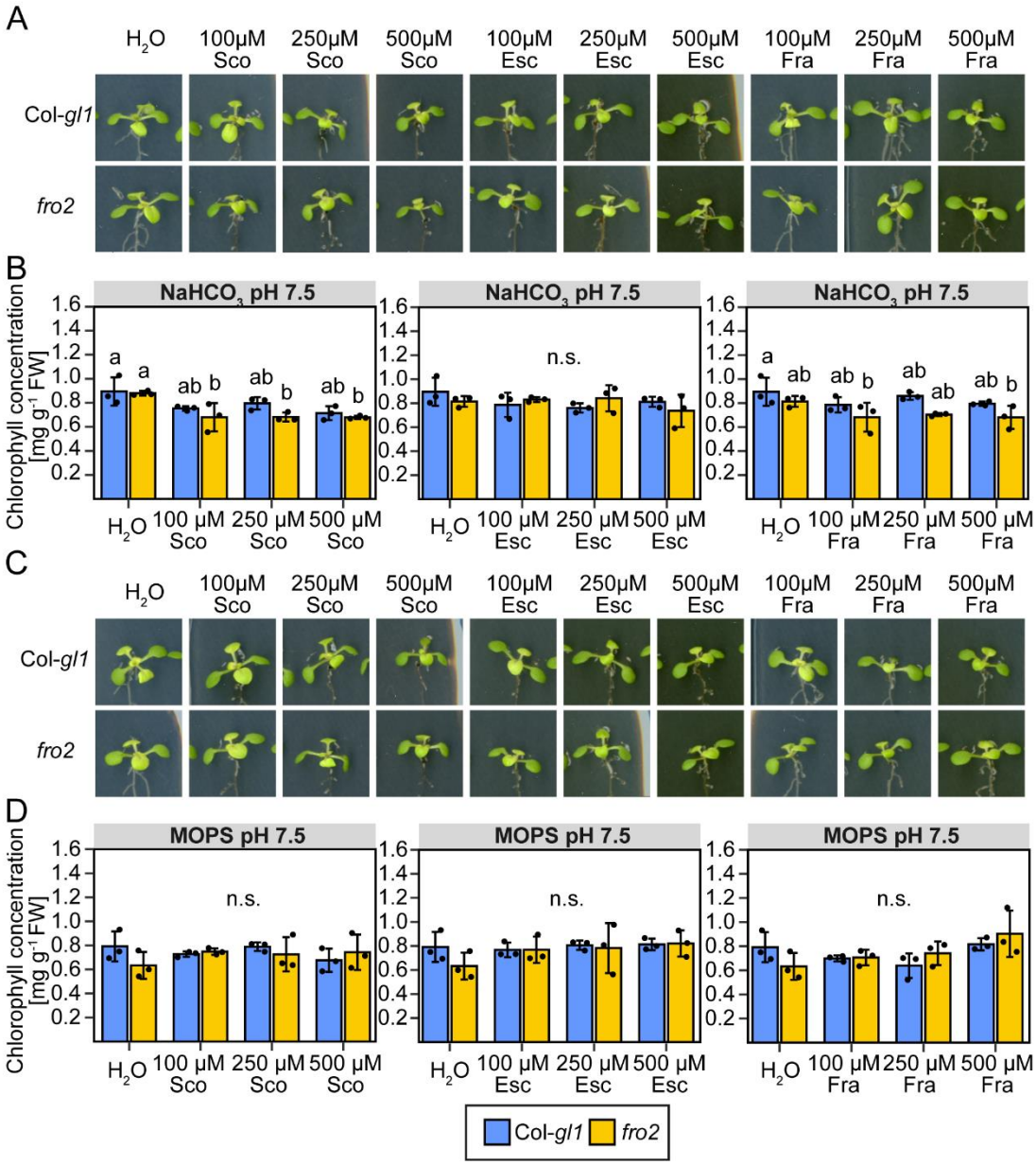

Annex Fig. 2. Influence of different concentrations of esculetin, fraxetin, and scopoletin on the growth of wild-type (Col-*gl1*) and *fro2* plants on Fe-limiting conditions at pH 7.5. (A-D) Plant appearance (A and C) and leaf chlorophyll concentration (B and D) of Col-*gl1* and *fro2* plants grown for 6 d under different conditions of low Fe availability at pH 7.5 with or without esculetin, fraxetin, and scopoletin. Plants were pre-cultured for 10 d on one-half strength MS medium with 40 µM NaFeEDTA (pH 5.6) and then transferred to one-half strength MS medium with 20 µM $FeCl_3$ buffered with either $NaHCO_3$ or MOPS to pH 7.5. The medium was supplemented with mQ-H_2O (mock) or 100, 250, or 500 µM esculetin, fraxetin, or scopoletin, respectively. Bars represent means ± s.d. (n = 3 biological replicates). Different letters indicate significant differences according to one-way ANOVA with post-hoc Tukey's test at $p \leq 0.05$. n.s.: not significant.

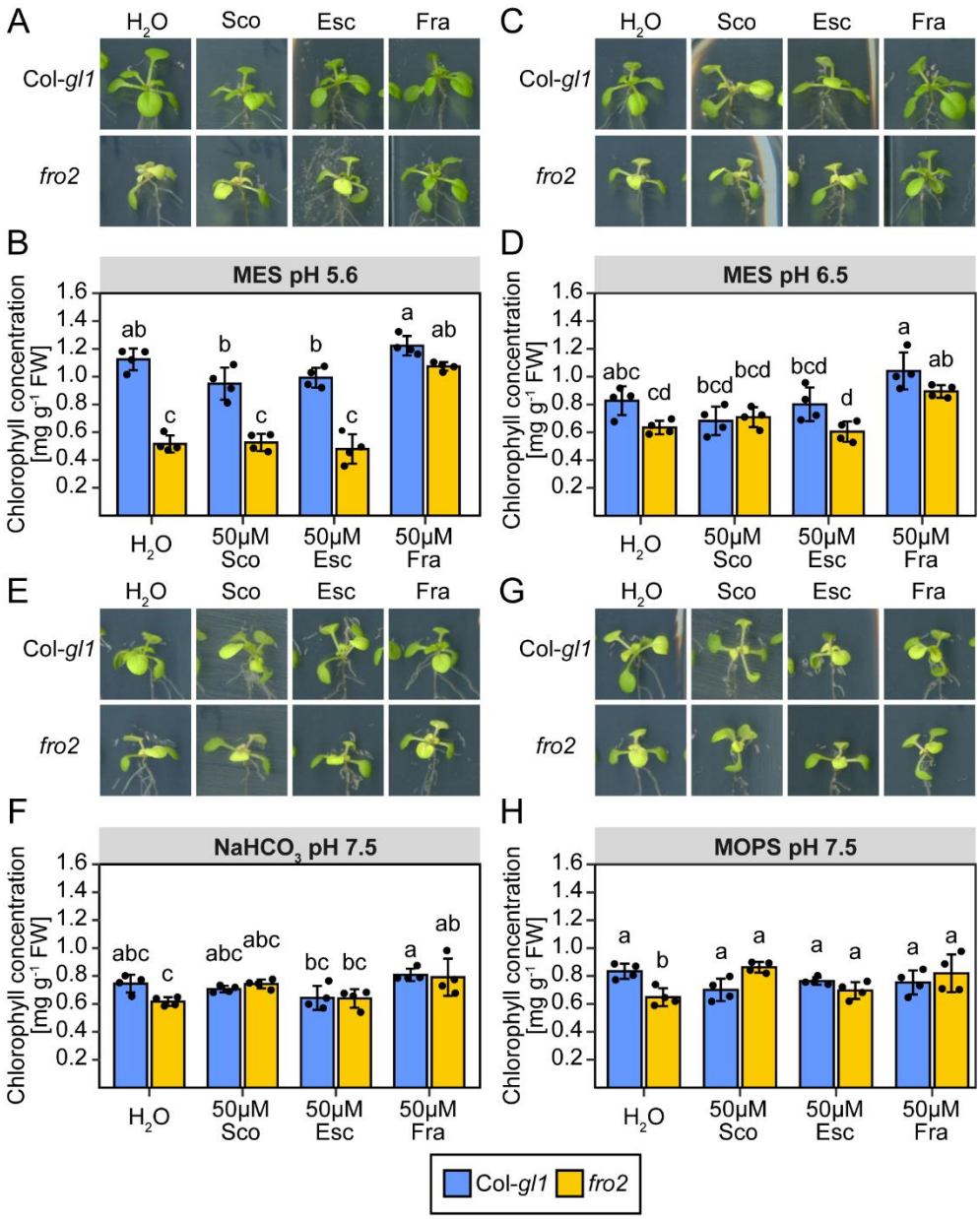

Annex Fig. 3. Influence of coumarins on Fe deficiency in *fro2* plants grown under different conditions of low Fe availability. (A-H) Plant appearance (A, C, E, G) and leaf chlorophyll concentration (B, D, F, H) of wild-type (Col-*gl1*) and *fro2* plants grown for 6 d under different conditions of low Fe availability with or without esculetin, fraxetin, and scopoletin. Ten-d-old seedlings pre-cultured for 10 d on one-half strength MS medium with 40 µM NaFeEDTA (pH 5.6) were transferred to one-half strength MS medium with 20 µM $FeCl_3$ buffered with either MES to pH 5.6 or pH 6.5, $NaHCO_3$ or MOPS to pH 7.5. The medium was supplemented with mQ-H_2O (mock) or 50 µM esculetin, fraxetin, or scopoletin, respectively. Bars represent means ± s.d. (n = 4 biological replicates). Different letters indicate significant differences according to one-way ANOVA or ANOVA on ranks with post-hoc Tukey's test at $p \leq 0.05$.

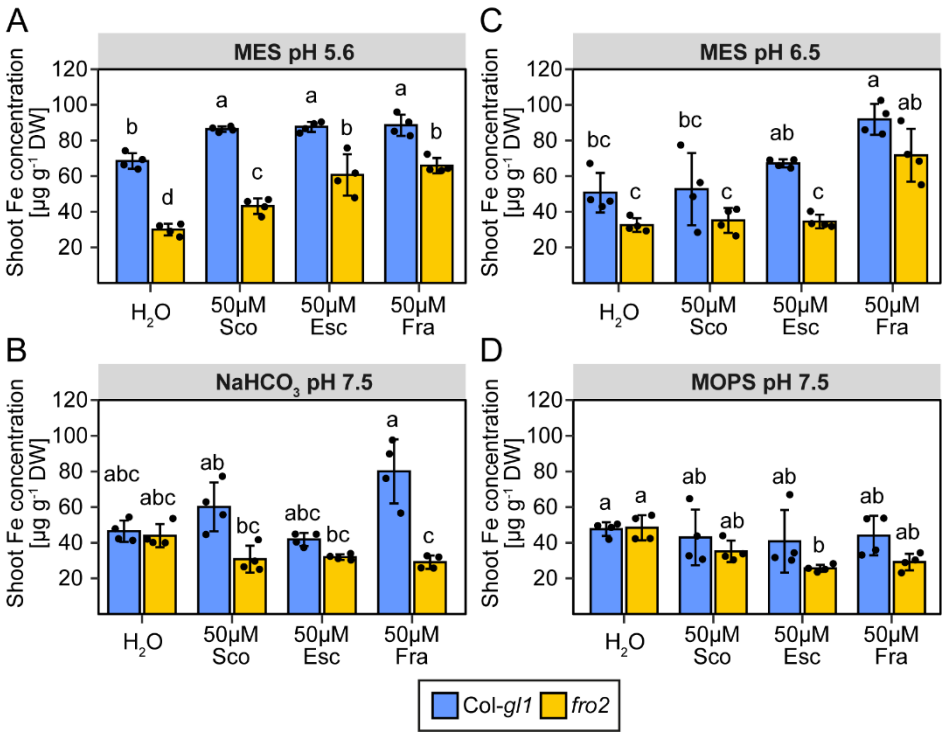

Annex Fig. 4. Influence of fraxetin supplementation on shoot Fe concentration of *fro2* plants under conditions of low Fe availability in dependence of pH. (A-D) Shoot Fe concentration in wild-type (Col-*gl1*) and *fro2* plants grown for 6d on different Fe-limiting conditions. Plants were pre-cultured for 10 d on one-half strength MS medium with 40µM FeEDTA (pH 5.6) and then transferred to one-half strength MS medium containing 20µM $FeCl_3$ buffered with either MES to pH 5.6 or pH 6.5, $NaHCO_3$ to pH 7.5, or MOPS to pH 7.5. The medium was supplemented with either mQ-H_2O, 50 µM esculetin, 50 µM fraxetin, or 50 µM scopoletin. Bars represent means ± s.d. (n = 4 biological replicates). Different letters indicate significant differences according to one-way ANOVA with post-hoc Tukey's test at $p \leq 0.05$.

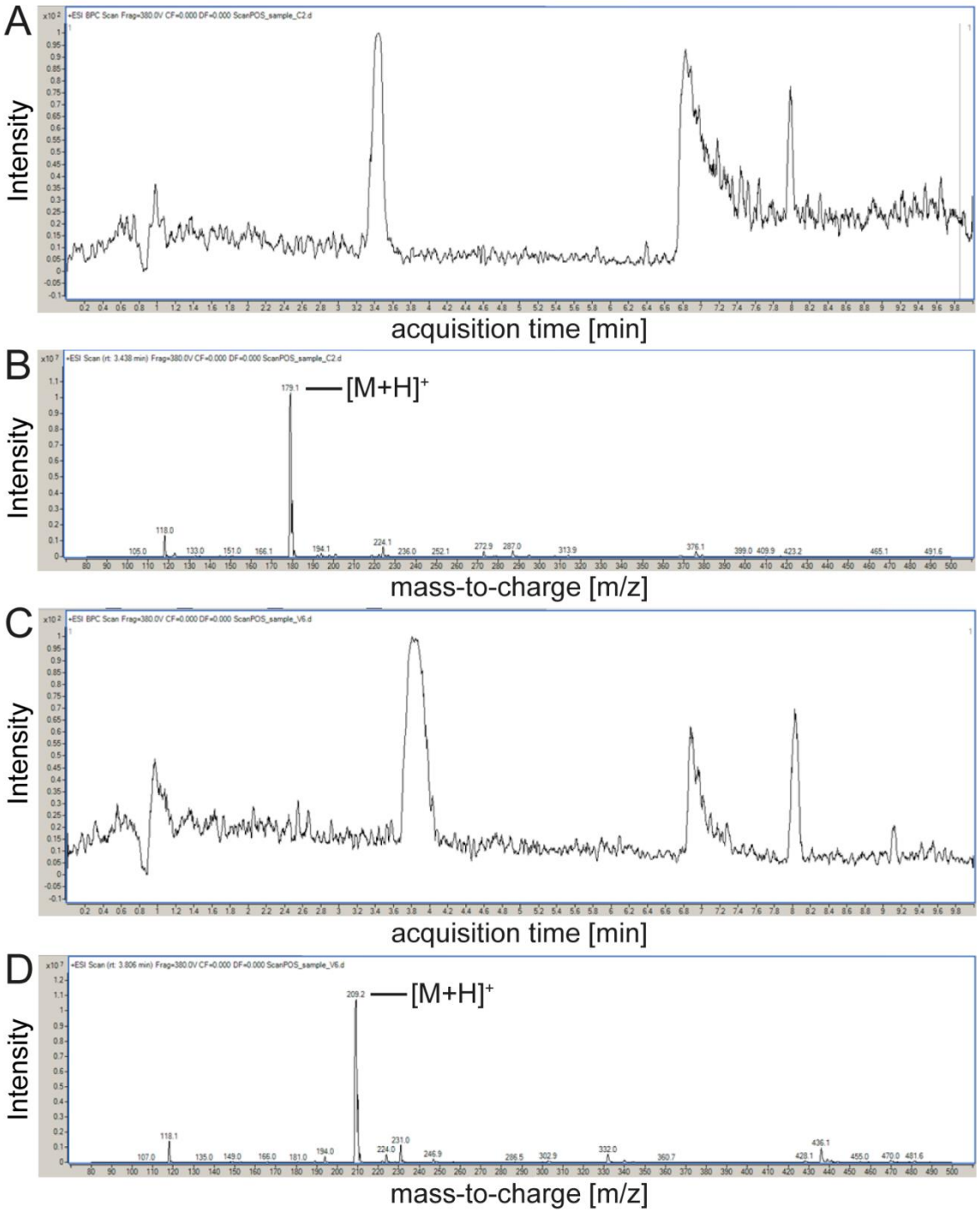

Annex Fig. 5. Analysis of Fe-esculetin and Fe-fraxetin complexes in positive ion mode. (A-D) Representative chromatogram (A and C) and mass spectra (B and D) of esculetin (A and B) and fraxetin (C and D), respectively, incubated with $FeCl_3$ at pH 5.5 and analyzed in positive ion mode. Esculetin and fraxetin were dissolved in MeOH and incubated with freshly prepared $FeCl_3$ solution adjusted to pH 5.5. The coumarin:Fe ratio was set to 3:1. Samples were incubated for 30 min at room temperature and 1000 rpm in darkness. After subsequent filtration, samples were analyzed by UPLC-MS/MS (Triple Quad). M = free ligand.

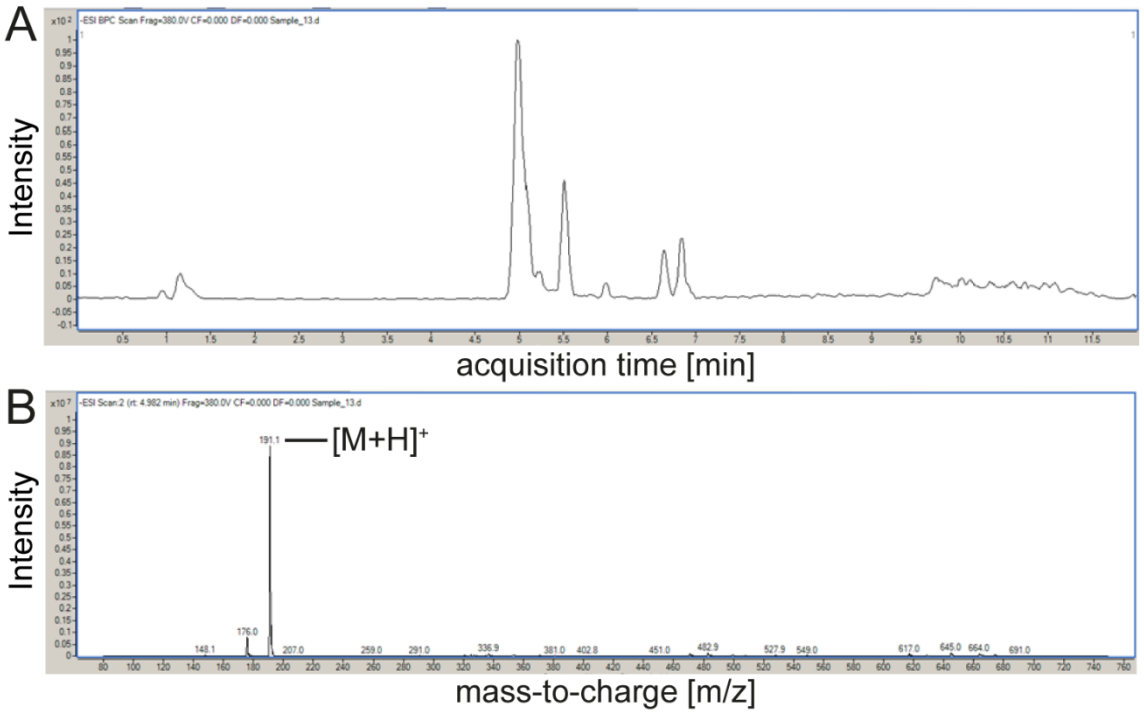

Annex Fig. 6. Analysis of Fe-scopoletin complexes in negative ion mode. (A-B) Representative chromatogram (A) and mass spectra (B) of scopoletin incubated with $FeCl_3$ at pH ~2.5 and analyzed in negative ion mode. Scopoletin was dissolved in MeOH and incubated with freshly prepared $FeCl_3$ solution adjusted to pH ~2.5. The coumarin:Fe ratio was set to 2:1. Samples were incubated for 30 min at room temperature and 1000 rpm in darkness. After subsequent filtration, samples were analyzed by UPLC-MS/MS (Triple Quad). M = free ligand.

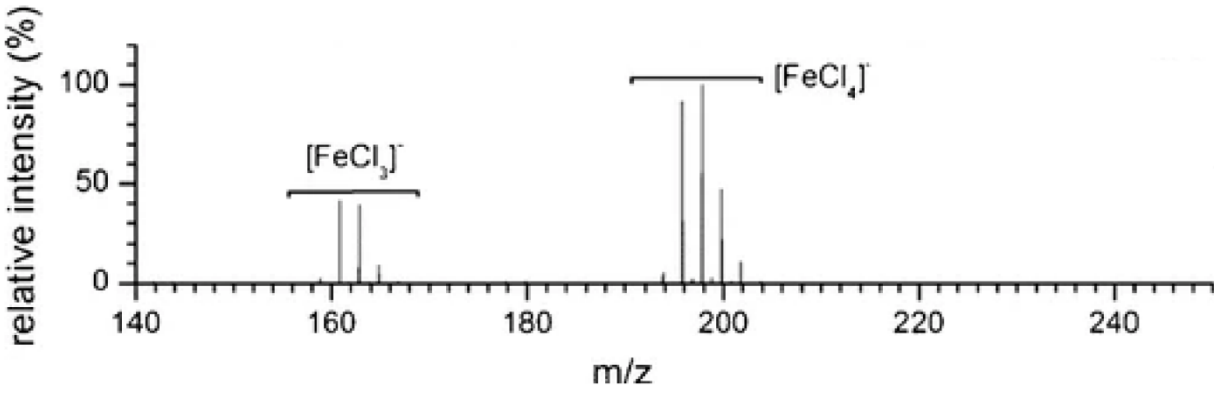

Annex Fig. 7. Expected negative mode electrospray mass spectrum of $FeCl_3$ according to (Zarzana *et al.*, 2015)**.**

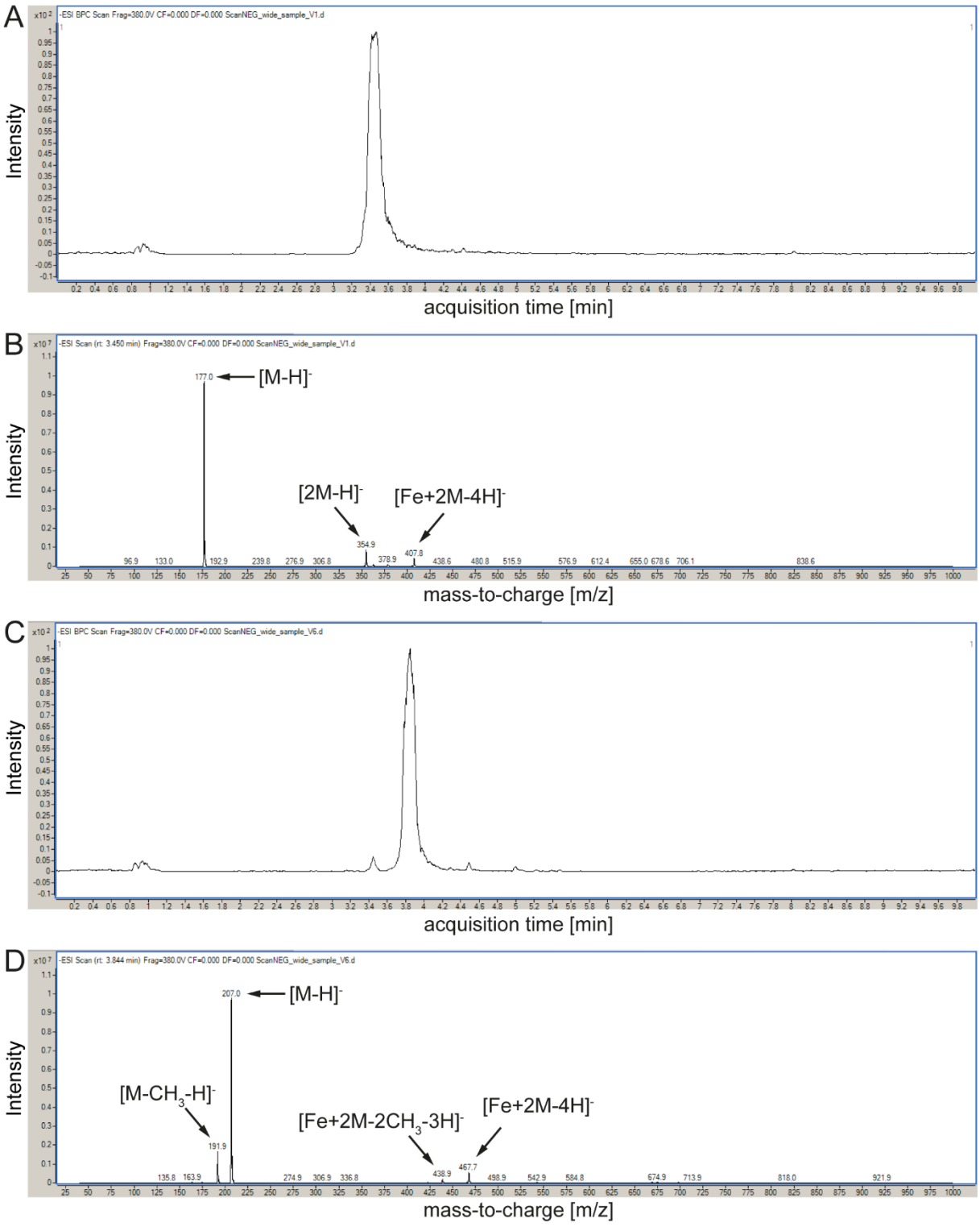

Annex Fig. 8. Detection of Fe-esculetin and Fe-fraxetin complexes with different stoichiometry. (A-D) Representative chromatogram for (A) esculetin and (C) fraxetin incubated with $FeCl_3$ at pH 5.5. Representative mass spectra for (B) esculetin and (D) fraxetin as indicated in A and C. Esculetin and fraxetin were dissolved in MeOH and incubated with freshly prepared $FeCl_3$ solution adjusted to pH 5.5. The coumarin:Fe ratio was set to 3:1. Samples were incubated for 30 min at room temperature and 1000 rpm in darkness. After subsequent filtration, samples were analyzed by UPLC-MS/MS (Triple Quad). Samples were analyzed in negative mode with extended mass range of m/z 1000. M = free ligand.

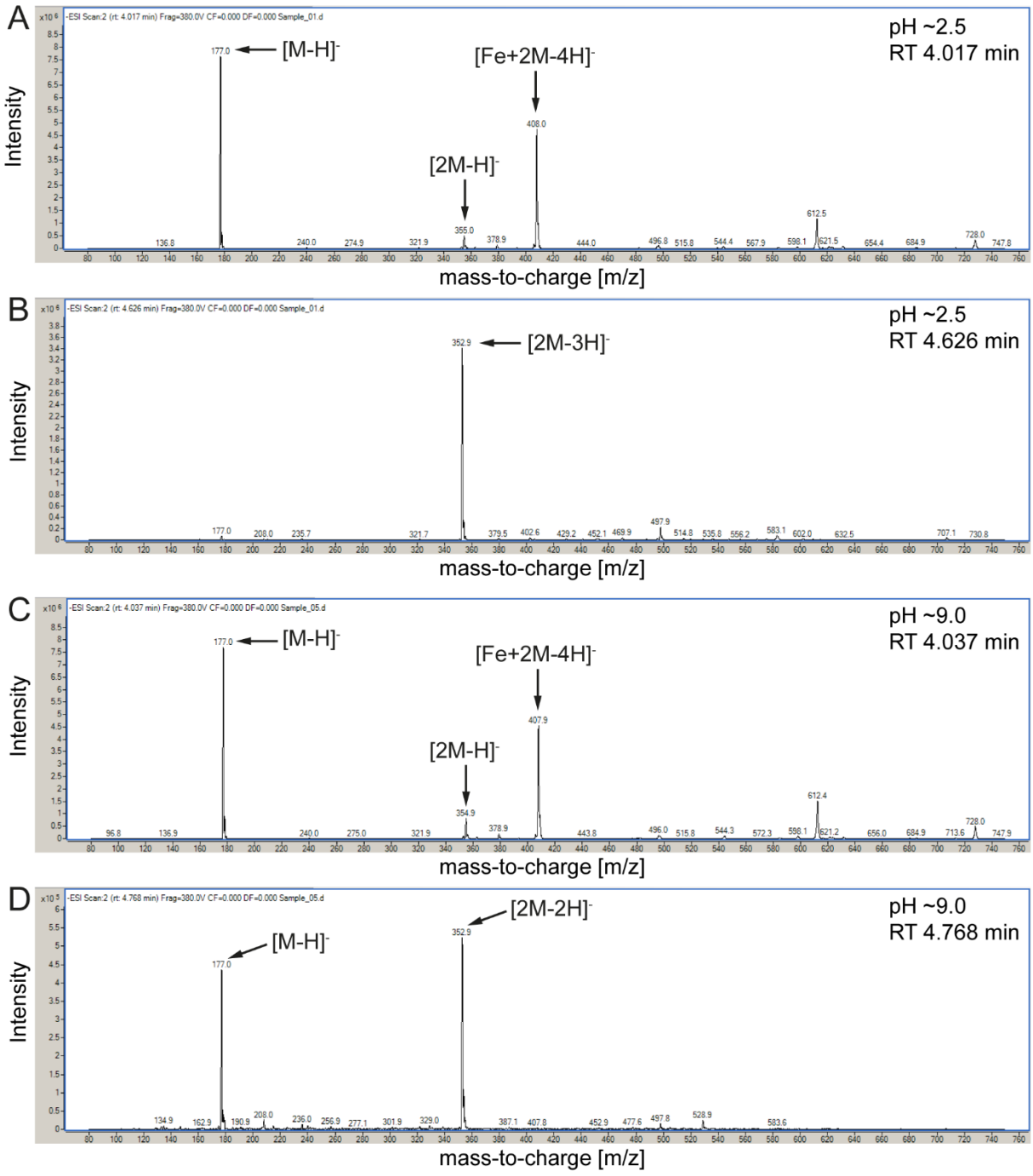

Annex Fig. 9. Detection of Fe-esculetin complexes at acidic and alkaline pH. (A-D) Representative mass spectra of esculetin incubated with $FeCl_3$ at pH ~2.5 and pH ~9.0 analyzed in negative mode. Esculetin was dissolved in MeOH and incubated with freshly prepared $FeCl_3$ solution adjusted to pH ~2.5 and pH ~9.0, respectively. The coumarin:Fe ratio was set to 2:1. Samples were incubated for 30 min at room temperature and 1000 rpm in darkness. After subsequent filtration, samples were analyzed by UPLC-MS/MS (Triple Quad). M = free ligand.

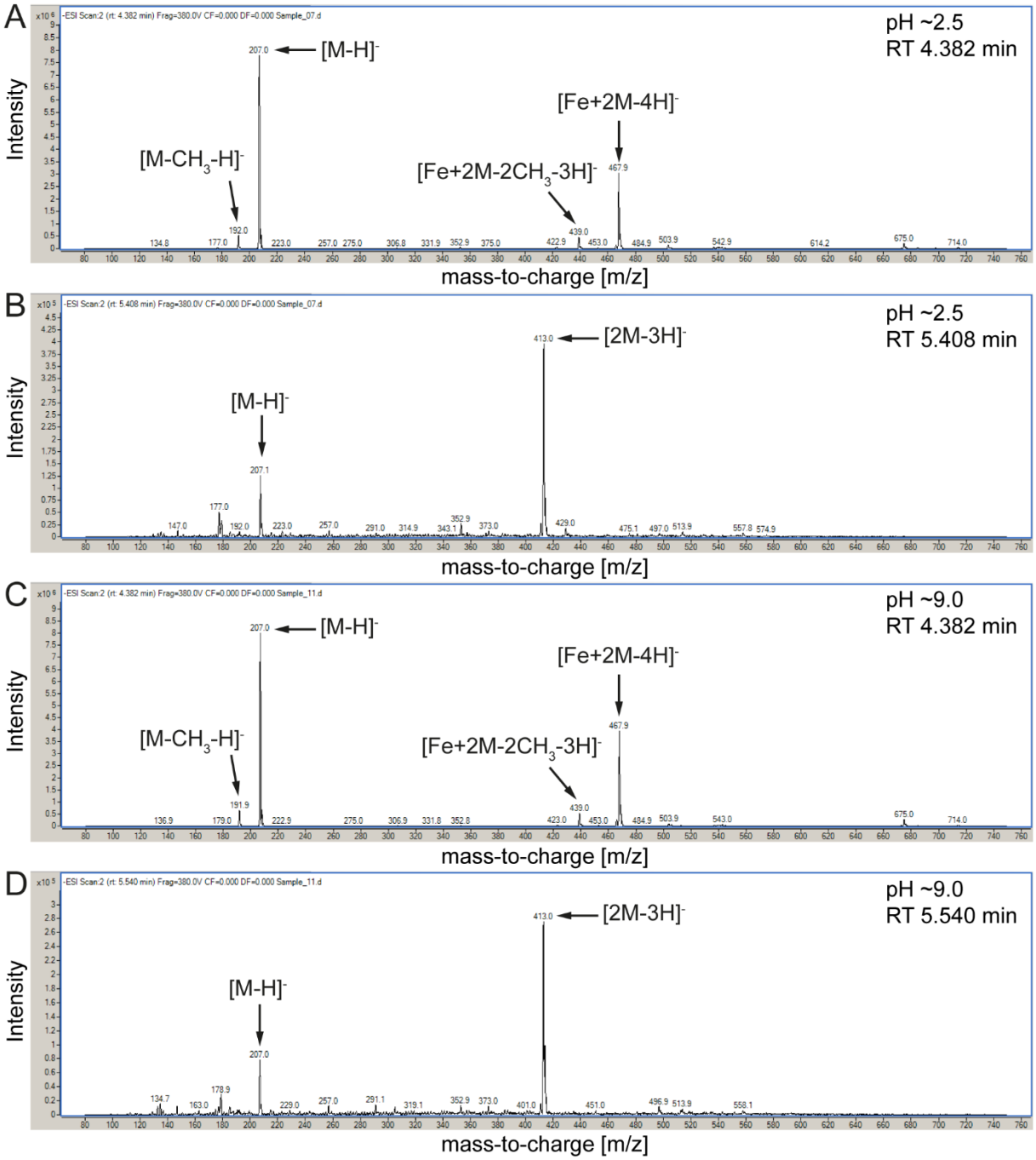

Annex Fig. 10. Detection of Fe-fraxetin complexes at acidic and alkaline pH. (A-D) Representative mass spectra of fraxetin incubated with $FeCl_3$ at pH ~2.5 and pH ~9.0 analyzed in negative mode. Fraxetin was dissolved in MeOH and incubated with freshly prepared $FeCl_3$ solution adjusted to pH ~2.5 and pH ~9.0, respectively. The coumarin:Fe ratio was set to 2:1. Samples were incubated for 30 min at room temperature and 1000 rpm in darkness. After subsequent filtration, samples were analyzed by UPLC-MS/MS (Triple Quad). M = free ligand.

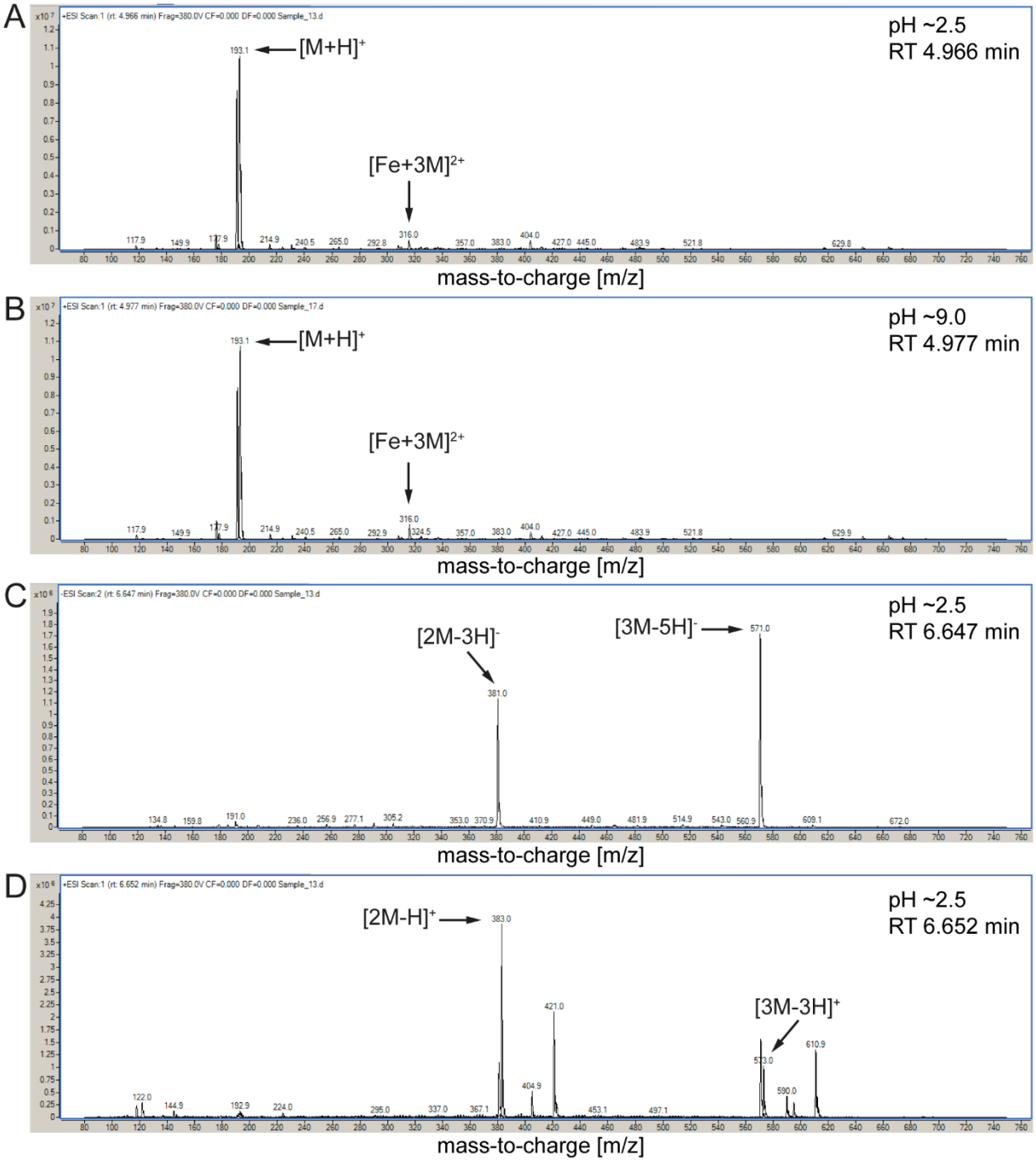

Annex Fig. 11. Detection of Fe-scopoletin species at acidic and alkaline pH. (A-D) Representative mass spectra of scopoletin incubated with $FeCl_3$ at pH ~2.5 and pH ~9.0 analyzed in positive (A, B, D) and negative (C) mode. Scopoletin was dissolved in MeOH and incubated with freshly prepared $FeCl_3$ solution adjusted to pH ~2.5 and pH ~9.0, respectively. The coumarin:Fe ratio was set to 2:1. Samples were incubated for 30 min at room temperature and 1000 rpm in darkness. After subsequent filtration, samples were analyzed by UPLC-MS/MS (Triple Quad). M = free ligand.

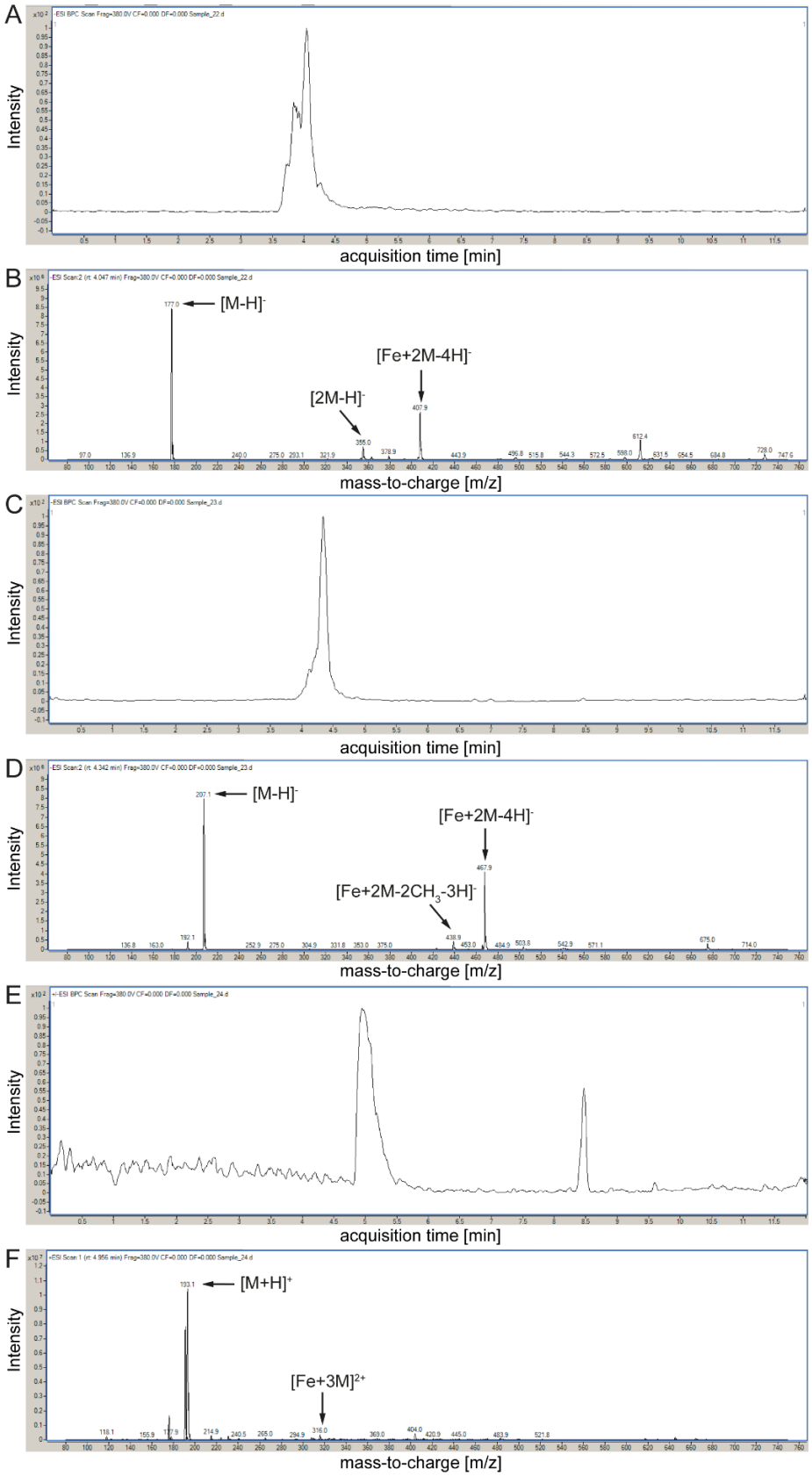

Annex Fig. 12. Detection of Fe-coumarin species without addition of external Fe. (A-F) Representative chromatograms (A, C, E) and mass spectra (B, D, F) of esculetin (A and B), fraxetin (C and D), and scopoletin (E and F) incubated in absence of external $FeCl_3$. Esculetin and fraxetin were analyzed in negative mode and scopoletin was analyzed in positive mode. Coumarins were dissolved in MeOH and incubated with mQ-H_2O. Samples were incubated for 30 min at 1000 rpm in darkness. After subsequent filtration, samples were analyzed by UPLC-MS/MS (Triple Quad). M = free ligand.

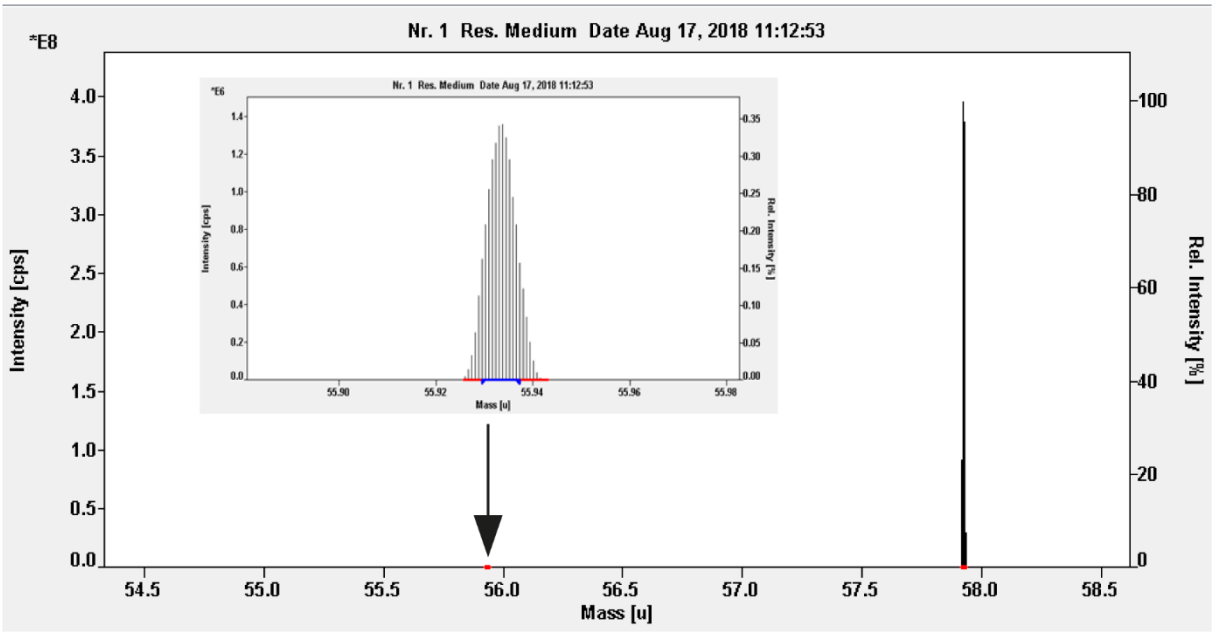

Annex Fig. 13. Verification of the $^{58}FeCl_3$ standard by ICP-MS. Mass spectrum of the $^{58}FeCl_3$ standard showing the relative intensity of the most prominent mass at 57.93 u and detailed view of the mass spectrum at 55.93 u.

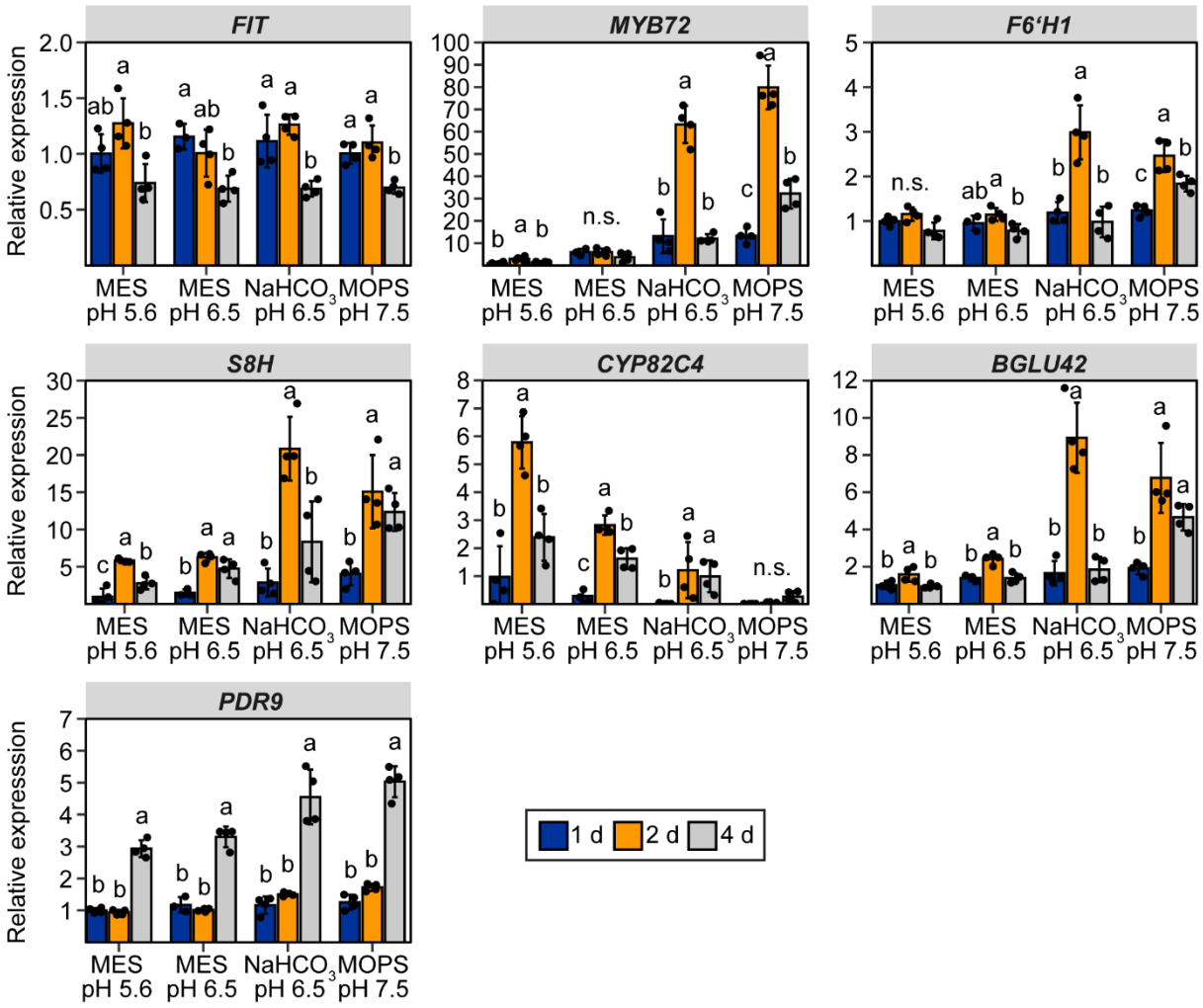

Annex Fig. 14. Analysis of the expression of genes involved in coumarin biosynthesis and secretion in plants supplemented with FeEDDHA. Relative expression levels of *FIT*, *MYB72*, *F6'H1*, *S8H*, *CYP82C4*, *BGLU42*, and *PDR9* as determined by RT-PCR in roots of wild-type plants (Col-0) grown in the presence of FeEDDHA under different pH and buffer conditions for 1 d, 2 d, and 4 d. After 10-d pre-culture on one-half strength MS medium with 40 µM FeEDTA (pH 5.6), plants were transferred to one-half strength MS medium with 80 µM FeEDDHA buffered with either MES to pH 5.6 or pH 6.5, $NaHCO_3$ to pH 6.5 (1 mM), or MOPS to pH 7.5. Relative expression levels are calculated as fold changes from plants grown for 1 d on MES pH 5.6. Bars represent means ± s.d. (n = 3-4 biological replicates). Different letters indicate significant differences according to one-way ANOVA with post-hoc Tukey's test at $p \leq 0.05$ or Welch's ANOVA with post-hoc Games-Howell test with $p \leq 0.05$ within the individual treatments. n.s.: not significant.

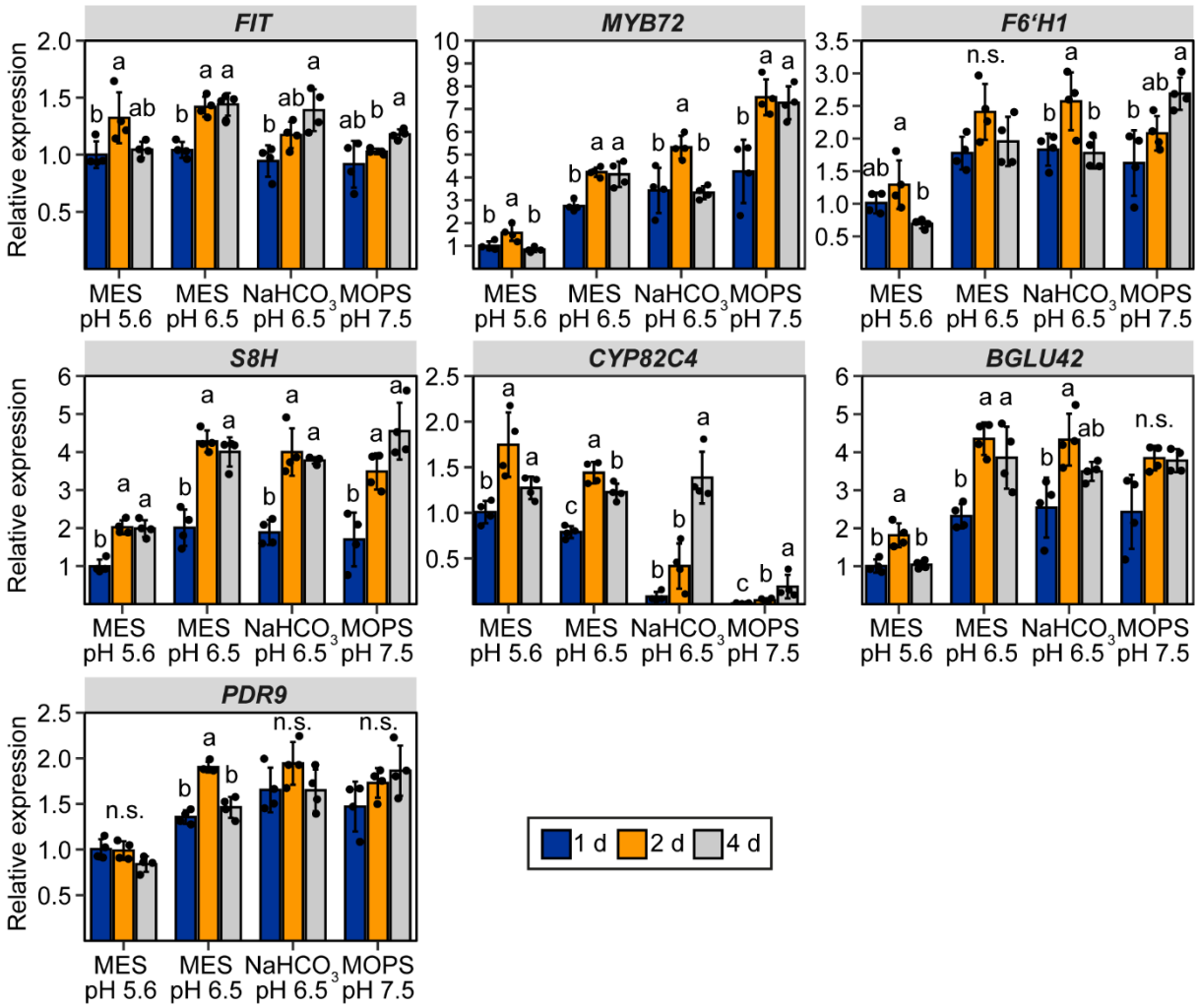

Annex Fig. 15. Analysis of the expression of genes involved in coumarin biosynthesis and secretion in plants supplemented with $FeCl_3$. Relative expression levels of *FIT*, *MYB72*, *F6'H1*, *S8H*, *CYP82C4*, *BGLU42*, and *PDR9* as determined by RT-PCR in roots of wild-type plants (Col-0) grown in the presence of $FeCl_3$ under different pH and buffer conditions for 1 d, 2 d, and 4 d. After 10-d pre-culture on one-half strength MS medium with 40 µM FeEDTA (pH 5.6), plants were transferred to one-half strength MS medium with 20 µM $FeCl_3$ buffered with either MES to pH 5.6 or pH 6.5, $NaHCO_3$ to pH 6.5 (1 mM), or MOPS to pH 7.5. Relative expression levels are calculated as fold changes from plants grown for 1 d on MES pH 5.6. Bars represent means ± s.d. (n = 3-4 biological replicates). Different letters indicate significant differences according to one-way ANOVA with post-hoc Tukey's test at $p \leq 0.05$ or Welch's ANOVA with post-hoc Games-Howell test with $p \leq 0.05$ within the individual treatments. n.s.: not significant.

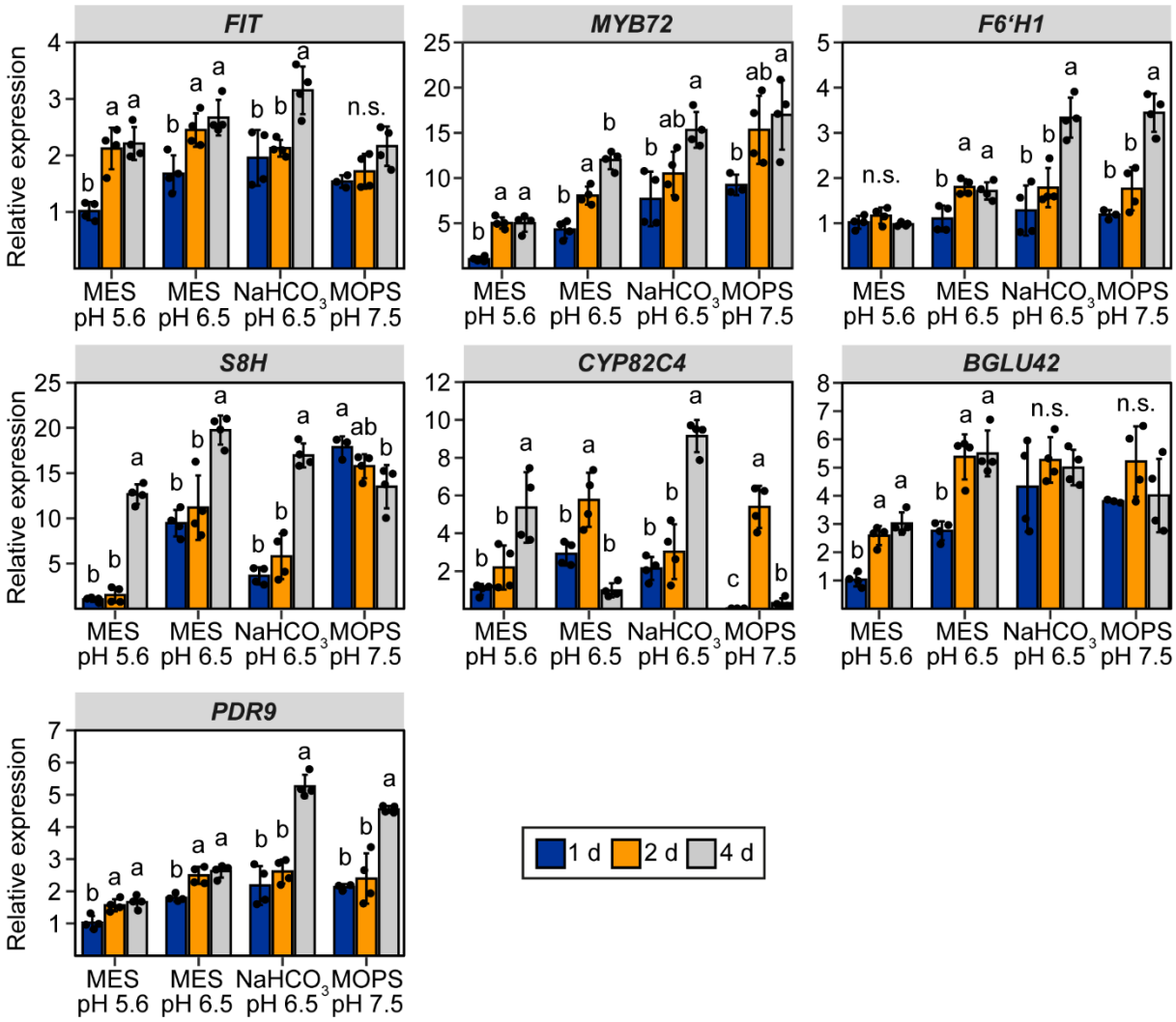

Annex Fig. 16. Analysis of the expression of genes involved in coumarin biosynthesis and secretion in plants grown in the absence of Fe. Relative expression levels of *FIT*, *MYB72*, *F6'H1*, *S8H*, *CYP82C4*, *BGLU42*, and *PDR9* as determined by RT-PCR in roots of wild-type plants (Col-0) grown in the absence of Fe under different pH and buffer conditions for 1 d, 2 d, and 4 d. After 10-d pre-culture on one-half strength MS medium with 40 µM FeEDTA (pH 5.6), plants were transferred to one-half strength MS medium without Fe but with 15 µM ferrozine buffered with either MES to pH 5.6 or pH 6.5, $NaHCO_3$ to pH 6.5 (1 mM), or MOPS to pH 7.5. Relative expression levels are calculated as fold changes from plants grown for 1 d on MES pH 5.6. Bars represent means ± s.d. (n = 3-4 biological replicates). Different letters indicate significant differences according to one-way ANOVA with post-hoc Tukey's test at $p \leq 0.05$ or Welch's ANOVA with post-hoc Games-Howell test with $p \leq 0.05$ within the individual treatments. n.s.: not significant.

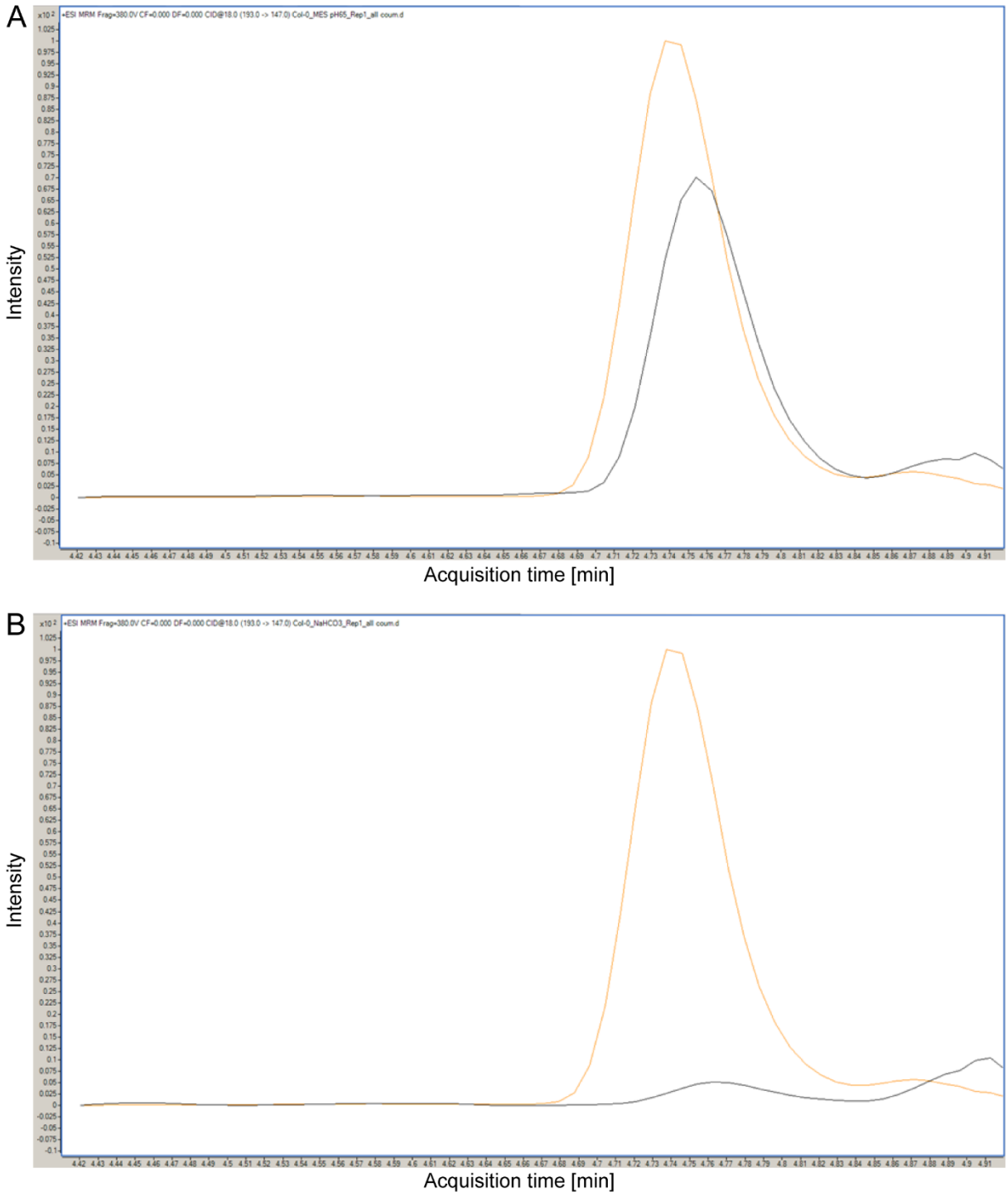

Annex Fig. 17. Signal intensity of 4-methyldaphnetin in root exudate samples collected in the presence of bicarbonate. (A and B) Chromatograms of the transition followed for 4-methyldaphnetin (m/z 193 → 147) for representative root exudate samples of plants grown at pH 6.5 buffered with MES (A) or bicarbonate (B) (Triple Quad). Orange line represents the signal intensity of 4-methyldaphnetin present in the coumarin calibration standard (final conc. 0.4 µg/mL); black line represents the signal intensity of 4-methyldaphentin in the respective exudate sample.

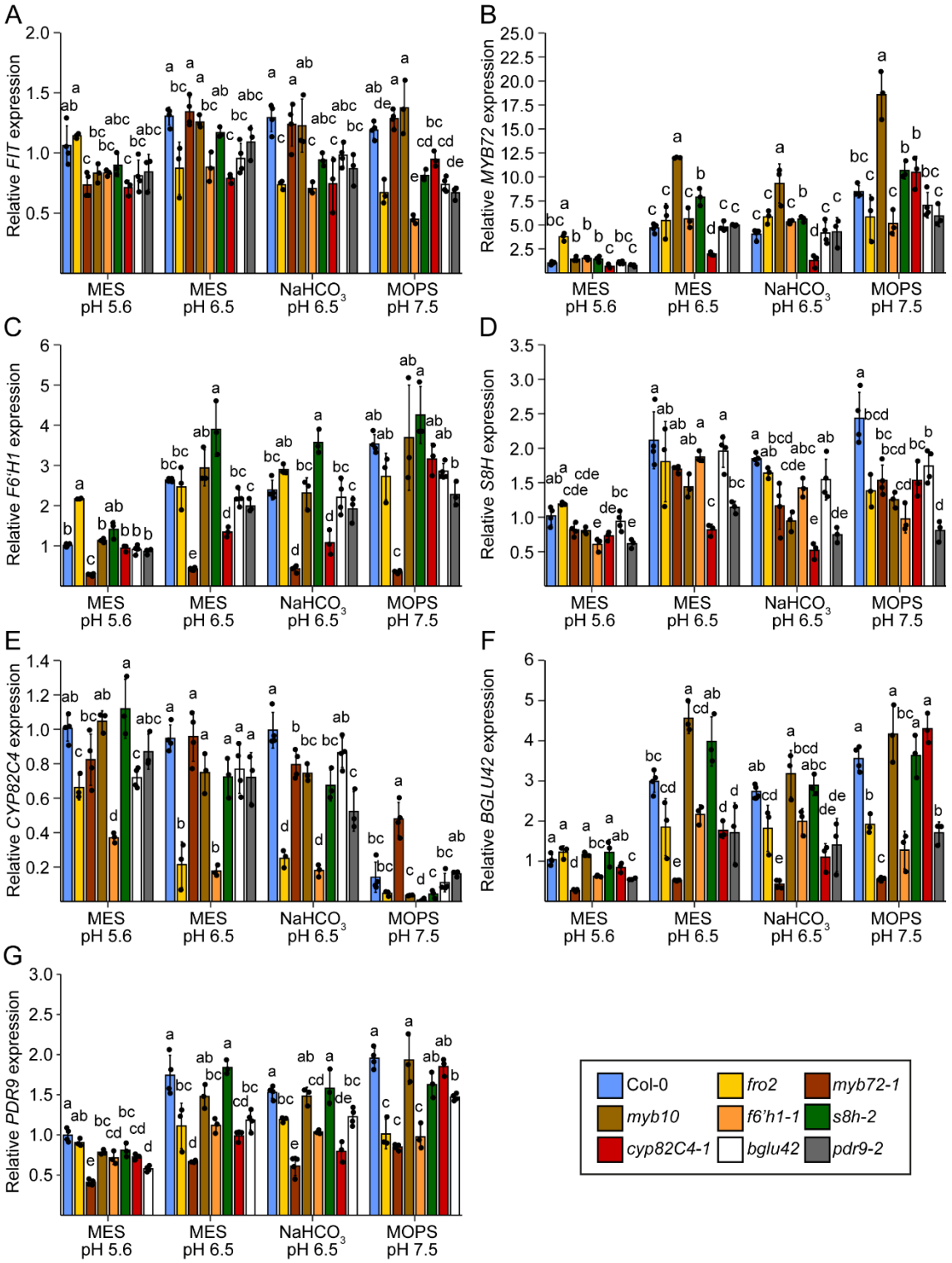

Annex Fig. 18. Expression of distinct genes involved in coumarin biosynthesis and secretion in wild-type (Col-0), *fro2*, and different coumarin biosynthesis and secretion mutants under different conditions of low Fe availability. (A-G) Relative expression levels of *FIT* (A), *MYB72* (B), *F6'H1* (C), *S8H* (D), *CYP82C4* (E), *BGLU42* (F), and *PDR9* (G) as determined by RT-PCR in roots of wild-type (Col-0), *fro2*, *myb72-1*, *myb10*, *f6'h1-1*, *s8h-2*, *cyp82C4-1*, *bglu42*, and *pdr9-2* plants grown under different conditions of low Fe availability for 4 d. Plants were pre-cultured on one-half strength MS medium with 40 µM FeEDTA (pH 5.6) and then were transferred to one-half strength MS medium with 20 µM $FeCl_3$ buffered with either MES to pH 5.6 or pH 6.5, $NaHCO_3$ to pH 6.5 (1 mM), or MOPS to pH 7.5. Relative expression levels were calculated as fold changes from wild-type plants grown for on MES pH 5.6. Bars represent means ± s.d. (n = 3-4 biological replicates; n = 3 technical replicates for wild-type plants). Different letters indicate significant differences according to one-way ANOVA with post-hoc Tukey's test at $p \leq 0.05$ or Welch's ANOVA with post-hoc Games-Howell test with $p \leq 0.05$ within the individual treatments.

8 Abbreviations

Å	angstrom (equal to a length of 10^{-10} m)
°C	degree Celsius
%	percentage
µ	micro
µg	microgram
µL	microliter
µm	micrometer
µM	micromolar
µmol	micromole
35S	CaMV *35S* promoter
bp	base pair
CaMV	cauliflower mosaic virus
cDNA	complementary DNA
cm	centimeter
C_t	cycle threshold
d	day
ddMS2	data dependent MS2
DNA	deoxyribonucleic acid
DTT	dithiothreitol
EDTA	ethylenediaminetetraacetic acid
EDDHA	ethylenediamine-N,N′-bis(2-hydroxyphenylacetic acid)
E_h	redox potential
ESI	electrospray ionization
FCR	ferric-chelate reductase
Fe	iron
For	forward
g	gram
GABI	German Plant Genome Research Program (Genomanalyse im biologischen System Pflanze)
gDNA	genomic DNA
GFP	green fluorescent protein
GOI	gene of interest
h	hour
HESI	heated electrospray ionization
HR-IPC-MS	high resolution inductively coupled plasma mass spectrometry
ICP-MS	inductively coupled plasma mass spectrometry
kg	kilogram
kV	kilovolt
L	liter
LC/MS	liquid chromatography mass spectrometry
LOQ	limit of quantification
m	meter
M	molar
M (in MS spectra)	free ligand
MES	2-(N-morpholino)ethanesulfonic acid

mg	milligram
min	minute
mL	milliliter
mm	millimeter
mM	millimolar
mΩ	milliohm
m/z	mass-to-charge ratio
MOPS	3-(N-morpholino)propanesulfonic acid
MRM	multiple reaction monitoring
MS	mass spectrometry
MS medium	Murashige and Skoog medium
MS/MS	(or MS2) tandem mass spectrometry
mQ-H_2O	milli-Q water
NCE	normalized collision energy
n.d.	not detected
NF	normalization factor
nm	nanometer
n.s.	not significant
PCR	polymerase chain reaction
pH	power of hydrogen
PI	propidium iodine
PPP	phenylpropanoid pathway
pro	promotor
qPCR	quantitative PCR
Rev	reverse
rpm	revolutions per minute
SAIL	Syngenta Arabidopsis Insertion Library
SALK	Salk Institute Genomic Analysis Laboratory
s.d.	standard deviation
sec	seconds
UPLC	ultra-performance liquid chromatography
UPLC-ESI-MS	UPLC - electrospray ionization liquid chromatography mass spectrometry
V	volt
v/v	volume per volume
w/v	weight per volume
XIC	extracted ion chromatogram

9 Acknowledgement

From my perspective, PhD is not something you achieve alone. You rather rely on the support of other from time to time, so it is teamwork. This page is devoted to all the people who supported me during the last four years and made this piece of work possible.

First of all, I would like to thank Prof. Dr. Nicolaus von Wirén for the opportunity to work on this project and for his support during the whole time. Without any further knowledge in plant biology, you gave me the chance to follow my curiosity and to learn about the beauty of plants.

I also would like to thank Prof. Dr. Edgar Peiter and Prof. Dr. Stephan Clemens for evaluating my thesis.

My deepest thanks to Dr. Ricardo Giehl. I literally do not know to express my gratefulness and appreciation for everything I was able to learn from you. Thank you for sharing your experience and knowledge of how to succeed in science and your support and encouragement throughout the whole time.

Many thanks also to our collaboration partners of the project including Dr. Walter Schenkeveld, Prof. Dr. Steffan Kraemer, Dr. Markus Puschenreiter, Dr. Theresa Rosenkranz, Prof. Dr. Günther Weber, and Matthias Baune for the good cooperation and the DFG for financial support.

Special thanks also to Yudelsy for excellent technical assistance with ICP-MS analysis and guidance and support for my UPLC-MS/MS measurements.

Thanks also to Annett, Jaqueline, and Elis for their excellent technical support especially during the end of my thesis and for just being there, making me smile, listening, and becoming good friends.

Another special person I would like to mention is my colleague and friend Sara. Thank you for understanding me even without any words, for your mental support, for cheering me up, and for taking me the promise to finish my PhD. Thank you for our extraordinary friendship.

I also would like to thank all the members from the Molecular Plant Nutrition group: Anja, Diana, Markus, Ying, Zhongtao, Zhaojun, Rodolfo, Loïse, Esin, Bijal, Mikel, Jingyi, Geeisy, Suresh, Goudham, Alex, Mo, Babara, Dagmar, Christine, Heike, Melanie, Andrea, Nicole, Marleen, and Elmarie. It was a pleasure to meet and to work with all of you.

Further, I want to acknowledge the continuous support from Mr. Geyer and his team especially Katrin Thiemann in the greenhouse.

Since life is more than just working all the time and chasing dreams, I also would like to thank Master Peter Wolf and all members from the Taekwondo school Tong-Il for teaching me about discipline and perseverance and what goes along with it as well as for giving me joy and the chance to be part of a great community. Taekwon.

Finally, I want to thank my family and Florian for their continuous support, their encouragement to follow my dreams and their unconditional love. I am so grateful to have you all in my life. I love you!

10 Curriculum Vitae

Name:	Vanessa Paffrath
Date of Birth:	27.05.1991
Place of Birth:	Berlin, Germany
Nationality:	German
Address:	Leibniz-Institute of Plant Genetics and Crop Plants Research (IPK), Department of Physiology and Cell Biology, Corrensstraße 3, 06466 Gatersleben, Germany

Education:

03/2017-01/2021	PhD Student at the Leibniz-Institute of Plant Genetics and Crop Plants Research (IPK), Department of Physiology and Cell Biology, Research Group: Plant Molecular Nutrition Supervisor: Prof. Dr. Nicolaus von Wirén enrolled at the Martin-Luther University Halle/Wittenberg, Germany, Institute for Biology Dissertation title: Iron mobilization and reduction by coumarin-type siderophores in roots of *Arabidopsis thaliana*
10/2011 – 09/2016	Technical University Berlin, Germany Master study course: Biotechnology Master thesis at the University of Tartu (Estonia) Institute of Technology, Proteomics Core Facility on the subject: Identification of precise sites of protein-RNA interactions *in vivo* by *in vivo* ultraviolet light-induced crosslinking and LC-MS/MS Bachelor study course: Biotechnology Graduation in 12/2014 Bachelor thesis in cooperation with BIOTRONIK SE & Co. KG, Berlin, Department of Quality Management - Biological Safety/ Biocompatibility on the subject: Method development for efficiency assessment of a cleaning machine for the reduction of chemical and particular impurities
08/2003 – 06/2011	Goethe Oberschule Berlin, Germany Graduation: academic high school diploma

Conferences and scientific training during the PhD study:

Conferences - oral presentations:

18.06.-21.06.2019 Iron mobilization and reduction by coumarin-type siderophores in *Arabiopsis*; 15th Plant Science Student Conference, IPB Halle (Saale)

Conferences - poster presentations:

09.07.-13.07.2018 Iron mobilization by coumarin-type siderophores in *Arabidopsis*; 19th International Symposium on Iron Nutrition and Interactions in Plants (Academia Sinica, Taipei, Taiwan)

19.06.-22.06.2018 Iron mobilization by coumarin-type siderophores in *Arabidopsis*; 14th Plant Science Student Conference; IPK Gatersleben

06.06.-09.06.2017 Iron mobilization by coumarin-type siderophores in *Arabidopsis*; 13th Plant Science Student Conference
IPB Halle (Saale)

Practical scientific training:

10.-12.12.2019 Early Carrere Writing Workshop (by Myles Axton)

20.-22.03.2019 Spring School IPK “Computational Biology Starter”

29.-31.01.2019 Q Exactive Operations (LC-MS user training)

12.-14.11.2018 Confocal Laser Scanning Microscopy

22.10.2018 Plant In vitro propagation and cryo-conservation

17.07.2018 Good Scientific Practice

03.-07.09.2018 GFBio - de.NBI Summer School 2018 Riding the Data Life Cycle!

Further activities:

04/2017-11/2019 Member of the IPK PhD Student Board
Member of the core organization committee for the 14th Plant Science Student Conference; IPK Gatersleben

Publications:

Alahmad, A.; Paffrath, V.; Clima, R.; Busch, J. F.; Rabien, A.; Kilic, E.; Villegas, S.; Timmermann, B.; Attimonelli, M.; Jung, K.; Meierhofer, D.: Papillary renal cell carcinomas rewire glutathione metabolism and are deficient in both anabolic glucose synthesis and oxidative phosphorylation. Cancers 11 (9), 1298 (2019), https://doi.org/10.3390/cancers11091298

Sarashgi, A., Puschenreiter, M., Baune, M., Paffrath, V., Oburger, E., Giehl, R. F. H., Rosenkranz, T.: Does the exudation of coumarins from Fe-deficient, soil-grown Brassicaceae species play a significant role in plant Fe nutrition?. Rhizosphere (19), 2021, https://doi.org/10.1016/j.rhisph.2021.100410

Gatersleben,

11 Eidesstattliche Erklärung/Declaration on oath

Hiermit versichere, dass ich die vorliegende Arbeit selbstständig verfasst habe, dass ich keine anderen Quellen und Hilfsmittel als die angegebenen benutzt habe und dass ich die Stellen der Arbeit, dich ich anderen Werken – auch elektronischen Medien – dem Wortlaut oder Sinn nach entnommen habe, in jedem Fall unter Angabe der Quelle als Entlehnung kenntlich gemacht habe. Die Arbeit wurde bisher in gleicher oder ähnlicher Form keiner anderen Institution oder Prüfungsbehörde vorgelegt.

I hereby declare that I have written the submitted thesis independently and without illicit assistance of third parties. I have not used any other reference and sources than those listed in the thesis or engaged any plagiarism. All references and sources used in the presented work are properly cited and acknowledged. Further, I declare that the presented work has not been previously submitted for the purpose of academic examination, either in its original or similar form, anywhere else.

Ort/Place, Datum/Date Unterschrift/ Signature

12 Erklärung über bestehende Vorstrafen und anhängige Ermittlungsverfahren/Declaration concerning Criminal Record and Pending Investigations

Hiermit erkläre ich, dass ich weder vorbestraft bin noch dass gegen mich Ermittlungsverfahren anhängig sind.

I hereby declare that I have no criminal record and that no preliminary investigations are pending against me.

Ort/Place, Datum/Date Unterschrift/ Signature